

**SUBCELLULAR LOCALIZATION OF HYPOXIA-INDUCIBLE FACTORS AND
HIF REGULATORY HYDROXYLASES IN RAT LIVER**

by

Zahida Khan

B.S. in Biochemistry, Simmons College, 1998

Submitted to the Graduate Faculty of the
University of Pittsburgh School of Medicine,
Department of Cellular and Molecular Pathology,
in partial fulfillment of the requirements for the degree of
Doctor of Philosophy

University of Pittsburgh

2006

UNIVERSITY OF PITTSBURGH
SCHOOL OF MEDICINE

This dissertation was presented

by

Zahida Khan

It was defended on

Tuesday, May 2, 2006

and approved by

Donna Beer Stolz, Ph.D., Chairperson
Assistant Professor, Department of Cell Biology and Physiology

Stephen C. Strom, Ph.D., Professor, Department of Pathology

Shi-Yuan Cheng, Ph.D., Associate Professor, Department of Pathology

Marie DeFrances, M.D., Ph.D., Assistant Professor, Department of Pathology

George K. Michalopoulos, M.D., Ph.D., Dissertation Director
Professor and Chairman, Department of Pathology

COPYRIGHT

This document is copyright free for educational and scientific development.

Permission was granted to the use of figures from:

1. Carmeliet, P., and R.K. Jain. (2000) Angiogenesis in cancer in other diseases. *Nature*, 407:249-257. (Copyright ©2000, Macmillan Publishers, Ltd.)
2. Ross M.A., C.M. Sander, T.B. Kleeb, S.C. Watkins, and D.B. Stolz. (2001) Spatiotemporal expression of angiogenesis growth factor receptors during the revascularization of regenerating rat liver. *Hepatology*, 34:1135-1148. (Copyright ©2001, John Wiley and Sons, Inc.)
3. Michalopoulos, G.K., and M.C. Defrances. (1997) Liver regeneration. *Science*, 276:60-66. (Copyright ©1997, AAAS)
4. Sato, T., O.N. El-Assal, T. Ono, A. Yamanoi, D.K. Dhar, and N. Nagasue. (2001) Sinusoidal endothelial cell proliferation and expression of angiopoietin/Tie family in regenerating rat liver. *J. Hepatol.* 34:690-698. (Copyright ©2001, Elsevier, Inc.)

Documentation of permission letters is on file with Zahida Khan

SUBCELLULAR LOCALIZATION OF HYPOXIA-INDUCIBLE FACTORS AND HIF REGULATORY HYDROXYLASES IN RAT LIVER

Zahida Khan, Ph.D.

University of Pittsburgh, 2006

ABSTRACT

Many signals involved in pathophysiology are controlled by hypoxia-inducible factors (HIFs), transcription factors that induce expression of hypoxia-responsive genes. HIFs are highly conserved master regulators of O₂ homeostasis. These factors are post-translationally regulated by a family of O₂-dependent HIF hydroxylases, whose members include four prolyl 4-hydroxylases (PHD1-4) and an asparaginyl hydroxylase (FIH-1). All HIF hydroxylases require molecular O₂, Fe²⁺, ascorbate, and 2-oxoglutarate as cofactors. We hypothesized that alterations in subcellular localization may provide an additional point of regulation for the HIF pathway in response to hypoxia. Most of these enzymes are abundant in resting liver, an organ which is itself unique due to its physiologic O₂ gradient, and they can exist in both nuclear and cytoplasmic pools. In this study, we analyzed the localization of endogenous HIFs and their regulatory hydroxylases in primary rat hepatocytes cultured under hypoxia-reoxygenation conditions. We observed an absence of nuclear HIF-1 α activation in hypoxic hepatocytes, even though several known HIF target genes were upregulated, suggesting that HIF-2 α and HIF-3 α are the predominant isoforms in liver. We show that in hepatocytes, hypoxia-reoxygenation targets HIF-1 α to the peroxisome rather than the nucleus, where it co-localizes with the von Hippel Lindau protein (VHL) and the HIF hydroxylases. Confocal immunofluorescence microscopy demonstrated that the HIF hydroxylases can translocate from the nucleus to the cytoplasm in response to hypoxia, with increased accumulation in peroxisomes upon reoxygenation. These results were confirmed via immuno-transmission electron microscopy and Western blotting. Surprisingly, in resting liver tissue, peri-venous localization of the HIF hydroxylases was detected, consistent with areas of low pO₂. This was in contrast to nuclear HIF-1 α , which was

undetectable in a number of liver injury models. In conclusion, these studies establish the peroxisome as a highly relevant site of subcellular localization and function for the endogenous HIF pathway in hepatocytes.

TABLE OF CONTENTS

LIST OF TABLES	X
LIST OF FIGURES	XI
LIST OF ABBREVIATIONS	XIII
PREFACE.....	XV
1.0 INTRODUCTION.....	1
1.1 THE HIF PATHWAY.....	1
1.1.1 Hypoxia-inducible factors	1
1.1.2 HIF regulatory hydroxylases	9
1.2 DOWNSTREAM EFFECTS OF THE HIF PATHWAY	15
1.2.1 Expression and localization.....	15
1.2.2 Insights from knock-out models	17
1.2.3 Direct targets of HIF.....	18
1.2.4 Role of HIF pathway in therapeutic applications	20
1.3 RELEVANCE OF THE HIF PATHWAY IN THE LIVER.....	22
1.3.1 Organization of the liver	22
2.0 RATIONALE AND HYPOTHESIS.....	27
2.1 HIF AND LIVER.....	27
2.2 GENERAL HYPOTHESIS.....	27
2.3 SPECIFIC AIMS	28
2.3.1 Specific Aim 1	28
2.3.2 Specific Aim 2	28
2.3.3 Specific Aim 3.....	28

3.0	MATERIALS AND METHODS	29
3.1	ANTIBODIES AND REAGENTS.....	29
3.2	ANIMAL MODELS AND CELL CULTURE	29
3.2.1	Isolation and culture of primary rat hepatocytes	29
3.2.2	Growth factor experiments	30
3.2.3	Hepatoma cell line culture, transplantation, and in vivo tumor formation.....	31
3.2.4	70% Partial hepatectomy (PHx) model	33
3.3	HISTOLOGIC METHODS.....	36
3.3.1	Immunohistochemistry.....	36
3.3.2	Hypoxyprobe™ immunohistochemistry	36
3.3.3	HIF-1α and HIF-2α immunohistochemistry.....	37
3.4	HIGH RESOLUTION IMAGING.....	38
3.4.1	Scanning laser confocal immunofluorescence microscopy	38
3.4.2	Immuno-transmission electron microscopy (Immuno-TEM).....	38
3.5	ANALYSIS OF CELLULAR PROTEINS.....	39
3.5.1	Preparation of nuclear extracts	39
3.5.2	Preparation of membrane-enriched fractions.....	39
3.5.3	Western blotting.....	39
3.5.4	Enzyme-linked immunosorbent assay (ELISA) for HIF-1α DNA-binding activity.....	40
3.6	ANALYSIS OF RNA.....	42
3.6.1	Isolation of RNA.....	42
3.6.2	Reverse-transcription polymerase chain reaction	42
3.6.3	Affymetrix gene array analysis.....	42
4.0	PEROXISOMAL LOCALIZATION OF HYPOXIA-INDUCIBLE FACTORS AND HIF REGULATORY HYDROXYLASES IN PRIMARY RAT HEPATOCYTES EXPOSED TO HYPOXIA-REOXYGENATION	44
4.1	INTRODUCTION	44
4.2	RESULTS	46
4.2.1	Establishment of hypoxic cultures of primary rat hepatocytes.....	46

4.2.2	Hypoxia does not induce nuclear localization of HIF-1 α in primary rat hepatocytes.....	47
4.2.3	HIF-1 α localizes to peroxisomes in primary rat hepatocytes	49
4.2.4	HIF hydroxylases localize to peroxisomes in resting liver	52
4.2.5	Expression of HIF hydroxylases in primary rat hepatocytes	54
4.2.6	Hypoxia-reoxygenation induces nuclear-to-cytoplasmic translocation and peroxisomal sequestration of HIF hydroxylases in cultured hepatocytes	54
4.2.7	Immuno-TEM and Western analysis confirm peroxisomal localization of HIF hydroxylases in cultured hepatocytes.....	59
4.2.8	Hypoxia-reoxygenation leads to peroxisomal localization of VHL	59
4.3	DISCUSSION.....	62
4.4	ACKNOWLEDGEMENTS:.....	67
5.0	ABSENCE OF NUCLEAR INDUCTION OF HIF-1 α IN RAT LIVER: IN VIVO AND IN VITRO STUDIES.	68
5.1	INTRODUCTION	68
5.1.1	Liver regeneration as a model for angiogenesis.....	68
5.1.2	Hepatocyte growth factor (HGF) in liver regeneration.....	71
5.1.3	Epidermal growth factor (EGF) in liver regeneration	73
5.1.4	Purpose of the experiments conducted in this chapter.....	74
5.2	RESULTS.....	75
5.2.1	HIF-1 α is undetectable in regenerating rat liver.	75
5.2.2	Absence of nuclear HIF-1 α induction in primary rat hepatocyte cultures.....	75
5.2.3	Analysis of hepatocyte gene expression in response to hypoxia	79
5.3	DISCUSSION.....	84
5.4	ACKNOWLEDGEMENTS	88
6.0	DISCUSSION	89
6.1	SUMMARY	89
6.2	POTENTIAL MECHANISMS OF PEROXISOMAL LOCALIZATION ..	90
6.2.1	The peroxisome as a site of PHD activity.....	90
6.2.2	O ₂ zonation in the liver (i.e., “How is liver different?”)	91

6.2.3	O ₂ -redirection hypothesis.....	92
6.3	FUTURE DIRECTIONS.....	95
6.3.1	Examination of putative peroxisomal targeting sequences (PTS sites)..	95
6.3.2	Pex mutants	98
6.3.3	Conditional knock-outs	99
6.3.4	Regulation of peroxisomal sequestration.....	100
6.4	CLINICAL SIGNIFICANCE TO PEROXISOME PROLIFERATION...	101
6.5	CONCLUSIONS.....	103
APPENDIX A		105
APPENDIX B		110
APPENDIX C		121
BIBLIOGRAPHY		148

LIST OF TABLES

Table 1: Biochemical comparison of human HIF family members.....	4
Table 2: Biochemical comparison of human HIF hydroxylases.....	12
Table 3: Growth factor supplementation used in normoxic HIF-1 α induction experiments for primary rat hepatocytes.....	31
Table 4: Antibodies and conditions used in this study.	34
Table 5: RT-PCR primer pairs used in this study.....	43
Table 6: Summary of confocal immunolocalization for endogenous members of the HIF pathway in primary rat hepatocytes.....	63
Table 7: Angiogenic growth factor receptors in liver regeneration.....	71
Table 8: Genes up-regulated by 4 hr. hypoxia in primary rat hepatocytes.....	80
Table 9: Genes down-regulated by 4 hr. hypoxia in primary rat hepatocytes.....	83
Table 10: Analysis of putative PTS1 sequences in members of the HIF pathway.....	96
Table 11: Analysis of putative PTS2 sequences in members of the HIF pathway.....	97
Table 12: Genes up-regulated by 4 hr. hypoxia in primary rat hepatocytes (complete list).....	111
Table 13: Genes down-regulated by 4 hr. hypoxia in primary rat hepatocytes (complete list).	122

LIST OF FIGURES

Figure 1: Structures of human HIF proteins.	5
Figure 2: Canonical model of HIF-1 α induction.	8
Figure 3: Modification of the HIF-1 α polypeptide by the HIF prolyl and asparaginyl hydroxylases.	13
Figure 4: Summary of known HIF target genes.	19
Figure 5: Tumor “invasive switch”.	21
Figure 6: Normal liver architecture.	23
Figure 7: Physiologic O ₂ gradient in the liver.	25
Figure 8: Subcellular O ₂ sinks in the liver.	26
Figure 9: Generation of JM1 rat hepatomas.	32
Figure 10: Rat liver regeneration following 70% partial hepatectomy (PHx).	33
Figure 11: Schematic of subcellular fractionation protocol.	41
Figure 12: Establishment of hypoxic cultures.	48
Figure 13: Absence of nuclear HIF-1 α induction in primary rat hepatocytes.	50
Figure 14: Comparison of hypoxic regions in syngeneic rat hepatomas.	51
Figure 15: Subcellular localization of endogenous HIFs in primary rat hepatocytes.	53
Figure 16: Subcellular localization of endogenous HIF hydroxylases in resting liver.	55
Figure 17: Expression of HIF hydroxylases in hepatocyte cultures.	56
Figure 18: Subcellular localization of endogenous PHD1 in hepatocytes.	57
Figure 19: Subcellular localization of endogenous HIF hydroxylases in cultured hepatocytes. .	58
Figure 20: Peroxisomal localization of endogenous HIF hydroxylases in hepatocytes.	60
Figure 21: Peroxisomal localization of VHL.	61
Figure 22: Liver revascularization following 70% PHx.	69
Figure 23: RT-PCR for <i>HIF-1α</i> expression over time.	76

Figure 24: Hepatocyte cultures maintained in DMSO.....	78
Figure 25: Overview of hypoxic gene expression data.....	79
Figure 26: Peroxisomes as a potential site of oxygen-redirection in hepatocytes.	94
Figure 27: Peroxisome proliferator activated receptor (PPAR) pathway.	102

LIST OF ABBREVIATIONS

aa = amino acid	DMEM = Dulbecco's modified Eagle's medium
ABC = avidin biotinylated enzyme complex	DMSO = dimethyl sulfoxide
AhR = aryl hydrocarbon receptor	DNA = deoxyribonucleic acid
AR = amphiregulin	EGF = epidermal growth factor
ARD1 = arrest defective 1 protein = HIF- α acetyl transferase	EGLN = egg-laying defect nine
ARNT = aryl hydrocarbon receptor nuclear translocator	EMSA = electrophoretic mobility shift assay
bHLH = basic helix-loop-helix	EPAS = endothelial PAS domain protein
BSA = bovine serum albumin	EPO = erythropoietin
CBP = cAMP response element binding protein binding protein	ER = endoplasmic reticulum
CoCl ₂ = cobalt chloride	FIH-1 = factor-inhibiting HIF-1
C-P4H = collagen prolyl 4-hydroxylase	FITC = fluorescein isothiocyanate
CTAD = C-terminal transactivation domain	Flk-1/KDR = fetal liver kinase-1/kinase insert domain-containing receptor = VEGFR-2
DAB = 3,3'-diaminobenzidine	Flt-1 = fms-like tyrosine kinase 1 = VEGFR-1
DFO = desferrioxamine	H&E = hematoxylin and eosin

HB-EGF = heparin-binding EGF
HBSS = Hank's balanced salt solution
HGF = hepatocyte growth factor
HIF = hypoxia-inducible factor
HPH = HIF prolyl hydroxylase
HRE = hypoxia response element
HRP = horseradish peroxidase
ID = inhibitory domain
IPAS = inhibitory PAS protein
kD = kilodalton
 K_m = Michaelis-Menten constant
met = met proto-oncogene
MOP = member of PAS protein
NATH = human N-acetyltransferase 1 protein
nt = nucleotide
NTAD = N-terminal transactivation domain
ODDD = O₂-dependent degradation domain
2-OG = 2-oxoglutarate
PAS = Per-Arnt-Sim
PBG = PBS with BSA and glycine
PBS = phosphate-buffered saline

PBST = phosphate-buffered saline with Tween-20
PCNA = proliferating cell nuclear antigen
PER = *Drosophila* periodic clock protein
PEX = peroxin
PHD = prolyl 4-hydroxylase domain-containing protein
PHx = partial hepatectomy
PPAR = peroxisome proliferator activated receptor
PTS = peroxisomal targeting sequence
pVHL = von Hippel-Lindau tumor suppressor protein
RNA = ribonucleic acid
ROS = reactive oxygen species
RT = room temperature
RT-PCR = reverse transcription-polymerase chain reaction
SD = standard deviation
SIM = *Drosophila* single-minded protein
 $t_{1/2}$ = half-life
TAD = transactivation domain
TBST = tris-buffered saline with Tween-20
VEGF = vascular endothelial growth factor

PREFACE

“In the name of Allah, the beneficent, the merciful.”

DEDICATION

This dissertation is dedicated in loving memory of the late Dr. Mary T. Walsh
Simmons College Chemistry Alumna, 1974
Boston University School of Medicine, Associate Professor of Biophysics
My Senior Thesis Advisor, 1997-1998
Advocate for M.D./Ph.D. Students Everywhere

ACKNOWLEDGEMENTS

Sunday, August 6, 2000—When I think back to the day of my White Coat Ceremony, I can still recall both the excitement and anticipation I felt as I embarked upon my first year of MD/PhD training. Would I be able to juggle the rigors of medical school, graduate school, adjusting to life in Pittsburgh, waiting for my husband to move here from Boston, making new friends and then watching them drift apart once they have graduated? Proceeding through the MSTP here at Pitt is truly an evolutionary process, and of all the training phases I have progressed through so far, I feel that in graduate school I learned the most practical experience in terms of maturity, independence, and challenging myself to overcome obstacles.

During these years, I am most grateful for the support of my mentors, teachers, colleagues, family, and friends. Dr. George Michalopoulos enabled me to develop my research

project in his laboratory based on novel ideas and thinking “outside of the box.” Dr. Donna Beer Stolz further strengthened my research endeavors by encouraging me to aim for a higher level both creatively and scientifically. I have always admired Donna’s upbeat attitude, undying energy, and contagious enthusiasm, and these attributes became a welcome refuge during the ups and downs of grad school.

I also appreciate the support and constructive criticism offered by the members of my Thesis Committee: Drs. Steve Strom, Shi-Yuan Cheng, and Marie Defrances. Marie has especially been inspirational in serving as a role model for future MSTP graduates from our Program. Dr. Strom’s contributions to my Committee were always down-to-earth, and I also appreciate his help in providing us with human tissues. Dr. Cheng offered valuable insights from a cancer biologist’s perspective, and I am also fortunate to have been one of his first two *Angiogenesis* students, since this class helped me shape a number of my hypotheses.

I would also like to acknowledge my fellow researchers and collaborators for their technical assistance and valuable discussions. First and foremost, I would like to thank Bill Bowen for his unrivaled surgical and perfusion skills. I am also indebted to all the members of Dr. Simon Watkins’ laboratory at the Center for Biologic Imaging, especially Mark Ross, Mara Sullivan, Dr. Fengli Guo, and Jason Devlin. The Affymetrix array experiments were performed by Dr. Jianhua Luo’s group. In our laboratory, Lindsay Barua, Yu Yang, and Aimee Katsigrelis helped me “tag team” enormous amounts of serial sectioning. James Shray (high school summer student) and Srey Gast (MSTP SURP-MS summer student) were both instrumental in maintaining and characterizing the JM1 hepatoma cells. Ken Dorko and Dr. Hongbo Cai (Strom laboratory) procured human livers for the HIF hydroxylase project. Finally, the following researchers all provided helpful suggestions and techniques during the many phases of my project: Dr. Russ Delude, Dr. Xiaonan Han (Delude laboratory), Dave Gallo (Billiar laboratory), Dr. Patricia Loughran (Billiar laboratory), Dr. Atsu Nakao (Murase lab), Dr. Denise Chan (Stanford University), Dr. Ya-Min Tian (Oxford University, England), and Dr. Deborah Stroka (University of Bern, Switzerland). Of our past laboratory members, I also greatly appreciate Dr. Elizabeth Powell for her patience and sensible advice during my first year of graduate school.

Most importantly, I would like to thank the one person, other than God, who has given me the strength and motivation to succeed in the Program and achieve my goals in becoming a physician-scientist one step-at-a-time. This person is Nasrullah Khan, my beloved husband and

very best friend. Although we have been married for nearly twelve years, it feels like I've known him for many lifetimes. It was his undying love and dedication that helped me get through the most trying times, often spending late nights and weekends with me in the lab to keep me company and to make sure I took breaks once in a while for food and drink.

I would also like to acknowledge the following grant support during my MD/PhD training: the University of Pittsburgh/Carnegie-Mellon University Medical Scientist Training Program Training Grant (NIH 5T32GM08208) and the McGowan Institute for Regenerative Medicine's Cellular Approaches to Tissue Engineering and Regenerative Medicine (CATER) Pre-Doctoral Fellowship (NIH/NIBIB 1T32EB001026).

With respect and much appreciation,

Zahida Khan

(a.k.a. "Za")

1.0 INTRODUCTION

1.1 THE HIF PATHWAY

Oxygen homeostasis is a highly conserved mechanism required for the survival of all organisms from bacteria to humans. In most settings, O₂ delivery and consumption increase with metabolic demand; however, extreme shifts in tissue oxygenation can be detrimental. Multicellular organisms exploit evolutionary machinery that senses and adapts to fluctuations in the pO₂ of their microenvironment. This O₂-responsive system is ubiquitous among metazoans, and it involves an intracellular balance between hypoxia-inducible factors (HIFs) and the hydroxylases by which they are regulated. Due to its physiologic O₂ gradient, the liver is a unique organ where maintenance of O₂ homeostasis is critical for its specialized functions. In this chapter, we will first describe the mechanisms of the HIF pathway in detail, and then examine its relevance to the liver in health and disease.

1.1.1 Hypoxia-inducible factors

With a few notable exceptions, HIFs are transcription factors that upregulate the expression of hypoxia-dependent genes when cellular O₂ is limiting (hypoxia). When O₂ is abundant (normoxia), HIFs undergo a series of post-translational hydroxylations, which render them transcriptionally inactive and target them for proteosomal degradation. The key players in this HIF regulatory pathway include HIF prolyl 4-hydroxylases (PHDs), HIF asparaginyl hydroxylase (FIH-1), and the von Hippel-Lindau tumor suppressor protein (pVHL), each of which will be described in turn. Hypoxia liberates HIFs from this inhibitory cycle, allowing them to stabilize and translocate to the nucleus where HIF-dependent transcription is initiated.

1.1.1.1 Discovery of HIF

As befitting with its role in O₂ homeostasis, the initial identification of HIF arose from pioneering studies involving the regulation of erythropoietin (EPO), a glycoprotein hormone secreted by the fetal liver and adult kidneys that is essential for erythropoiesis and maintenance of erythroid progenitor cells (1, 2). It is well known that local O₂ tension is a major determinant of EPO production, which in turn facilitates systemic O₂ delivery. Since O₂ consumption rises with metabolic demand, the O₂-carrying capacity of the blood increases over time as more erythrocytes are produced to fulfill tissue oxygenation requirements.

Interestingly, the best characterized model for studying the regulation of *Epo* gene expression is the Hep3B human hepatoma cell line, which was shown by Goldberg in 1987 to upregulate *Epo* mRNA in response to hypoxia (1% O₂) or cobalt chloride (CoCl₂); however, at that time the prevailing view was that this *Epo* transcription depended on an as yet undiscovered “O₂-sensing heme protein” (3, 4). In 1991, Gregg Semenza and colleagues published the first of several definitive works that provided a molecular basis for the increase in *Epo* in response to hypoxia. Using mice expressing a hypoxia-inducible human *Epo* transgene, they identified *cis*-acting DNA sequences that were cell-type specific: sequences within the immediate 3' flanking region of the human *Epo* gene directed expression specifically in hepatocytes, but not in the renal cortex; therefore, human *Epo* transcription initiation sites were differentially utilized in liver and kidney (5). Semenza *et al.* (6) next demonstrated via DNase I footprint analyses and electrophoretic mobility shift assays (EMSAs/gel shifts) that at least two “hypoxia-inducible nuclear factors” found in anemic mouse liver nuclear extracts could bind to a 3' enhancer element of the human *Epo* gene. Semenza and Wang (7) then cloned the minimal 50-nt 3' enhancer element into chloramphenicol acetyltransferase (CAT) reporter vectors, which were transiently transfected into Hep3B cells for *in vitro* experiments. Mutational analyses and EMSAs revealed the first evidence that the binding of a “hypoxia-induced nuclear factor” and a “constitutive factor” at this hypoxia-response element (HRE) was required for transcriptional activation of the human *Epo* gene; furthermore, the hypoxia-induced DNA binding was sensitive to cyclohexamide treatment, indicating that this nuclear factor was induced via *de novo* protein synthesis (7). This DNA-binding activity was also inhibited by treatment with either the protein kinase inhibitor 2-aminopurine or calf intestinal alkaline phosphatase, suggesting a requirement for protein phosphorylation (8).

The race to unveil the identity of this mysterious nuclear factor was now gaining momentum. Semenza's group (8) proposed the existence of a putative "hypoxia-inducible factor-1" (HIF-1). Although the still unidentified HIF-1 protein(s) could not be studied directly, the laboratory used EMSAs to further characterize the kinetics of its DNA-binding activity in response to hypoxia, which were noted to be extremely rapid ($t_{1/2} < 1$ min. for either association or dissociation) (8). These results were further corroborated using the same methods in a number of EPO- and non-EPO-producing mammalian (human and rodent) cell lines (9). Since HIF-1 was induced by a common mechanism in all cells examined, this suggested a general role for HIF-1 in the transcriptional response to hypoxia.

In 1995, Wang and Semenza finally reported the biochemical purification and characterization of HIF-1 protein from both EPO-producing Hep3B and non-EPO-producing HeLa S3 cells, treated with either hypoxia or CoCl_2 (10). In solution, HIF-1 existed predominantly as a heterodimer consisting of two subunits: a 120-kD HIF-1 α and a 90-94-kD HIF-1 β . Both subunits contacted DNA directly in the major groove (8, 10). After cloning, screening, and antibody production, Semenza's group (11) revealed later that HIF-1 was not a heme-containing protein at all. HIF-1 α was closely related to the *Drosophila* single-minded (Sim) protein, while HIF-1 β was identical to the mammalian aryl hydrocarbon receptor nuclear translocator (ARNT) of the dioxin-responsive pathway. All of these proteins contained a basic helix-loop-helix (bHLH) and a Per-ARNT-Sim (PAS) domain, both of which were necessary for protein dimerization and DNA binding at a 5'-RCGTG-3' consensus sequence (12-14). HIF-1 was thus unequivocally defined as a bHLH-PAS heterodimeric transcription factor which not only mediated the transcriptional response to hypoxia but also was itself regulated by cellular O_2 tension.

1.1.1.2 Members of the HIF family

Although HIF-1 is considered the master regulator of hypoxic gene expression, numerous studies have reported the existence of other HIFs as well. Recognized members of the HIF family of transcription factors are summarized in Table 1. These include three hypoxia-inducible HIF- α subunits (HIF-1 α , HIF-2 α /EPAS1, HIF-3 α /IPAS) and three constitutively-expressed HIF- β subunits (HIF-1 β /ARNT1, HIF-2 β /ARNT2, and HIF-3 β /ARNT3). Any HIF- α can dimerize with

any HIF- β ; however, HIF- α subunits dimerize exclusively with HIF- β subunits, (15-17). In contrast, HIF- β subunits can also dimerize with aryl hydrocarbon receptors (AhRs) and Sim proteins, providing cross-talk with xenobiotic metabolism and central nervous system development, respectively (18, 19).

Table 1: Biochemical comparison of human HIF family members.

HIF- α subunits are hypoxia-induced while HIF- β subunits are constitutive. Any HIF- α can dimerize with any HIF- β ; however, HIF- α subunits dimerize exclusively with HIF- β subunits. Note that HIF-3 β has only been identified in *M. musculus*. The polarity index is the predicted percentage of amino acid hydrophathy. This compilation is based on information retrieved from *UniProt* (20).

Primary Name	Alternate Nomenclature	# aa	Predicted Molecular Mass (Da)	Predicted Isoelectric Point (pI)	Predicted Polarity Index (%)	Human Gene Location	UniProt Accession #
HIF-1α	<ul style="list-style-type: none"> Member of PAS Protein 1 (MOP1) ARNT-Interacting Protein 	826	92,670	5.45	54.36	14q23	Q16665
HIF-2α	<ul style="list-style-type: none"> Member of PAS Protein 2 (MOP2) Endothelial PAS Domain Protein 1 (EPAS2) HIF-1α-Like Factor (HLF) HIF-Related Factor (HRF) 	870	96,459	6.55	49.77	2p21	Q99814
HIF-3α	<ul style="list-style-type: none"> Inhibitory PAS domain protein (IPAS) 	669	72,461	6.36	46.19	19q13	Q66K72
HIF-1β	<ul style="list-style-type: none"> Aryl Hydrocarbon Receptor Nuclear Translocator 1 (ARNT1), 2 isoforms 	789 774	86,636 84,948	6.82 7.00	52.34 51.81	1q21	P27540 (2 splicing variants)
HIF-2β	<ul style="list-style-type: none"> Aryl Hydrocarbon Receptor Nuclear Translocator 2 (ARNT2) 	706	77,612	7.08	50.71	15q25	Q9HBZ2
HIF-3β (based on data from <i>M. musculus</i>)	<ul style="list-style-type: none"> Aryl Hydrocarbon Receptor Nuclear Translocator 3 (ARNT3), 5 isoforms Brain and muscle ARNT-like 1 (BMAL1) Aryl hydrocarbon receptor Nuclear translocator-like protein 1 (ARNTL) 	742 625 613 626 222	79,949 68,614 67,200 68,684 25,060	7.15 7.14 7.44 7.14 9.70	48.65 49.28 48.61 49.20 55.41	N/A	Q9WTL8 (5 splicing variants)

With regard to HIF- α subunits, a closer inspection of their primary structure offers valuable clues about their functional role in the cell. Comparison of cDNAs encoding human, mouse, and rat HIF-1 α reveals >90% homology of amino acids (11, 21-24). The organization of HIF-1 α and HIF-2 α polypeptides is also very similar. As depicted in Figure 1, the aforementioned bHLH and PAS domains are located at the N-terminus, while the C-terminus consists of a number of important regulatory domains. There are two transactivation domains

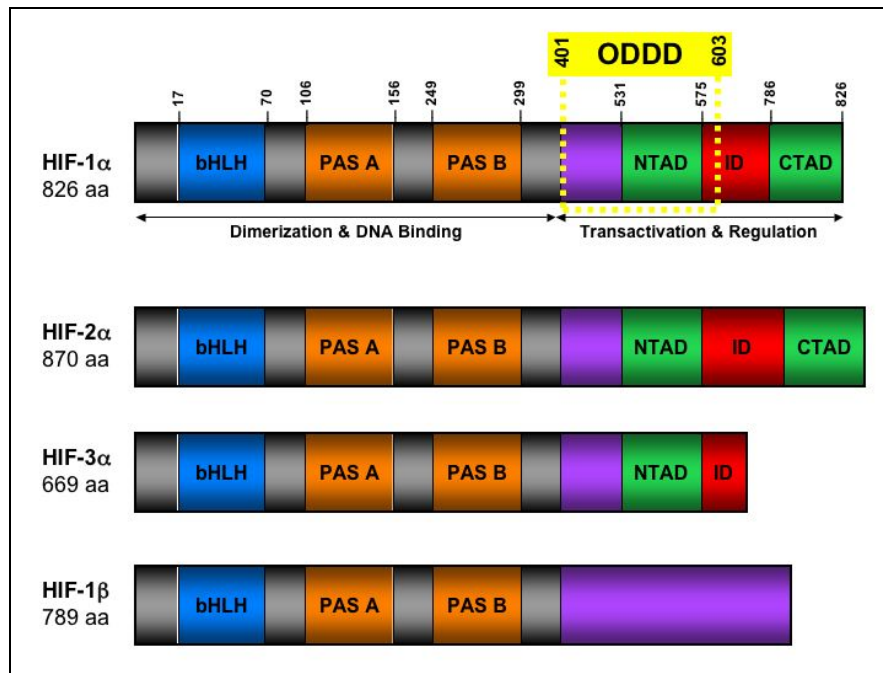


Figure 1: Structures of human HIF proteins.

All members contain an N-terminal basic helix-loop-helix (bHLH) domain and two Per-ARNT-Sim (PAS A and B) sub-domains, which are necessary for protein dimerization and DNA binding. The regulatory regions of HIF-1 α and HIF-2 α are comprised of two transactivation domains (NTAD and CTAD) within the C-terminus, separated by an inhibitory domain (ID). FIH-1 hydroxylates Asn-803 in the HIF-1 α CTAD. Lys-532 in the HIF-1 α O₂-dependent degradation domain (ODDD) is acetylated by ARD1/NATH. PHDs hydroxylate Pro-402 and Pro-564 in the ODDD, leading to HIF- α degradation. The constitutive HIF-1 β lacks these regulatory sequences. A novel variant of the bipartite-type nuclear localization signal (NLS) has also been identified in the C-terminus of the human HIF- α subunits (25). [Figure based on (17)]

(NTAD and CTAD) within the C-terminus, separated by an inhibitory domain (ID) (26). These regulatory domains are not present in the constitutive HIF-1 β . The transactivation domains bind to transcriptional co-activators in hypoxia. Specifically, binding of CTAD to the cysteine/histidine rich CH-1 domain of the transcriptional co-activator p300 leads to enhanced HIF transcriptional activity (27-29). This interaction is blocked in normoxia when a key

asparagine residue in the CTAD (Asn-803 of human HIF-1 α , Asn-851 of human HIF-2 α) is β -hydroxylated by the O₂-dependent asparaginyl hydroxylase, FIH-1 (30-32). In accordance with this, deletion of the ID results in increased HIF transcriptional activity in the presence O₂ (26).

In addition to controlling transcriptional activity, the central portions of the HIF-1 α and HIF-2 α C-termini (aa residues ~400-600) also contain regulatory sequences essential for protein stability. In general, 31% of all HIF-1 α residues are proline, glutamic acid, serine, or threonine (PEST) residues, which are common to many proteins targeted for rapid intracellular degradation (11, 33). Most importantly, two proline residues (Pro-402 and Pro-564) in the O₂-dependent degradation domain (ODDD) are critical in directing turnover of HIF- α subunits (34). Each of these prolines is located within conserved Leu-X-X-Leu-Ala-Pro motifs (LXXLAP, where X is any amino acid), which act as substrates for O₂-dependent HIF PHDs (35, 36). In normoxia, the presence of hydroxyproline at positions 402 and/or 564 leads to HIF- α degradation, whereas inhibition of prolyl hydroxylation results in stabilization of HIF- α subunits in hypoxic conditions.

Although the ODDD is predominantly regulated by hydroxylation, other O₂-dependent post-translational modifications may also exist. The ODDD contains a specific lysine (Lys-532 in HIF-1 α) which is a target of the arrest defective 1 protein (ARD1, not to be confused with an earlier ARD1 = ADP-ribosylation factor domain protein 1) (37, 38). ARD1 forms a complex with the human N-acetyltransferase 1 protein (NATH), which together can directly transfer an acetyl group from acetyl-CoA to Lys-532 in normoxia (39). This novel mechanism enhances the interaction of pVHL with HIF-1 α or HIF-2 α , leading to maximal degradation. Additional modulation of HIF by cellular metabolites will be addressed in later chapters.

In contrast to the other HIFs, less is known about HIF-3 α . As seen in Figure 1, the HIF-3 α polypeptide is much shorter. Although HIF-3 α contains an ODDD which is modified by prolyl hydroxylation, it does not possess a lysine for acetylation (40). Moreover, it appears to be regulated predominantly by alternative splicing. At least six splice variants of human HIF-3 α have been identified (41). Most striking is the production of a 307-aa “decoy” known as inhibitory PAS protein (IPAS), which is composed of bHLH and PAS domains, but lacks nearly all of the C-terminal regulatory sequences needed for transactivation (42). This splicing variant of the HIF-3 α locus may act as a dominant-negative regulator by heterodimerizing preferentially

with other HIFs and forming a transcriptionally inactive complex (43). In certain tissues, this alternative splicing is hypoxia-induced, suggesting a mechanism to counter-regulate excessive HIF-1 α activity (43).

1.1.1.3 Current model of HIF regulation

In general, HIF- α stability and activity are directly related to the primary structure described above. This involves the functional association and dissociation of HIF- α with various regulatory proteins, most of which are influenced by cellular O₂ levels and energy status. Before elaborating on these precise interactions, an overview of the current model of HIF induction is helpful. Since HIF-1 α was the first to be identified (9), it serves as the prototype for studying cellular mechanisms of O₂-sensing. Figure 2 illustrates the canonical series of events which regulate HIF-1 α activity.

Under normoxic conditions, cytosolic HIF-1 α proteins are constitutively expressed but rapidly degraded due to post-translational hydroxylations. The 120-kD HIF-1 α subunit consists of both the asparagine-containing CTAD and the proline-rich ODDD (26, 35). These domains, which are essential for HIF function, are enzymatically modified by recently identified non-heme HIF hydroxylases (FIH-1 and PHDs, respectively), members of a dioxygenase superfamily whose activity requires 2-oxoglutarate (2-OG), Fe(II), ascorbate, and most importantly molecular O₂. As seen in Figure 2, when O₂ is abundant, hydroxylation of two prolines in the ODDD by PHDs allows the pVHL to recognize HIF-1 α (36). Specifically, the largely hydrophobic β -domain of pVHL contains two critical hydrophilic residues (His-115 and Ser-111), which must hydrogen bond with either hydroxyproline or H₂O molecules (44, 45). As the substrate recognition unit of the E3 ubiquitin ligase multiprotein complex (elongins B and C, cullin2, Ring-box 1), pVHL tags HIF-1 α for polyubiquitination and degradation by the 26s proteasome (36, 46). Recognition of HIF-1 α is unlike that of any other ubiquitinated proteins, which instead rely on phosphorylation (47). This continuous turnover results in the short half-life of HIF-1 α in room air (11). Furthermore, normoxia inhibits HIF-1 α transcriptional activity via FIH-1, which hydroxylates an asparagine in the CTAD, providing yet another brake in the system (31).

Due to their requirement for molecular O₂, the HIF hydroxylases can be considered principal O₂ sensors within the cell, preventing aberrant HIF-dependent transcription in the

presence of O₂. Accordingly when cells undergo hypoxic stress (Figure 2), the hydroxylation and subsequent degradation of HIF-1α is inhibited, and this step is the chief O₂ “sensing” mechanism (48, 49). Consequently, HIF-1α stabilizes, accumulates in the cytoplasm, and translocates to the nucleus, where it forms a heterodimer with its constitutively expressed, 94-kD nuclear binding partner, HIF-1β (50). The recruitment of the transcriptional co-activators CREB-binding protein (CBP) and p300 to the CTAD (transactivation) enables the bHLH-PAS domains of the HIF-1 heterodimer to bind to HRE core consensus sequences (5'-RCGTG-3') in the promoter or enhancer regions of target genes (6, 29, 51). This initiates hypoxia-induced transcription.

Interestingly, hypoxia-independent nuclear induction of HIFs can also be achieved *in vitro* by chemical mimetics and certain growth factors (Figure 2) (52-54). Potent chemical

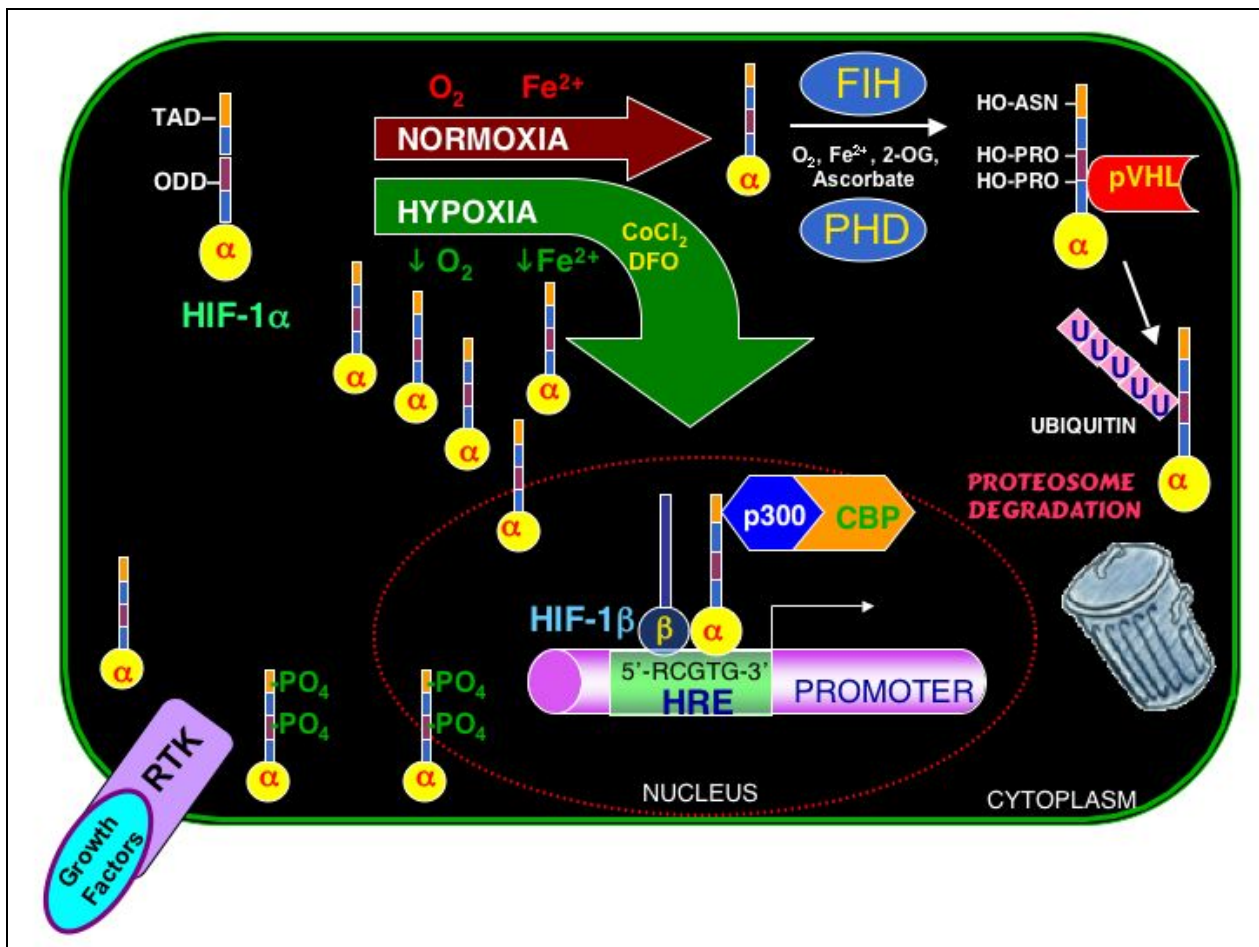


Figure 2: Canonical model of HIF-1α induction.

HIF-1α protein subunits are rapidly degraded in normoxia, but stabilize and translocate to the nucleus in hypoxia. Hydroxylation reactions may occur in the nucleus or the cytoplasm. HIF-1α also accumulates in response to inhibitors of PHDs (DMOG) or proteasomes (MG-132). Hypoxia-independent nuclear induction of HIF-1α can be achieved with chemical mimetics (DFO, CoCl₂) or via phosphorylation downstream of certain growth factors/receptor tyrosine kinases (RTKs).

inducers of HIF-1 α *in vitro* include the addition of Fe²⁺ chelators such as desferrioxamine (DFO), or transition metals such as Co²⁺, Ni²⁺, and Mn²⁺, to normoxic cell cultures, and this is thought to interfere with pVHL-dependent degradation by inhibiting HIF hydroxylase activity (55). Additional feedback loops will be discussed in the next section.

1.1.2 HIF regulatory hydroxylases

Prior to the discovery of HIF hydroxylases, various theories were proposed regarding how cells “sense” O₂ and regulate HIF. The simplest model, proposed by Semenza himself (56), involved hemoproteins, in which sensing is determined by the presence or absence of bound O₂. For example, the bacterium *R. meliloti* utilizes a two-component O₂ signaling system consisting of FixL, a hemoprotein kinase that is active in the deoxygenated state, and FixJ, a transcription factor that is active when phosphorylated by FixL (57). Although HIF-1 α itself was not found to contain heme, the model O₂ sensor for mammalian cells was proposed to involve one or more hemoproteins as well. What emerged in the years that followed was instead an exquisitely sensitive and complex mechanism of HIF regulation, much more so than anticipated by the experts in the field.

1.1.2.1 Discovery of HIF prolyl hydroxylases

Unlike Semenza’s characterization of HIF-1 α , the very recent discovery of the HIF regulatory hydroxylases involved a combined effort of several teams, whose findings were published almost simultaneously. Preliminary reports in 2001 suggested that the O₂-dependent hydroxylation of two conserved proline residues (Pro-402 and -564) in the ODDD of human HIF-1 α triggered pVHL-binding and proteosomal targeting (46, 48). Within months of these initial findings, the enzymes catalyzing these hydroxylations were identified, and an evolutionarily conserved mechanism of HIF regulation was revealed (36, 58).

Epstein *et al.* (58) first demonstrated the existence of a HIF- α homolog (*CeHIF-1*) in *C. elegans*. Similar to mammals, the regulation of this homolog in roundworms is dependent on a conserved mechanism of prolyl hydroxylation followed by targeting to a VHL homolog, VHL-1.

Mutant worms lacking *vhl-1* constitutively express *CeHIF-1*, similar to the RCC4 cells derived from patients with VHL syndrome. Furthermore, *in vitro*-translated *CeHIF-1* did not bind to VHL-1 unless it was incubated with worm extract, and mutation of Pro-621 in *CeHIF-1* eliminated interaction with VHL, suggesting a requirement for prolyl hydroxylase activity. Addition of known competitive inhibitors of collagen prolyl 4-hydroxylase (C-P4H) led to HIF-1 stabilization *in vitro* and *in vivo*. These findings were similar to those found in mammalian cells, exposing an evolutionarily conserved mechanism of proline hydroxylation.

Since worms containing inactivating mutations in each of two C-P4H isoforms showed normal *CeHIF-1* regulation, Epstein *et al.* (58) then predicted that the putative *CeHIF-1* prolyl hydroxylase would belong to the 2-OG-dependent dioxygenase superfamily, which shares a common β -barrel jelly roll motif. This criteria led to them to the *egl-9* (egg-laying defect-9) gene, which encoded a protein product of previously unknown function; although in 1983, *egl-9* mutant worms were shown to be unable to lay eggs, but produced normal offspring which violently burst from the parental worm following gestation (59). The *egl-9* gene product in worms was found to be a 2-OG-dependent dioxygenase, thus defining a novel class of prolyl hydroxylase.

Using the *egl-9* sequence, Epstein *et al.* (58) then identified three ubiquitously expressed mammalian EGL-9 homologs, designated prolyl hydroxylase domain-containing proteins (PHD1, PHD2, PHD3), each of which hydroxylated human HIF-1 α at Pro-564. The proline residues modified in both worm and mammalian HIF-1 α proteins are contained in a conserved core LXXLAP motif. In mammalian cells, the PHD isoforms acted differentially on prolyl hydroxylation sites within HIF-1 α , and recombinant enzyme activity was directly modulated by O₂ tension, providing the first substantiated mechanism for O₂-sensing within the HIF pathway.

1.1.2.2 HIF hydroxylase family members

Until the aforementioned reports, the only mammalian protein known to contain hydroxyproline was collagen; however, the HIF PHDs differ from the well-characterized C-P4H in many respects. For instance, the substrate composition for C-P4H is the tripeptide X-pro-gly, which is much shorter than the minimal ~19-mer HIF-derived peptide necessary for optimal PHD activity (60). Furthermore, recombinant C-P4H isoforms showed no activity against the HIF-1 α peptide

in vitro (46). Finally, the collagen-modifying C-P4H resides in the endoplasmic reticulum, an unlikely site for prolyl hydroxylation of HIF-1 α (36).

As shown in Table 2, new members of the HIF hydroxylase family have since been described. Oehme *et al.* (61) were the only group to describe a putative fourth HIF prolyl hydroxylase, PHD4 (PH-4). Like PHD1-3, PHD4 over-expressed in cellular reporter assays suppressed HIF-1 α activity, and this was dependent on consensus proline residues in the ODDD. The authors concluded that PHD4 might be related to cellular O₂ sensing; however, no further studies have been published on this enzyme.

In contrast to PHD4, the most unusual addition to the HIF regulatory hydroxylase family is factor inhibiting HIF-1 (FIH-1), the HIF asparaginyl hydroxylase, which was identified shortly after the PHDs. Lando *et al.* (31) reported that transactivation of HIF-2 α at the CTAD was independent but closely similar to PHD O₂-sensing, since similar effects were observed with the same enzyme co-factors and inhibitors. β -hydroxylation of Asn-851 on human HIF-2 α correlated with that of Asn-803 of HIF-1 α (30), and this activity was soon demonstrated to result from FIH-1 (31, 62).

Although FIH-1 requires similar co-factors as the O₂-dependent PHDs, some key differences have also been noted. To date, crystal structures have only been solved for FIH-1 (63, 64) and the FIH-1/HIF-1 α peptide complex (65). Examination of these structures reveals that FIH-1 contains a double-stranded β -barrel jelly roll core motif similar to other 2-OG dioxygenases, and it must form a homodimer for productive substrate-binding and catalysis (66). Sequence analysis further identified FIH-1 not only as a 2-OG dioxygenase, but also as a member of the Jumonji (JmjC) family of putative transcription factors. A significant number of JmJC proteins may actually be hydroxylases involved in signaling (65).

Interestingly, FIH-1 is not the only enzyme known to catalyze hydroxylation of asparagine. There also exists a human EGF aspartyl/asparaginyl β -hydroxylase (EGFH), which can hydroxylate both Asp and Asn residues in EGF domains of proteins such as the coagulation factors VII, IX, and X (67). The physiologic role of EGF hydroxylation is still unclear; however, it has been proposed to be involved both in the Notch pathway and as a tumor suppressor (68).

Table 2: Biochemical comparison of human HIF hydroxylases.

This family includes four HIF prolyl 4-hydroxylases (PHDs) and one HIF asparaginyl hydroxylase (FIH-1). EGL stands for “egg-laying defect” in *Drosophila* nomenclature. The polarity index is the predicted percentage of amino acid hydrophathy. This compilation is based on information retrieved from *UniProt* (20).

Primary Name	Alternate Nomenclature	# aa	Predicted Molecular Mass (Da)	Predicted Isoelectric Point (pI)	Predicted Polarity Index (%)	Human Gene Location	UniProt Accession #
PHD1	<ul style="list-style-type: none"> EGL nine homolog 2 (EGLN2) HIF prolyl hydroxylase 3 (HPH3) Estrogen-induced tag 6 (EIT6) Falkor (in <i>M. musculus</i>) 	407	42,650	8.08	40.29	19q13	Q96KS0
PHD2	<ul style="list-style-type: none"> EGL nine homolog 1 (EGLN1) HIF prolyl hydroxylase 2 (HPH2) 	426	46,021	8.67	44.60	1q42	Q9GZT9
PHD3	<ul style="list-style-type: none"> EGL nine homolog 3 (EGLN3) HIF prolyl hydroxylase 1 (HPH1) SM-20 (in <i>R. norvegicus</i>) 	239	27,261	7.85	42.26	14q13	Q9H6Z9
PHD4	Putative HIF prolyl hydroxylase 4 (PH-4), 3 isoforms	502 423 563	56,661 47,210 63,112	6.32 6.73 6.36	46.22 44.44 44.58	N/A	Q9NXG6 (3 splicing variants)
FIH-1	<ul style="list-style-type: none"> Hypoxia-inducible factor 1 alpha inhibitor (HIF1AN) Hypoxia-inducible factor asparagine hydroxylase 	349	40,285	5.71	45.85	10q24	Q9NWT6

1.1.2.3 HIF hydroxylase reactions

The generalized reaction scheme for PHDs and FIH-1 is given in Figure 3. Within the cell, PHD2 in particular is believed to be the key O₂-sensing mechanism which regulates HIF-1 α activity (49). Normoxic degradation of HIF-1 α is initiated via hydroxylation of Pro-402 and Pro-564 in the presence of O₂. In contrast, hypoxia and/or Fe(II) depletion prevents this hydroxylation from occurring. Since these enzymes are dioxygenases, for every proline that is hydroxylated, 2-OG (α -KG) must also be hydroxylated. The intermediate product of the 2-OG hydroxylation is immediately decarboxylated to give succinate.

Interestingly, this reaction has been exploited using traditional biochemical methods to measure the activity of human PHD enzymes (60). In these assays, a 19-residue peptide substrate was synthesized with an identical sequence as the C-terminal hydroxylation site of human HIF-1 α . The assay involved measuring the radioactivity of $^{14}\text{CO}_2$ formed during the hydroxylation-coupled decarboxylation of 2-oxo[1- ^{14}C]glutamate to succinate in a closed vessel. The reaction mixture also contained FeSO_4 , ascorbate, and extracts from transfected cells which expressed recombinant PHDs.

Based on these experiments and further mutational analysis, PHD1, PHD2, and PHD3 were all found to hydroxylate human HIF-1 α at Pro-564 (60). In contrast, only PHD1 and PHD2

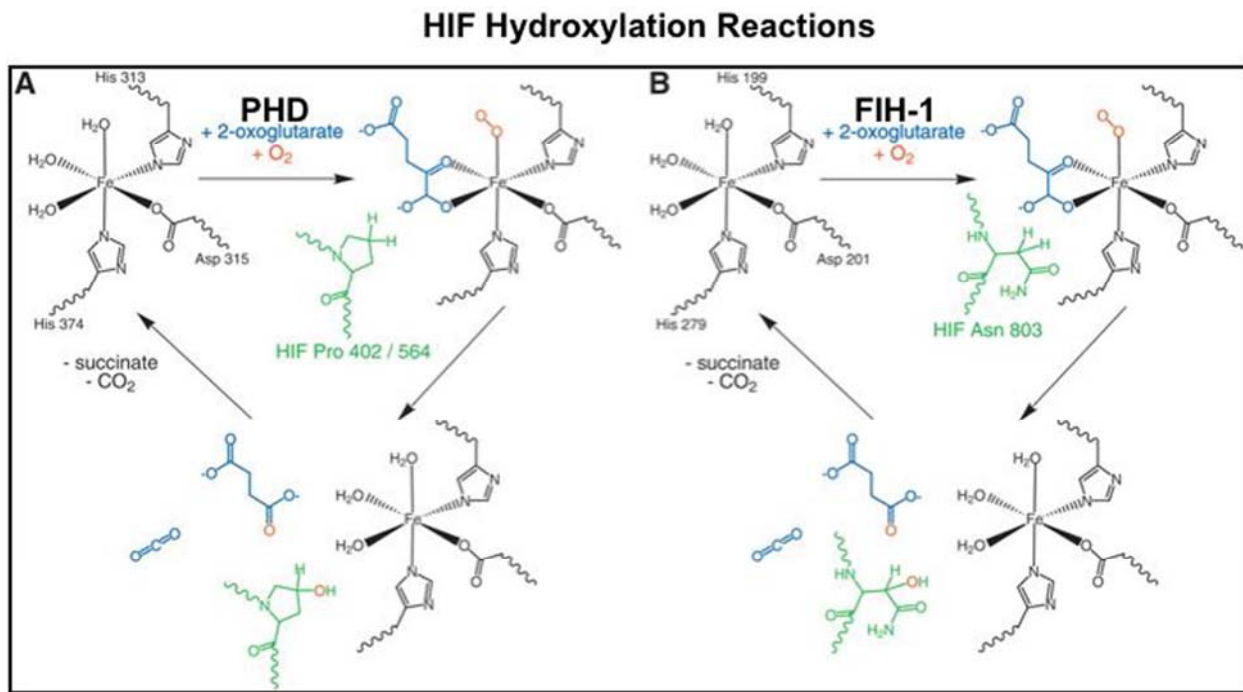


Figure 3: Modification of the HIF-1 α polypeptide by the HIF prolyl and asparaginyl hydroxylases. PHD/EGLN/HPH hydroxylates human HIF-1 α at Pro-402 and Pro-564 (A) while FIH-1 hydroxylates Asn-803 (B). The active sites contain Fe(II) coordinated by a His-XAsp...His triad. The enzymes bind 2- (2-OG, α -KG), the HIF polypeptide substrate, and O₂, acting as dioxygenases to hydroxylate both HIF-1 α and 2-. In the course of the reaction, molecular O₂ is consumed and the hydroxylated 2- undergoes decarboxylation to give succinate and CO₂. The HIF hydroxylases are considered non-equilibrium enzymes, since they cannot directly catalyze the reverse reaction, at least not by a process involving reformation of dioxygen. Figure adapted from (69).

could hydroxylate Pro-402, the second site of prolyl hydroxylation and VHL binding (58). Moreover, Michaelis-Menten enzyme kinetic assays revealed that PHD1-3 have a relatively high K_m for O₂ (pO₂ of 230-250 μM) when compared to the C-P4H (~ 40 μM) (60). This high K_m is

slightly above atmospheric pO₂, implicating that the PHDs' sensitivity to physiologic changes in pO₂ is rate-limiting for their activity (60). Consequently, changes in cellular O₂ concentration are directly transduced into changes in the rate at which HIF-1 α is hydroxylated, ubiquitinated, and degraded.

This is not completely true for FIH-1, whose *K_m* (~90 μ M) was found to be less than half that of the PHDs (70). Moreover, its catalytic properties in response to the required substrates of HIF hydroxylases are also distinct. As a result, FIH-1 has been shown to reduce HIF-1 α transcriptional activity even at low O₂ tensions (31, 71). This suggests that a hypoxic “window” may exist in which HIF-1 α subunits could accumulate (due to lack of prolyl hydroxylation) yet still undergo asparaginyl hydroxylation.

1.1.2.4 Regulation of HIF hydroxylases

Just as the HIF hydroxylases function in regulating HIF, novel mechanisms are also emerging for the regulation of these enzymes. For example, *PHD2* and *PHD3* mRNA expression is also enhanced by HIF (72-74), providing a negative feedback mechanism that limits accumulation of HIF-1 α in long-term hypoxia and accelerates its degradation upon reoxygenation (75). In contrast, hypoxia can also induce the accumulation of the ring finger proteins Siah1 and Siah2, which polyubiquitinate PHD1 and PHD3 for proteosomal degradation (76). Even more puzzling is the finding by Erez *et al.* (77) in HCT116 cells that human *PHD1* mRNA expression is down-regulated in hypoxia due to binding of HIF-1 β (ARNT) to the *PHD1* promoter. These feedback loops allow cells to rapidly accommodate to both acute and chronic changes in O₂ availability.

Differences in the regulation of PHDs are still being investigated. For instance, PHD2 but not the others has been shown to contain an N-terminal MYND-type zinc finger domain, which inhibits its catalytic activity (78). Novel interactions of PHDs with other proteins are also emerging, such as with MORG-1 (79) and OS-9 (80). Mitochondria have been linked to the metabolic regulation of PHDs, and will be discussed in more detail in later chapters.

1.2 DOWNSTREAM EFFECTS OF THE HIF PATHWAY

1.2.1 Expression and localization

As a master regulator of cellular O₂ homeostasis, the HIF pathway is considered a ubiquitous evolutionary adaptation to life in an aerobic world. However, upon closer inspection, tissue- and cell-type-specific patterns do exist regarding the expression and distribution of HIF components

1.2.1.1 Expression and distribution of HIFs

In contrast to the rather ubiquitous distribution of HIF-1 β (81), distinct expression patterns have been described for the HIF- α isoforms, and these differences imply non-redundant functions. Due to the rapid turnover of HIF- α subunits, there are only limited reports of protein localization in normal tissues. Talks *et al.* (82) analyzed a wide range of normal human tissues using novel monoclonal antibodies they generated against HIF-1 α and HIF-2 α . They found very little to no expression of either protein in any normal tissue, with the exception of bone marrow cells expressing HIF-2 α (82). These cells were identified as macrophages, and closer inspection revealed HIF-2 α -positive macrophages in lung, lymph node, spleen, brain, and liver (Kupffer cells) (82). These findings were contradicted by Stroka *et al.*, (83), who were able to localize HIF-1 α protein in mouse brain, kidney, liver, and heart using their own novel chicken (IgY) anti-HIF-1 α polyclonal antibody.

Studies analyzing HIF mRNA expression in various tissues are more abundant, but offer less functional insight. Expression of *HIF-1 α* mRNA is highest in the kidney and heart, while that of *HIF-2 α* is highest in placenta, lung, heart, and liver (21, 84). HIF-2 α may play a significant role in lung development, since elevated levels of HIF-2 α have been noted in this tissue compared to HIF-1 α (84). Interestingly, *HIF-1 α* mRNA is constitutively expressed in placental development, whereas *HIF-2 α* expression increases with gestational age (85). The latter coincides with the increases in vascularization, since endothelial cells are known to highly express *HIF-2 α* . Furthermore, in tissues where both *HIF-1 α* and *HIF-2 α* are co-expressed, each is localized to a distinct cell population. For example, in the brain, *HIF-1 α* is specific to neuronal cells, while *HIF-2 α* is limited to non-parenchymal cells (86).

These differences have also been observed in various types of cancer cells. In breast cancer cell lines, HIF-1 α was required for the hypoxic induction of many target genes, and when *HIF-1 α* was inactivated, this induction could not be recapitulated by *HIF-2 α* rescue (87). In contrast, HIF-2 α was identified as the major HIF- α isoform in RCC cells (87).

Recently, a differential pattern was also described in embryonic stem (ES) cells, which were not found to exhibit HIF-2 α transcriptional activity, suggesting possible inhibition by a HIF-2 α -specific transcriptional repressor (88). Similarly, in immortalized mouse embryonic fibroblasts (MEFs), hypoxia-induced gene expression occurred solely through the action of HIF-1 α , while endogenous HIF-2 α remained inactive due to cytoplasmic trapping (89). Furthermore, Covello *et al.* (90) found that in primary murine ES cells, targeted replacement of *HIF-1 α* by a *HIF-2 α* “knock-in” (KI) allele promoted tumor growth, increased microvessel density, and increased VEGF, TGF- α , and cyclin D1. These KI embryos also showed expanded expression of HIF-2 α -specific target genes, especially *Oct-4*, a transcription factor essential for maintaining stem cell pluripotency, survival, and maintenance (91). These and other studies suggest the non-redundant role of HIFs in development.

Much less is known about the expression and function of HIF-3 α . *HIF-3 α* mRNA was localized to adult skeletal muscle, thymus, lung, brain, heart, and kidney (92). At least six alternatively spliced isoforms of *HIF-3 α* are thought to exist. One such isoform, IPAS, functioned as a negative regulator (“decoy”) of HIF target gene expression in cerebellar Purkinje cells and in the corneal epithelium of the eye under hypoxic conditions, formed heterodimers with other HIF- α subunits, and prevented their binding to HREs (42, 43). This inhibitory role of IPAS may be important for maintaining avascularity in the otherwise hypoxic microenvironment of the cornea.

1.2.1.2 Expression and distribution of HIF hydroxylases

Due to their more recent discovery, studies on the expression patterns of HIF hydroxylases are more limited. Lieb *et al.* (93) reported on their distribution in mouse tissues. PHD1 protein was detected in testis, heart, brain, liver, kidney, and lung, but not in skeletal muscle. In contrast, PHD2 protein was localized in heart, brain, liver, skeletal muscle, kidney, and lung, but not in testis. Its abundance has also been noted in adipose tissue (94). PHD3 is unique in that it has a rat

ortholog, SM20, whose expression was previously documented in vascular smooth muscle cells and rat sympathetic neurons (95-97). SM20 is expressed in rat brain, skeletal muscle, kidney, and lung, but not in testis, liver, or spleen (95). Although similar findings were observed for PHD3 in mice, it was also found to be particularly abundant in liver (93). Regarding FIH-1, Soilleux *et al.* (98) generated novel monoclonal antibodies and localized FIH-1 in a wide range of human epithelial tissues, including esophagus, stomach, intestine, liver, gall bladder, salivary glands, pancreas, renal tubules, breast, and ovary.

1.2.2 Insights from knock-out models

Due to the embryonic lethality associated with most knock-outs, conditional knock-outs and silencing experiments have allowed further investigation into the differential functions of HIF components.

1.2.2.1 Knock-out models of HIFs

Homozygous knock-outs for HIF-1 α , HIF-2 α , and HIF-1 β are embryonic lethal; however, the underlying causes of this non-viability appear surprisingly different. In wild-type embryos, HIF-1 α expression increases between E8.5 and E9.5; although, the *HIF-1 α ^{+/+}* and *HIF-1 α ^{-/-}* embryos are indistinguishable at E8.5-E8.75 (99). Complete loss of HIF-1 α results in developmental arrest and death by E11, due to major malformations of the heart and vasculature (99-101). A reduced number of somites and neural fold defects are also observed (102). Surprisingly, the vascular defects were correlated with mesenchymal cell death, since elevated VEGF expression was detected in *HIF-1 α ^{-/-}* embryos (101). In contrast, *HIF-2 α ^{-/-}* embryos develop normal systemic vasculature, but do not survive beyond E16.5 due to impaired fetal lung maturation and catecholamine insufficiency (103, 104). Pathologic findings were also observed in the eye, skeletal muscle, liver, testis, and bone marrow (hematopoiesis) of these knock-outs, and these were associated with mitochondrial abnormalities in sites of high energy demand (105, 106).

Although several investigators are actively pursuing tissue-specific HIF conditional knock-outs, there are very few published reports on these models (107, 108). Interestingly, a recent report by Helton *et al.* (109) demonstrated that a brain-specific knock-out of HIF-1 α

reduces rather than increases hypoxic-ischemic damage, consistent with a pro-apoptotic role of HIF-1 α . This suggests that HIF-1 α loss-of-function may be protective in some tissues.

1.2.2.2 Knock-out models of HIF hydroxylases

Currently, there are no published reports on knock-out models for any of the HIF hydroxylases. The only related studies rely heavily on siRNA to silence PHD1, PHD2, and PHD3 in various human cell lines, resulting in isoform-specific patterns for PHDs (49, 110). Berra *et al.* (49) reported that PHD2 silencing was sufficient to stabilize and activate HIF-1 α in normoxia in all of the human cell lines investigated, while silencing of PHD1 or PHD3 had no effect on HIF-1 α stability either in normoxia or hypoxia-reoxygenation. Based on these results, they concluded that PHD2 is the key O₂ sensor of the cell, by setting low steady-state levels of HIF-1 α in normoxia (49).

Appelhoff *et al.* (110) further demonstrated that each PHD could regulate HIF-1 α and HIF-2 α subunits in a non-redundant manner in various cell lines, and that the contribution of each PHD was strongly dependent on enzyme abundance. Specifically, PHD2 was more active at hydroxylating HIF-1 α over HIF-2 α , while PHD3 exerted the opposite effect. In addition to this selectivity, each enzyme also exhibited specificity in hydroxylating one or both of the conserved proline residues within each HIF- α isoform. Although these silencing experiments may be limited in scope, they do provide some clues into the differential functions of HIF hydroxylases *in vivo*.

1.2.3 Direct targets of HIF

It is estimated that 1-2% of all human genes are regulated by hypoxia (111). Many such genes may be hypoxia-induced but lack HREs, implying cooperative effects with other non-HIF transcription factors (112). There are currently over 70 *bona fide* target genes of HIF-1, and these are involved in diverse cellular functions, including angiogenesis, energy metabolism, motility, and survival (Figure 4). Although the HIF-1 α and HIF-2 α subunits are structurally similar in

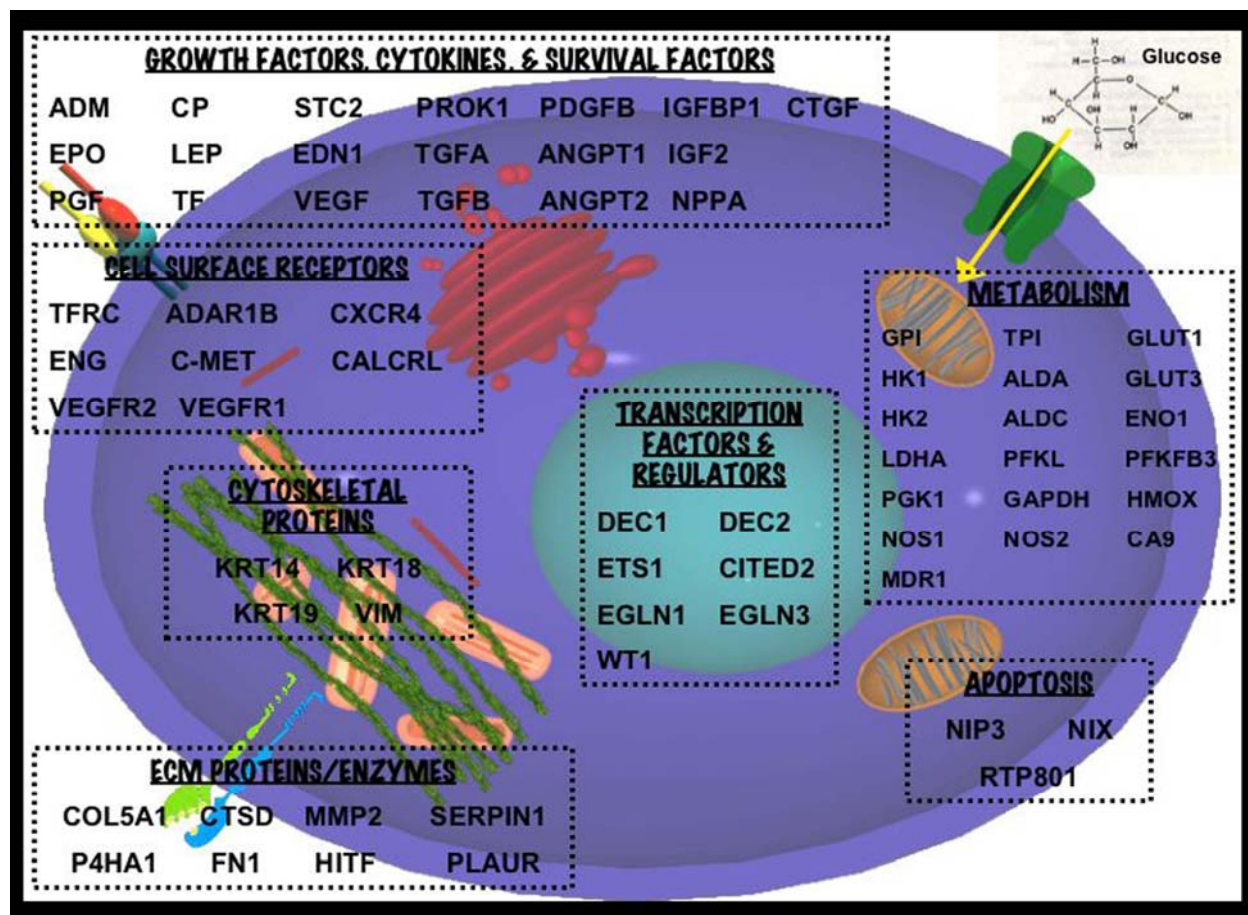


Figure 4: Summary of known HIF target genes.

Compilation of Gene ID's is based on lists published in (113-115). The abbreviated gene ID's encode the following proteins: ADM, adrenomedullin; ADRA1B, α_1 β -adrenergic receptor; ALD, aldolase A and C; ANGPT, angiopoietin 1 and 2; CA9, carbonic anhydrase IX; CALCRL, calcitonin receptor-like receptor; CITED2, CREB-binding protein (CBP)/p300-interacting transactivator (p35srj); C-MET, met proto-oncogene (HGF receptor); COL5A1, collagen V α_1 -subunit; CP, ceruloplasmin; CTGF, connective tissue growth factor; CTSD, cathepsin D; CXCR, chemokine receptor-4; DEC, differentiated embryo chondrocyte expressed 1 and 2; EDN, endothelin-1; EGLN, egg-laying defect nine-1 and 3 (HIF PHD2 and PHD3); ENG, endoglin; ENO, enolase-1; EPO, erythropoietin; ETS1, erythroblastosis virus transforming sequence; FN, fibronectin-1; GAPDH, glyceraldehyde-3-phosphate dehydrogenase; GLUT, glucose transporter 1 and 3; GPI, glucose phosphate isomerase; HITF, human intestinal trefoil factor; HK, hexokinase 1 and 2; HMOX, heme oxygenase; IGF, insulin-like growth factor-2; IGFBP, insulin-like growth factor binding protein-1; KRT, keratin 14, 18, and 19; LDHA, lactate dehydrogenase A; LEP, leptin; MDR1, multi-drug resistance P-glycoprotein; MMP2, matrix metalloproteinase; NIP3, BCL2/adenovirus E1B 19-kDa-interacting protein; NIX, NIP3-like; NPPA, atrial natriuretic peptide; NOS, nitric oxide synthase (iNOS and eNOS); P4HA1, collagen prolyl-4-hydroxylase α_1 -subunit; PFKFB3, 6-phosphofructo-2-kinase/fructose-2,6-bisphosphatase-3; PFKL, phosphofructokinase L; PGF, placental growth factor; PGK, phosphoglycerate kinase-1; PLAUR, urokinase-type plasminogen activator receptor (uPAR); PROK, prokineticin (endocrine gland-derived VEGF); RTP801, DNA-damage-inducible transcript 4 (DDIT4, REDD1); SERPIN1, plasminogen activator inhibitor-1; STC, stanniocalcin; TF, transferrin; TFRC, transferrin receptor; TGF, transforming growth factor- α and - β ; TPI, triose phosphate isomerase; VEGF, vascular endothelial growth factor; VEGFR, VEGF receptor-2/flk-1 and VEGF receptor-1/flt-1; VIM, vimentin; WT-1, Wilms' tumor suppressor.

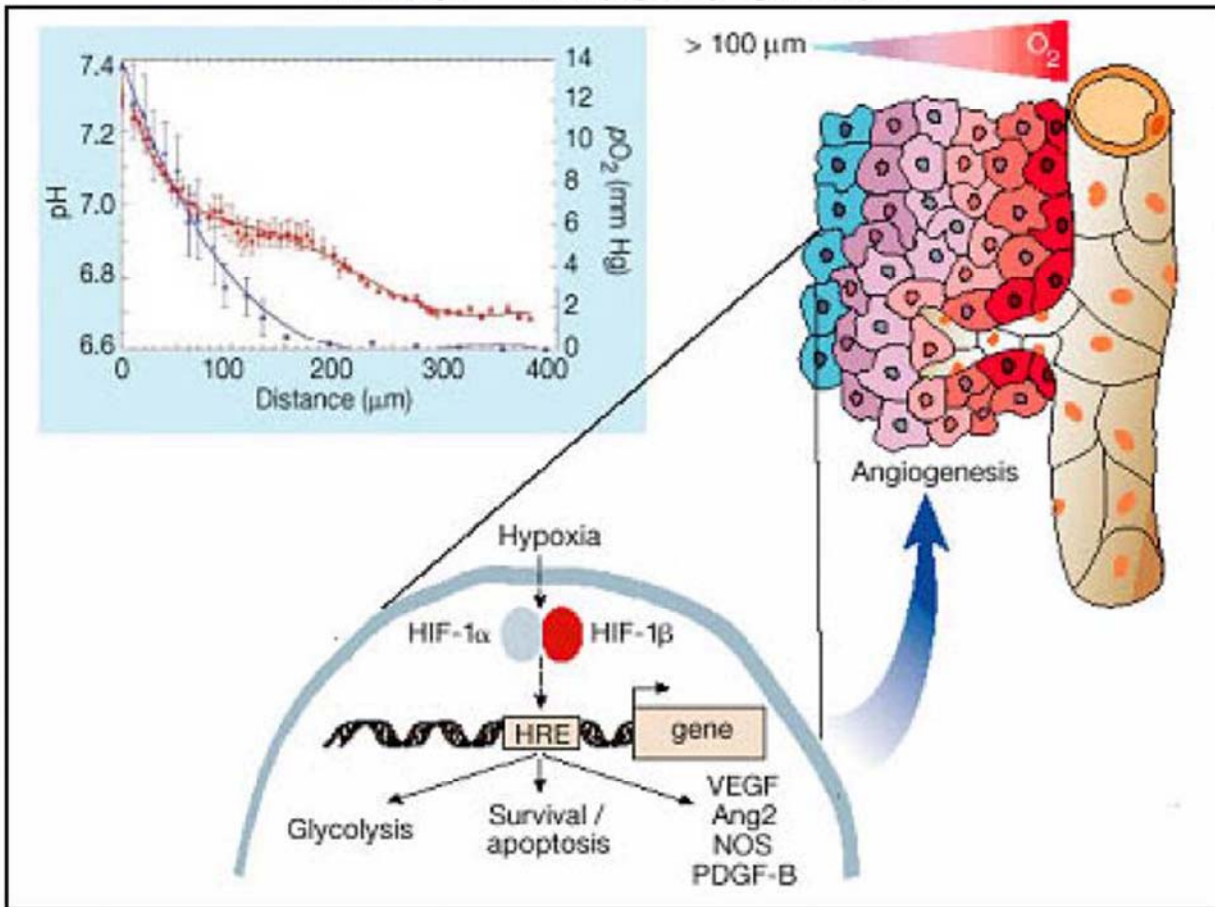
their DNA-binding and dimerization domains, they differ in their transactivation domains, implying they may have unique target genes and require distinct transcriptional co-factors. For instance, the hypoxic induction of glycolytic enzymes is regulated by HIF-1 α but not HIF-2 α (116, 117). In contrast, TGF- α appears to be a preferred HIF-2 α target (90). These findings are not surprising, given the considerable differences observed in the HIF-null mice.

1.2.4 Role of HIF pathway in therapeutic applications

1.2.4.1 Repression of HIF activity

Perhaps the most direct line of evidence between HIF-1 α and tumor progression resides in the VHL cancer syndrome. Aside from this rare disease, the global effects of HIF-1 α have been well-established in the tumor literature, and entire conferences have been devoted to tumor hypoxia and angiogenesis. As depicted in Figure 5, when tumors outgrow their (abnormal) blood supply, hypoxia represents a positive stimulus for invasion. Clinically, tumor hypoxia tends to indicate a poor outcome and increased risk of distant metastases. When compared to normal adjacent tissue, HIF-1 α is overexpressed in a majority human cancers and their metastases (118). The increased malignancy of hypoxic tumors can be attributed to the selection of apoptosis-resistant cells and induction of angiogenic factors. In aggressive cancers, even over-expression and nuclear translocation of PHD2, the chief O₂ sensor, are associated with less-differentiated and highly proliferative tumors, suggesting that PHD-activating agents would not be sufficient to down-regulate HIF-1 α in some tumors (119). In contrast, loss of HIF-1 α or HIF-1 β results in reduced tumor growth, decreased angiogenesis, and increased radio-sensitivity (118, 120). Currently, several pharmacological inhibitors of HIF-1 α are in all phases of development and clinical trials [reviewed in (89)]. Similar agents which exploit the hypoxic microenvironment are also being investigated as potential anti-inflammatory agents and as hypoxia-specific cytotoxins.

Tumor “Invasive Switch”



From: Carmeliet and Jain (2000), *Nature* 407:249-257

Figure 5: Tumor “invasive switch”.

As tumors outgrow their (abnormal) blood supply, hypoxia represents a positive stimulus for invasion. Clinically, tumor hypoxia tends to indicate a poor outcome and increased risk of distant metastases. When compared to normal adjacent tissue, HIF-1 α is over-expressed in 70% of human cancers and their metastases. The increased malignancy of hypoxic tumors can be attributed to the selection of apoptosis-resistant cells and induction of angiogenic factors. Figure reproduced from (121) with permission from Macmillan Publishers Ltd.

1.2.4.2 Activation of HIF activity

In recent years, constitutive activation of HIF-1 α has been gaining attention as a means of inducing therapeutic angiogenesis, mainly since preliminary studies of VEGF delivery alone stimulated an increase in abnormal blood vessels that were dilated, tortuous, and edematous (122). Phase II clinical trials are in progress for delivery of a constitutively active adenoviral construct (Ad2/HIF-1 α /VP16) to treat patients with peripheral vascular disease and advanced coronary artery disease (123). The results of these trials have yet to be reported.

It is interesting to note that, very recently, a family with erythrocytosis was found to carry a hereditary loss-of-function mutation in PHD2 (124). This link has heightened the awareness for another potential application that harnesses HIF-1 α activity, namely the stimulation of erythropoiesis in patients suffering from anemia of chronic disease, such as in renal failure. Clinical trials are currently under way for orally active, small molecule inhibitors of PHD enzymes for patients with chronic kidney disease. These agents would act to induce endogenous *EPO* expression along with the mobilization and utilization of iron stores. Since the life-span of an erythrocyte is 120 days, of growing concern is whether or not long-term use of these agents for HIF-mediated erythropoiesis would also carry tumorigenic potential.

1.3 RELEVANCE OF THE HIF PATHWAY IN THE LIVER

1.3.1 Organization of the liver

Much of the liver's organization is governed by its central role in removing toxins from the blood and in maintaining normal blood composition and homeostasis. Figure 6 illustrates the basic histo-architecture of the liver. The liver is organized into lobules which take the shape of polygonal prisms. Each lobule is generally hexagonal in cross-section and is centered around a central vein (branch of the hepatic vein), with portal triads at each corner. Within each lobule, hepatocytes are arranged into cords separated by adjacent sinusoids. The fenestrated endothelium lining the sinusoids lies immediately adjacent to the cords, with no basement membrane and a

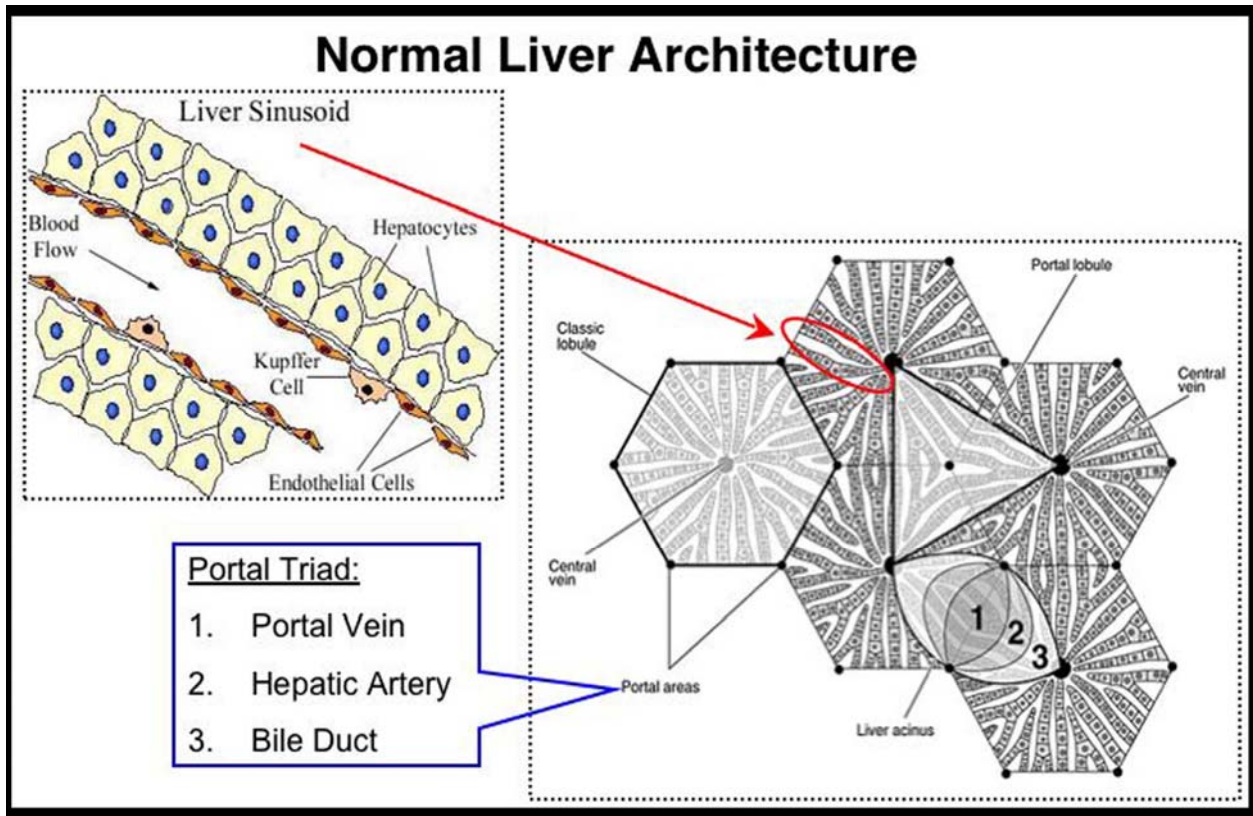


Figure 6: Normal liver architecture.

For orientation purposes, the histo-architecture of liver can be defined in terms of classic lobules, portal lobules, or liver acini.

small amount of connective tissue (primarily collagen type III and glycosaminoglycans), so that each hepatocyte is bathed on two faces by blood plasma. Within the hepatic cords lies a network of bile canaliculi, allowing passage of bile through inter-cellular channels which drain into the nearest branch of the bile duct. This specialized hepatic architecture optimizes the liver's parallel functions as an exocrine gland, endocrine gland, as well as a blood filter.

1.3.1.1 The hepatic microenvironment

Most of the pioneering work on HIF-1 α was done in hepatoma cell lines (8, 11); however, much less is known about its function in normal liver. Due to the liver's zoned architecture (Figure 7), a physiologic O₂ gradient exists between peri-portal (high O₂) and peri-venous (low O₂) regions. Consequently, the liver provides an ideal setting for the study of hypoxia-regulated genes and O₂-dependent zonation of hepatocyte and NPC functions. Unlike other organs, the liver's blood supply originates from two sources: the hepatic artery (25%) and the hepatic portal

vein (75%). As a result, the pO_2 of peri-portal blood is 60-65 mm Hg ($\sim 8\% O_2$), which is much lower than the systemic arterial pO_2 of ~ 100 mm Hg. Peri-portal hepatocyte functions include oxidative metabolism, gluconeogenesis, ureagenesis, and bile formation (125). In contrast, peri-venous blood has a pO_2 of 30-35 mm Hg ($\sim 4\% O_2$), and hepatocytes in this zone are more capable of glycolysis, liponeogenesis, and xenobiotic metabolism (125).

Clearly, the liver's functional zonation has been extensively mapped out. Surprisingly very few studies exist detailing the function and localization of the HIF pathway in liver. These published reports will be discussed in further detail in the context of Chapter 5.

1.3.1.2 Subcellular O_2 sinks in liver

To say that the liver is a highly metabolic organ is an understatement. It receives over 25% of the total resting cardiac output and it expends over 20% of the body's resting O_2 consumption (126). In hepatocytes, the chief sites of O_2 consumption are mitochondria, smooth ER, and peroxisomes (126). Although all three organelles can be considered subcellular O_2 sinks in the liver, only the mitochondrial respiratory chain is coupled to oxidative-phosphorylation and ATP synthesis.

Of particular interest to the liver's specialized function are peroxisomes. Unlike mitochondria, the peroxisomal respiratory chain is not coupled to ox-phos and energy production. Peroxisomes consume 10-30% of total cellular O_2 consumption in the liver, but the number of peroxisomes is 10-15 times less than that of mitochondria ($\sim 1\%$ of a hepatocyte's total cell volume) (126). Therefore, on a per unit basis, peroxisomes may consume a significant amount of O_2 as compared to mitochondria, especially in less-oxygenated peri-venous hepatocytes. The subcellular distribution of O_2 within and between the aforementioned organelles are illustrated in Figure 8, and these interactions will be discussed in more detail in later chapters.

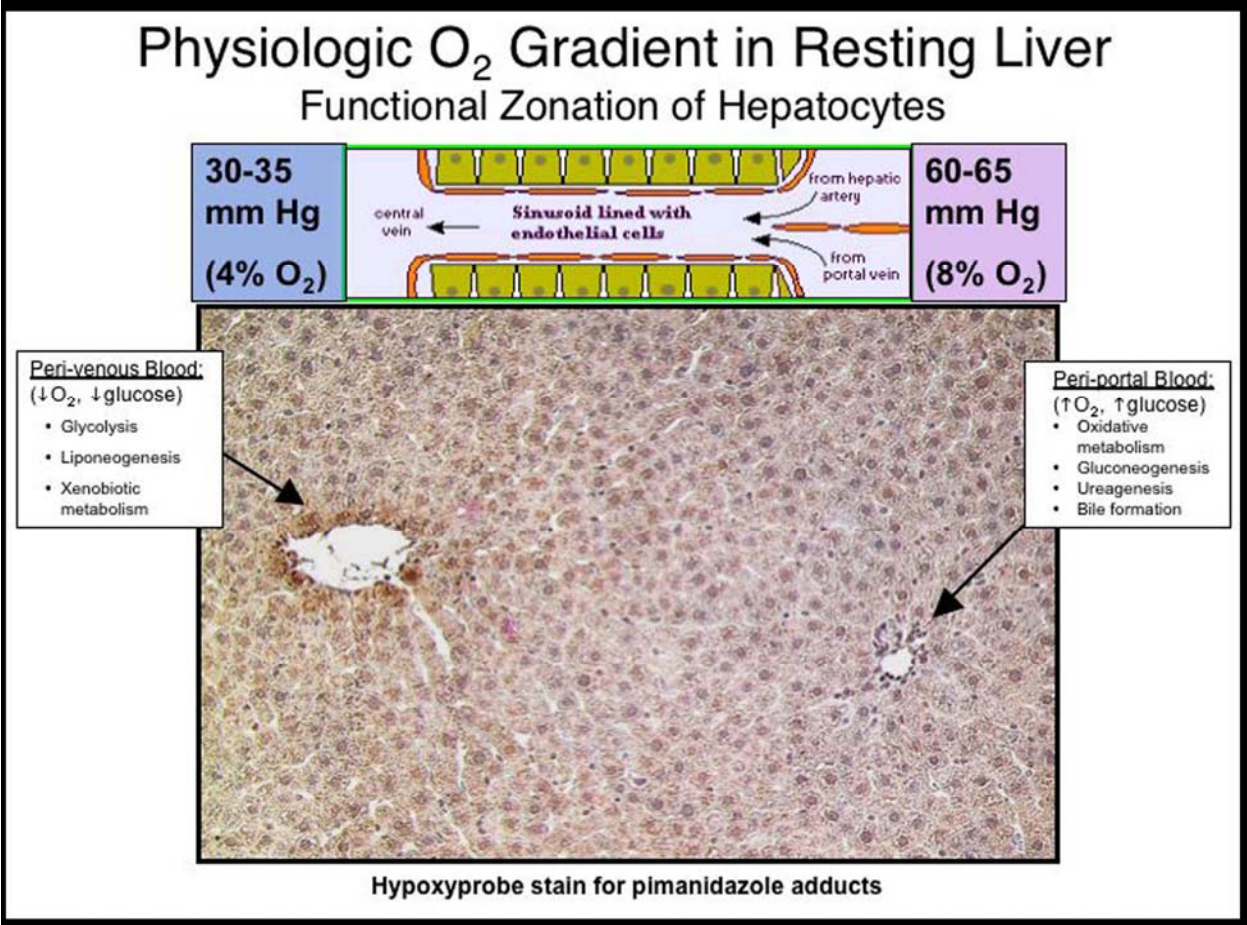


Figure 7: Physiologic O₂ gradient in the liver.
 Hypoxyprobe immunohistochemistry for pimanidazole adducts demonstrates the O₂ zonation in resting rat liver. As blood enters the sinusoid, it undergoes a ~50% drop in oxygenation from peri-portal to peri-venous hepatocytes. Hepatic gradients of O₂ and nutrients result in a functional zonation of hepatocytes.

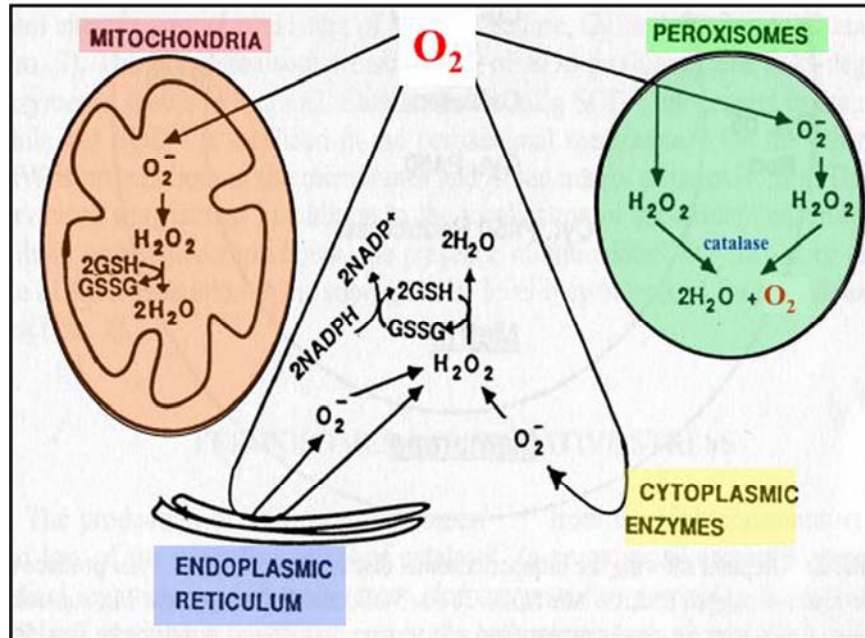


Figure 8: Subcellular O_2 sinks in the liver.

O_2 is consumed in various metabolic reactions in different cellular compartments. In the liver, mitochondria, smooth ER, and peroxisomes are the major sites. Unlike mitochondria, the peroxisomal respiratory chain is not coupled to ox-phos and energy production. Peroxisomes consume 10-30% of total cellular O_2 consumption in the liver, but the number of peroxisomes is 10-15 times less than that of mitochondria (~1% of a hepatocyte's total cell volume). Therefore, on a per unit basis, peroxisomes may consume a significant amount of O_2 as compared to mitochondria, especially in less-oxygenated peri-venous hepatocytes. Figure is based on (126).

2.0 RATIONALE AND HYPOTHESIS

2.1 HIF AND LIVER

Although the liver's unique oxygenation, functional zonation, and metabolic requirements have been extensively studied, little is known about what role the HIF pathway plays in this specialized microenvironment. If such a role does exist in the liver, it is unclear whether the HIF pathway is regulated in the same manner as in other organs. Moreover, very limited and often contradictory information exists regarding HIF activity in liver diseases and injury models (127-130). Understanding these mechanisms at the molecular level may help advance our knowledge of liver disease and treatment.

2.2 GENERAL HYPOTHESIS

Based on the liver's physiologic O₂ gradient, alterations in the zonal distribution and subcellular localization of members of the HIF pathway may provide a novel means of HIF regulation in hepatocytes.

2.3 SPECIFIC AIMS

2.3.1 Specific Aim 1

To investigate the hypoxia-dependent and –independent induction and transcriptional activation of HIF-1 α in primary rat hepatocyte cultures. This is addressed in Chapters 4 and 5.

2.3.2 Specific Aim 2

To investigate the subcellular localization of HIFs and HIF regulatory hydroxylases in rat liver and in primary rat hepatocyte cultures. This is addressed in Chapter 4.

2.3.3 Specific Aim 3

To determine the spatio-temporal expression and localization of HIF-1 α in regenerating rat liver. This is addressed in Chapter 5.

3.0 MATERIALS AND METHODS

3.1 ANTIBODIES AND REAGENTS

All chemicals were from Sigma (St. Louis, MO) and Fisher Scientific (Pittsburgh, PA), unless otherwise noted. Antibody sources and conditions are outlined in Table 4.

3.2 ANIMAL MODELS AND CELL CULTURE

3.2.1 Isolation and culture of primary rat hepatocytes

Animals were treated according to the guidelines of the Institutional Animal Care and Use Committee of the University of Pittsburgh. Rat hepatocytes were isolated from male Fisher 344 rats (Harlan, Indianapolis, IN) using a modified two-step collagenase perfusion (131, 132). Freshly isolated hepatocytes of >90% viability, as assessed by Trypan blue exclusion, were added to plating media (MEM containing 50 µg/mL bovine insulin and 0.1% gentamycin). Hepatocytes were plated on rat-tail collagen I-coated cultureware at a density of 3-4 x10⁶ cells/100-mm plastic dish or 1-2 x10⁵ cells/22-mm glass coverslip (BD Biocoat, Bedford, MA), incubated at 37°C (5% CO₂), and checked for adherence of monolayers after 2–4 hr. Once adhered, the media was changed to serum-free basal Hepatocyte Growth Media (HGM, without ITS, dexamethasone, or growth factors) (133). The next day, normoxic cells were cultured for 6

hr. at 37°C in a standard 5% CO₂ humidified incubator (Heraeus, Ashville, NC), while hypoxic cells were cultured for 6 hr. at 37°C in a 1% O₂ ProOxC system balanced with 5% CO₂/95% N₂ (Biospherix, Redfield, NY). This degree of hypoxia was chosen based on established protocols for HIF-induced transcription (134). Duplicate hypoxic cultures were also returned for reoxygenation overnight (18 hr.) in the normoxic incubator. Hypoxic culture was evaluated using Hypoxyprobe-1 Plus (Chemicon, Temecula, CA) detection of pimanidazole adducts (135). Cell survival was confirmed by both 3-(4,5-Dimethylthiazol-2-yl)-2,5-diphenyltetrazolium bromide (MTT) viability and lactate dehydrogenase (LDH) cytotoxicity assays (Biovision, Mountain View, CA) (136, 137). At the indicated time point, hepatocytes were harvested immediately on ice for protein or RNA, or fixed in 2% paraformaldehyde for imaging (described below).

3.2.2 Growth factor experiments

For investigation of hypoxia-independent induction of HIF-1 α by growth factors, primary rat hepatocytes were isolated and plated as described above. The next day, cells were cultured for 6-16 hr. in HGM supplemented with one of the growth factors listed in Table 3. Control culture medium consisted of HGM without added ITS, dexamethasone, or growth factors.

Table 3: Growth factor supplementation used in normoxic HIF-1 α induction experiments for primary rat hepatocytes.

The control medium was basal Hepatocyte Growth Medium (without Dex, ITS, HGF, or EGF). Hepatocytes were cultured for 6-16 hr. under these conditions. Growth factors were from R&D Systems (Minneapolis, MN).

Growth Factor or Supplement	Final Concentration
HGF	4 x 10 ⁻⁵ g/L
EGF	2 x 10 ⁻⁵ g/L
ITS	1 g/L
TGF α	2 x 10 ⁻⁵ g/L
TGF- β 1	5 x 10 ⁻⁶ g/L
AR	4 x 10 ⁻⁵ g/L
Dex	1 x 10 ⁻⁷ M
PGE2	1 x 10 ⁻⁵ M
CoCl ₂	5-10 x 10 ⁻⁵ M
DFO	5-10 x 10 ⁻⁵ M
DMSO	2% (v/v)

3.2.3 Hepatoma cell line culture, transplantation, and in vivo tumor formation

Previously frozen stocks of JM1 Fisher 344 rat hepatoma cells (138) were grown in T-75 flasks containing DMEM supplemented with 2 mM glucose, 2 mM L-glutamine, 10% fetal bovine serum, and 0.1% gentamycin. Once confluent, JM1 cells were trypsinized and washed in Hank's balanced salt solution (HBSS). Three million cells were transplanted into each liver of 8-10 wk old, 180-200g, male Fisher 344 rats via surgical injection with a 26-G needle into the superior mesenteric vein. Negative control rats were injected with cell-free HBSS. After 2 and 4 wk. of syngeneic engraftment, rats were injected i.p. with 100mg/kg dose of Hypoxyprobe (pimonidazole hydrochloride) hypoxia marker 1 hr. before sacrificing, then tumors were harvested, snap-frozen, and/or processed for histology. Formalin-fixed tissues were embedded in

paraffin blocks. A total of two series were performed, each consisting of three rats: control (vehicle alone), 2 wk. hepatoma, and 4 wk. hepatoma. The generation of JM1 liver tumors is chronicled in Figure 9.

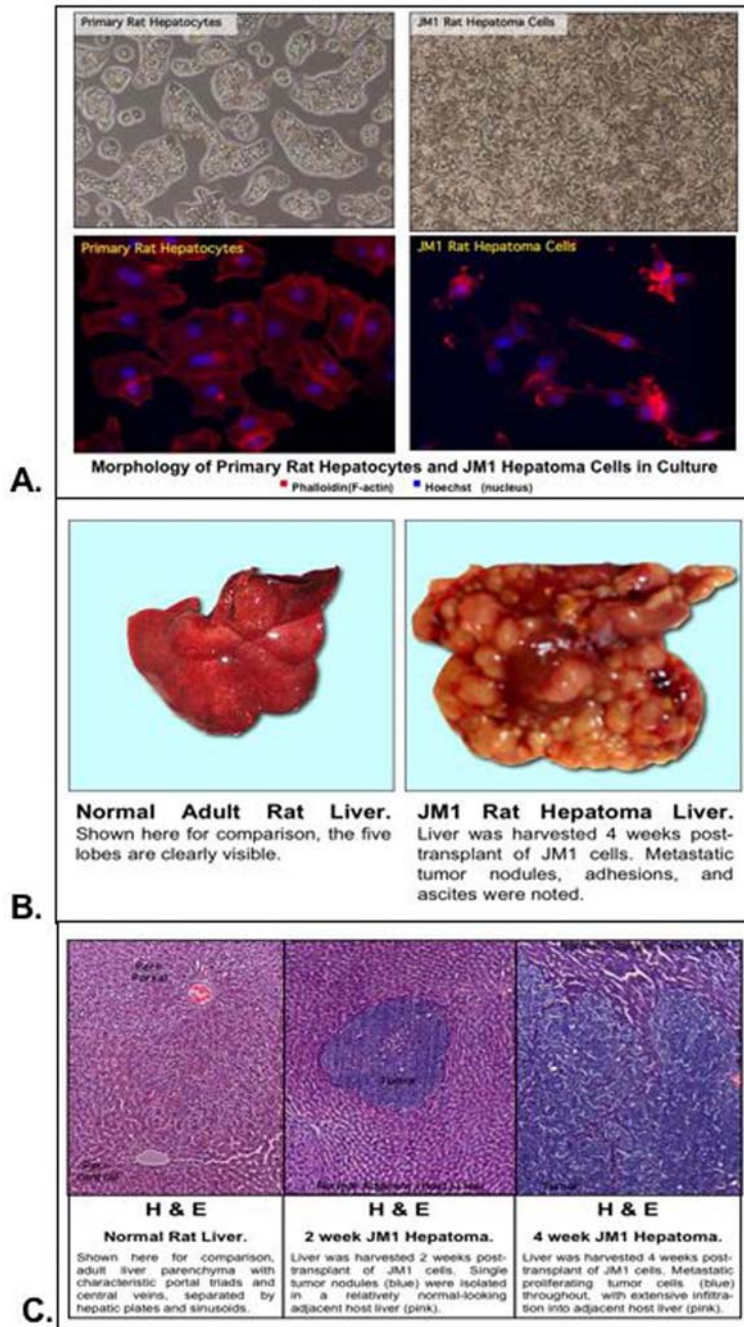


Figure 9: Generation of JM1 rat hepatomas.

A. Morphologic comparison of primary rat hepatocytes and the syngeneic JM1 rat hepatoma cell line. B. Gross morphology normal rat liver compared to 4 wk. JM1 hepatomas. Normal adjacent host liver is compressed between multiple tumor nodules. C. Hematoxylin and eosin (H & E) stain shows JM1 tumor progression over time.

3.2.4 70% Partial hepatectomy (PHx) model

Animals were treated according to the guidelines of the Institutional Animal Care and Use Committee of the University of Pittsburgh. Male Fisher 344 rats (10-12 wk old, 180-200 g) were anesthetized with isoflurane inhalant and 70% PHx (Figure 10) was performed as described by Higgins and Anderson (139). For sham operations, only the xyphoid process was removed. A total of four PHx series were performed, using the following time-points of regeneration after 70% PHx: 0, 1, 3, 6, and 12 hr.; 1, 2, 3, 4, 5, 6, and 7 days.

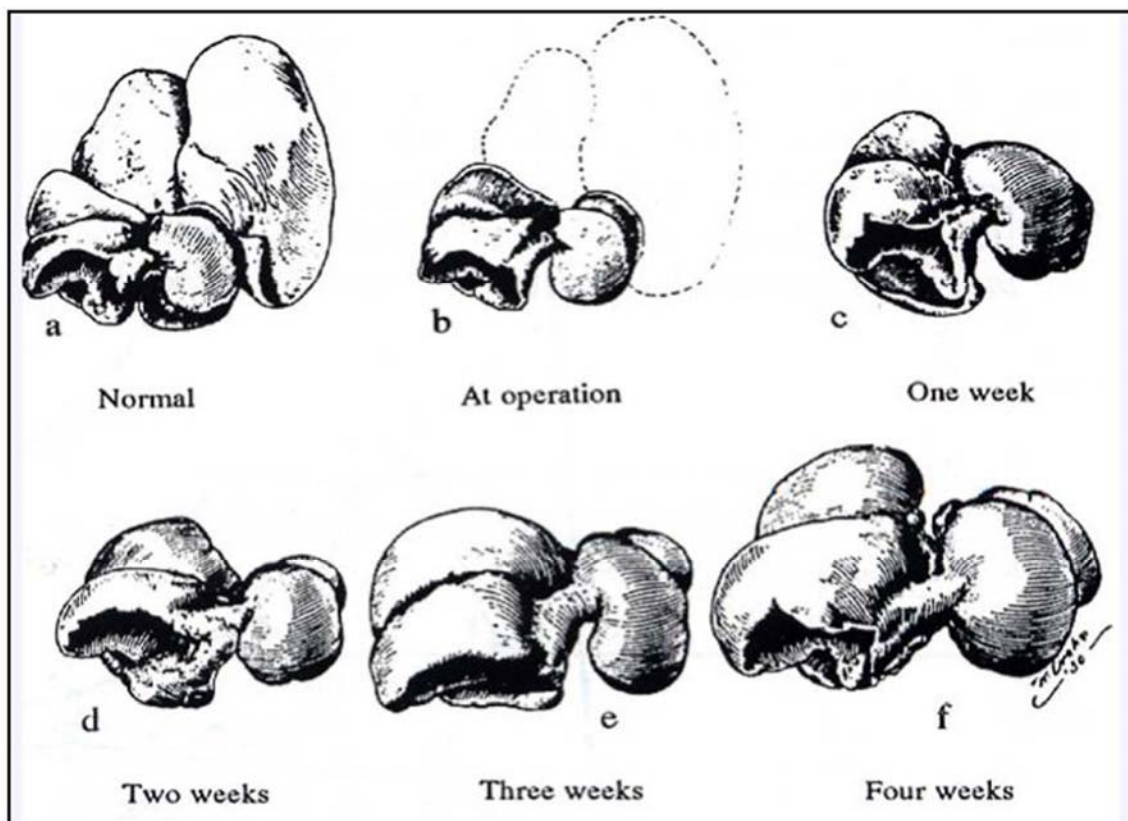


Figure 10: Rat liver regeneration following 70% partial hepatectomy (PHx). Liver of a normal rat at operation (the excised lobes are outlined) and at 1 to 4 wk. after PHx. The liver mass is restored by compensatory hyperplasia of the remnant lobes. Figure from (139).

Table 4: Antibodies and conditions used in this study.

Epitope	Primary Antibody Dilution (Source)	Fluorescence Secondary Antibody Dilution (Source)	Gold-Conjugated	HRP Conjugated	Biotinylated
			Secondary Antibody for Immunoelectron Microscopy Dilution (Source)	Secondary Antibody for Western Blotting Dilution (Source)	Secondary Antibody for Immunohistochemistry Dilution (Source)
HIF-1α	1:500 WB NB100-105 1:1000 IHC NB100-131 1:100 IF NB100-123 All Ms mAb (NO)	Gt anti-Ms Cy3 1:1000 (JA)	N/A	Dky anti-Ms IgG 1:75,000 (JA)	Anti-Ms ImmPRESS reagent (VE)
HIF-2α	NB100-132 Ms mAb 1:100 IF	Gt anti-Ms Cy3 1:1000 (JA)	N/A	N/A	N/A
HIF-3α	601-401-435 Rbt pAb 1:100 IF (RO)	Gt anti-Rbt IgG Alexa 488 1:500 (MO)	N/A	N/A	N/A
HIF-1β	NB100-110 Rbt pAb 1:100 IF (NO)	Gt anti-Rbt IgG Alexa 488 1:500 (MO)	N/A	N/A	N/A
PHD1	NB100-310 Rbt pAb 1:1000 WB, IHC 1:100 IF 1:50 TEM (NO)	Gt anti-Rbt IgG Alexa 488 1:500 (MO)	Gt anti-Rbt IgG 10-nm gold 1:25 (AM)	Dky anti-Rbt IgG 1:75,000 (JA)	Gt anti-Rbt IgG 1:500 (CH)
PHD2	NB100-138 Rbt pAb 1:1000 WB, IHC 1:200 IF 1:50 TEM (NO)				
PHD3	NB100-139 Rbt pAb 1:1000 WB, IHC 1:100 IF 1:50 TEM (NO)				
PHD4	NB100-295 Rbt pAb 1:100 WB, IF 1:1000 IHC 1:50 TEM (NO)				
FIH-1	NB100-428 Rbt pAb 1:100 WB 1:1000 IHC 1:200 IF 1:50 TEM (NO)				

Table 4: Antibodies and conditions used in this study: Continued

Epitope	Primary Antibody Dilution (Source)	Fluorescence Secondary Antibody Dilution (Source)	Gold-Conjugated Secondary Antibody for Immunoelectron Microscopy Dilution (Source)	HRP Conjugated Secondary Antibody for Western Blotting Dilution (Source)	Biotinylated Secondary Antibody for Immunohistochemistry Dilution (Source)
VHL	SC1535-R20 Gt pAb 1:100 IF	Dky anti-Gt IgG Alexa 488 1:500 (MO)	N/A	N/A	N/A
Catalase (peroxisomes)	Ms mAb 1:50 TEM (SI)	N/A	Gt anti-Ms 5-nm gold 1:25 (AM)	N/A	N/A
	W90080C Shp pAb 1:1000 WB 1:200 IF (BI)	Dky anti-Shp IgG Cy3 1:200 (JA)	N/A	Dky anti-Shp IgG 1:20,000 (JA)	N/A
PMP70 (peroxisomes)	ALX210205C100 Rbt pAb 1:500 WB (AL)	N/A	N/A	Dky anti-Rbt IgG 1:75,000 (JA)	N/A
Pan-Actin (loading control)	MAB1501 Ms mAb 1:2000 WB (CH)	N/A	N/A	Dky anti-Ms IgG 1:75,000 (JA)	N/A

Methods Abbreviations: Dky = donkey, Gt = goat, IF = immunofluorescence, IHC = immunohistochemistry, mAb = monoclonal antibody, Ms = mouse, pAb = polyclonal antibody, Rbt = rabbit, Shp = sheep, TEM = immuno-transmission electron microscopy, WB = Western blotting.

Company Abbreviations (in parentheses): AL = Alexis Corp., San Diego, CA; AM = Amersham, Uppsala, Sweden; BI = Biodesign International, Saco, ME; CH = Chemicon, Temecula, CA; NO = Novus Biologicals, Littleton, CO.; JA = Jackson ImmunoResearch Labs, West Grove, PA; MO = Molecular Probes, Eugene, OR; RO = Rockland Immunochemicals, Gilbertsville, PA; VE = Vector Laboratories, Burlingame, CA; SA = Santa Cruz Biotechnologies, Santa Cruz, CA; SI = Sigma, St. Louis, MO.

3.3 HISTOLOGIC METHODS

3.3.1 Immunohistochemistry

Serial sections of formalin-fixed or zinc-fixed liver tissue were cut at 5- μ m thickness onto Superfrost Plus glass slides (Fisher Scientific, Pittsburgh, PA) and heat-fixed 1 hr. at 65°C. With the exception of Hypoxyprobe, HIF-1 α , and HIF-2 α , all immunohistochemistry was performed using the Vectastain Elite ABC kit according to manufacturer's protocol (Vector Laboratories, Burlingame, CA). Briefly, after deparaffinization and rehydration of sections, endogenous peroxidase activity was quenched 20 min. in methanol containing 3% H₂O₂, and 10 min. of antigen retrieval was performed in boiling 10 mM citrate buffer (pH 6.0) with slow cooling. Sections were blocked 30 min. at room temperature (RT) with Blueblock (Thermo Electron, Pittsburgh, PA), then incubated with primary antibodies overnight at 4°C. Primary-deleted negative controls for background were treated with the antibody diluent alone. After incubation for 30 min. at RT with affinity-purified biotinylated secondary antibodies, sections were treated with ABC reagent followed by DAB chromagen (Vector). All sections were counterstained in hematoxylin, dehydrated, and coverslipped with Cytoseal (Richard-Allan Scientific, Kalamazoo, MI).

3.3.2 HypoxyprobeTM immunohistochemistry

Hypoxia-dependent activation of nitroheterocyclic drugs such as pimonidazole by cellular nitroreductases leads to the formation of intracellular adducts between the drugs and cellular macromolecules (140). Because this covalent binding is maximal in the absence of oxygen, detection of bound adducts by monoclonal antibodies provides an assay for estimating the degree of cellular hypoxia within tissues or cells (140). Hypoxyprobe staining for pimonidazole adducts

was performed according to manufacturer's protocol (Chemicon). Sections were deparaffinized, rehydrated, quenched, and subjected to antigen retrieval as described above. After a TBST wash, sections were blocked 30 min. at RT with 1% BSA in TBST, then incubated 30 min. at RT with 1:50 Hypoxyprobe-1 Mab1 FITC-conjugated mouse monoclonal IgG1 primary antibody. Primary-deleted negative controls for background were treated with the antibody diluent (1% BSA in TBST) alone. Sections were washed twice in TBST, then incubated 30 min. at RT with 1:50 mouse anti-FITC HRP-conjugated secondary antibody. After two TBST washes, DAB chromagen was applied for 10 min. at RT. The brown color reaction was stopped by a brief ddH₂O wash, then sections were counterstained in Harris' hematoxylin, blued in TBST, dehydrated, cleared, and coverslipped with Cytoseal.

3.3.3 HIF-1 α and HIF-2 α immunohistochemistry

Mouse ImmPRESS reagent kit was used according to manufacturer's protocol (Vector). Sections were deparaffinized, rehydrated, quenched, and subjected to antigen retrieval as described above. After a PBS wash, sections were blocked 30 min at RT with 2.5% normal horse serum, then incubated 1 hr at RT with 1:1000 mouse monoclonal anti-HIF-1 α or anti-HIF-2 α primary antibodies. Primary-deleted negative controls for background were treated with the antibody diluent (1% BSA in PBS) alone. Sections were washed twice in PBS, then incubated 30 min at RT with pre-diluted ImmPRESS anti-mouse IgG HRP-conjugated secondary antibody. After two PBS washes, DAB chromagen was applied for 10 min at RT. The brown color reaction was stopped by a brief ddH₂O wash, then sections were counterstained in Harris' hematoxylin, blued in PBS, dehydrated, cleared, and coverslipped with Cytoseal.

3.4 HIGH RESOLUTION IMAGING

3.4.1 Scanning laser confocal immunofluorescence microscopy

Primary rat hepatocytes cultured on coverslips were placed on ice and rapidly washed in cold PBS containing 1:200 dilution of protease and phosphatase inhibitor cocktails (Sigma), then fixed in 2% paraformaldehyde in PBS for 15 min, and processed as described (141). Briefly, cells were rinsed 3 times in PBS, rinsed 3 times in PBS with BSA and glycine (PBG), permeabilized with 0.1% Triton X-100 in PBG for 20 min, and then blocked in 2% BSA in PBG for 30 min at RT. Primary antibodies in PBG were added to cells for 1 hr at RT. Samples were washed 5 times in PBG, and then secondary antibodies in PBG were added for 1 hr at RT. Samples were washed 3 times in PBG, 3 times in PBS, counterstained with Hoechst dye, and then coverslipped using Gelvatol. Primary-deleted negative controls for background were treated with the antibody diluent alone. HIF-1 α and HIF-2 α immunofluorescence staining was performed using a modification of the method recommended by the manufacturer (Novus Biologicals, Littleton, CO). Briefly, cells were permeabilized and blocked overnight at 4°C with 2% BSA/0.1% Triton-X 100 in PBS. Subsequent labeling was performed in 0.5% BSA in PBS. All fluorescence labeling was imaged on a Fluoview 1000 confocal scanning microscope (Olympus, Melville, NY). Imaging conditions were maintained at identical settings within each antibody labeling experiment.

3.4.2 Immuno-transmission electron microscopy (Immuno-TEM)

Rat livers were perfused-fixed and cultured primary rat hepatocytes were fixed in 2% paraformaldehyde in PBS (1 hr. for cells, overnight for tissues), processed, and analyzed as described (141). Sections were observed on a JEM 1210 electron microscope (JEOL, Peabody, MA).

3.5 ANALYSIS OF CELLULAR PROTEINS

3.5.1 Preparation of nuclear extracts

For HIF Western analysis, nuclear proteins from both snap-frozen rat liver tissue and primary hepatocytes cultured on 5 x 100-mm collagen-coated plates were extracted as described by Runge *et al.*; however, no milk was included in the hypotonic buffer (142).

3.5.2 Preparation of membrane-enriched fractions

Hepatocytes cultured on 5 x 100-mm plates were washed and scraped into 10 mL of ice-cold isotonic isolation buffer [0.1 mM EDTA, 250 mM sucrose, 4% PEG-6000, 5 μ M MES (pH 7.4), plus fresh 1:100 protease/phosphatase inhibitor cocktails (Sigma)], resuspended in 2 mL of isolation buffer, and lysed by nitrogen cavitation (Parr Bomb, 600 psi/15 min.) on ice (141). The resulting cell lysate (CL) was centrifugated for 10 min. at 10,000xg to separate a nuclear fraction (NF, pellet) and a cytosolic/membrane fraction (CMF, supernatant). Following ultracentrifugation (10 min. at 100,000xg, Beckman Airfuge, A-100 rotor) of the CMF, intact peroxisomes were obtained in the organelle-enriched membrane fraction (MF, heavy pellet) and cytoplasmic proteins remained in the cytosolic fraction (CF, final supernatant). The MF was solubilized in 1% SDS. All fractions were stored at -80°C until use. Isolation of intact peroxisomes in the MF was confirmed via Western blotting for PMP70, a peroxisomal membrane protein. A schematic of the isolation can be seen in Figure 11.

3.5.3 Western blotting

Protein concentrations were determined by BCA assay (Pierce, Rockford, IL), then 20-50 μ g of protein were heated to 65°C in 2x Laemmli buffer, slowly cooled, and separated on 10% or 12% SDS-PAGE gels (143). After electrotransfer onto Immobilon PVDF membranes (Millipore, Bedford, MA), protein bands were reversibly stained with Ponceau S to confirm complete

transfer. Membranes were blocked 1 hr. in tris-buffered saline with Tween-20 (TBST) containing 5% non-fat dry milk (NFDM), then incubated overnight at 4°C with primary antibodies diluted in 1% or 5% NFDM/TBST. Membranes were washed and incubated 1.5 hr. at RT with HRP-conjugated secondary antibodies diluted in 1% NFDM/TBST. After several TBST washes, membranes were incubated with Supersignal West Pico enhanced chemiluminescence (ECL) and exposed to CL-Xposure film (Pierce, Rockford, IL). For Western blots designed for maximum sensitivity, three mouse anti-HIF-1 α monoclonal antibodies (NB100-131, NB100-123, NB100-105; Novus) were combined and used at 1:500 on Western blots containing 50-100 μ g of nuclear extracts.

3.5.4 Enzyme-linked immunosorbent assay (ELISA) for HIF-1 α DNA-binding activity

To ensure that the samples' salt and detergent concentrations were compatible with this ELISA-based transcription factor assay, nuclear extracts were prepared using buffers accompanying the kit, and the Trans-AM ELISA for HIF-1 α DNA-binding was used according to manufacturer's protocol (Active Motif, Carlsbad, CA) (144).

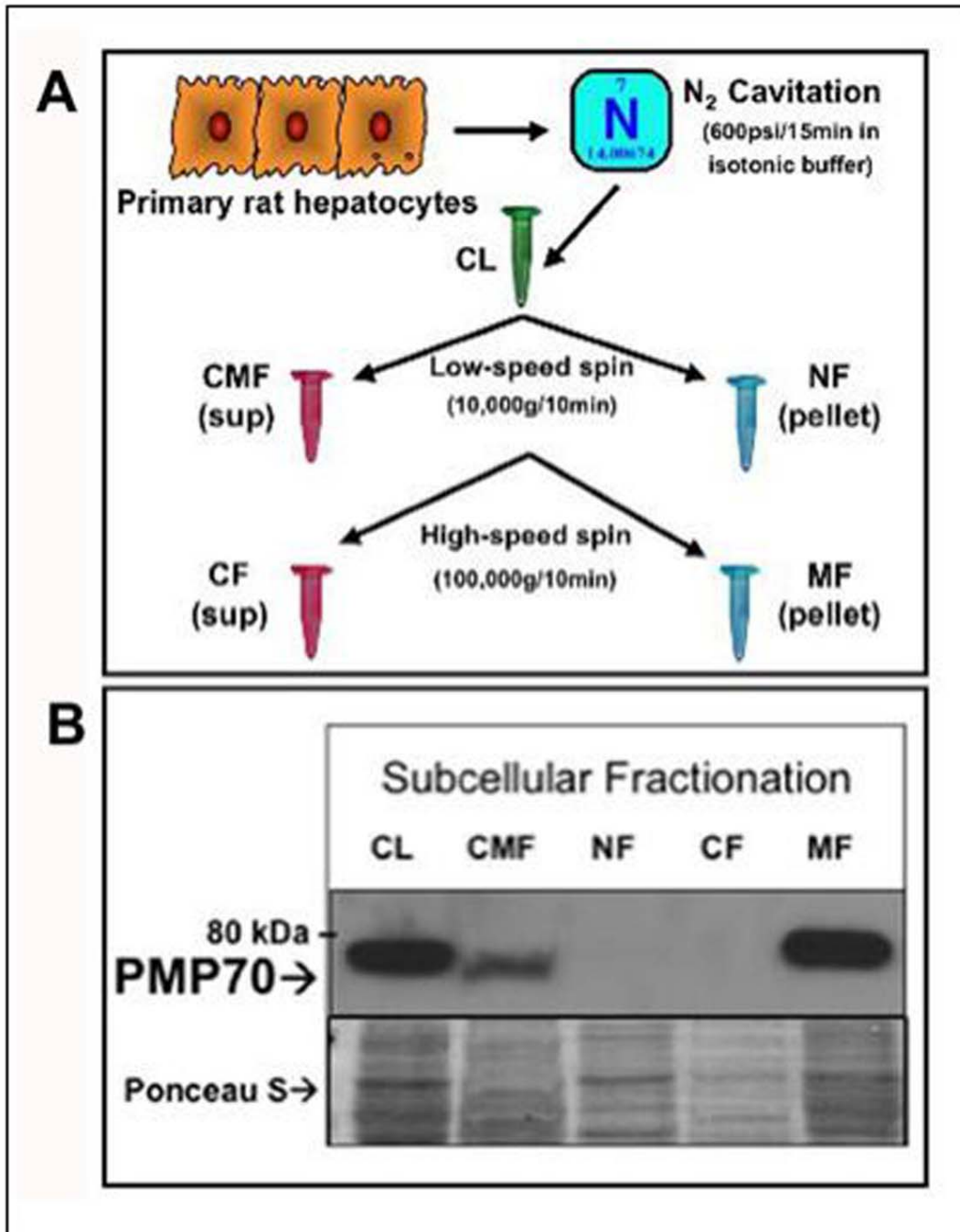


Figure 11: Schematic of subcellular fractionation protocol.

A. Subcellular fractionation of primary rat hepatocytes in an isotonic buffer [0.1 mM EDTA, 250 mM sucrose, 4% PEG-6000, 5 μ M MES (pH 7.4), plus fresh protease/phosphatase inhibitor cocktails (Sigma)] was used to obtain intact peroxisomes in the membrane-enriched fraction (MF). B. PMP-70 western blot confirms isolation of intact peroxisomes in MF.

3.6 ANALYSIS OF RNA

3.6.1 Isolation of RNA

Cells were lysed in RNazol B (Iso-Tex, Friendswood, TX) and total RNA was purified using the RNeasy kit with DNase treatment (QIAGEN, Valencia, CA).

3.6.2 Reverse-transcription polymerase chain reaction

Total RNA (500 ng) was reverse-transcribed and the resulting cDNA template was amplified with hot-start PCR using Jumpstart ReadyMix Taq polymerase according to manufacturer's recommendations (Sigma, St. Louis, MO). Primer pairs are outlined in Table 5. PCR products were visualized on 1.2% agarose-TBE gels, stained with ethidium bromide, and imaged with AlphaImager software (Alpha Innotech, San Leandro, CA).

3.6.3 Affymetrix gene array analysis

At the indicated time-points, primary rat hepatocytes cultured in triplicate 10-cm plates were pooled, lysed in Trizol (Invitrogen, Carlsbad, CA) and processed as described (145) for gene expression analysis using rat U34A arrays (Affymetrix, Santa Clara, CA), in collaboration with Dr. Jianhua Luo (University of Pittsburgh, Microarray Center). Data analysis was performed using a fully-functional demo version of GeneSifter software (downloadable at <http://www.genesifter.net/web/trial.html>; VizX Labs, Seattle, WA).

Table 5: RT-PCR primer pairs used in this study.

Gene Target	Accession Number (all are rat)	Forward Primer (FP) Reverse Primer (RP)	Size (bp)
HIF-1α	AF057308	5'-TGCTTGGTGCTGATTTGTGA-3' 5'-GGTCAGATGATCAGAGTCCA-3'	209
HIF-2α	RNO277828	5'-TGACTTCACTCATCCTTGCGACCA-3' 5'-ATTCATAGGCAGAGCGGCCAAGTA-3'	443
HIF-3α	RNO277827	5'-AAGAAGGGTATCCCAGGCAACAGT-3' 5'-TGTACGGAGCCAACATCTCCAAGT-3'	361
HIF-1β	U61184	5'-TGCACCAACACCAACGTGAAGAAC-3' 5'-TGGTTGTGCTGATGTTGGCTGAAC-3'	915
PHD1	NM_001004083	5'-AGCAACAGCACTACCCATAGCAGT-3' 5'-TGTGACACGGGTAATTGAACACCT-3'	755
PHD2	NM_178344	5'-AAGATCACCTGGATCGAGGGCAA-3' 5'-TCGCTCGTCTGCATCGAAATACCA-3'	426
PHD3	NM_019371	5'-AGAGGCACCCTTGAAACCCTAACA-3' 5'-TTGCTTGAAAGTCTGCATGGCTG-3'	897
FIH-1	XM_219961	5'-TGCAGCAAACACTCAATGACACCG-3' 5'-TCAAGAGGCAAGGGTGAGAAACCT-3'	821
VEGF-A all isoforms	NM_031836	5'-CTCACCAAAGCCAGCACATA-3' 5'-AAATGCTTTCTCCGCTCTGA-3'	160
PAI-1	NM_012620	5'-GACAATGGAAGAGCAACATG-3' 5'-ACCTCGATCTTGACCTTTTG-3'	205
ADM	NM_012715	5'-GGCAGCATTGAACAGTCG-3' 5'-AAGGCAGTGGCTCAGACC-3'	223
GAPDH	NM_017008	5'-CTCACTGGCATGGCCTTCCG-3' 5'-ACCACCCTGTTGCTGTAGCC-3'	200
β-actin	BC063166	5'-GAGCTATGAGCTGCCTGACG-3' 5'-AGCACTTGCGGTCCACGATG-3'	361

4.0 PEROXISOMAL LOCALIZATION OF HYPOXIA-INDUCIBLE FACTORS AND HIF REGULATORY HYDROXYLASES IN PRIMARY RAT HEPATOCYTES EXPOSED TO HYPOXIA-REOXYGENATION

Zahida Khan,^{1,3,4} Donna B. Stolz Ph.D.,^{2,3} and George K. Michalopoulos M.D., Ph.D.^{1,3}

Cellular and Molecular Pathology,¹ Cell Biology and Physiology,² McGowan Institute of Regenerative Medicine,³ and Medical Scientist Training Program,⁴ University of Pittsburgh School of Medicine, Pittsburgh, PA 15261 USA

(submitted in April 2006 to *Am. J. Pathol.*)

4.1 INTRODUCTION

Oxygen homeostasis relies on highly conserved mechanisms required for the survival of nearly all organisms. In most settings, O₂ delivery and consumption increase with metabolic demand; however, extreme shifts in tissue oxygenation can be detrimental. Mammalian cells employ an O₂-responsive pathway to sense and to adapt to fluctuations in their microenvironment. This ubiquitous system involves hypoxia-inducible factors (HIFs), transcription factors that upregulate the expression of hypoxia-responsive genes. HIFs are members of the basic helix-loop-helix Per-ARNT-Sim (bHLH-PAS) family of transcription factors, which includes three HIF- α subunits (HIF-1 α , HIF-2 α /EPAS1, HIF-3 α /IPAS) and three HIF- β subunits (HIF-1 β /ARNT1, HIF-2 β /ARNT2, and HIF-3 β /ARNT3). HIF- α subunits dimerize exclusively with HIF- β subunits. In contrast, HIF- β subunits can also dimerize with aryl hydrocarbon receptors (AHRs), providing cross-talk with xenobiotic metabolism (18).

HIF-1 α was first identified by Wang and Semenza (9), and it serves as the prototype for studying cellular mechanisms of O₂-sensing. Under normoxic conditions, cytosolic HIF-1 α proteins are constitutively expressed but rapidly degraded due to post-translational hydroxylations. HIF-1 α consists of both an asparagine-containing transactivation (CTAD) domain (26) and a proline-rich oxygen dependent degradation domain (ODDD) (35), both of which are essential for HIF function. These domains are enzymatically modified by recently identified non-heme HIF asparaginyl and prolyl hydroxylases, members of a dioxygenase superfamily whose activity requires 2-oxoglutarate (2-OG), Fe(II), ascorbate, and most importantly molecular O₂. When O₂ is abundant, hydroxylation of key prolines in the ODDD by HIF prolyl 4-hydroxylases (PHDs)* allow the von Hippel-Lindau tumor suppressor protein (pVHL) to tag HIF-1 α for polyubiquitination and subsequent proteasomal degradation (36, 46). This continuous turnover results in the very short half-life of HIF-1 α in normoxic conditions (11). Furthermore, normoxia curtails HIF-1 α transcriptional activity via the asparaginyl hydroxylase, factor-inhibiting HIF-1 (FIH-1), which acts on an asparagine residue in the CTAD (31), providing yet another brake in the system.

Due to their requirement for molecular O₂, the HIF hydroxylases can be considered principal O₂ sensors within the cell, preventing aberrant HIF-dependent transcription in the presence of O₂. Accordingly, when cells undergo hypoxic stress, the hydroxylation and degradation of HIF-1 α is inhibited (48, 49). As a result, HIF-1 α stabilizes, accumulates in the cytoplasm, and translocates to the nucleus, where it forms a heterodimer with its constitutively expressed nuclear binding partner, HIF-1 β (50). Following transactivation (29, 51), HIF-1 heterodimer binds to hypoxia-response elements (HREs), consensus sequences in the promoter or enhancer regions of target genes (6). To date, over seventy HIF-induced genes have been identified, encoding such adaptive proteins as EPO, VEGF-A, iNOS, PAI-1, c-MET, IGFBP-1, and all glycolytic enzymes [reviewed in (113, 114)].

*The HIF prolyl 4-hydroxylases were termed PHDs, EGLNs, or HPHs by various groups. In this paper we refer to the PHD nomenclature. PHD1/PHD2/ PHD3 are equivalent to HPH3/HPH2/HPH1 or EGLN2/EGLN1/EGLN3, respectively.

Due to its physiologic O₂ gradient, the liver is a unique organ where maintenance of O₂ homeostasis is critical for its specialized function. Despite much of the pioneering work on HIF originating in hepatoma cell lines (6), little is known about its regulation in the liver itself. Unlike other organs, liver receives most of its blood supply from the portal vein, which carries venous blood with lower O₂ tension. This gradient can further be disrupted by chronic liver disease or acute insults such as ischemia-reperfusion injury. O₂ zonation is therefore an additional consideration when studying the HIF pathway in liver, and perivenous mRNA expression of all three HIF- α subunits has been described (146). Although PHD1-3 are highly expressed in mouse liver (93), the significance of HIF hydroxylases in hepatic physiology and pathology is largely unexplored. To better understand how the *endogenous* HIF pathway is affected by hypoxia/reoxygenation, we investigated the subcellular distribution of HIFs and their regulatory hydroxylases in primary rat hepatocytes. We show that in hepatocytes, HIF-1 α targets to the peroxisome rather than the nucleus, where it co-localizes with VHL and the HIF hydroxylases. Peroxisomal sequestration may provide an additional point of regulation for HIF signaling in the liver.

4.2 RESULTS

4.2.1 Establishment of hypoxic cultures of primary rat hepatocytes

To investigate the effects of hypoxia-reoxygenation on endogenous HIF proteins in hepatocytes, we first characterized our *in vitro* culture system. We isolated and plated primary rat hepatocytes, allowing them to adhere and equilibrate overnight (18 hr.). The following day, we cultured them under conditions of 6 hr. normoxia (control), 6 hr. hypoxia (1% O₂), or 6 hr. hypoxia followed by overnight reoxygenation. To confirm initially that our hepatocytes were indeed hypoxic, we utilized the hypoxia marker pimanidazole (Figure 12A), a nitroheterocyclic drug whose hypoxia-dependent activation by cellular nitroreductases leads to the formation of covalent intracellular adducts between cellular macromolecules and the drug itself (135). As seen in Figure 12A and subsequent images, staining of nuclei (Hoechst) and F-actin (phalloidin) confirms that the cells

were viable. We also routinely assessed hepatocyte viability and found that hypoxic cultures had ~73.7% viability (MTT assay) and ~20.6% cytotoxicity (LDH assay) compared to normoxic controls (Figure 12B). Analysis of gene expression by RT-PCR next confirmed the hypoxic induction of HIF target genes *PAI-1*, *adrenomedullin*, and *VEGF-A*, but not *GAPDH* (Figure 12C).

4.2.2 Hypoxia does not induce nuclear localization of HIF-1 α in primary rat hepatocytes

After our assessment of hypoxic culture conditions, we next sought to investigate the expression of endogenous HIFs in primary rat hepatocytes, beginning with HIF-1 α . Interestingly, although we observed expression of *HIF-1 α* via RT-PCR (Figure 13A), we were unable to detect by either imaging or Western blotting a nuclear induction of HIF-1 α protein in hypoxic primary rat hepatocytes. We repeated our experiments using parallel cultures of primary rat hepatocytes and JM1 cells, a syngeneic rat hepatoma cell line derived from Fisher 344 rat

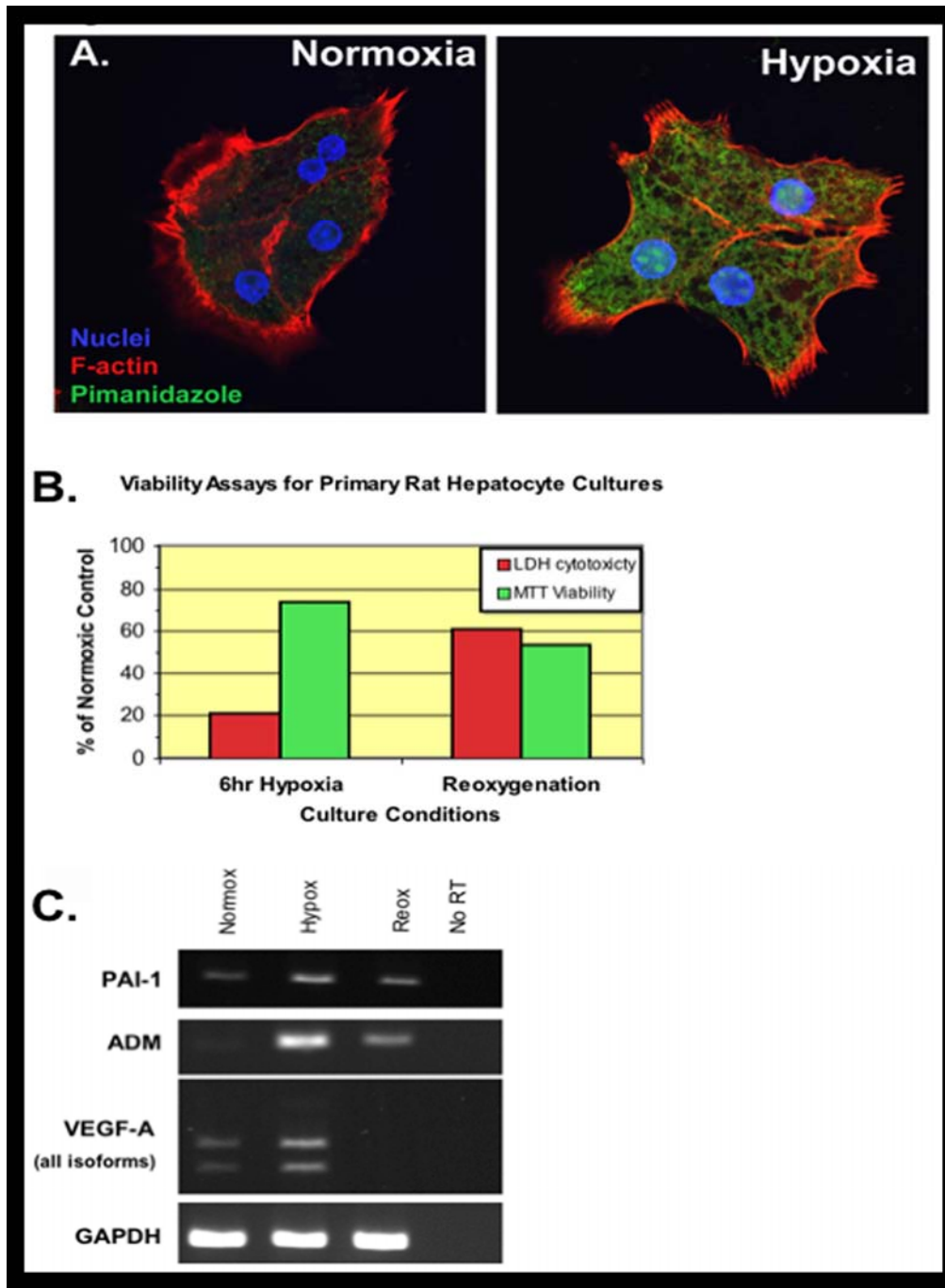


Figure 12: Establishment of hypoxic cultures.

Primary rat hepatocytes were cultured for 6 hr. in normoxic (control) or hypoxic (1% O₂) incubators. Parallel hypoxic cultures were returned to the normoxic incubator for overnight reoxygenation. A. Confocal immunofluorescence of pimanidazole adducts (green) in hepatocytes after 6 hr. of hypoxia confirms hypoxic incubation. B. Representative data from MTT and LDH viability assessments are shown as % of normoxic control. C. RT-PCR demonstrates upregulation of known HIF target genes, *PAI-1*, *adrenomedullin*, and *VEGF-A*, indicating hepatocytes are responding to hypoxia.

hepatocytes (138). Even when analyzed using identical experimental conditions, we could only detect nuclear HIF-1 α in the JM1 cells and not the hepatocytes. As seen in Figure 13B-C, the absence of nuclear HIF-1 α in hepatocytes can be observed in both confocal immunofluorescence and maximum sensitivity Western blots. An ELISA-based DNA-binding assay confirmed this lack of HIF-1 α responsiveness in hepatocytes (Figure 13D). Furthermore, when JM1 cells were re-introduced into normal Fisher 344 rat livers, the resulting tumors contained numerous hypoxic regions (Figure 14A-C). The tumor cells highly expressed nuclear HIF-1 α in these regions; however, the normal adjacent compressed liver contained only cytoplasmic HIF-1 α staining (Figure 14D-E), indicating that such an excessive and chronic hypoxic insult to the liver was inadequate to induce nuclear HIF-1 α in hepatocytes. Taken together, the results in Figures 12, Figure 13 and Figure 14 provide evidence that although hepatocytes do respond to hypoxia, the contribution of HIF-1 α to this adaptation may be minor or transient at best.

4.2.3 HIF-1 α localizes to peroxisomes in primary rat hepatocytes

As shown in Figure 13C, although HIF-1 α does not translocate to the hepatocyte nucleus in hypoxia, there appears to be an increase HIF-1 α in the cytoplasm. Given our unexpected findings, we decided to further dissect the punctate cytoplasmic labeling we observed for HIF-1 α in hypoxic hepatocytes. Confocal immunofluorescence (Figure 15A) revealed that endogenous HIF-1 α (green) co-localized (yellow) with the peroxisomal membrane protein PMP70 (red) in hepatocytes subjected to reoxygenation following hypoxia. Since HIF-1 α was recently shown to play the least active role in primary rat hepatocytes co-transfected with HIF- α expression vectors and IGFBP-1 reporter gene constructs (147), we next decided to compare the distribution

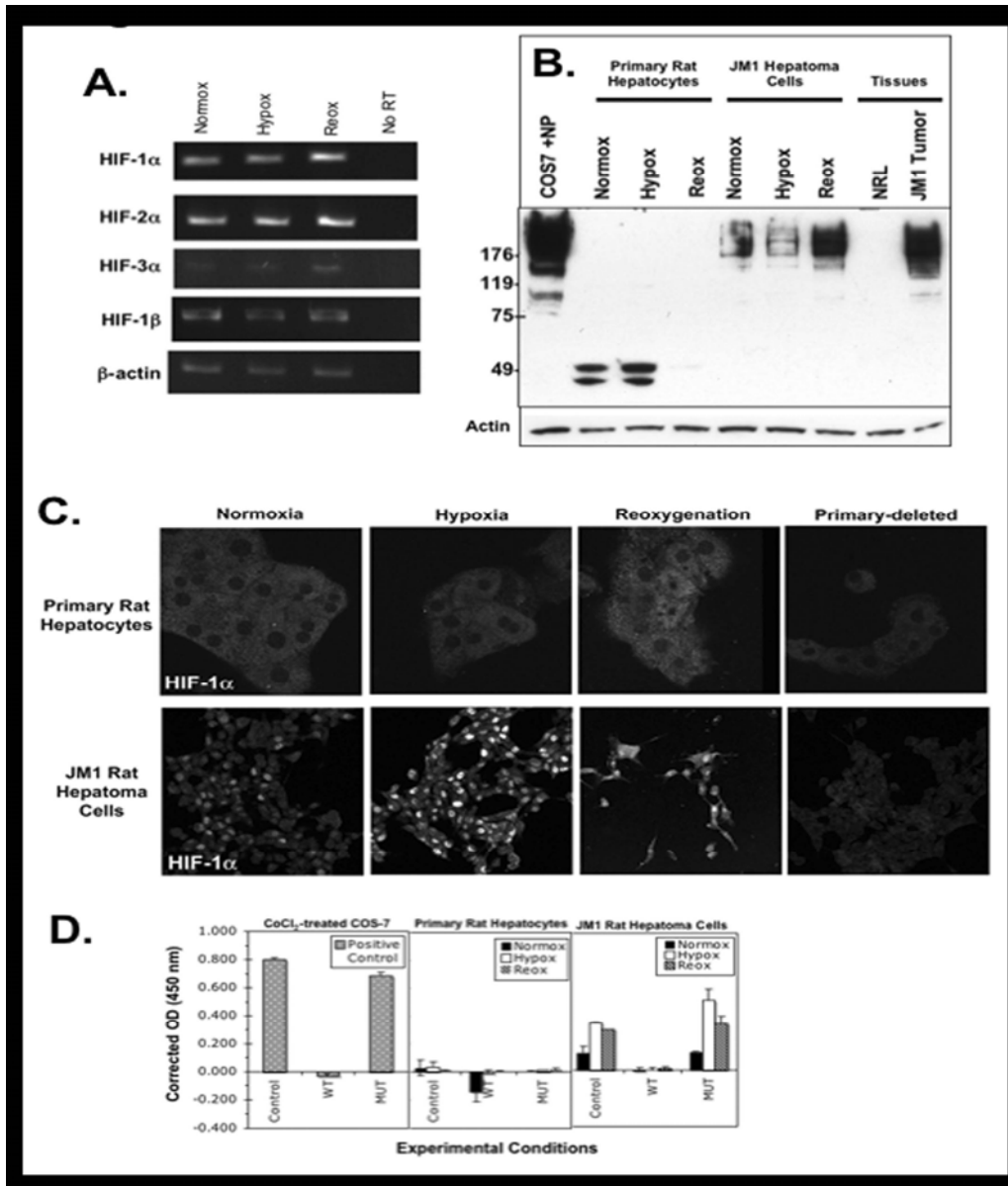


Figure 13: Absence of nuclear HIF-1 α induction in primary rat hepatocytes. Primary rat hepatocytes were cultured for 6 hr. in normoxic (control) or hypoxic (1% O₂) incubators. Parallel hypoxic cultures were returned to the normoxic incubator for overnight reoxygenation. **A.** RT-PCR shows expression of HIF-1 α , HIF-2 α , HIF-3 α , and the constitutive HIF-1 β in hepatocytes cultures. **B.** Maximum sensitivity Western blot of nuclear extracts reveals lack of HIF-1 α induction in primary hepatocytes compared to tumor cells. A similar pattern is observed in normal rat liver (NRL) tissue vs. JM1 tumor tissue. **C.** Scanning confocal immunofluorescence demonstrates nuclear localization of HIF-1 α in syngeneic JM1 rat hepatoma cells, but not in primary rat hepatocytes. **D.** HIF-1 α DNA-binding, as assessed by transcription factor ELISA, further confirms a lack of HIF-1 α activation in hepatocyte nuclear extracts. Positive control was CoCl₂-treated COS-7. The results in Figures 12 and 13 demonstrate that although hepatocytes do respond to hypoxia, the contribution of HIF-1 α to this response may be minor or very transient.

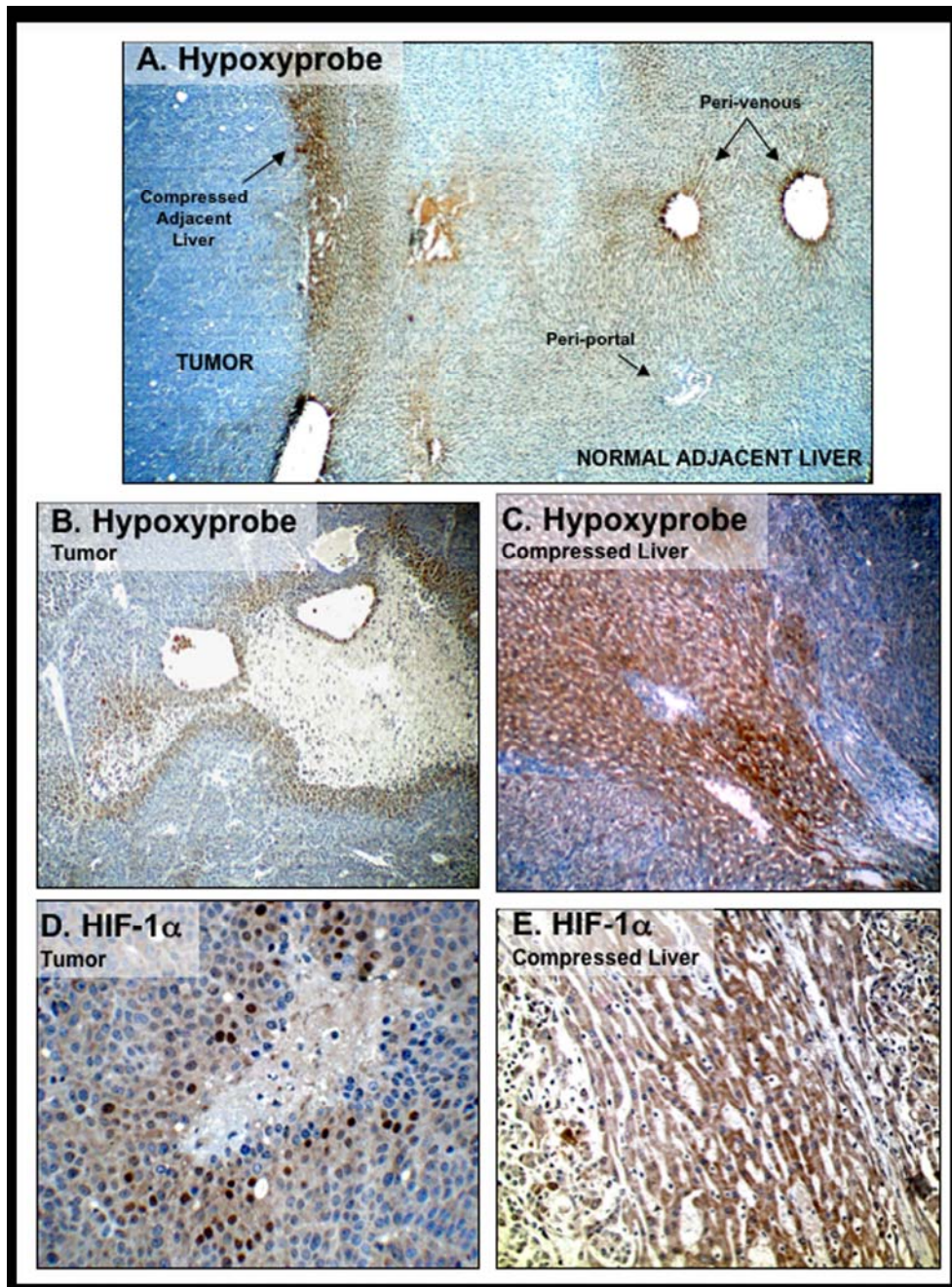


Figure 14: Comparison of hypoxic regions in syngeneic rat hepatomas. JM1 Fisher 344 rat hepatoma cells were transplanted into livers of same-strain rats. After 4 wk. of tumor formation, rats were injected i.p. with Hypoxyprobe marker. A. Low power view of hypoxic regions contained in tumor and compressed normal adjacent (host) liver. B. Hypoxic cells outline necrotic region of tumor. C. Hypoxic host liver is compressed by tumors extending bilaterally. D. HIF-1 α -positive tumor cells surround necrotic center, corresponding to hypoxic regions in B. E. Absence of HIF-1 α nuclear labeling in adjacent hepatocytes, despite being compressed in hypoxic regions (C).

patterns of other endogenous HIF transcription factors in response to hypoxia. In contrast to HIF-1 α , we did observe a nuclear induction of HIF-2 α in hepatocytes, but this was only following reoxygenation experiments (Figure 15B). HIF-2 α (green) co-localized (yellow) with HIF-1 β (red), the constitutive nuclear binding partner of HIF- α . There was also an increase in cytoplasmic HIF-2 α , but this was not co-localized to peroxisomes (data not shown). Interestingly, basal levels of HIF-3 α (green) were observed in the nuclei of normoxic (control) hepatocytes, and this HIF-3 α shifted *out* of the nucleus in hypoxia (Figure 15C). Unlike HIF-2 α , HIF-3 α did co-localize (yellow) with the peroxisomal enzyme catalase (red), suggesting a similar targeting as HIF-1 α .

4.2.4 HIF hydroxylases localize to peroxisomes in resting liver

Since much less is known about the HIF regulatory hydroxylases in comparison to the HIF transcription factors, we decided to expand our study to include the subcellular distribution of HIF hydroxylases in intact rat and human liver. As seen in Figure 16A, there is a zoned distribution of PHD4 around the central veins, and this zonal pattern is similar for the other HIF hydroxylases examined. This was surprising, since the perivenous hepatocytes are exposed to the lowest pO₂ along the liver's physiologic O₂ gradient, making this region less suited for HIF hydroxylase activity. At higher magnification, we found that in perivenous areas, HIF hydroxylases localized to some hepatocyte nuclei; however, there was also an intense punctate labeling in the cytoplasm (Figure 16B-C). These findings were intriguing given the paucity of prior reports on endogenous HIF hydroxylases in normal tissue and liver in particular. We next performed additional high-resolution studies to identify the subcellular localization of endogenous HIF hydroxylases in resting rat liver. The particulate pool of HIF hydroxylases in the hepatocyte cytoplasm was contained in specific organelles. PHD2 and PHD3 localized to mitochondria as well as peroxisomes (Figure 16D). As demonstrated by immuno-TEM in Figure 16E, PHD2 co-localizes in peroxisomes, which are identified by both catalase and the recognizable urate oxidase crystalline core. Although localization of transiently transfected PHD3 (SM20) has been described previously in rat sympathetic neurons (97), peroxisomal localization has never been reported for any of the known HIF hydroxylases. Interestingly,

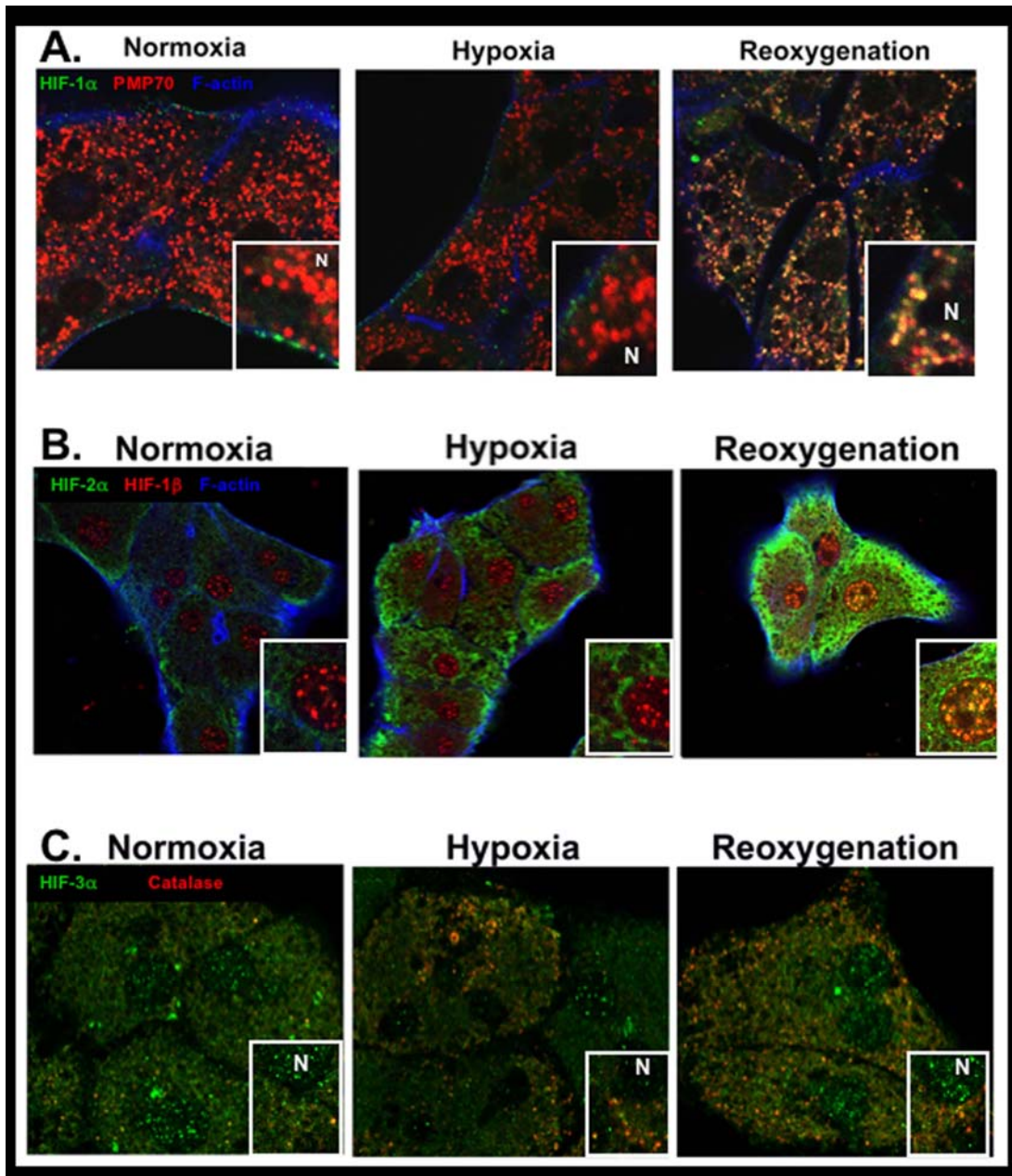


Figure 15: Subcellular localization of endogenous HIFs in primary rat hepatocytes. Primary rat hepatocytes were cultured for 6 hr. in normoxic (control) or hypoxic (1% O₂) incubators. Parallel hypoxic cultures were returned to the normoxic incubator for overnight reoxygenation. A. Confocal scanning laser immunofluorescence microscopy demonstrates HIF-1 α (green) co-localization (yellow) with the peroxisomal membrane marker PMP-70 (red) following reoxygenation. Note the “donut-like” red outline of the peroxisomes. Hepatocyte membranes are labeled with phalloidin (blue), and HIF-1 α (green) is also co-localized here (2000x mag, N = nucleus). B. Unlike HIF-1 α , hypoxia-reoxygenation leads to nuclear induction of HIF-2 α (green), which co-localizes (yellow) with the constitutive HIF-1 β (red) (1000x mag). C. Nuclear HIF-3 α (green) is observed in normoxic hepatocytes, and hypoxia-reoxygenation leads to co-localization with catalase (red) in peroxisomes (2000x mag, N = nucleus).

unlike the other HIF hydroxylases, PHD1 also localized to the bile canalicular membrane of hepatocytes (Figure 18).

4.2.5 Expression of HIF hydroxylases in primary rat hepatocytes

To investigate the effects of hypoxia-reoxygenation on HIF hydroxylases in hepatocytes, we once again utilized our *in vitro* culture system. We analyzed gene expression by RT-PCR of the HIF hydroxylases with available rat sequences, *PHD1-3* and *FIH-1*, in our hepatocyte cultures and found an upregulation of *PHD3* but not *PHD2* by 6 hr of hypoxia (Figure 17A). This is in contrast to previous reports by others that *PHD2* and *PHD3* are both hypoxia-induced genes; however, those findings were based on longer hypoxic incubation times (18 hr.) (73).

4.2.6 Hypoxia-reoxygenation induces nuclear-to-cytoplasmic translocation and peroxisomal sequestration of HIF hydroxylases in cultured hepatocytes

We next employed our *in vitro* hypoxia-reoxygenation model to further characterize the dynamic relationship of subcellular localization and HIF hydroxylases in hepatocytes in culture. As seen in Figure 18, scanning laser confocal immunofluorescence microscopic analysis revealed that endogenous PHD1 (green) shifts from the nucleus to the cytoplasm in hypoxia, and this shuttling is reversed upon reoxygenation. As nuclear PHD1 decreases, more PHD1 is associated with the hepatocyte membrane, and there is an increase in PHD1 colocalization (yellow) with catalase (red) in peroxisomes. Although nuclear PHD1 is restored with reoxygenation, peroxisomes still appear to sequester a sizable fraction of PHD1. Figure 19A-D shows analogous findings for PHD2-4 and FIH-1; however, only PHD1 localizes to the bile canaliculi (Figure 18). The peroxisomal pool exists in normoxia, but increases with hypoxia-reoxygenation. This finding is observed even with PHD4 (Figure 19C), which is the least expressed of the HIF hydroxylases in these hepatocyte cultures, suggesting a common sequestration event among these family members.

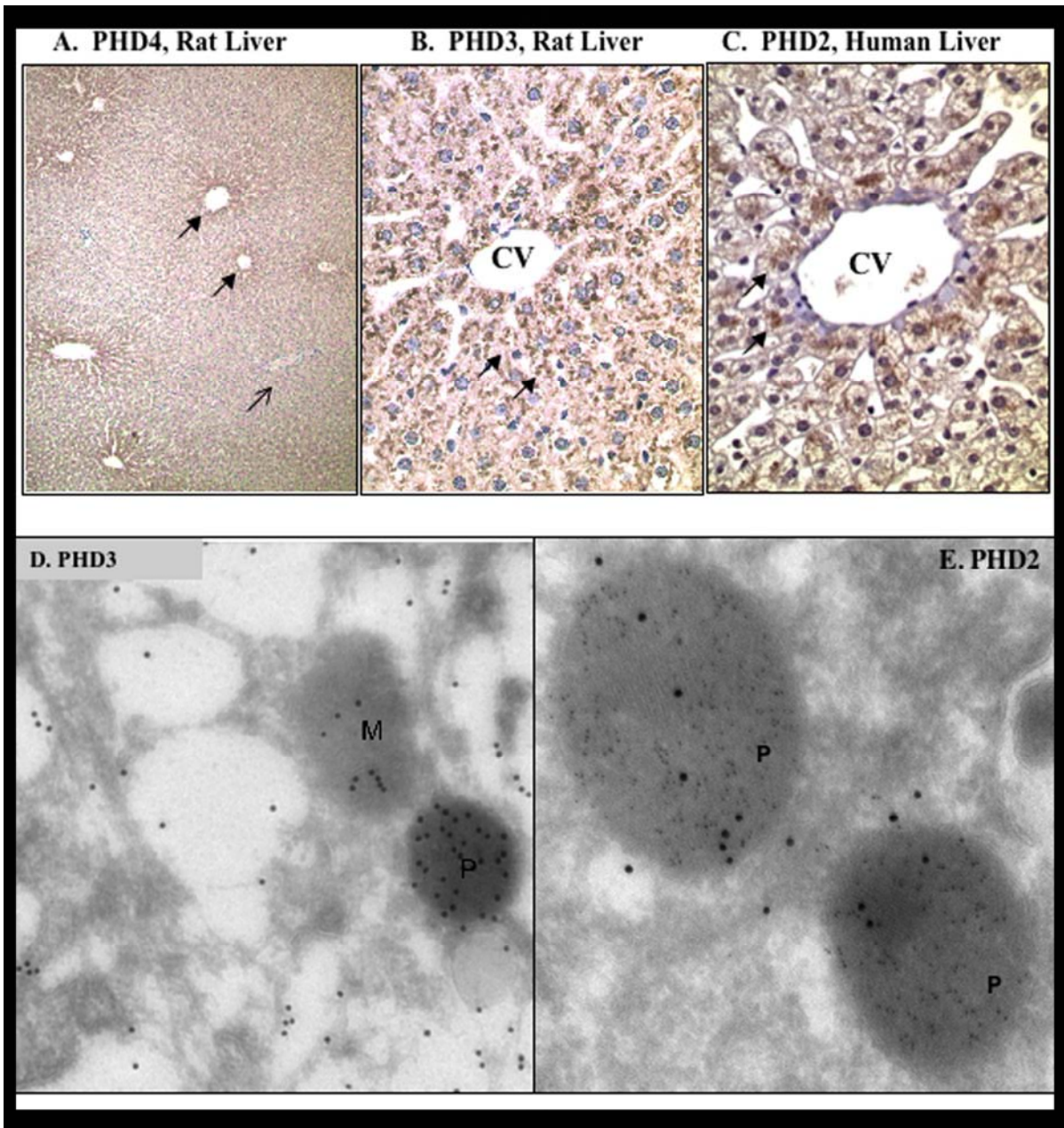


Figure 16: Subcellular localization of endogenous HIF hydroxylases in resting liver.

Shown here are representative images of localization patterns observed. A-C. Perivenous (heavy arrows) gradient distribution of PHD4 in rat liver, with sparing of peri-portal regions (light arrow, 100x mag). Punctate labeling (arrows) is observed in perivenous hepatocytes for PHD3 (B) in rat liver and PHD2 (C) in human liver (600x mag, CV = central vein). D. Immuno-TEM showing PHD3 in peroxisomes (P) and in mitochondria (M) of rat liver. E. PHD2 in rat liver is labeled with 10-nm gold particles, and peroxisomes are identified by catalase (smaller 5-nm gold particles) and the urate oxidase crystalline core.

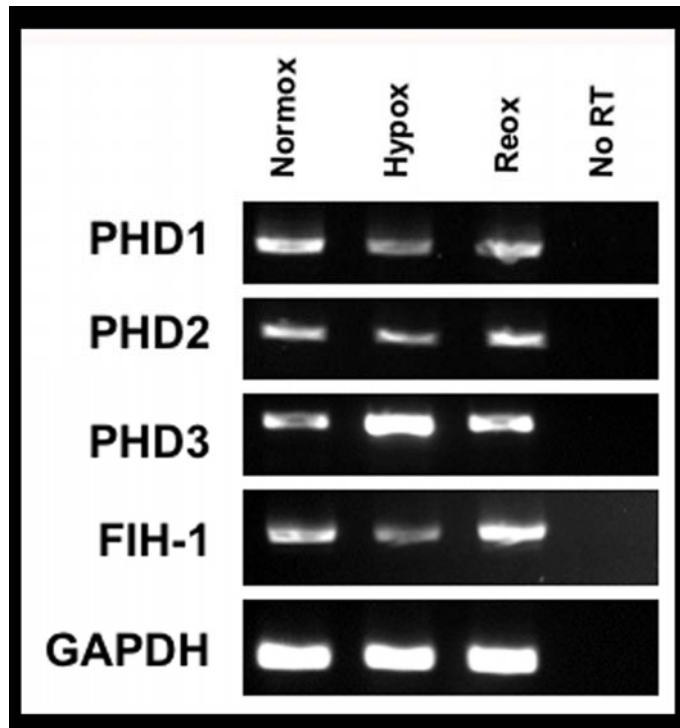


Figure 17: Expression of HIF hydroxylases in hepatocyte cultures. Primary rat hepatocytes were cultured for 6 hr. in normoxic (control) or hypoxic (1% O₂) incubators. Parallel hypoxic cultures were returned to the normoxic incubator for overnight reoxygenation. RT-PCR analysis of total RNA is shown for HIF hydroxylases. *PHD3* expression is induced by hypoxia, consistent with published reports. Repeated analyses using human *PHD4* primers were unsatisfactory, and at present the rat sequence for *PHD4* is not available.

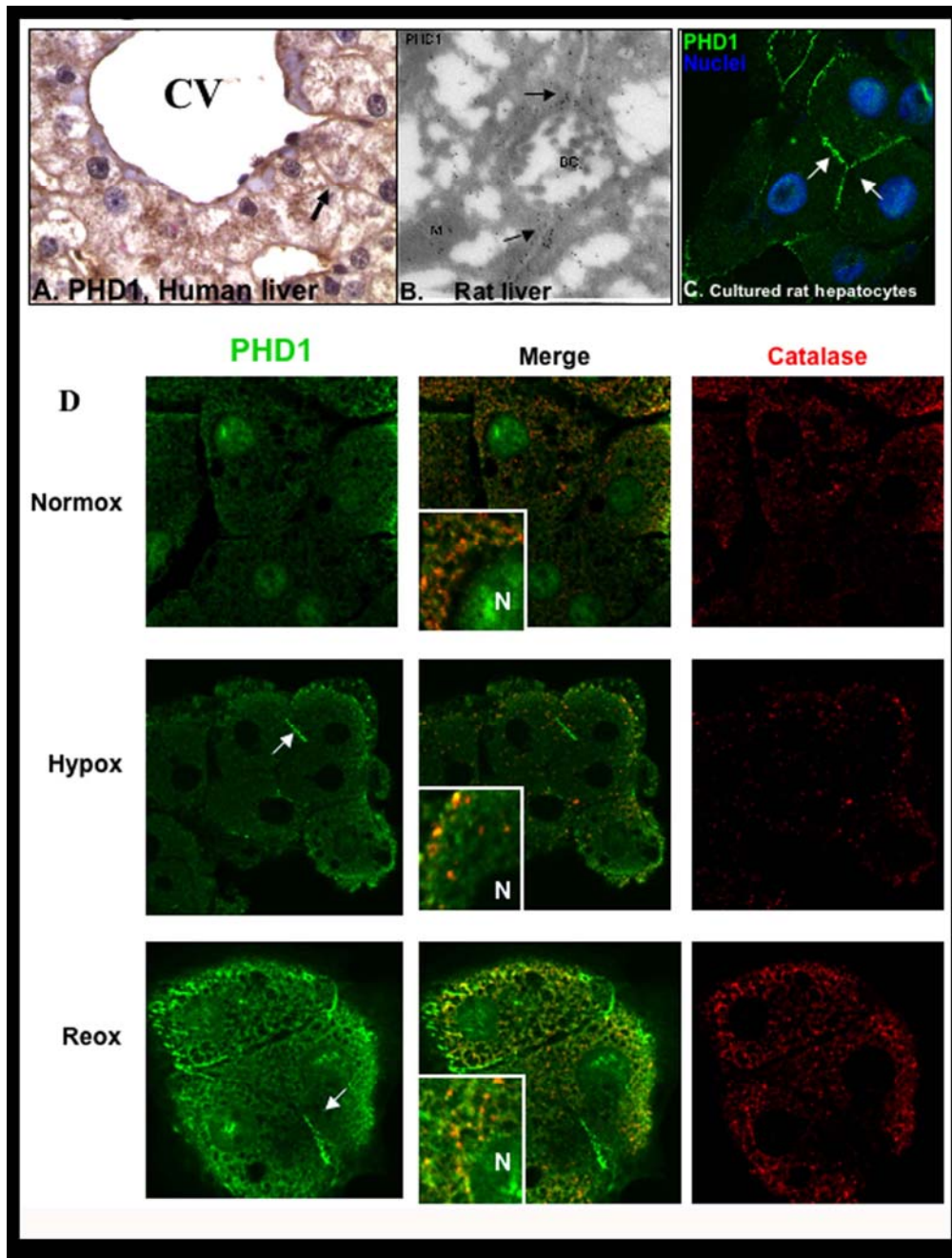


Figure 18: Subcellular localization of endogenous PHD1 in hepatocytes.

A. PHD1 is found in the bile canaliculi (BC) of resting human liver (1000x mag, CV = central vein). **B.** Immuno-TEM showing PHD1 localized to the BC of rat liver. **C.** PHD1 on the membranes of cultured primary rat hepatocytes (arrows, 1000x mag). **D.** Confocal immunofluorescence microscopy visualizing cells labeled with catalase (red) and PHD1 (green). As with the other HIF hydroxylases, hypoxia-reoxygenation results in a reversible nuclear-to-cytoplasmic translocation for PHD1. Increased peroxisomal co-localization (yellow, see insets) is also observed in response to these treatment conditions; however, unlike the other HIF hydroxylases, PHD1 also localizes to the hepatocyte membrane (arrows, N = nucleus, 2000x mag).

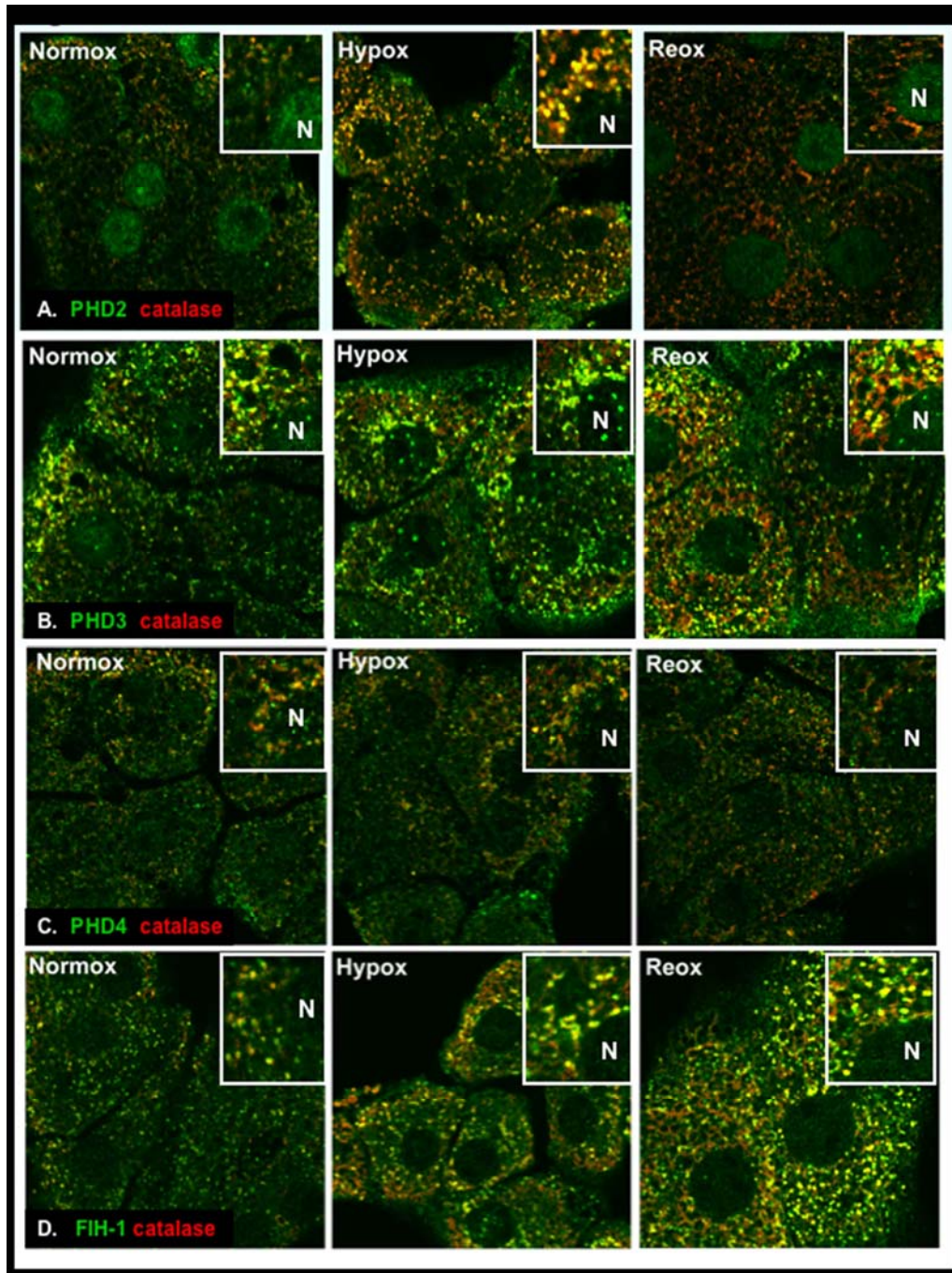


Figure 19: Subcellular localization of endogenous HIF hydroxylases in cultured hepatocytes. Primary rat hepatocytes were cultured for 6 hr. in normoxic (control) or hypoxic (1% O₂) incubators. Parallel hypoxic cultures were returned to the normoxic incubator for overnight reoxygenation. Confocal immunofluorescence microscopy was used to visualize cells labeled with catalase (red) and each of the HIF hydroxylases (green). In general, hypoxia-reoxygenation results in increased peroxisomal co-localization (yellow, see insets); however, each hydroxylase has distinct levels of expression. A. PHD2, B. PHD3. C. PHD4. D. FIH-1 (N = nucleus, magnification = 2000x).

4.2.7 Immuno-TEM and Western analysis confirm peroxisomal localization of HIF hydroxylases in cultured hepatocytes

To verify our microscopic observations, we commenced additional studies on primary rat hepatocytes. Immuno-TEM of hypoxic hepatocytes in culture confirmed the presence of PHD2 in peroxisomes, identified by catalase and the urate oxidase crystalline core (Figure 20A). This was also noted for the other HIF hydroxylases, with PHD4 showing the least amount of labeling. As shown for PHD3 (Figure 20B), there is a striking lack of it in the nucleus compared to the peroxisome in these cells. We next performed subcellular fractionation of hepatocytes in an isotonic buffer in order to obtain a “heavy pellet” containing an organelle-enriched membrane fraction (MF). Immunoblotting of the MFs isolated from cultured rat hepatocytes further confirmed the presence of PHD1-3 and FIH-1 in the peroxisome-containing fractions (Figure 20C). Hypoxia-reoxygenation also altered the size of some HIF hydroxylases, suggesting either post-translational modifications or the existence of other isoforms. For instance, we observed a decrease in the faster-migrating species of the nuclear PHD1 doublet, which has also been described by others (110, 148).

4.2.8 Hypoxia-reoxygenation leads to peroxisomal localization of VHL

Having identified the presence of HIF-1 α and PHDs in peroxisomes, we next investigated whether VHL, known to be associated with the transport of HIF-1 α , also resided here. As the substrate recognition unit of the E3 ubiquitin ligase multiprotein complex (elongins B and C, cullin2, Ring-box 1), pVHL tags hydroxylated HIF-1 α for polyubiquitination and degradation by the 26s proteasome (36, 46). As seen in Figure 21, VHL does co-localize in peroxisomes with HIF-1 α and catalase. These findings may suggest a potential link between HIF-1 α shuttling to the peroxisomes and HIF hydroxylation.

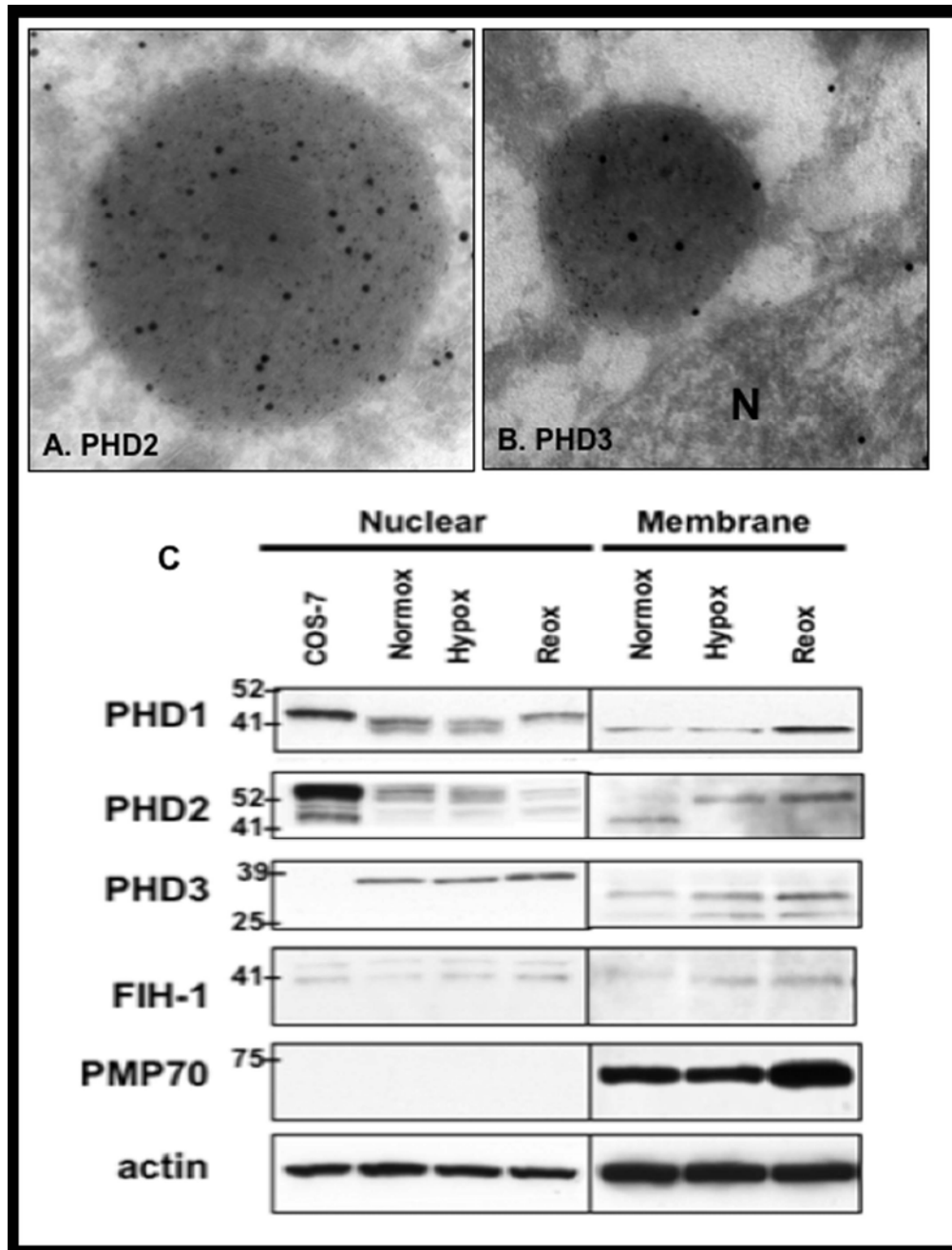


Figure 20: Peroxisomal localization of endogenous HIF hydroxylases in hepatocytes.

A-B. Immuno-TEM of hypoxic primary rat hepatocytes. PHD2 (A) and PHD3 (B) are labeled with large gold particles, while peroxisomes are identified by catalase (5 nm gold particles) and the urate oxidase crystalline core (N = nucleus). **C.** Subcellular fractionation in an isotonic buffer was used to obtain both a nuclear fraction (NF) and intact peroxisomes in the organelle-enriched membrane fraction (MF). Western blots showing localization of HIF hydroxylases in the MF and NF of primary rat hepatocytes. PHD4 was undetectable in either fraction via Western blot. COS-7 cell nuclear extract was used as positive control. PMP-70 western blot confirms isolation of intact peroxisomes in MF.

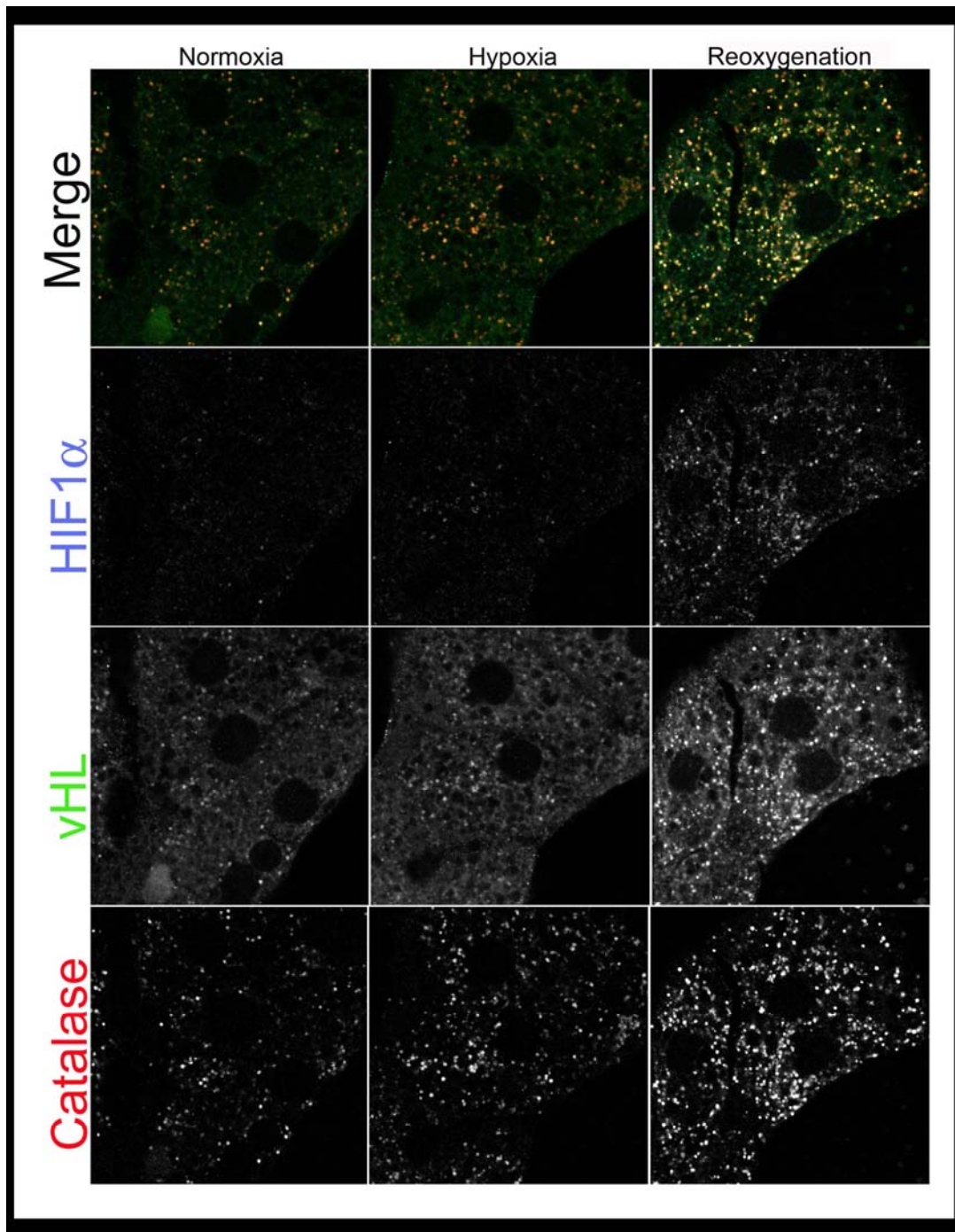


Figure 21: Peroxisomal localization of VHL.

Primary rat hepatocytes were cultured for 6 hr. in normoxic (control) or hypoxic (1% O₂) incubators. Parallel hypoxic cultures were returned to the normoxic incubator for overnight reoxygenation. Confocal scanning laser immunofluorescence microscopy demonstrates the peroxisomal colocalization of HIF-1 α (blue), catalase (green), and VHL (red) in hepatocytes subjected to hypoxia-reoxygenation (2000x mag).

4.3 DISCUSSION

The subcellular localization patterns of endogenous HIFs and HIF regulatory hydroxylases in our primary rat hepatocyte cultures are summarized in Table 6. Interestingly, although we observed both expression of *HIF-1 α* via RT-PCR (Figure 13A) and an upregulation of HIF target genes (Figure 12C), we were unable to detect by either imaging, Western blot, or ELISA a nuclear induction of HIF-1 α protein in hypoxic primary rat hepatocytes (Figure 13). This may be due to the predominance of other HIF- α species in hepatocytes, since HIF-2 α did translocate to the nucleus following hypoxia-reoxygenation. In addition, the role of nuclear HIF-3 α in normoxic hepatocytes is less clear, since several splice variants are known to exist, including those that may act as “decoys” (*e.g.*, IPAS) which negatively regulate the other HIF- α subunits (43). It was recently demonstrated that HIF-2 α and HIF-3 α were the predominant activators of hypoxia-induced IGFBP-1 transcription in transfected primary rat hepatocytes (147). The minor role of HIF-1 α in hepatocytes may be due to its translocation to peroxisomes rather than to the nucleus in hypoxia. This peroxisomal import is accompanied (or perhaps facilitated) by the HIF regulatory hydroxylases and VHL in hypoxia-reoxygenation.

Our observations of VHL in hepatocytes are intriguing given that Groulx and Lee (149) found in HeLa cells that VHL engages in a constitutive nuclear-cytoplasmic shuttle unaffected by pO₂ or levels of nuclear HIF- α substrate. The peroxisomal targeting sequences PTS1 and PTS2 are consensus sequences which are involved in peroxisomal import, and they are recognized by the peroxisomal import receptors Pex5 and Pex7, respectively [reviewed in (150)]. Upon closer examination of the primary sequence of VHL, we identified a potential 100% canonical PTS2 import sequence in the N-terminal side of the middle of the molecule, making this PTS site the most potentially active among the protein sequences we compared. Furthermore, even if a protein's sequence is not 100% identical to the canonical PTS sites, other enzymes have been described that target to the peroxisome with similar, but non-conventional PTS sequences; these include acetoacetyl-CoA thiolase (151), alanine:glyoxylate aminotransferase (152), isopentenyl diphosphate dimethylallyl diphosphate isomerase (153), and iNOS (141, 154). In fact, very large protein oligomers lacking PTS motifs have been shown to “piggy-back” onto other conventional peroxisomal proteins and gain entry into the peroxisomal matrix in their native configuration

Table 6: Summary of confocal immunolocalization for endogenous members of the HIF pathway in primary rat hepatocytes.

Protein	Treatment Condition			Comments on Localization
	Normoxia	Hypoxia	Reoxygenation	
HIF-1α	Membrane	Membrane	Cytoplasm	<ul style="list-style-type: none"> • Peroxisomal in reoxygenation • Not in nucleus
HIF-2α	Cytoplasm	Cytoplasm	Nucleus Cytoplasm	<ul style="list-style-type: none"> • Not in peroxisomes
HIF-3α	Nucleus Cytoplasm	Cytoplasm	Nucleus Cytoplasm	<ul style="list-style-type: none"> • Peroxisomal • Leaves nucleus in hypoxia
HIF-1β	Nucleus	Nucleus	Nucleus	<ul style="list-style-type: none"> • Constitutive
PHD1	Nucleus	Cytoplasm Membrane	Nucleus Cytoplasm Membrane	<ul style="list-style-type: none"> • Peroxisomal • Bile canaliculi
PHD2	Nucleus Cytoplasm	Cytoplasm	Nucleus Cytoplasm	<ul style="list-style-type: none"> • Peroxisomal in hypoxia • Some mitochondrial
PHD3	Nucleus Cytoplasm	Nucleus Cytoplasm	Nucleus Cytoplasm	<ul style="list-style-type: none"> • Peroxisomal • Some mitochondrial
PHD4	Nucleus Cytoplasm	Nucleus Cytoplasm	Nucleus Cytoplasm	<ul style="list-style-type: none"> • Peroxisomal • Lowest abundance • Very novel enzyme
FIH-1	Nucleus Cytoplasm	Nucleus Cytoplasm	Nucleus Cytoplasm	<ul style="list-style-type: none"> • Peroxisomal
VHL	Cytoplasm	Cytoplasm	Cytoplasm	<ul style="list-style-type: none"> • Peroxisomal • Not in nucleus

(155). Specifically, the largely hydrophobic β -domain of VHL contains two critical hydrophilic residues (His-115 and Ser-111), which must hydrogen bond with either hydroxyproline or H₂O molecules (44, 45). Theoretically, VHL could gain entry into the peroxisome while complexed with HIF-1 α and its associated HIF hydroxylase(s), and hydroxylated HIF-1 α may serve as an intermediate between them. Since achieving highly efficient transfection of primary hepatocyte cultures can be a challenge, additional experiments in liver-specific VHL-null cells (156) would provide further clues about the peroxisomal import of these proteins.

The significance of our findings can be further extrapolated to the liver's microenvironment, where hepatocytes and neighboring cells are exposed to a physiologic gradient of O₂ and other nutrients from the portal circulation. Not only does the portal vein contribute significantly to the liver's blood supply, there is a ~50% drop in pO₂ along the course of the sinusoid toward the central vein, from 60-65 mm Hg (afferent) to 30-35 mm Hg (efferent) (157). Since basal HIF-1 α is constitutively expressed but rapidly degraded, there must exist a mechanism to poise the cell for swift responses to hypoxic insult, while at the same time keeping nuclear levels of HIF-1 α in check when not needed. Nuclear HIF hydroxylases are thought to participate in the regulation of HIF-1 α turnover and activity, since the degradation of HIF-1 α can occur with the same half-life in both the nucleus and the cytoplasm (158). This indicates that, unlike p53 which must exit the nucleus prior to its degradation, both nuclear and cytoplasmic proteasomes are fully competent to degrade HIF-1 α in an O₂-dependent manner, thereby preventing even ongoing HIF transcriptional activity. Moreover, *in vitro* enzyme kinetics assays have found that PHD2 and PHD3 possess the highest relative prolyl hydroxylation activities (159), suggesting that the robust expression of these enzymes in resting liver would counter-act much of the HIF-1 α activity one would have expected to find in peri-venous hepatocytes. This lack of HIF-1 α activity is in contrast to organs such as the adult kidney, which acts as an important physiologic O₂ sensor and rapidly adapts to systemic hypoxia by increasing EPO production [reviewed in (160)].

In general, the PHDs can shuttle from the hepatocyte nucleus to the cytoplasm in response to hypoxia. Upon reoxygenation, there exists a substantial pool of endogenous HIF hydroxylases sequestered in peroxisomes, which is a novel finding. In contrast to the HIFs, subcellular localization of HIF hydroxylases has only been published for cell lines transfected to over-express each respective enzyme. Mitochondrial localization has been shown for the PHD3

homolog, SM20 (97), and we observed some mitochondrial localization in hepatocytes as well (Figure 16D). In U2OS cells expressing transiently transfected human HIF hydroxylase-GFP fusion proteins, the localization of PHD1 was completely nuclear, PHD2 and FIH-1 were mostly cytoplasmic, and PHD3 was homogenously distributed between the nucleus and the cytoplasm (161). In contrast, transfection of COS-1 cells revealed both nuclear and cytoplasmic distribution for PHD1-3 and FIH-1 (98). When FLAG-tagged PHD4 was transiently transfected in COS-7 cells, it excluded the nucleus and localized to the endoplasmic reticulum; although, no consensus ER retention signal was identified in its peptide sequence (94). These pioneering experiments may be useful in predicting the diverse functions of HIF hydroxylases in different cell types; however, they only add to the complexity of how and where these O₂-dependent hydroxylases are shuttled in response to hypoxia. To date, a detailed analysis of the subcellular localization of *endogenous* HIF hydroxylases in primary cells has not been published.

In this study, we identify dynamic changes in subcellular localization of HIF-1 α , VHL, and the HIF regulatory hydroxylases, all of which co-localize to peroxisomes in hepatocytes. The question remains as to whether these enzymes are actively hydroxylating key proline residues while sequestered. Prior to the discovery of HIF regulation, collagen was the only known hydroxyproline-containing protein. Unlike the collagen prolyl 4-hydroxylase, which acts on the tripeptide X-pro-gly, the HIF PHDs require a much longer (~19mer) minimal HIF-derived peptide for optimal activity (60). Furthermore, each PHD may preferentially hydroxylate one or both of the two proline residues in the HIF-1 α ODDD, suggesting specialized roles for acute and chronic adaptation (60). Interestingly, a short but growing list is emerging for O₂-dependent hydroxylation of non-HIF proteins by PHDs and FIH-1, such as the large subunit (Rbp1) of RNA polymerase II (162). Even though the PHDs are highly conserved and ubiquitously expressed, there is also evidence of alternative splicing, with some variants no longer capable of hydroxylating HIF- α (60). In general, numerous hydroxylases exist in peroxisomes as well as in the bile canaliculi, where PHD1 also co-localized. Although we observed a peroxisomal pool of HIF-1 α in hepatocytes, we are uncertain if any of the HIF hydroxylases sequestered in peroxisomes still retain their activity, and if so, what their potential substrates may be. In the case of iNOS, a non-conventional peroxisomal enzyme in hepatocytes, the fraction of iNOS sequestered in peroxisomes is an inactive monomer, perhaps protecting the cell from incompetent enzyme (154). On the other hand, phytanoyl Co-A hydroxylase is a classic PTS2-

containing enzyme which leads to Refsum's disease if defective (163). Not only is phytanoyl Co-A hydroxylase active in peroxisomes, it is actually a member of the same O₂-, Fe²⁺-, and 2-oxoglutarate-dependent oxygenase family as the HIF hydroxylases; therefore, within the peroxisomes there may exist a medium containing the co-factors necessary for PHD and FIH-1 activity (164). Modification of existing biochemical techniques for measuring hydroxylated HIF peptides *in vitro* could provide an alternative method for testing enzymatic activity of HIF hydroxylases in intact peroxisomes.

The *in vitro* hypoxia-reoxygenation model alters the O₂ availability necessary for HIF hydroxylase function. A potential mechanism for targeting HIF hydroxylases to other organelles may involve the oxygen-redirection hypothesis [reviewed in (165)], which states that inhibition of mitochondrial respiration may lead to subcellular redirection of O₂ from mitochondria to non-respiratory O₂-dependent compartments. In hepatocytes, the peroxisome represents one such compartment, constituting ~1% of total cell volume, yet consuming up to 30% of the O₂ in resting liver (166). Inhibitors of mitochondrial respiration such as NO have been shown to increase PHD activity and decrease nuclear HIF-1 α in hypoxia, due to subcellular O₂ redirection from mitochondria to PHDs (167, 168). A very recent study by Papandreou *et al.* (169) in cell lines has shown that HIF-1 can actively down-regulate mitochondrial O₂ consumption by repressing the TCA cycle. This results in adaptation to hypoxia, since mitochondrial O₂ redistribution leads to a relative increase in intracellular O₂ concentration and availability. The effects of HIF-1 on mitochondria were found to be functional, not structural, and decreased cell death was observed in chronic hypoxia. Other groups have also linked the TCA cycle as a "metabolic switch" for cellular adaptation to hypoxia, due to its production of intermediates such as the PHD co-factor 2-OG (170, 171).

In summary, we have identified an unexpected subcellular distribution pathway in hepatocytes in response to hypoxia, where both HIF-1 α and the O₂-sensing hydroxylases which regulate it are all shuttled to the peroxisome, such that nuclear induction of HIF-1 α is undetectable. It would be interesting to elucidate the molecular mechanisms of this sequestration in more detail, and to determine precisely how VHL or other carrier proteins might be functioning in hepatocytes. Further consideration should also be given to the effects of required HIF hydroxylase co-factors (Fe²⁺, 2-OG, ascorbate), as well to glucose itself, since like O₂ the latter is also distributed across a gradient in the liver. Finally, *in vivo* correlations with ischemia-

reperfusion models may provide new insights on how HIF regulatory hydroxylases are altered in liver injury. In conclusion, our results suggest a novel site for the regulation of the O₂-dependent HIF pathway in hepatocytes, and they expand upon the role of peroxisomes as an O₂ sink in the redox microenvironment of the liver.

4.4 ACKNOWLEDGEMENTS:

We greatly appreciate our colleagues for their technical assistance and helpful discussions: William Bowen, Mark Ross, Dr. Fengli Guo, Mara Sullivan, Dr. Patricia Loughran, Lindsay Barua, Aimee Katsigrelou, Srey Gast, and James Shray.

5.0 ABSENCE OF NUCLEAR INDUCTION OF HIF-1 α IN RAT LIVER: IN VIVO AND IN VITRO STUDIES.

(Portions of 5.1. Introduction were reproduced from Appendix A: Michalopoulos, G.K., and **Z. Khan**. (2005) Liver regeneration, growth factors, and amphiregulin. *Gastroenterology* 128:503-506.)

5.1 INTRODUCTION

5.1.1 Liver regeneration as a model for angiogenesis

The set of events triggering liver regeneration after acute loss of hepatic mass has been the subject of much investigation over the last twenty years (reviewed in (172)). Following normal resection, as in 70% partial hepatectomy (PHx) in the rat, the liver will restore 100% of its lost mass within six days after surgery (139). Despite this amazing regenerative capacity, there is still much to be learned about the molecular interactions of distinct liver cell types in normal liver growth and repair, as well as how these signals are altered in disease states.

Due to the predictable nature of revascularization and controlled tissue growth following PHx, the study of liver regeneration using the rat PHx model provides an ideal and efficient setting for investigating the spatiotemporal mechanisms of angiogenesis at the molecular level. Liver regeneration involves a series of highly coordinated processes involving the restoration of parenchymal cells (hepatocytes and biliary epithelium), non-parenchymal cells (NPCs), and hepatic microarchitecture, while simultaneously maintaining normal liver function. Specifically, hepatocytes are the first cells to proliferate after PHx, initially forming avascular islands of 10-12

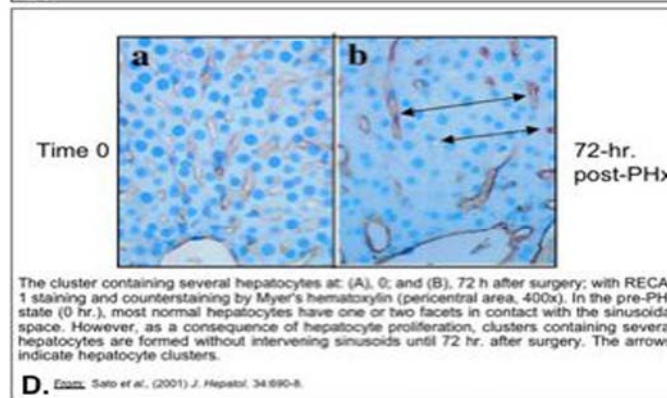
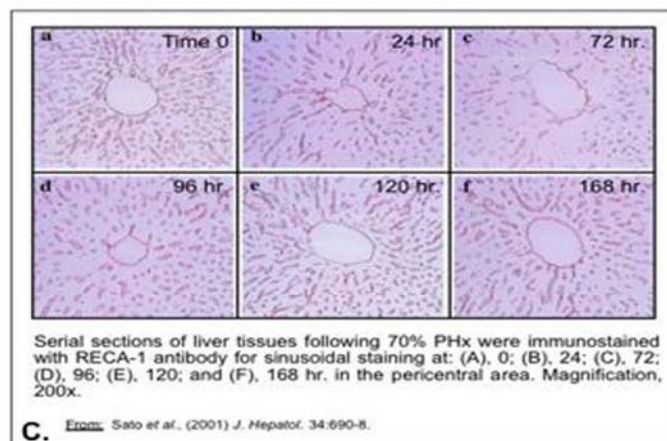
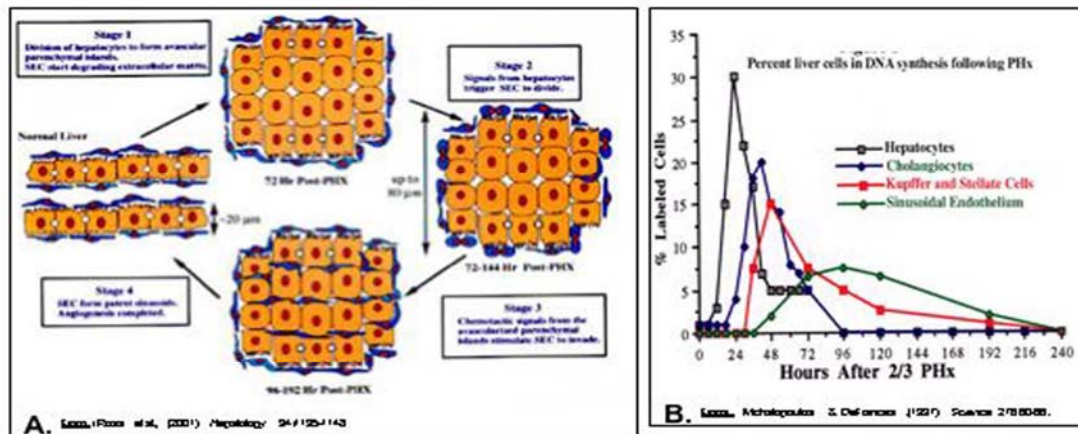


Figure 22: Liver revascularization following 70% PHx.
A. The timing and stages of angiogenic events during liver regeneration. Figure A reproduced from (174) with permission from John Wiley & Sons, Inc., Hoboken, NJ. **B.** Proliferation of liver cell compartments after 70% PHx. Parenchymal cells divide first, followed by non-parenchymal cells. Figure B reproduced from (172) with permission from AAAS, Washington, DC. **C.** Restoration of sinusoidal architecture following 70% PHx. **D.** Avascular hepatocyte islands in regenerating rat liver. Figures C-D reproduced from (175) with permission from Elsevier, Inc., Philadelphia, PA.

cells, and it is not until days 4-8 after PHx that neighboring sinusoidal endothelial cells (SECs) are recruited to migrate, proliferate, and repopulate these islands (Figure 22) (173, 174). Thus angiogenesis is considered a later event in liver regeneration, presumably in response to hypoxic “hot spots” with avascular hepatocyte islands.

Hypoxia-induced signals are essential for both normal and pathologic angiogenesis. In regenerating rat liver, the spatiotemporal expression of angiogenic growth factors and receptors has been described (

Table 7). By day three post-PHx, the critical time-point before revascularization of avascular hepatocyte islands, peak vascular endothelial growth factor (VEGF) expression is observed in hepatocytes (periportal > pericentral), with the VEGF₁₈₈ isoform predominating (176-178). This is followed by expression of angiopoietin-1 (Ang-1), which peaks at day four post-PHx and is needed for vessel stabilization and pericyte recruitment (175). Angiopoietin-2 (Ang-2), which is important for vascular remodeling, gradually increases to peak at day seven post-PHx (175). Beginning three days after PHx, the following receptors are upregulated on SECs: VEGFR-1/flt-1 (also on hepatocytes; role is less clear), VEGFR-2/flk-1 (main VEGF receptor), Tie-1 (orphan receptor), Tie-2 (main Ang receptor), PDGF-R β , and EGF-R (174).

In the past, these signals were considered necessary for SEC proliferation and survival, but in fact, recent *in vitro* co-culture experiments suggest they may also promote hepatocyte-SEC interactions important for both cell types. For instance, a comprehensive investigation in mice showed that VEGF could stimulate hepatocyte proliferation *in vivo*, but it could do so *in vitro* only if co-cultured with SECs (179). In co-cultures, hepatocyte-produced VEGF stimulated SEC proliferation via VEGFR-2/flk-1; however, VEGFR-1/flt-1 activation in SECs was not associated with cell proliferation; instead, it caused production of HGF, which in turn induced proliferation of hepatocytes.

A more complex example involves the *in vitro* characterization of long-term hepatic organoid cultures originating mostly from isolated primary rat hepatocytes (145). In these “roller bottle” co-cultures, the corticosteroid dexamethasone (Dex) suppressed growth and induced hepatocytic (HNF4+) maturation, while HGF and EGF were needed for development of non-epithelial elements. When cultures were treated with Dex alone, there was a suppression of gene expression for *HIF-1 α* , along with the angiogenic factors *VEGF*, *VEGFR-2/flk-1*, and *neuropilin-1*, and these cultures contained neither connective tissue nor biliary epithelium. These findings support a link between the HIF-1 α /VEGF axis and liver vascularization, which may mimic

paracrine and juxtacrine interactions between hepatocytes and NPCs in the liver microenvironment.

Table 7: Angiogenic growth factor receptors in liver regeneration.
This table was modified from (174).

Receptor	Time of Receptor Up-regulation on Endothelial Cell Membrane by Western Blot	Cellular Location of Receptor Up-regulation
Flt-1 (VEGF-R1)	4 -10 days	Up-regulation on SECs, larger amounts in arterioles than seen in veins. Also seen on hepatocytes in resting and proliferating liver.
Flk-1/KDR (VEGF-R2)	3 - 8 days	Predominantly on large vessels, small amounts observed on SECs.
Tie-1	2-14 days	SECs surrounding avascular islands
Tie-2 (tek)	2-14 days	Large vessels and SECs
PDGF-Rβ	3-12 days	Large vessels and SECs, stellate cells
EGF-R	Constitutive 3-14 days	Sinusoids, small amount on large vessels during regeneration
c-Met	Constitutive no change	Small amounts on large vessels, higher expression on hepatocyte canaliculi, bile ductules
FGF-R1 (Fig)	ND	Hepatocytes
FGF-R2 (Bek)	ND	ND

5.1.2 Hepatocyte growth factor (HGF) in liver regeneration

All of the aforementioned factors may contribute to a precisely-timed mechanism of controlled angiogenesis in response to hypoxia; however, regeneration of the hepatic parenchyma is

governed by other factors as well. Rapid changes in gene expression and activation of growth factors, receptors and transcription factors begin immediately after PHx (180-183). These stimuli have been shown to have effects on liver and on hepatocytes in culture. The effects of growth factors are mediated through their respective receptors. Two receptor-ligand, growth factor-signaling systems appear to be mainly involved in liver regeneration: hepatocyte growth factor (HGF) and its receptor (met), and epidermal growth factor (EGF) and its relatively large family of ligands and co-receptors. HGF/met signaling has been extensively studied and its role in liver regeneration will only be briefly summarized here, as follows:

- a. HGF levels in liver and circulating blood rise soon after PHx (184). The source for this early rise is HGF released by remodeling of the liver extracellular matrix (ECM) initiated by urokinase. HGF is known to be bound to liver ECM in large amounts (185).
- b. New HGF is synthesized in liver from 3-48 hr. post-PHx (186).
- c. HGF receptor (met) is tyrosine-phosphorylated within five min. post-PHx (182).
- d. Infusion of HGF into normal livers initiates hepatocyte DNA synthesis and is associated with dramatic increase in hepatic mass (187).
- e. Elimination of the HGF receptor (met) specifically in the liver eliminates the capacity of the liver to regenerate following 70% PHx (188, 189).
- f. Genetic deletion of either HGF or its receptor is associated with embryonic lethality with abnormalities primarily in placenta and secondarily in the liver (190).
- g. Generation of a mouse expressing a conditional knockout of the HGF gene in liver demonstrated impaired liver regeneration (191).

5.1.2.1 Crosstalk between hypoxia and HGF pathways:

Interestingly, a number of studies have suggested a role for the HGF/met pathway in hypoxia signaling; however, the majority of these studies focus on cancer biology. In a series of elegant

experiments, Pennacchietti *et al.* (192) demonstrated that hypoxia promotes invasive growth of tumors by transcriptional activation of the *met* proto-oncogene. This over-expression of *met* was in direct response to HIF-1 α induction, thereby providing a mechanism for sensitizing tumor cells to HGF stimulation. Subsequent reports have also confirmed hypoxia-induced *met* up-regulation in human salivary gland cancer cell lines (193) and papillary carcinoma of the thyroid (194).

There are conflicting reports in the hypoxia literature regarding HGF itself. In HepG2 cells, HGF stimulation was found to increase HIF-1 α transcription and translation in an NF- κ B-dependent mechanism (195). Increased *PAI-1* and *uPA* expression was also observed in HGF-treated HepG2 cells (196), and this was dependent on HIF-1 α activation downstream of PI3K/JNK (197). Studies of HGF in hypoxic non-cancer cells are minimal. In vascular smooth muscle cells and in endothelial cells, hypoxia decreased HGF at both mRNA and protein levels (198). The hypoxia mimetic CoCl₂ was shown to down-regulate HGF mRNA in cultured rat cardiac myocytes (199). When exposed to anoxic culture, a dramatic decrease was observed for HGF in myofibroblastic hepatic stellate cells and for *met* in primary rat hepatocytes (129). Furthermore, addition of HGF to cultured aortic endothelial cells (200) and primary hepatocytes (201) rescued them from hypoxia-induced apoptosis. These studies, though ambiguous, tend to support a cytoprotective and anti-apoptotic role for HGF in hypoxic conditions.

5.1.3 Epidermal growth factor (EGF) in liver regeneration

Compared to the simplicity of the HGF-*met* (single ligand-single receptor) system, the relationship of the EGF receptor (EGFR) and its ligands is quite complicated. EGFR was the first receptor demonstrated to play a role in liver regeneration. A seminal report by Rubin *et al.* (202) showed that EGFR was phosphorylated and down-regulated following PHx. In reality, there are four EGFR family members: ErbB (HER), ErbB-2 (HER-2, NEU), ErbB-3 (HER-3), and ErbB-4 (HER-4) (203, 204). Of these, HER-4 does not appear to be expressed in adult or embryonic liver (205). Aside from EGF, there are many ligands for EGFR, including transforming growth factor alpha (TGF α), amphiregulin (AR), heparin-binding EGF (HB-EGF), cripto, epiregulin and betacellulin (206, 207).

5.1.3.1 Crosstalk between hypoxia and EGF pathways:

Involvement of the EGF/EGFR pathway in hypoxia signaling is less clear. Hypoxia has been shown to increase expression of AR (208) and HB-EGF (209). Hypoxia and EGF can synergistically enhance VEGF expression and angiogenesis in a number of cancer types (210, 211); however, some studies report that this mechanism involves hypoxia-independent stabilization of HIF-1 α protein via phosphorylation (54, 212, 213). As with HGF, EGF has also been shown to rescue cells from hypoxia-induced apoptosis (214-216). In addition, studies of HB-EGF demonstrated cytoprotective effects on intestinal epithelial cells exposed to hypoxia (217, 218). These findings may point to a role for EGF in cell survival during hypoxic stress.

5.1.4 Purpose of the experiments conducted in this chapter

Classic experiments in muscle, correlating mean capillary density to increased metabolic demand (219), have shown that angiogenesis can be regulated specifically by O₂ availability. Due to the significant role of hypoxia in this process, it is not surprising that HIF-1 α can induce multiple genes involved in induction, sprouting, and maintenance of blood vessels. Liver revascularization is a well-characterized process in which a number of known HIF target genes are up-regulated, yet as can be inferred from the HIF literature, very little is known about the regulatory role of HIF-1 α in this normal angiogenic response. Most of the pioneering work on HIF-1 α was done in tumor cell lines (8, 10); however, its functional role in liver, if any, is still unclear. Due to the liver's zoned architecture, a physiologic O₂ gradient exists between periportal (high O₂) and peri-venous (low O₂) regions. Consequently, the liver may provide an ideal setting for the study of hypoxia-induced genes and O₂-dependent zonation of hepatic functions.

In the experiments we are about to describe, we investigated the role of HIF-1 α in regenerating rat liver following PHx. We further attempted to identify potential mechanisms of HIF-1 α regulation in primary rat hepatocyte cultures. These *in vitro* studies were initially designed to examine hypoxia-dependent induction of HIF-1 α in hepatocytes, which could then activate VEGF transcription and support SEC proliferation. Due to the extensive repertoire of growth factors that peak during liver regeneration, we expanded our *in vitro* exploration to include hypoxia-independent induction of HIF-1 α by growth factors. Finally, we performed

microarray gene expression analysis to identify hypoxia-induced genes in primary rat hepatocytes. In this chapter, we provide further evidence that HIF-1 α is not a key regulator of liver revascularization, nor does it play any discernable major role in the response of hepatocytes to hypoxia.

5.2 RESULTS

5.2.1 HIF-1 α is undetectable in regenerating rat liver.

In order to study HIF-1 α induction in liver regeneration, we isolated nuclear extracts from frozen rat liver tissues harvested at the following time-points after 70% PHx: 0, 1, 3, 6, and 12 hr.; 1, 2, 3, 4, 5, 6, and 7 days. HIF-1 α western blots were performed repeatedly using 20-50 μ g of nuclear extracts and 1:100 dilution of various primary antibodies (using those in Table 4 of [3.2 Methods](#) chapter, as well as several rabbit polyclonals); however, no HIF-1 α was ever detected in the Western blots of these samples. To further identify any presence of HIF-1 α in regenerating rat liver, we performed immunohistochemistry on paraffin sections (formalin-fixed or zinc-fixed) and immunofluorescence staining on frozen sections (snap-frozen or perfusion-fixed). After repeated experiments, we could not conclusively detect nuclear HIF-1 α in these samples.

5.2.2 Absence of nuclear HIF-1 α induction in primary rat hepatocyte cultures.

In hypoxic cultures of rat hepatocytes, we were unable to detect nuclear localization of HIF-1 α protein via immunofluorescence, immunocytochemistry, or Western blots of 50-100 μ g of nuclear proteins (as described in the previous chapter). We also obtained negative results even when hepatocytes were cultured and harvested over time in a sealed Hypoxic Culture System, fitted with an airlock transfer chamber and an O₂-controlled glove box (Coy Lab Products, Grass lake, MI; courtesy of Billiar lab). Ideally, this system provided us with several advantages for studying HIF-1 α . First, culture plates were transferred in and out of the incubator, so that a

number of time-points could be analyzed in a single experiment. Second, the transfer chamber allowed equilibration of all buffers and media to 1% O₂ in <3 min., and solutions were bubbled with this gas to further deoxygenate them. Third, the sealed glove box, also maintained at 1% O₂ and 37°C, allowed for media changes, harvesting, and other manipulations without exposing the cultures to room air. All of these features provided us with a prudent but efficient system for studying HIF-1 α *in vitro*, since it has been shown that reoxygenation of anoxic culture medium can occur within two minutes of exposure to room air (220). Despite these painstaking efforts, we still could not detect HIF-1 α nuclear protein using this custom-built Hypoxic Culture System; although, we were consistently able to detect expression *HIF-1 α* mRNA at the time-points analyzed (Figure 23). This discrepancy may be due to the rapid kinetics of HIF-1 α degradation and its post-translational regulation by the more abundant PHDs.

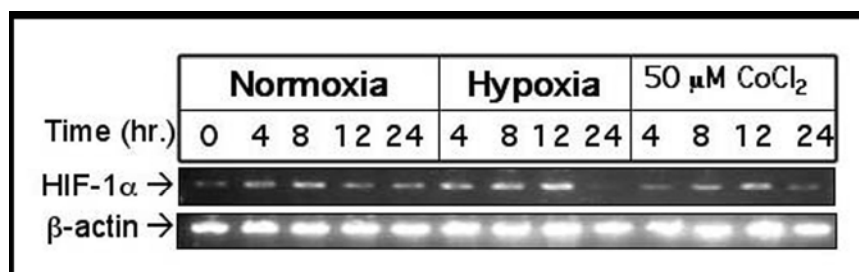


Figure 23: RT-PCR for *HIF-1 α* expression over time. Primary rat hepatocytes cultured in hypoxic conditions (1% O₂) in a sealed Hypoxic Culture System show an increase in *HIF-1 α* mRNA expression over time, which diminishes by 24 hr. in culture. Despite the continuous expression of *HIF-1 α* at the RNA level, we were unable to detect HIF-1 α nuclear protein.

Regarding hypoxia-independent induction of HIF-1 α , we decided to incorporate this in our *in vitro* experiments, due to the massive upregulation of growth factors and their receptors in regenerating liver, which may act preferentially or synergistically with hypoxia. In total, we tested the following factors in culture: HGF, EGF, Dex, ITS, TGF- α , TGF- β 1, AR, PGE2, and VEGF-A (details listed in Table 3 of [3.2.2. Methods](#) chapter). After screening for all of these growth factors via repeated Western blotting and immunofluorescence microscopy, no reproducible change in HIF-1 α was seen despite some early encouraging results.

Since our HIF-1 α experiments repeatedly gave inconsistent results, an additional concern was the possibility that in the short-term, hepatocyte cultures were de-differentiating as soon as the first day after perfusion and isolation. To maintain hepatocytes in a differentiated state over seven days, we supplemented our serum-free HGM with Dex, ITS, and 2% DMSO (221). Based

on hepatocyte morphology, presence of bile canaliculi, and albumin expression (Figure 24), we selected day two cultures to be a well-differentiated phenotype for future experiments. Using confocal immunofluorescence microscopy, we still could not detect HIF-1 α in these well-differentiated cultures; although, nuclear HIF-1 β was constitutive. Furthermore, the HIF regulatory hydroxylases, which are more highly expressed in hepatocytes, were also undetectable. Closer examination revealed abnormal mitochondria in these cells, which was also noted in the original paper by Isom *et al.* (221). Since we are now more familiar with the crucial role of mitochondria in O₂-sensing and redirection (169, 171), it is possible that the DMSO supplementation in some way disrupted essential components of the HIF pathway.

Hepatocyte Cultures Maintained in DMSO

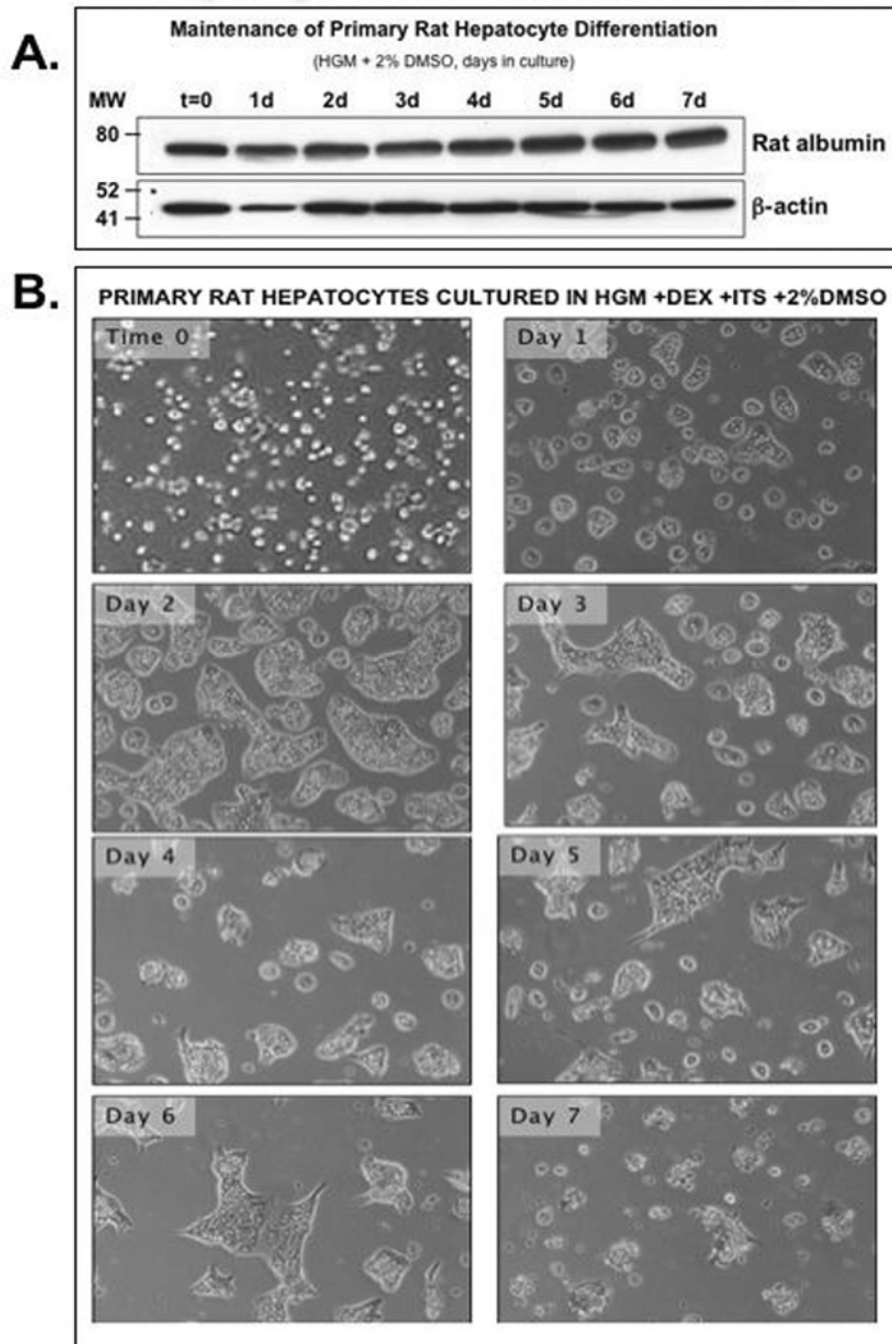


Figure 24: Hepatocyte cultures maintained in DMSO. Primary rat hepatocytes were cultured for one week in serum-free HGM supplemented with Dex, ITS, and 2% DMSO to prevent de-differentiation. **A.** Western blot showing that rat albumin expression was maintained over time. **B.** Hepatocyte morphology appeared well-differentiated on days two and three, and bile canaliculi are readily observed in these cultures.

5.2.3 Analysis of hepatocyte gene expression in response to hypoxia

To further investigate the hypoxia-responsive gene expression profile in primary rat hepatocytes, we performed Affymetrix microarray analysis on total RNA isolated from 4 hr. hypoxic cultures and normoxic controls. A total of 15923 rat genes were probed, including ESTs. As shown in Figure 25, only 2% of these genes were up-regulated by hypoxia, while 12% of the total were down-regulated. Interestingly, 88% of the genes showed no significant changes in 4 hr. hypoxic cultures of primary rat hepatocytes. The eleven highest and lowest expressed genes are listed in Table 8 and Table 9, respectively (the complete data tables have been included in Appendices B and C). Most of the up-regulated genes were unexpected, but some known HIF targets were also increased. However, since we did not detect HIF-1 α protein in our hypoxic cultures, these instead may be induced by primarily by the other HIF- α isoforms which exist in hepatocytes (147).

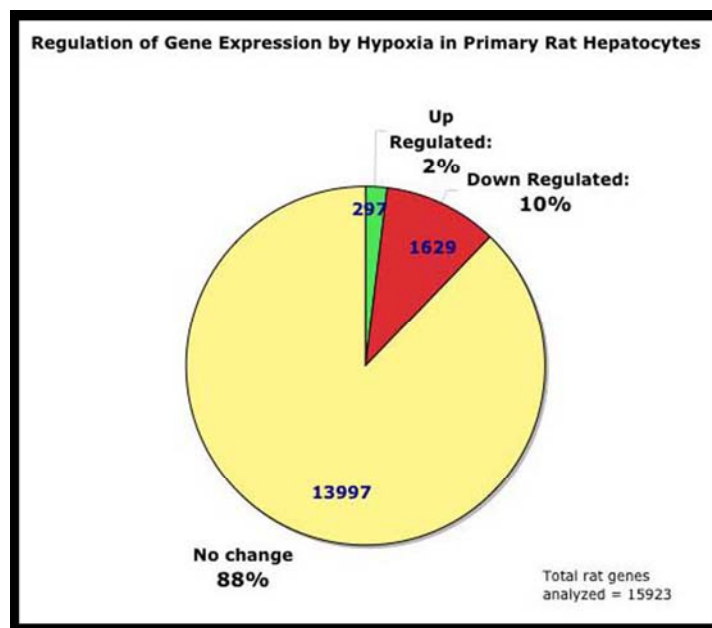


Figure 25: Overview of hypoxic gene expression data. Primary rat hepatocytes were cultured for 4 hr. in hypoxic and normoxic (control) conditions, and total RNA was subjected to Affymetrix analysis using Rat U34A arrays. Data was further analyzed using a fully-functioning demo version of GeneSifter software (<http://www.genesifter.net/web/trial.html>).

Table 8: Genes up-regulated by 4 hr. hypoxia in primary rat hepatocytes.

This list represents the eleven most induced rat genes, showing increased expression of four-fold or higher, as identified by Affymetrix analysis and GeneSifter software. Several of the genes listed are involved in the immune response. *ADM* and *IGFBP-1* are known HIF target genes. Ratio = hypoxic/normoxic signals. Cellular function was obtained from *UniProt* database. (Complete data set is in [Appendix B](#)).

#	Gene Name	Gene Identifier	Ratio	p-value	Cellular Function (UniProt)	Reference (if HIF target)
1	Pineal specific PG25 protein (PG25, ESM1)	NM_022604	7.78	4.52E-02	Endothelial cell-specific molecule 1 precursor; Secreted protein; Potent lung endothelial cell-leukocyte interactions; Pineal gland specific; Contains IGFBP domain.	N/A
2	Macrophage inflammatory protein-1 alpha receptor gene (CCR1, LOC57301)	NM_020542	6.82	7.18E-03	Integral membrane protein of G-protein coupled receptor 1 family; Angiotensin II receptor activity; Rhodopsin-like receptor activity; Receptor for CCL3 chemokine [both contribute to HCC progression (222)].	N/A
3	Granulocyte-macrophage colony stimulating factor (GM-CSF, CSF2)	U00620	6.55	3.46E-02	Secreted cytokine; Stimulates growth and differentiation of hematopoietic precursors from various lineages, including granulocytes/Mφ/eos/RBC.	N/A
4	Adrenomedullin (ADM).	NM_012715	5.26	8.96E-07	HIF-induced in cardiomyocytes; Potent hypotensive and vaso-dilator peptide; Expressed in adrenal glands, lung, kidney, heart, spleen, duodenum and submandibular glands.	(223) (224) (225)

Table 8: Genes up-regulated by 4 hr. hypoxia in primary rat hepatocytes. Continued

#	Gene Name	Gene	Ratio	p-value	Cellular Function (UniProt)	Reference (if HIF target)
		Identifier				
5	Chemokine orphan receptor-1 (RDC1, CMKOR1)	NM_053352	5.26	4.47E-03	Up-regulated by hypoxia in adult rat lung (226); Multi-pass membrane protein of G-protein coupled receptor 1 family; Orphan receptor; Putative calcitonin gene-related peptide (CGRP1) receptor.	N/A
6	Stearoyl-Coenzyme A desaturase-2 (SCD2)	NM_031841	4.90	3.00E-03	aka Acyl-CoA desaturase-2, Fatty acid desaturase-2, Δ9-desaturase-2; ER membrane protein; Metal-binding; Terminal component of liver microsomal stearyl-CoA desaturase system; utilizes O ₂ and e ⁻ from reduced cytochrome b5 to catalyze insertion of a double bond into fatty acyl-CoA substrates, such as palmitoyl-CoA and stearyl-CoA.	N/A
7	IgG Fc receptor III, low affinity (FCGR3)	NM_053843	4.53	6.12E-03	Membrane protein forms multi-subunit complexes; Surface receptor for Fc region of complexed IgG; Expressed on NK cells and Mφ.	N/A
8	Glutaredoxin-1 (thioltransferase) (GLRX1)	NM_022278	4.34	7.84E-05	Cytoplasmic; Has glutathione-disulfide oxidoreductase activity in the presence of NADPH and glutathione reductase; Reduces LMW disulfides and proteins.	N/A

Table 8: Genes up-regulated by 4 hr. hypoxia in primary rat hepatocytes. Continued

#	Gene Name	Gene Identifier	Ratio	p-value	Cellular Function (UniProt)	Reference (if HIF target)
9	Insulin-like growth factor binding protein-1 (IGFBP1)	NM_013144	4.11	1.81E-03	HIF-induced in hepatocytes; Secreted protein binds equally well to IGF1 and IGF2 to prolong their half-life; Can inhibit or stimulate growth-promoting effects of IGFs in cell culture; Alter interaction of IGFs with their cell surface receptors.	(147) (227) (228)
10	Cathepsin K (CTSK)	NM_031560	4.09	8.04E-03	Secreted member of peptidase C1 family; Broad proteolytic activity; Involved in osteoclastic bone resorption and may participate partially in the disorder of bone remodeling; Displays potent endoprotease activity against fibrinogen at acidic pH; May function in ECM degradation.	N/A
11	Activating transcription factor-3 (ATF3, LRF-1)	NM_012912	4.03	5.92E-04	aka Liver Regeneration Factor; cAMP-dependent transcription factor binds to CRE consensus sequences; Rapidly and highly induced in regenerating liver and mitogen-stimulated cells; Also found in skeletal/smooth muscle and some tumor cells.	N/A

Table 9: Genes down-regulated by 4 hr. hypoxia in primary rat hepatocytes.

This list represents the eleven most suppressed rat genes, showing decreased expression of four-fold or higher, as identified by Affymetrix analysis and GeneSifter software. These genes have no published associations with hypoxia. Ratio = hypoxic/normoxic signals. Cellular function was obtained from *UniProt* database. (Complete data set is in [Appendix C](#)).

#	Gene Name	Gene Identifier	Ratio	p-value	Cellular Function (UniProt)
1	Cyclin D (CCND1)	X75207	-8.28	1.09E-02	G1/S-specific cyclin-D1; Essential for control of cell cycle; Interacts with CDK4 and CDK6 protein kinases.
2	Novel kinesin-related protein (KIF1D, KIF1C)	BF417285	-5.99	8.72E-03	Probable molecular motor protein; Belonging to the kinesin-like motor family; involved in Golgi-ER vesicular transport; Regulates podosome dynamics in Mφ.
3	Cytochrome c oxidase subunit VIa polypeptide 2, heart (COX6A2)	NM_012812	-5.39	4.95E-02	Heart/muscle isoform of Cytochrome c oxidase subunit VIa; Mitochondrial inner membrane protein; One of the nuclear-coded polypeptide chains of Cytochrome c oxidase, the terminal oxidase in mitochondrial electron transport.
4	Insulin-like 6 (INSL6)	NM_022583	-4.92	7.25E-03	Secreted insulin-like peptide precursor; Member of insulin family; Specific to testis and prostate; Possible role in sperm development and fertilization.
5	Recoverin (RCVRN)	NM_080901	-4.80	3.03E-05	Ca ⁺⁺ -binding protein in photoreceptor; Controls phosphorylation of the visual receptor rhodopsin by inhibiting rhodopsin kinase (GRK-1); Functions in visual perception of the retina; Also a para-neoplastic antigen in cancer-associated retinopathy.
6	Pepsinogen F protein (PEPF, PGA5)	NM_021753	-4.61	2.52E-03	Zymogen of gastric mucosa; For proteolysis and peptidolysis; Member of peptidase A1 family.
7	Bcl-2 modifying factor (BMF)	NM_139258	-4.55	1.44E-02	Bcl-2 family member; Positive regulator of apoptosis; Interacts with MCL1, BCL2, BCL2L1/BCL-XI and BCL2L2/BCL-w; Interacts with the myosin V actin motor complex through its binding to DLC2; Involved in oligodendroglial differentiation.

Table 9: Genes down-regulated by 4 hr. hypoxia in primary rat hepatocytes. Continued

#	Gene Name	Gene Identifier	Ratio	p-value	Cellular Function (UniProt)
8	Tektin 1 (TEKT1)	NM_053508	-4.46	3.64E-02	Filament-forming protein co-assembled with tubulins to form ciliary and flagellar microtubules; Specific to testes; Found in spermatocytes/spermatids (possible role in spermatogenesis)
9	Calcium-calmodulin-dependent protein kinase phosphatase (PPM1F)	AB023634	-4.28	3.08E-05	Dephosphorylates concomitantly deactivates the critical autophosphorylation site of CaMKII; Partner of PIX2; Found in brain; Promotes apoptosis.
10	G protein-coupled receptor kinase 6, splice variant C (GRK6, GPRK6)	AF040750	-4.13	1.29E-02	Membrane-bound member of Ser/Thr protein kinase family; Specifically phosphorylates the activated forms of G protein-coupled receptors; Expressed in brain.
11	Phosphatidylinositol 3-kinase p45 subunit (PIK3R1)	D64048	-4.08	3.89E-02	Regulatory subunit for PI3K; Structurally similar to p55PIK; Generated by alternative splicing of the p85alpha gene.

5.3 DISCUSSION

Certain organs, such as the kidney (229) and spleen (230) have the limited ability to regenerate after injury; however, the most profound regenerative capacity is observed in the liver. Remarkably, normal liver function is maintained throughout the regenerative process, even as liver mass and structure are restored. Since revascularization is a major component of regeneration, we attempted to investigate the role, if any, of HIF-1 α in the regulation of this normal angiogenic response. Although we attempted repeated experiments with several modifications, we were unable to detect HIF-1 α in regenerating rat liver. Furthermore, as illustrated in this and the previous chapter, we did not observe a strong or consistent nuclear

induction of endogenous HIF-1 α in primary rat hepatocyte cultures, despite the up-regulation of several HIF target genes by hypoxia.

Our results differ from some previous studies of endogenous HIF-1 α in rat liver. For example, Kietzmann *et al.* (146) examined the mRNA and protein localization of HIF-1 α , -2 α , and -3 α in resting rat liver, and found some conflicting results. Increased mRNAs of all three HIFs were located predominantly in the peri-venous hepatocytes. In contrast, nuclear localization of all three HIF proteins was the highest in both peri-portal and peri-venous hepatocytes, which contradicts the well-known physiologic O₂ gradient pattern previously characterized by this group in liver [reviewed in (125, 231)]. A significant cytoplasmic accumulation of all three HIF proteins was localized in the distal peri-venous zone as well, but there was also a basal cytoplasmic HIF-1 α evenly distributed in all hepatocytes. Interestingly, the endothelial cells lining the central vein also expressed the mRNAs and proteins of all three HIFs. It should be noted that the immunolocalization was performed with rabbit polyclonal anti-HIF antibodies generated by their own lab, which are not commercially available. In summary, the authors demonstrated a peri-venous distribution of HIF- α mRNAs, but not proteins. Their explanation for this discrepancy was that peri-portal hepatocytes may be able to manage on the baseline expression and stabilization of cytoplasmic HIF- α protein subunits via post-translational mechanisms, while peri-venous hepatocytes must also rely on transcriptional upregulation of HIFs in order to function.

It should be noted that all *in vitro* HIF studies published by Kietzmann have utilized HIF-1 α over-expression vectors in primary rat hepatocytes, transfected using the method of calcium phosphate precipitation (146, 147, 232-234). None of their published findings are based on endogenous HIF-1 α expression in hepatocytes. They have also recently demonstrated that HIF-2 α and HIF-3 α , but not HIF-1 α , were the predominant activators of hypoxia-induced IGFBP-1 transcription in primary rat hepatocytes co-transfected with each HIF- α expression vector and an IGFBP-1 reporter gene construct (147). Although these latter experiments rely heavily on the extreme case of HIF over-expression in primary cells, they do support our findings indirectly, since we also could not identify a major role for HIF-1 α in hepatocytes.

With regard to the function of HIF in liver regeneration, one published report from Maeno *et al.* (235) claims to have found a significant HIF-1 α expression in regenerating rat liver,

showing a peak in HIF-1 α nuclear protein and mRNA at 24 hr. after PHx. They conclude that this “may be related to sinusoidal endothelial reconstruction,” since it precedes both a transient decrease in liver blood flow and an increase in *VEGF* and *flt-1* expressions.

There are numerous experimental flaws in this paper. First, much of the revascularization data they presented was already published in a previous paper (175). Second, although their PHx series consisted of five rats per time-point, no shams were performed in their experiments. Sham operations are necessary controls when monitoring changes in the first 24 hr. of liver regeneration, and their studies included 6, 12, and 24-hr. time-points. When studying HIF-1 α in particular, sham operations are essential at every time-point studied, since anesthetizing and/or killing the animal can itself be a cause of respiratory depression and tissue ischemia. Third, the authors use β -actin as a housekeeping (loading) control during normalization, even though the β -actin clearly changes during liver regeneration. Fourth, the HIF-1 α immunohistochemistry data is presented at low-power. Only the 24-hr time-point shows the peri-portal region at higher magnification, which is then compared to all of the other time-points shown at lower magnification. Although Maeno *et al.*'s histologic observations are difficult to interpret, they report that the peak in nuclear HIF-1 α was observed only in peri-portal hepatocytes, while the less-oxygenated peri-venous hepatocytes expressed neither nuclear nor cytoplasmic HIF-1 α . These results are contradictory to those of Kietzmann *et al.* (146).

When analyzed in the context of other published reports, our data fit well with the theory that compared to other organs, liver is different in both its response and adaptation to hypoxia. Unlike other organs, the liver receives most of its blood supply from the portal vein, which carries venous blood with lower O₂ tension. The pO₂ of peri-portal blood is 60-65 mm Hg, compared to 100 mm Hg for systemic arterial blood (125). Furthermore, there is a ~50% drop in oxygenation along the sinusoid, such that the pO₂ of peri-venous blood is 30-35 mm Hg (125). As a result, certain regions of the liver are exposed to a mild but chronic hypoxia. The hepatocytes residing in this microenvironment must somehow adapt to this physiologic hypoxia and prevent aberrant HIF-1 α activation when it is not necessary. Consequently, one would expect HIF-1 α induction only in extreme cases of hepatic injury, and not in the relatively benign setting of liver regeneration following PHx.

In light of this possibility, we also performed some additional experiments in more severe liver injury models. It should be noted however, that neither we nor other independent

investigators could detect nuclear HIF-1 α even in cirrhotic livers (data not shown), which are known to contain hypoxic regions with increased VEGF expression, fibrogenesis, and abnormal regenerative capacity (130). Even when we compared post-transplant rat livers *versus* kidneys, both of which had undergone ischemia-reperfusion injury, we were able to demonstrate nuclear HIF-1 α induction only in the kidney but not in the liver (data not shown). The kidney's responsiveness to HIF-1 α activation is not surprising, given its O₂-sensing function in erythropoiesis, when a rapid adaptation to systemic hypoxia causes increased EPO production and red cell mass [reviewed in (160)].

In support of our findings, a very recent study by Bianciardi *et al.* (236) investigated levels of HIF-1 α and apoptosis in the organs of rats exposed to chronic *in vivo* hypoxia (10% O₂ for 2 wk.). Interestingly, while HIF-1 α was markedly increased in brain, gastrocnemius muscle, and the renal cortex, it was undetectable in heart and liver. In the renal medulla, HIF-1 α protein was high in both normoxia and hypoxia. In contrast, apoptosis was significantly increased only in heart; it was undetectable in other organs. Based on these observations, the authors concluded that the response of HIF-1 α in chronic hypoxia can be a sustained phenomenon, but not in all organs. Since each organ has its own O₂ requirement, blood supply, and O₂ consumption (237), it is most likely that each responds differently as well. It should be noted that Bianciardi's data is in contrast to that of Stroka *et al.* (83), who found that in mice exposed to short-term hypoxia (6% O₂ for 12 hr.), there was widespread nuclear labeling of HIF-1 α in hepatocytes (but not endothelial cells), with no pattern of zonal distribution; however, Stroka's experiments relied on the generation of a novel chicken (IgY) polyclonal anti-HIF-1 α antibody that is not commercially available.

In conclusion, despite our extensive attempts to localize HIF-1 α in rat liver, we must conclude that it plays little if any role in the hepatic response to hypoxia. The other possibility is that the highly unstable nature of HIF-1 α protein results in a rapid and transient response; however, our experiments using the sealed Hypoxic Culture System make this highly unlikely, since this incubator has several modifications specifically designed to maintain hypoxic conditions throughout the HIF experiments. Furthermore, we have observed nuclear localization of HIF-2 α and HIF-3 α in the previous chapter, suggesting that these HIFs may be the more active isoforms in the liver.

Due to the liver's unique relatively low-O₂ blood supply and zoned O₂ gradient, the absence of HIF-1 α activation may provide a reasonable adaptation to the chronic physiologic hypoxia for hepatocytes in the liver microenvironment. If hepatocytes were dependent on regulating the anoxia pathways in the same manner as other cell types, hepatocytes would respond as though they were continually in a hypoxic state. Our results suggest that hepatocytes have instead adapted to a chronic hypoxic environment by “dampening” the conventional HIF-1 α -dependent responses seen in other cells; moreover, hepatocytes have transferred the regulation of HIF-1 α from nucleus/cytoplasm to peroxisomes. The latter are most likely the sites within peri-venous hepatocytes with the highest O₂ tension. This renders them as perhaps the only sites in which the relatively “hypoxic” hepatocytes can still find enough O₂ to allow the PHD enzymes to function and to regulate HIFs as though the rest of the cell was in a standard normoxic environment. Potential mechanisms on this theory of “O₂ redirection” will be addressed further in [Chapter 6](#).

5.4 ACKNOWLEDGEMENTS

We greatly appreciate our colleagues for their technical assistance and helpful discussions: William Bowen, Mark Ross, Dave Gallo, Dr. Jianhua Luo, and Dr. Russ Delude.

6.0 DISCUSSION

6.1 SUMMARY

In this study, we analyzed the localization of endogenous HIFs and their regulatory hydroxylases in primary rat hepatocytes cultured under hypoxia-reoxygenation conditions. We observed an absence of nuclear HIF-1 α activation in hypoxic hepatocytes, even though several known HIF target genes were upregulated, suggesting that HIF-2 α and HIF-3 α may be the predominant active transcriptional isoforms in these cells. We show that in hepatocytes, hypoxia-reoxygenation targets HIF-1 α to the peroxisome rather than the nucleus, where it co-localizes with VHL and the HIF hydroxylases. We further demonstrated that the HIF hydroxylases can translocate from the nucleus to the cytoplasm in response to hypoxia, with increased accumulation in peroxisomes upon reoxygenation. Surprisingly, in resting liver tissue, perivenous localization of the HIF hydroxylases was detected, consistent with areas of low pO₂. This was in contrast to nuclear HIF-1 α , which was undetectable in resting liver, regenerating liver, and even in liver injury models. Alterations in subcellular localization may provide an additional point of regulation for the HIF pathway in response to hypoxia. These data establish the peroxisome as a highly relevant site of subcellular localization and function for the *endogenous* HIF pathway in hepatocytes.

6.2 POTENTIAL MECHANISMS OF PEROXISOMAL LOCALIZATION

6.2.1 The peroxisome as a site of PHD activity

We have identified dynamic changes in subcellular localization of both hypoxia-inducible factors and the HIF regulatory hydroxylases utilizing hypoxic cultures of primary rat hepatocytes. Specifically, we observed peroxisomal localization of HIF-1 α and HIF-3 α in our hypoxia-reoxygenation experiments, and this can now be viewed in parallel with the peroxisomal localization of HIF hydroxylases under identical conditions. The absence of hypoxic nuclear induction of HIF-1 α in primary rat hepatocytes may be attributed to its rapid post-translational degradation pathway, which involves the highly abundant PHDs. The question still remains as to whether these enzymes are actively hydroxylating key proline residues in peroxisomes.

Prior to the discovery of PHD enzymes, collagen was the only known hydroxyproline-containing protein. Unlike the collagen prolyl 4-hydroxylase (P4H), a HIF-induced enzyme which acts on the tripeptide X-pro-gly, the HIF PHDs require a much longer (~19mer) minimal HIF-derived peptide for optimal activity (60). Furthermore, each PHD may preferentially hydroxylate one or both of the two proline residues in the HIF-1 α ODDD, suggesting specialized roles for acute and chronic adaptation (60). The actions of PHDs on HIFs are also not equivalent. PHD2 was found to selectively hydroxylate HIF-1 α more than HIF-2 α , while PHD3 had the exact opposite effect (110). There is currently a short but growing list emerging for O₂-dependent hydroxylation of non-HIF proteins by PHDs and FIH-1, such as the large subunit (Rbp1) of RNA polymerase II (162). Even though the PHDs are highly conserved and ubiquitously expressed, there is also evidence of alternative splicing, with some splice variants no longer capable of hydroxylating HIF- α (60).

Numerous hydroxylases exist in peroxisomes as well as in the bile canaliculi, where PHD1 also co-localized. In very preliminary experiments, we did note a peroxisomal pool of hydroxylated HIF-1 α in hypoxic hepatocytes (data not shown) using a rabbit polyclonal antibody (gift of Dr. Ya-Min Tian, Oxford University) which detects hydroxylated HIF-1 α over unhydroxylated forms in a ratio of 9:1 (238); however, further confirmatory studies are necessary. Although this may be promising, we are uncertain if any of the HIF hydroxylases sequestered in

peroxisomes still retain their activity, and if so, what their potential substrates may be for hydroxylation. In the case of the non-conventional peroxisomal enzyme iNOS, the fraction of iNOS sequestered in peroxisomes is an inactive monomer, perhaps functioning to protect hepatocytes from incompetent enzyme (154). This scenario may also apply to the HIF hydroxylases. PHDs are non-equilibrium enzymes, since they do not catalyze the reverse reaction (110). Consequently, the control of enzyme abundance, as in sequestration, would be a major determinant of substrate hydroxylation and ultimately HIF regulation.

On the other hand, phytanoyl Co-A hydroxylase is a classic PTS2-containing enzyme which leads to Refsum's disease if defective (163). Not only is phytanoyl Co-A hydroxylase active in peroxisomes, it is actually a member of the same O_2 -, Fe^{2+} -, and 2-oxoglutarate-dependent oxygenase family as the HIF hydroxylases; therefore, within the peroxisomal milieu there does exist the co-factors required for PHD and FIH-1 activity (164).

Unfortunately, standard hydroxyproline assays cannot be used to monitor PHD activity, since they may be influenced by other confounding proteins such as collagen. Furthermore, since hydroxylated HIF-1 α is an intermediate for degradation, the results of such assays may be unreliable due to protein instability and rapid turnover. Although rabbit polyclonal antibodies have been generated by several labs to hydroxylated HIF-1 α at either hydroxyproline positions -402 or -564 (238-241), these are still not commercially available. Biochemical techniques for measuring hydroxylated HIF peptides *in vitro* have provided an alternate method for studying the activity of recombinant PHDs over-expressed in cell culture (60); however, this can be technically challenging for testing enzymatic activity of *endogenous* HIF hydroxylases in intact peroxisomes, especially when working with primary cells. Until a more efficient method is developed and standardized, the potential enzymatic activity of peroxisomal HIF hydroxylases will remain unresolved.

6.2.2 O_2 zonation in the liver (i.e., "How is liver different?")

The significance of our subcellular localization findings can be further extrapolated to the liver's microenvironment, where hepatocytes and neighboring cells are exposed to a physiologic gradient of O_2 and other nutrients from the portal circulation. Not only does the portal vein contribute significantly to the liver's blood supply, there is a ~50% drop in pO_2 along the course

of the sinusoid toward the central vein, from 60-65 mm Hg (afferent) to 30-35 mm Hg (efferent) (157). Since basal HIF-1 α is constitutively expressed but rapidly degraded, there must exist a mechanism to poise the cell for swift responses to hypoxic insult, while at the same time keeping nuclear levels of HIF-1 α in check when not needed.

In most cells including transfected primary rat hepatocytes, PHD2 functions as the “chief” O₂ sensor, maintaining low levels of HIF-1 α in normoxic and mildly hypoxic conditions (49, 147). Nuclear HIF hydroxylases are thought to participate in the regulation of HIF-1 α turnover and activity, since the degradation of HIF-1 α can occur with the same half-life in both the nucleus and the cytoplasm (158). This indicates that, unlike p53 which must exit the nucleus prior to its degradation, both nuclear and cytoplasmic proteasomes are fully competent to degrade HIF-1 α in an O₂-dependent manner, thereby preventing even ongoing HIF transcriptional activity. Moreover, *in vitro* enzyme kinetics assays have found that PHD2 and PHD3 possess the highest relative prolyl hydroxylation activities (159), suggesting that the robust expression of these enzymes in resting liver would counter-act much of the HIF-1 α activity one would have expected to find in peri-venous hepatocytes. This would explain some of the paradoxical findings reported by Maeno *et al.* (235) and Kietzmann *et al.* (146) in rat liver.

6.2.3 O₂-redirection hypothesis

The *in vitro* hypoxia-reoxygenation model utilized in our experiments alters key parameters necessary for HIF hydroxylase function. A potential mechanism for HIF hydroxylases targeting to the peroxisome may involve the O₂-redirection hypothesis [reviewed in (165)]. Inhibition of mitochondrial respiration may lead to subcellular redirection of O₂ from mitochondria to non-respiratory O₂-dependent compartments (Figure 26). A very recent study by Papandreou *et al.* (169) in cell lines has shown that HIF-1 can actively down-regulate mitochondrial O₂ consumption by repressing the tricarboxylic acid (TCA/Citric Acid/Kreb's) cycle. This results in adaptation to hypoxia, since mitochondrial O₂ redistribution leads to a relative increase in intracellular O₂ concentration and availability. The effects of HIF-1 on mitochondria were found to be functional, not structural, and decreased cell death was observed in chronic hypoxia.

Furthermore, since HIF-1 induces the expression of glycolytic genes, increased glycolysis would be necessary to produce energy when low O₂ could not support oxidative phosphorylation within the mitochondria.

Other groups have also linked the TCA cycle as a “metabolic switch” for cellular adaptation to hypoxia (170, 171, 242). Selak *et al.* (170) identified a mitochondria-to-cytosol signaling pathway that links mitochondrial dysfunction to oncogenic events. In this case succinate, which accumulates as a result of succinate dehydrogenase (SDH) inhibition/mutations in tumor cells, inhibits the PHDs in the cytosol, since increased succinate results in decreased activity of TCA cycle enzymes via negative feedback. This results in less production of the intermediate 2-OG (α -KG). The shortage of 2-OG, a required co-factor for HIF hydroxylases, inhibits PHD activity and leads to stabilization and activation of HIF-1 α . HIF overexpression has also been reported with biallelic loss of fumarate hydratase in hereditary RCC, where excess fumarate acts as a competitive inhibitor of PHDs (243).

In hepatocytes, the three major subcellular sites of O₂ consumption are mitochondria, peroxisomes, and smooth ER; however, only mitochondria are coupled to oxidative-phosphorylation and ATP synthesis. Although they are present in all eukaryotic cells except mature erythrocytes, peroxisomes are particularly abundant in hepatocytes, constituting ~1% of the total cell volume and consuming 10-30% of O₂ in resting liver (166). Since peri-venous hepatocytes are exposed to low O₂ and glucose concentrations, their capacity for oxidative-phosphorylation is reduced. Subcellular O₂ could be shunted to peroxisomes, and this would account for the increased peri-venous localization of HIF hydroxylases in resting liver.

The added stress conditions of hypoxia-reoxygenation on hepatocytes could exaggerate the redistribution of subcellular O₂ to peroxisomes, and as the cell’s chief O₂ sensors, PHDs would also shuttle by an unknown mechanism to the peroxisomal O₂ sink. Inhibitors of mitochondrial respiration such as NO have been shown to increase PHD activity and decrease HIF-1 α in hypoxia, due to subcellular O₂ redirection from mitochondria (167, 168). Furthermore, H₂O₂ and O₂^{-•} are the predominant ROS exported from mitochondria, but since the majority of O₂^{-•} is dismutated to H₂O₂, a rather constant flow of H₂O₂ is generated by mitochondria, accounting for ~40% of the liver’s total H₂O₂ production (244). Due to its membrane permeability, H₂O₂ would require detoxification by peroxisomal catalase, leading to the formation of H₂O and more molecular O₂.

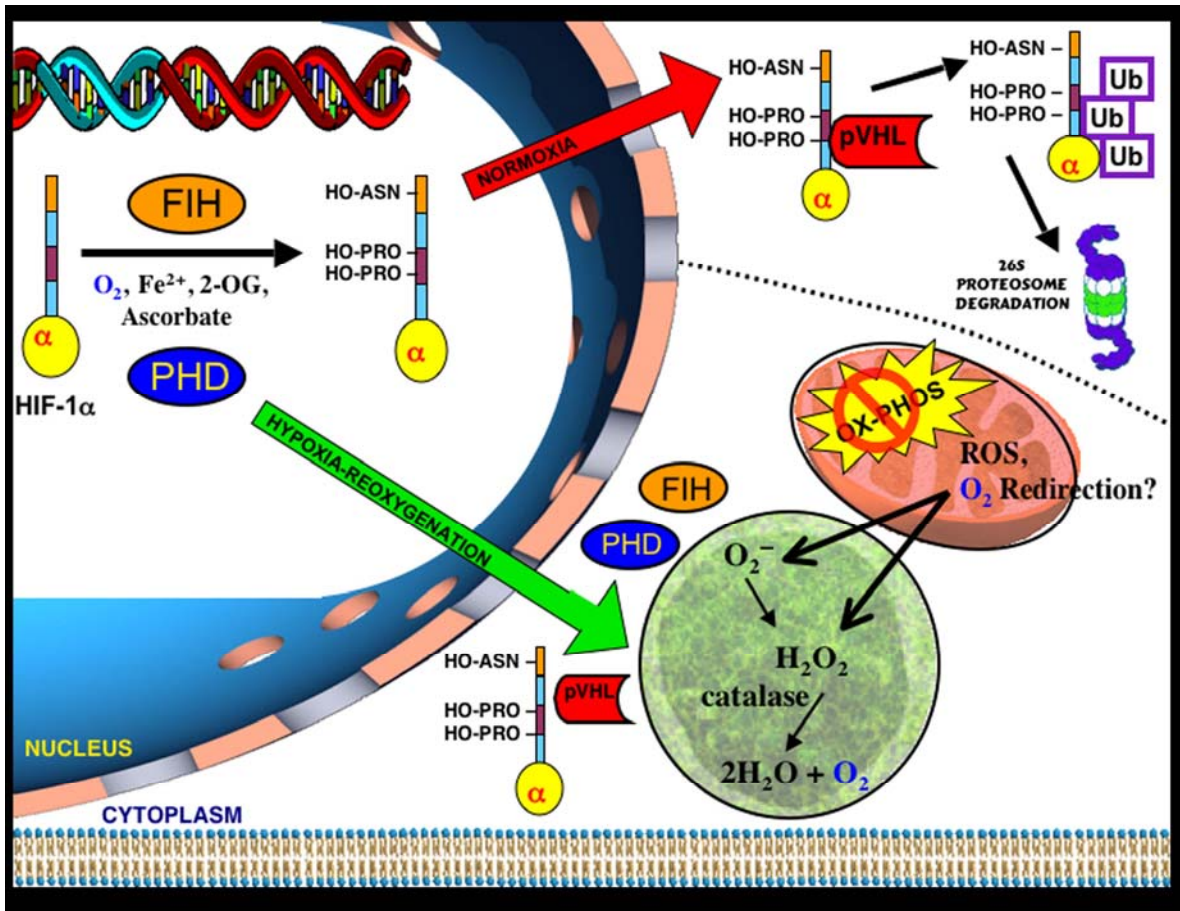


Figure 26: Peroxisomes as a potential site of oxygen-redirection in hepatocytes. Potential interactions of the HIF pathway with peroxisomes are illustrated. When O_2 is abundant, HIF hydroxylases reside in the nucleus, where they actively hydroxylate HIF-1 α for subsequent degradation. Inhibition of mitochondrial respiration by hypoxia may lead to subcellular redirection of O_2 from mitochondria to non-respiratory O_2 -dependent compartments, such as peroxisomes in liver. Hypoxia-reoxygenation would lead to an increase in ROS, including H_2O_2 , which would then be detoxified in peroxisomes by catalase. Since O_2 is a product of this reaction, peroxisomes can be considered as a major site of both O_2 production and consumption. Such an O_2 sink could be “sensed” and targeted by the HIF hydroxylases.

All of this could contribute to the peroxisome functioning as an O_2 sink even in resting hepatocytes. Since these organelles are not as abundant in other cell types, previous localization studies may have been unable to discern the distinct peroxisomal localization of endogenous HIF hydroxylases that we have observed in hepatocytes. It should be noted however that several protective mechanisms must work in concert to defend the liver against hypoxic insult and maintain its remarkable regenerative capacity. For example, ischemia/reperfusion injury

experiments performed on rat liver have shown that although catalase activity was reduced, the activities of most other peroxisomal anti-oxidants actually increased or remained the same (245). Of course, any of these protective enzymes can be saturated by the over-production of free radicals, and a mounting debate still exists regarding the precise role of ROS in HIF regulation itself.

6.3 FUTURE DIRECTIONS

6.3.1 Examination of putative peroxisomal targeting sequences (PTS sites)

To extrapolate on potential mechanisms for these proteins shuttling into peroxisomes, we analyzed the peptide sequences of these enzymes for putative peroxisomal targeting sequences (PTS1 or PTS2), consensus sequences which are involved in peroxisomal import [reviewed in (150)]. PTS1 is located at the extreme C-terminus of most known peroxisomal matrix proteins, and it contains a conserved tripeptide (Ser-Lys-Leu-COOH); although, a number of acceptable substitutions can exist. PTS2 is an alternate localization sequence found on the N-terminal half of some peroxisomal enzymes, and it consists of (Arg/Lys)-(Leu/Val/Ile)-X₅-(His/Glu)-(Leu/Ala). PTS1 and PTS2 are recognized by the peroxisomal import receptors (peroxins) Pex5 and Pex7, respectively. We identified a number of putative PTS1 and PTS2 sites in the primary sequences of some of our proteins, as summarized in Table 10 and Table 11. Of those listed in Table 10, VHL has a 100% canonical PTS2 import sequence in the N-terminal side of the middle of the molecule, making this PTS site the most potentially active among the protein sequences we compared. It should be noted however that other proteins have been described that target to the peroxisome with similar, but non-conventional PTS sequences. In fact, very large protein oligomers lacking PTS motifs have been shown to “piggy-back” onto other conventional peroxisomal proteins and gain entry into the peroxisomal matrix in their native configuration (155).

Table 10: Analysis of putative PTS1 sequences in members of the HIF pathway.

Accepted Sequence(s)		PTS1 Sequence (Pex5) Canonical C-Terminus				Accession Number	Comments
			S, A, L, C	K, H, R	L, M		
Protein	Species	-4	-3	-2	-1		
Urate Oxidase	Rat	P	S	R	L	NP_446220	303 AA Canonical PTS1
Catalase	Rat	K	A	N	L	NP_036652.1	527 AA Non-canonical PTS1
PHD1	Rat	S	K	D	V	AY228140	223 AA Extra AA at C-Terminus; Potential Terminal AA at -2 unlike substitution
PHD2	Rat	S	K	D	V	P59722	222 AA Extra AA at C-Terminus
PHD3	Rat	L	A	K	D	Q62630	355 AA Terminal AA non-conventional, unlike substitution
PHD4	Human	R	V	E	L	Q9NXG6	502 AA No Consensus
	Mouse	R	V	E	L	Q8BG58	503 AA No Consensus
FIH-1	Rat	G	R	Y	N	XP_219961	349 AA No Consensus
HIF-1 α	Rat	D	Q	V	N	NP_077335	823 AA No Consensus
HIF-2 α	Rat	D	Q	A	T	CAB96612	874 AA No Consensus
HIF-3 α	Rat	A	Q	T	H	Q9JHS2	662 AA No Consensus
VHL	Rat	E	G	V	H	AAA86874.1	184 AA No Consensus

Rat sequences are not available for PHD4 at this time.

Other proteins that target to the peroxisome with similar, but non-canonical PTS1 signals:

1. iNOS (-TRL): Barroso *et al.*, *J Biol Chem* 1999;274:36729-36733; Stolz *et al.*, *Hepatology* 2002;36:81-93; Loughran *et al.*, *PNAS*, 2005;102(39)13837-13842.
2. Acetoacetyl-CoA thiolase (-QKL): Olivier *et al.*, *J Lipid Res.* 2000; 41:19211935.
3. Isopentenyl diphosphate dimethylallyl diphosphate isomerase (-HRM): Paton *et al.*, *J Biol Chem* 1997; 272:18945-18950.

Table 11: Analysis of putative PTS2 sequences in members of the HIF pathway.

Accepted Sequences Protein/Species	PTS2 Sequence (Pex7)					Canonical (other active substitutes) Comments:
	R/K (S)	L/V/I	X _n	H/Q	L/A (V,E,F)	
Acetyl-CoA C-acyltransferase A35725/Rat	R	L	X ₅	H	L	100% PTS2 Sequence N-Terminus of molecule
Catalase NP_036652.1/Rat	R	I	X ₅	H	A	100% PTS2 Sequence N-Terminus of molecule
PHD1 AY228140/Rat	R	V	X ₅	S	V	At C-Terminus, (2 nd half of molecule)
	K	I	X ₅	K	E	At N-Terminus (1 st half of molecule)
PHD2 P59722/Rat	R	I	X ₄	K	A	In C-Terminus, (2 nd half of molecule)
	K	I	X ₅	K	E	At N-Terminus (1 st half of molecule)
PHD3 Q62630/Rat	R	L	X ₅	C	V	At N-Terminus (1 st half of molecule)
	R	L	X ₅	K	E	In middle of molecule
	R	I	X ₅	S	F	At C-Terminus (2 nd half of molecule)
	C	V	X ₅	Q	L	In middle of molecule
	P	L	X ₅	Q	A	At N-Terminus (1 st half of molecule)
	K	V	X ₄	W	L	At N-Terminus (1 st half of molecule)
	K	I	X ₄	I	V	In middle of molecule
PHD4 Q8BG58/Mouse	R	L	X ₅	Q	M	In middle of molecule
	R	L	X ₅	L	A	In middle of molecule
	Q	V	X ₅	H	F	At N-Terminus (1 st half of molecule)
	V	V	X ₄	H	F	At N-Terminus (1 st half of molecule)
FIH-1 XP_219961/Rat	R	L	X ₅	R	A	At N-Terminus (1 st half of molecule)
	K	I	X ₅	G	F	In middle of molecule
	K	W	X ₅	Q	E	At N-Terminus (1 st half of molecule)
HIF-1α NP_077335/Rat	S	L	X ₅	V	L	In middle of molecule
	R	L	X ₅	R	V	At N-Terminus (1 st half of molecule)
	R	V	X ₅	D	A	At N-Terminus (1 st half of the molecule)
	R	V	X ₅	K	A	In C-Terminus, not likely candidate
	R	V	X ₄	S	E	In C-Terminus, not likely candidate
	S	I	X ₄	H	A	100% but 4 AA separation, middle of molecule
	R	I	X ₅	Y	E	In middle of molecule
	K	L	X ₄	D	L	At N-Terminus (1 st half of molecule)
	K	L	X ₅	S	L	In middle of molecule
	K	L	X ₄	K	L	In middle of molecule
	K	L	X ₅	E	A	In middle of molecule
	K	V	X ₅	H	I	In middle of molecule
	R	S	X ₅	H	A	In middle of molecule
	S	I	X ₄	H	A	100% but 4 AA separation, middle of molecule

Table 11: Analysis of putative PTS2 sequences in members of the HIF pathway. Continued

Accepted Sequences	PTS2 Sequence (Pex7)					Canonical (other active substitutes) Comments:
	R/K (S)	L/V/I	X _n	H/Q	L/A (V,E,F)	
HIF-2α CAB96612/Rat	S	L	X ₅	N	F	In C-Terminus, not likely candidate
	R	L	X ₅	F	E	In C-Terminus, not likely candidate
	R	L	X ₅	S	E	At N-Terminus (1 st half of molecule)
	R	L	X ₅	E	A	In middle of molecule
	K	L	X ₅	Y	E	In C-Terminus, not likely candidate
	K	V	X ₅	Q	V	100% Canonical but at N-Terminal half
	K	I	X ₅	L	F	In middle of molecule
	R	S	X ₅	H	A	In middle of molecule
	E	V	X ₅	H	E	At N-Terminus (1 st half of molecule)
	K	L	X ₄	Q	L	In C-terminus, not likely candidate
HIF-3α Q9JHS2/Rat	S	L	X ₅	R	R	In middle of molecule
	S	L	X ₅	H	E	100% Canonical but at C Terminus, not likely candidate
	S	V	X ₅	S	L	In C-terminus, not likely candidate
	R	V	X ₅	V	L	In middle of molecule
	K	V	X ₅	H	M	In middle of molecule
	S	E	X ₄	H	L	At N-Terminus (1 st half of molecule)
T	I	X ₄	H	F	In C-terminus, not likely candidate	
R	A	X ₅	H	E	In C-terminus, not likely candidate	
vHL AAA86874.1/Rat	R	I	X ₅	H	L	100% canonical, middle of molecule
	R	L	X ₅	S	L	In middle of molecule

6.3.2 Pex mutants

In yeast, the mechanism of peroxisomal import and biogenesis has been described in detail. Proteins targeted to the peroxisome are docked at the peroxisomal membrane after binding in the cytoplasm to Pex5 or Pex7. It is unclear whether peroxisomal shuttling of HIF components is facilitated by these receptors. Directly silencing PTS sequences and/or *Pex* genes may shed light on whether the HIF pathway localizes to peroxisomes via conventional mechanisms; however, transfection methods for primary rat hepatocytes are often inefficient and even cytotoxic, especially when compounded with the added stress of hypoxic culture.

Although peroxisomes are particularly abundant in hepatocytes, these organelles are present in all eukaryotic cells except mature erythrocytes (166). The availability of human fibroblast cell lines which lack functional peroxisomes may provide us with basic insights regarding peroxisomal import. For example, a number of *Pex*-mutant skin fibroblasts are

available, which have been immortalized from patients with Zellweger (Cerebro-Hepato-Renal) syndrome, a recessive peroxisomal disease with an incidence of 1 in 25,000 to 50,000 births (246, 247). Zellweger syndrome is the most severe form of peroxisomal disorders—it is apparent at birth and results in death within the first year of life. The Zellweger cell lines we have acquired include mutants which lack Pex5, Pex7, and Pex5/Pex7, so that both conventional and non-conventional import pathways can be considered. Non-human *Pex*-mutant cell lines have also been described (248).

Even more relevant is the generation of a *PEX5*^{-/-} knock-out mouse, whose biochemical, serological, and pathological parameters are similar to those found in Zellweger patients (247, 249, 250). Functional peroxisomes are not detected in the livers of these mice, and instead the non-imported catalase is mislocalized to the cytoplasm and nucleus. Structural and functional alterations of mitochondria were also observed, leading to dysfunction of the respiratory chain enzymes and an over-production of ROS. The implications of these liver defects in subcellular localization of the HIF pathway have not been explored.

6.3.3 Conditional knock-outs

As mentioned earlier, VHL has a 100% canonical PTS2 import sequence in the N-terminal side of the middle of the molecule, making this PTS site the most potentially active among the protein sequences we examined. We observed an increase in peroxisomal VHL following hypoxia-reoxygenation, which co-localized with HIF-1 α . Our results for VHL in hepatocytes are intriguing given that Groulx and Lee (149) found in HeLa cells that VHL engages in a constitutive nuclear-cytoplasmic shuttle unaffected by pO₂ or levels of nuclear HIF- α substrate. Theoretically, VHL could gain entry into the peroxisome while complexed with HIF-1 α and its associated HIF hydroxylase(s), and hydroxylated HIF-1 α may serve as an intermediate between them.

Although homozygous disruption of *VHL* in mice results in embryonic lethality at E9-E11, liver-specific conditional knock-outs have been generated using albumin-*cre-loxP*-mediated recombination (156). This results in hepatocyte-specific inactivation of *VHL*. In this model, heterozygous mice developed cavernous hemangiomas in their livers, with an increased incidence at older age (90% of mice at ages 12-17 mos.). Prior to age 12 mos., only 50% of the

mice developed vascular tumors. Over time, the lesions formed large blood-filled vascular cavities, hepatocellular steatosis, and foci of increased vascularization; however, no cancer was ever detected in these animals. In contrast, patients with VHL syndrome rarely develop cavernous hemangiomas of the liver, and renal cell carcinoma is the hallmark of this cancer syndrome.

The *VHL* conditional knock-outs could be incorporated in future studies on peroxisomal import. *In vivo* investigation of the localization of HIFs, PHDs, and FIH-1 could be monitored over time as the cavernous hemangiomas develop. In addition, primary hepatocytes isolated from young and old mice could be subjected to hypoxia-reoxygenation experiments. These models would help clarify the role of VHL, if any, in the peroxisomal import process. Furthermore, since *VHL* inactivation directly affects HIF degradation (and so indirectly the enzyme activity of HIF hydroxylases), it would be a suitable, non-carcinogenic model for studying aberrant angiogenesis in liver pathology.

6.3.4 Regulation of peroxisomal sequestration

It should be noted that due to the limitations of our basic hypoxic chamber (Biospherix), we were only able to study single time-point cultures. By utilizing the more advanced hypoxic chamber/sealed glove box (Coy Labs), additional time course experiments could be performed that monitor the kinetics of peroxisomal import during specific hypoxia-reoxygenation treatments. This system can also be used to adjust the degree of hypoxia by gradually stepping up or down, so that the peroxisomal shuttling can be studied in relation to O₂ concentration, in effect simulating the peri-portal/peri-venous O₂ gradient of the liver (251-255).

As previously mentioned, another aspect of regulation involves the cell's energy status, since metabolic "switching" also effects the HIF pathway. This is especially significant for the liver, since like O₂, key nutrients (*e.g.*, glucose, lipids) and metabolites are also distributed across a gradient supplied by the hepatic portal vein. In our *in vitro* experiments, we have thus far only characterized the effects of one variable, that being O₂. It would be interesting to compare these findings to changes in the required HIF hydroxylase co-factors (Fe²⁺, 2-OG, ascorbate), as well to glucose itself. These experiments would give us a better understanding of the complex

mechanisms governing peroxisomal sequestration in resting liver and in ischemia/reperfusion injury.

6.4 CLINICAL SIGNIFICANCE TO PEROXISOME PROLIFERATION

Understanding HIF regulation is of course necessary for studying liver pathobiology, such as the underlying causes of cold ischemia/warm reperfusion injury or tumor angiogenesis. Our unexpected findings on the peroxisomal localization of the HIF pathway may offer new insights in another mechanism of liver carcinogenesis, involving the peroxisome proliferator activated receptor (PPAR) pathway [reviewed in (256)]. The PPARs were identified in rodents as members of the soluble nuclear receptor superfamily, and they were originally named for their unique property of inducing peroxisome volume and density (peroxisome proliferation) in the liver (257). As shown in Figure 27, PPARs can be activated by natural fatty acids and the fibrate class of anti-hyperlipodemic drugs. PPAR α was the first to be identified, followed by PPAR β/δ and PPAR γ (258, 259) Although the latter two share significant sequence homology with PPAR α , they are not involved in mediating peroxisome proliferation.

PPARs are found in all mammalian species examined to date, and they have evolved as critical physiologic modulators, by responding to endogenous ligands and transcriptionally regulating genes involved in lipid and glucose metabolism and transport, and associated energy homeostasis. Despite these important functions, studies involving hypoxia and PPARs are surprisingly inadequate, and none of these reports have been published for the liver. Zhang *et al.* (260), found that hypoxia increased the mRNA and protein of both PPAR α and HIF-1 α in A549 lung cancer cells; furthermore, this PPAR α induction was decreased after treatment with HIF-1 α anti-sense oligonucleotides. In contrast, hypoxia led to a decrease in PPAR α expression in intestinal epithelial cells, which was directly correlated to increased HIF-1 α binding to an HRE in the PPAR α promoter and also reversed by HIF-1 α anti-sense (261). This is one of the few reports of HIF-1 α directly down-regulating a target gene. In cardiac myocytes, hypoxia was found to indirectly deactivate PPAR α by decreasing RXR α levels, leading to an overall

PPAR Pathway

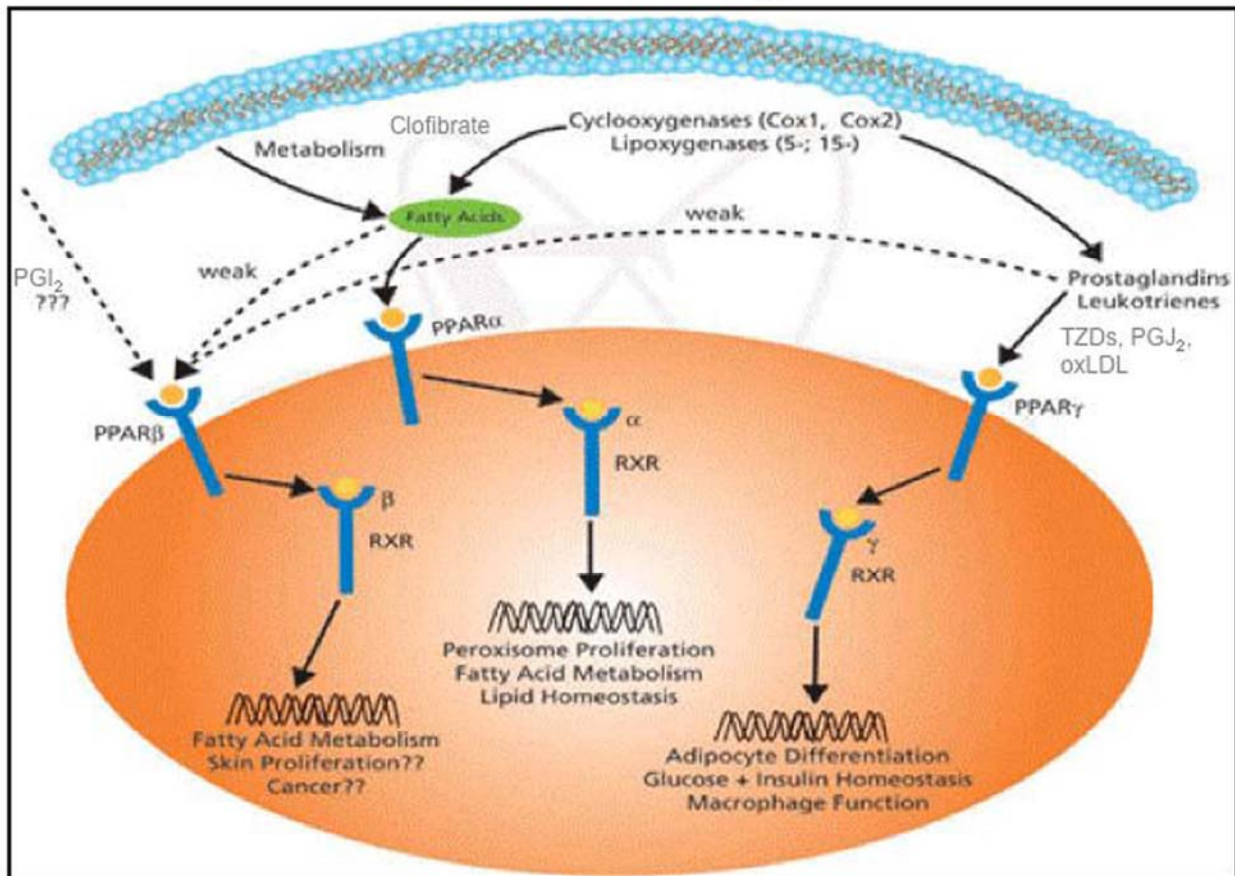


Figure 27: Peroxisome proliferator activated receptor (PPAR) pathway.

In response to ligand binding, PPARs undergo a conformational change in protein structure, allowing for dissociation of co-repressor proteins that inhibit transcription. They then heterodimerize with the nuclear receptor, retinoid-X receptor (RXR), to regulate transcription. Only PPAR α is involved in mediating peroxisome proliferation. Clofibrate is a hypolipodemic agent. Thiazolidinedione (TZD) is an anti-diabetic agent. Note that the connection with COX2/prostaglandins is also important, since these interact with the HIF pathway. One of many pathway slides freely downloadable from *Sigma* for educational purposes. (http://www.sigmaaldrich.com/Area_of_Interest/Life_Science/Cell_Signaling/Scientific_Resources/Pathway_Slides_Charts.html).

reduction in PPAR α /RXR α heterodimer DNA-binding activity (262). Chen *et al.* (263) reported that hypoxia was found to increase levels of HIF-1 α but not PPAR γ in 3T3-L1 adipocytes. Finally, the CBP/p300-interacting protein, CITED2, has been shown to act as a co-regulator of both PPARs and HIF-1 α , since both of these share the same CBP/p300 transcriptional co-activators (264, 265). The significance of these findings to the liver's physiology and zoned metabolic function are unknown.

The most classic finding of PPAR α -induced toxicity is hepatocarcinogenesis, which may be species-specific [(266), reviewed in (267)]. Although the role of PPAR α is well-established as a potent inducer of liver tumors in rodents, there is considerable controversy over whether ligands of PPAR α cause liver cancer in humans. This is significant due to the use of clofibrate and other anti-hyperlipodemic agents, which have been prescribed to patients for over thirty years (268), yet there is no epidemiological evidence that these drugs increase the risk of liver cancer. A plausible explanation for this species-specific difference may be due to the significantly lower levels (10- to 20-fold) of PPAR α in human *versus* rodent liver (269-271).

Of particular concern since the early 1980's is the use of polyvinyl chloride plastics in everyday household items. At least one-third of these plastics contain phthalate esters, liquid plasticizers used in the production of pliable plastic products such as footwear, vinyl toys, hospital I.V. tubing, and blood bags (272). Once phthalates are metabolized to monoesters, they become weak agonists of PPAR α (273, 274). Prolonged administration of phthalates, in doses comparable to those occurring in human exposures, appear to have a cumulative effect on the liver (272), but once again there are species-dependent differences in peroxisome proliferation and frank hepatocarcinogenesis (275, 276). Undoubtedly, the more we learn about the role of peroxisomes in liver pathology, more elusive it becomes.

6.5 CONCLUSIONS

In conclusion, we have identified an unexpected subcellular distribution pattern in hepatocytes in response to hypoxia, where both HIF-1 α and the O₂-sensing hydroxylases which regulate it are all shuttled to the peroxisome, such that nuclear induction of HIF-1 α is undetectable. It would be interesting to elucidate the molecular mechanisms of this import in more detail, and to determine precisely how VHL or other carrier proteins might be involved in hepatocytes. Further consideration should also be given to the effects of metabolic "switching" on subcellular localization. Finally, *in vivo* correlations with ischemia-reperfusion injury and/or peroxisome proliferation models may provide new insights on how HIF regulatory hydroxylases are altered in liver pathobiology. In conclusion, our results suggest a novel site for the regulation of the O₂-

dependent HIF pathway in hepatocytes, and they expand upon the role of peroxisomes as an O₂ sink in the redox microenvironment of the liver.

APPENDIX A

MICHALOPOULOS, G.K., AND **Z. KHAN**. (2005) LIVER REGENERATION, GROWTH FACTORS, AND AMPHIREGULIN. *GASTROENTEROLOGY* 128:503-506.

Liver Regeneration, Growth Factors, and Amphiregulin

See article on page 424.

The sequence of events triggering liver regeneration after acute loss of hepatic mass has been the subject of much investigation during the past 20 years.¹ Rapid changes in gene expression and activation of receptors and transcription factors occur immediately after partial hepatectomy (PHx).^{2,3} Several potential signaling stimuli are released in the liver or in circulation after the loss of hepatic parenchyma. These stimuli have effects on liver and on hepatocytes (or other hepatic cells) in cul-

ture. Such stimuli include cytokines (eg, tumor necrosis factor α , interleukin-6, norepinephrine, transforming growth factor [TGF]- β 1) and several growth factors. Cytokines are not direct mitogens for hepatocytes in culture and, after removal of their effects (eg, in mouse genetic models or by pharmacologic agents), liver regeneration is retarded or decreased, but hepatic mass is eventually restored nonetheless. Although this may suggest that the role of cytokines is not critical or essential, this should not imply that the events they mediate are not important or that they do not actually occur. The preponderance of evidence suggests that the cytokine

effects facilitate optimal timing and orchestration of the early signaling events after PHx, summarized under the term priming of hepatocytes.⁴

The effects of growth factors are mediated through their receptors. Two receptor-ligand and growth factor signaling systems appear to be mainly involved in liver regeneration: hepatocyte growth factor and its receptor (Met) and the epidermal growth factor receptor (EGFR) and its relatively large family of ligands and coreceptors. The receptor for EGFR was the first one that was shown to play a role in liver regeneration. A seminal publication by Earp et al⁵ showed that EGFR was phosphorylated and downregulated after PHx, suggesting binding of ligands and endocytosis.

The signaling scenario related to EGFR family members and its ligands is quite complex. The EGFR itself (also known as ErbB or HER) is a member of a family of four. The other members are ErbB-2 (HER-2, NEU), ErbB-3 (HER-3), and ErbB-4 (HER-4).⁶ Of these, HER-4 is expressed in only a limited number of tissues and it does not appear to be expressed in adult or embryonic liver. There are many ligands for EGFR, including epidermal growth factor (EGF), TGF- α , amphiregulin, heparin-binding EGF (HB-EGF), cripto, epiregulin, and betacellulin.

All of these considerations are relevant in putting in context the significant findings presented by Berrain et al⁷ in this issue of *GASTROENTEROLOGY*. The authors found that amphiregulin, a ligand for EGFR, is expressed early (within 30 minutes) during liver regeneration after PHx. In addition, they also found that liver regeneration is substantially decreased and retarded in mice with homozygous deletion of amphiregulin. The findings suggest a unique role for amphiregulin that cannot be substituted by the other ligands for EGFR. The time course of expression of amphiregulin corresponds well with the pattern of tyrosine phosphorylation of the EGFR, which previous work has shown is dramatically enhanced at 60 minutes after PHx.⁸

Previous studies have shown that deletion of other EGFR ligands does not have much impact on liver regeneration or liver development. The first one to be investigated in that regard was TGF- α . Similar to amphiregulin, TGF- α expression also rises soon after PHx.⁹ TGF- α is a strong mitogen for hepatocytes in culture, and its production by hepatocytes (which also express EGFR) suggests that TGF- α drives liver regeneration via an autocrine loop. Careful measurement of the TGF- α protein levels, however, showed that the increase in TGF- α protein levels was rather modest.⁹ It is not clear whether TGF- α produced by hepatocytes during liver regeneration stimulates proliferation (or other functions)

on hepatocytes or whether it provides paracrine mitogenic stimuli for adjacent cells expressing EGFR (stellate cells, endothelial cells, or bile duct epithelial cells). Surprisingly, mice with homozygous deletion of TGF- α have essentially normal liver regeneration and liver embryonic development.¹⁰ These findings were interpreted to be caused by the complementary action of the other EGFR ligands. In that scheme, however, it would be expected that removal of any other EGFR ligands would have no effect because stimulation of EGFR could be equally accomplished by the other members of the EGFR ligand family. The findings presented in the article by Berrain et al⁷ suggest that this is not the case. EGFR ligands are not equally interchangeable because removal of amphiregulin seriously affects liver regeneration whereas removal of TGF- α has no effect.

Removal of EGF has not been attempted by genetic mechanisms. Low levels of EGF are seen in male mice after removal of the salivary glands. Sialadenotomized mice have lower levels of EGF in the plasma and they also have deficient liver regeneration,¹¹ although the decrease in regeneration did not appear to be as intense as described in the article by Berrain et al.⁷ Deficient liver regeneration was also recently described in mice with homozygous deletions of another EGFR ligand, HB-EGF.¹² Liver regeneration was moderately decreased. Decreased DNA synthesis in the HB-EGF-deficient mice was observed at the early time points (30 and 36 hours) after PHx but it increased at subsequent times, becoming more than that seen in the wild-type animals.

The above findings clearly show that the EGFR ligands, despite the fact that they share the same receptor, have differing effects, not only during liver regeneration but also in most other biologic processes. To understand the basis for this phenomenon, one needs to dissect the complexity of the signaling of the ErbB receptor family members. ErbB signaling has evolved into a highly complex network of 4 closely related receptors and at least 10 different ligands. This diversification allows for a multi-layered network of regulation for ErbB signal input, processing, and output. Although all EGFR ligands can induce ErbB signaling, their expression patterns differ and their effector functions are nonoverlapping, ranging from cell motility and proliferation to growth inhibition. Most EGF family members are synthesized as transmembrane precursors, and these may have juxtacrine interactions aside from their soluble counterparts.¹³ In addition, HB-EGF, amphiregulin, and the neuregulins all contain heparin-binding domains that allow retention by extracellular matrix components.

In trying to understand the selective effects of removing some of the EGFR ligands, we need to focus on the intricate pathways of interaction among EGFR, the other members of the ErbB family, and the 10 ligands involved in the process. The dimerization of ErbB receptors is an intricate process that defines their signaling profile. ErbB proteins can form homodimers or heterodimers, with the latter being more stable. There is a distinct hierarchy that prefers ErbB-2 in heterodimer formation, and this is influenced by the structure of the ligand itself. Crucial to understanding the findings of the work by Berasain et al⁷ is the fact that different ligands exhibit distinct abilities to recruit and direct specific ErbB partners, and this ligand affinity ultimately influences signal strength and duration. Of the 10 possible dimer combinations, activated ErbB-2 heterodimers show the highest affinity ligand binding and a greater potency. ErbB-2 also exhibits a constitutively high basal kinase activity, and it is most closely linked to human cancer. ErbB2 is the major binding partner for EGFR.¹⁴ EGFR can be activated by EGF, TGF- α , HB-EGF, amphiregulin, betacellulin (BTC), and epiregulin. Unlike the other ErbB proteins, EGFR is coupled to the phospholipase C γ pathway. All ErbB receptors are coupled either directly or indirectly to the Ras- and Shc-activated mitogen-activated protein kinase pathways. ErbB-2 is a ligandless receptor because no direct ligand can induce ErbB-2 homodimers.¹⁵ Homodimers of ErbB-2 or ErbB-3 cannot activate ErbB signaling. The signal processing and output layers for ErbB receptors are a finely tuned network that involves receptor trafficking, as well as hidden multiple downstream cascades of enzymes, adaptor proteins, second messengers, and transcription factors. It should be noted that ErbB proteins, like other receptors, are synthesized, recycled, and shuttled to specific cellular locations even in the absence of any activating ligands. Once activated, the ErbB receptor-ligand complex is endocytosed in clathrin-coated pits. As a specific example, activated EGFR-ErbB-2 heterodimers are very potent for a number of reasons. ErbB-2-containing complexes are more stable at the cell surface.¹⁶ By decreasing the rate of ligand dissociation from the cognate receptor EGFR, ErbB-2 heterodimers remain at the cell surface longer and undergo a slower rate of endocytosis when compared with EGFR homodimers. Furthermore, once in early endosomes, internalized EGFR-ErbB-2 heterodimers are selected for recycling, whereas EGFR homodimers are continuously degraded.¹⁷ The preferential recycling of EGFR-ErbB-2 heterodimers allows a rapid return of this potent heterodimer to the cell

surface for another round of activation. ErbB-2 is also unique in that it is the only ErbB that is a substrate for the Hsp90 chaperone, which acts to further promote ErbB-2 folding and trafficking.¹⁸ Thus, even though ErbB-2 may be thought of as a ligandless receptor, its emerging role as a master regulator of ErbB signaling is quite extensive. The complexity of the pathways involved in ErbB receptor dimerization, ligand binding, endocytosis, and so on, create ample room for several alternative outcomes after ligand-receptor interactions. The protein structures formed from allosteric interactions between the ErbB receptors and their ligands determine the outcome of all further processing of the ligand-receptor complex and the signaling associated with it.

In view of all the complex effects of EGFR and its ligands in liver regeneration, it is surprising that there are no apparent effects on liver embryonic development in mice with genetic deletion of EGFR. Several studies using different strains of mice have reported an array of findings that appear to be specific to the mouse strains. These effects range from embryonic lethality caused by placental abnormalities or neonatal death caused by pulmonary defects or lack of lethality during either embryonic or neonatal stage of life.¹⁹ All strains of mice, however, eventually present with abnormalities in the central nervous system, characterized by neurodegeneration seen in frontal cortex, olfactory bulb, and thalamus, with massive neuronal apoptosis and enhanced expression of c-fos.²⁰ Hepatic abnormalities have not been described in any of the strains. It is possible (but not very likely) that the lack of EGFR is compensated by actions of the other members of the receptor family, specifically ErbB-2 and ErbB-3, because ErbB-4 is not expressed in liver.²⁰ The alternative interpretation is that, although undoubtedly EGFR contributes signaling of some importance to liver during embryonic development, the impact is not critically vital. Equally unimpressive in terms of liver embryonic development are the effects of deletion of any one of the ligands of EGFR examined so far (TGF- α , HB-EGF, amphiregulin). Mice are born with apparently normal overall anatomy and histology and no abnormalities are seen in liver (or most other tissues). Although one could argue that removal of any one of the EGFR ligands is compensated by the presence of the others, the findings by Berasain et al⁷ strongly suggests that EGFR ligand-induced signaling is not interchangeable from one ligand to the other. The combination of the findings by Berasain et al⁷ and those from the genetic deletion studies of EGFR ligands suggest that the functions of

the EGFR ligand system are just not critically important for liver embryonic development as they appear to be for liver regeneration.

Overall, the findings of the accumulated literature suggest that the pathways of stimulation of hepatocyte proliferation are quite complex, but EGFR and Met are playing very important roles. Other signaling pathways such as Notch/Jagged²¹ and c-kit,²² neuropeptide and the α -1 receptor²³ are also involved. The integration of all these pathways into an easy scheme remains a challenge. In this complex signaling environment, the findings of Berasain et al⁷ clearly show that amphiregulin appears to play a specific and unique role.

GEORGE K. MICHALOPOULOS
ZAHIDA KHAN

Department of Pathology
University of Pittsburgh School of Medicine
Pittsburgh, Pennsylvania

References

1. Michalopoulos GK, DeFrances MC. Liver regeneration. *Science* 1997;276:60–66.
2. Slick DB, Mars WM, Petersen BE, Kim TH, Michalopoulos GK. Growth factor signal transduction immediately after two-thirds partial hepatectomy in the rat. *Cancer Res* 1999;59:3954–3960.
3. Fausto N. Liver regeneration. *J Hepatol* 2000;32:19–31.
4. Webber EM, Brub J, Pierce RH, Fausto N. Tumor necrosis factor primes hepatocytes for DNA replication in the rat. *Hepatology* 1998;28:1226–1234.
5. Rubin RA, O'Keefe EJ, Earp HS. Alteration of epidermal growth factor-dependent phosphorylation during rat liver regeneration. *Proc Natl Acad Sci U S A* 1982;79:776–780.
6. Earp HS, Dawson TL, Li X, Yu H. Heterodimerization and functional interaction between EGF receptor family members: a new signaling paradigm with implications for breast cancer research. *Breast Cancer Res Treat* 1995;35:115–132.
7. Berasain C, Garcia-Trevijano ER, Castillo J, Erroba E, Lee DC, Prieto J, Avila MA. Amphiregulin: an early trigger for liver regeneration in mice. *Gastroenterology* 2005;128:424–432.
8. Webber EM, FitzGerald MJ, Brown PJ, Bartlett MH, Fausto N. Transforming growth factor- α expression during liver regeneration after partial hepatectomy and toxic injury, and potential interactions between transforming growth factor- α and hepatocyte growth factor. *Hepatology* 1993;18:1422–1431.
9. Russell WE, Dempsey PJ, Sitaric S, Peck AJ, Coffey RJ Jr. Transforming growth factor- α (TGF α) concentrations increase in regenerating rat liver: evidence for a delayed accumulation of mature TGF α . *Endocrinology* 1993;133:1731–1738.
10. Russell WE, Kaufmann WK, Sitaric S, Luetteke NC, Lee DC. Liver regeneration and hepatocarcinogenesis in transforming growth factor- α -targeted mice. *Mol Carcinog* 1996;15:183–189.
11. Jones DE Jr, Tran-Patterson R, Cui DM, Dawn D, Estell KP, Miller DM. Epidermal growth factor secreted from the salivary gland is necessary for liver regeneration. *Am J Physiol* 1995;268:G872–878.
12. Mitchell C, Hinson M, Jackson LF, Fox R, Lee DC, Campbell JS, Fausto N. HB-EGF links hepatocyte priming with cell cycle progression during liver regeneration. *J Biol Chem* 2004 (e-pub ahead of print).
13. Wong ST, Winchell LF, McCune BK, Earp HS, Tabbid J, Massague J, Herman B, Lee DC. The TGF- α precursor expressed on the cell surface binds to the EGF receptor on adjacent cells, leading to signal transduction. *Cell* 1989;56:495–506.
14. Tzahar E, Waksman H, Chen X, Levkowitz G, Karunakaran D, Lavie S, Ratzkin BJ, Yarden Y. A hierarchical network of intrareceptor interactions determines signal transduction by Neu differentiation factor/neuregulin and epidermal growth factor. *Mol Cell Biol* 1998;18:5276–5287.
15. Klapper LN, Glathe S, Waksman H, Hynes NE, Andrews GC, Sela M, Yarden Y. The ErbB-2/HER2 oncoprotein of human carcinomas may function solely as a shared coreceptor for multiple stroma-derived growth factors. *Proc Natl Acad Sci U S A* 1999;96:4995–5000.
16. Lanferink AE, Pinkas-Nramani R, van de Poll ML, van Vugt MJ, Klapper LN, Tzahar E, Waksman H, Sela M, van Zoelen EJ, Yarden Y. Differential endocytic routing of homo- and heterodimeric ErbB tyrosine kinases confers signaling superiority to receptor heterodimers. *Embo J* 1998;17:3385–3397.
17. Levkowitz G, Waksman H, Zamir E, Kam Z, Oved S, Langdon WY, Begunot L, Geiger B, Yarden Y. c-Cbl/SK-1 regulates endocytic sorting and ubiquitination of the epidermal growth factor receptor. *Genes Dev* 1998;12:3663–3674.
18. Neckers L. Her2/Neu inhibitors as novel cancer chemotherapeutic agents. *Trends Mol Med* 2002;8(suppl):S55–S61.
19. Sibilla M, Steinbach JP, Stingl L, Aguzzi A, Wagner EF. A strain-independent postnatal neurodegeneration in mice lacking the EGF receptor. *EMBO J* 1998;17:719–731.
20. Carver RS, Stevenson MC, Schoving LA, Russell WE. Diverse expression of ErbB receptor proteins during rat liver development and regeneration. *Gastroenterology* 2002;123:2017–2027.
21. Kohler C, BellAW, Bowen WC, Monga SP, Fleig W, Michalopoulos GK. Expression of Notch-1 and its ligand Jagged-1 in rat liver during liver regeneration. *Hepatology* 2004;39:1056–1065.
22. Ren X, Hogaboam C, Carpenter A, Collett L. Stem cell factor restores hepatocyte proliferation in IL-6 knockout mice following 70% hepatectomy. *J Clin Invest* 2003;112:1407–1418.
23. Cruise JL, Knechtle SJ, Bollinger RR, Ruhn C, Michalopoulos G. Alpha 1-adrenergic effects and liver regeneration. *Hepatology* 1987;7:1189–1194.

Address requests for reprints to: George K. Michalopoulos, MD, PhD, Department of Pathology, University of Pittsburgh School of Medicine, S-410 Biomedical Science Tower, Pittsburgh, Pennsylvania 15261. e-mail: michalopoulos@upmc.edu; fax: (412) 648-9846.

© 2005 by the American Gastroenterological Association
0016-5085/05/13411/\$30.00
doi:10.1053/j.gastro.2004.12.039

APPENDIX B

**GENES UP-REGULATED BY 4 HR. HYPOXIA IN PRIMARY RAT HEPATOCYTES
(COMPLETE LISTING).**

Table 12: Genes up-regulated by 4 hr. hypoxia in primary rat hepatocytes (complete list). This list represents all 159 rat genes with increased expression, as identified by Affymetrix analysis and GeneSifter software. Ratio = hypoxic/normoxic signals. ESTs were filtered out.

#	Gene Name	Gene ID	Gene Identifier	Ratio	p-value	Reference, if HIF target
1	Pineal specific PG25 protein (Pg25)	Esm1	NM_022604	7.78	4.52E-02	
2	Macrophage inflammatory protein-1 alpha receptor gene (LOC57301)	Ccr1	NM_020542	6.82	7.18E-03	
3	Granulocyte-macrophage colony stimulating factor (GM-CSF)	Csf2	U00620	6.55	3.46E-02	
4	Adrenomedullin (Adm).	Adm	NM_012715	5.26	8.96E-07	(223-225)
5	Chemokine orphan receptor 1 (Rdc1)	Cmkor1	NM_053352	5.26	4.47E-03	
6	Stearoyl-Coenzyme A desaturase 2 (Scd2)	Scd2	NM_031841	4.90	3.00E-03	
7	Fc receptor, IgG, low affinity III (Fcgr3)	Fcgr3	NM_053843	4.53	6.12E-03	
8	Glutaredoxin 1 (thioltransferase) (Glx1)	Glx1	NM_022278	4.34	7.84E-05	
9	Insulin-like growth factor binding protein 1 (Igfbp1)	Igfbp1	NM_013144	4.11	1.81E-03	(147, 227, 228)
10	Cathepsin K (Ctsk)	Ctsk	NM_031560	4.09	8.04E-03	
11	Activating transcription factor 3 (Atf3)	Atf3	NM_012912	4.03	5.92E-04	
12	Vimentin (Vim)	Vim	NM_031140	3.98	3.08E-02	
13	Guanine nucleotide binding protein gamma subunit 11 (Gng11)	Gng11	NM_022396	3.95	3.23E-03	
14	Selenoprotein P, plasma, 1 (Sepp1)	Sepp1	NM_019192	3.94	2.26E-02	

#	Gene Name	Gene ID	Gene Identifier	Ratio	p-value	Reference, if HIF target
15	Aldehyde reductase 1 (low Km aldose reductase) (5.8 kb PstI fragment, probably the functional gene) (Akr1b1)	Aldr1	NM_012498	3.92	3.28E-04	
16	Pyruvate kinase 3 (Pkm2)	Pkm2	NM_053297	3.85	1.55E-02	(277)
17	Potassium inwardly-rectifying channel, subfamily J, member 12 (Kcnj12)	Kcnj12	NM_053981	3.84	3.26E-02	
18	Monocarboxylate transporter (Mct3)	Slc16a3	NM_030834	3.75	5.26E-04	
19	Acyl-coenzyme A:cholesterol acyltransferase (Soat1)	Soat1	NM_031118	3.73	1.31E-02	
20	Vanilloid receptor-like protein 1 (Vrl1)	Trpv2	NM_017207	3.69	2.78E-02	
21	Adipocyte lipid-binding protein (LOC84378)	Fabp4	NM_053365	3.60	1.46E-03	
22	Lymphocyte cytosolic protein 2 (SH2 domain-containing leukocyte protein of 76kD) (Lcp2)	Lcp2	NM_130421	3.50	1.83E-02	
23	Fc receptor, IgG, low affinity III (Fcgr3)	Fcgr3	NM_053843	3.49	7.96E-03	
24	Interleukin 1 receptor antagonist gene (Il1rn)	Il1rn	NM_022194	3.37	3.15E-04	
25	Rat leukocyte common antigen (L-CA)	Ptprc	M10072	3.37	2.58E-02	
26	Matrix metalloproteinase 3 (Mmp3)	Mmp3	NM_133523	3.30	4.67E-04	(278)
27	Chemokine receptor LCR1	Cxcr4	U54791	3.30	1.45E-03	(279)
28	Brain-enriched membrane-associated protein tyrosine phosphatase (BSM)-1	Ptpro	D45412	3.29	9.68E-05	

#	Gene Name	Gene ID	Gene Identifier	Ratio	p-value	Reference, if HIF target
29	Tyrosine protein kinase pp60-c-src	Src	BI282912	3.24	1.58E-02	
30	Factor-responsive smooth muscle protein (SM-20)	Egln3	NM_019371	3.22	1.01E-02	(73)
31	SH3 domain-containing adapter protein isoform SETA-1x23 (SETA)	Sh3kbp1	AF230520	3.18	1.29E-02	
32	MRC OX-45 surface antigen.	Cd48	X13016	3.17	1.01E-03	
33	Plasminogen activator inhibitor 2 type A (Pai2a)	Serpib2	NM_021696	3.14	2.29E-02	
34	CXC chemokine receptor	Cxcr4	AA945737	3.08	1.58E-02	(279)
35	Heme oxygenase (Hmox1)	Hmox1	NM_012580	3.07	2.74E-04	(280)
36	Adenosine A2a-receptor (Adora2a)	Adora2a	NM_053294	3.01	3.08E-04	
37	Calcitonin receptor-like receptor (Calclrl)	Calclrl	NM_012717	2.98	2.78E-02	(281)
38	Pim-1 oncogene (Pim1), mRNA.	Pim1	NM_017034	2.96	1.67E-02	(282)
39	Clone ndf04 neu differentiation factor	Nrg1	U02315	2.91	7.90E-04	
40	Serine (or cysteine) proteinase inhibitor, clade E (nexin, plasminogen activator inhibitor type 1), member 1 (PAI-1, Serpine1)	Serpine1	NM_012620	2.90	5.66E-04	(233, 234, 283)
41	Cyclooxygenase 2	Ptgs2	U03389	2.85	3.24E-03	
42	Matrix metalloproteinase 10 (Mmp10)	Mmp10	NM_133514	2.84	5.27E-05	
43	Amelogenin (Amel)	Amelx	NM_019154	2.82	2.31E-02	
44	solute carrier family 1, member 3	Maf	BG376037	2.79	9.96E-03	
45	Matrix metalloproteinase 12	Mmp12		2.78	9.93E-03	

#	Gene Name	Gene ID	Gene Identifier	Ratio	p-value	Reference, if HIF target
	(Mmp12)		NM_053963			
46	Gamma-glutamyltransferase-like activity 1 (Ggta1)	Ggta1	NM_019235	2.78	2.33E-02	
47	Brain glucose-transporter protein (GLUT-1)	Slc2a1	BI284218	2.77	5.94E-05	(284)
48	Fc gamma receptor	Fcgr2b	X73371	2.75	6.71E-05	
49	CXC chemokine receptor	Cxcr4	AA945737	2.72	3.57E-03	(279)
50	Collagenase (UMRCas)	Mmp13	M60616	2.70	2.52E-03	
51	Inducible prostaglandin E synthase (iPGES)	Ptges	AB048730	2.70	5.64E-04	
52	Tissue inhibitor of metalloproteinase 3	Timp3	AA893169	2.62	3.02E-02	
53	Enzymatic glycosylation-regulating gene (Gcnt1)	Gcnt1	NM_022276	2.61	3.96E-02	
54	Matrix metalloproteinase 9 (gelatinase B, 92-kDa type IV collagenase) (Mmp9)	Mmp9	NM_031055	2.61	2.03E-02	
55	Growth response protein (CL-6) (LOC64194)	Insig1	NM_022392	2.60	3.86E-04	
56	Golgi SNAP receptor complex member 1 (Gosr1).	Gosr1	NM_053584	2.57	2.80E-02	
57	Epithelial membrane protein 1 (Emp1).	Emp1	NM_012843	2.56	1.74E-03	
58	CASP8 and FADD-like apoptosis regulator (Cflar)	Cflar	NM_057138	2.55	9.23E-03	
59	5S rRNA gene (clone pRA5S2).	-	X83747	2.52	4.84E-03	
60	Solute carrier family 21 (organic anion transporter), member 12 (Slc21a12, OAT-PE)	Slco4a1	NM_133608	2.51	3.37E-02	
61	Sodium/potassium-transporting ATPase gamma chain	Fxyd2	AF129400	2.50	1.67E-02	
62	Arginase 1, liver (Arg1)	Arg1		2.49	2.54E-03	(285)

#	Gene Name	Gene ID	Gene Identifier	Ratio	p-value	Reference, if HIF target
			NM_017134			
63	Embigin (Emb)	Emb	NM_053719	2.48	7.77E-03	
64	N-methyl-D-aspartate receptor subunit (NMDAR2D-1).	Grin2d	D13213	2.48	3.73E-03	
65	GABA transaminase (GABA-T)	Abat	U29701	2.42	3.98E-03	
66	Heat shock protein 70-1 (Hspa1a)	Hspa1a	NM_031971	2.37	2.00E-02	
67	Fatty acid binding protein 6 (bile acid-binding protein) (Fabp6)	Fabp6	NM_017098	2.35	5.07E-03	
68	Interleukin 6 (interferon, beta 2) (Il6)	Il6	NM_012589	2.33	2.09E-03	
69	Synaptotagmin 10	Syt10	AF375463	2.29	4.51E-02	
70	Mink-related peptide 2 (Kcne3)	Kcne3	NM_022235	2.26	2.92E-03	
71	Small inducible cytokine subfamily, member 2 (Scyb2)	Cxcl2	NM_053647	2.23	2.44E-03	
72	Rat (diabetic BB) MHC class II alpha chain RT1.D alpha (u).	RT1-Da	Y00480	2.23	7.02E-03	
73	Myristoylated alanine rich C kinase substrate	Marcks	M59859	2.22	1.27E-02	
74	BCL2-related protein A1 (Bcl2a1)	Bcl2a1	NM_133416	2.22	1.27E-03	
75	Proteoglycan peptide core protein (Pgsg)	Pgsg	NM_020074	2.21	2.71E-03	
76	NADPH oxidase beta subunit gp91-phox gene (Cybb)	Cybb	NM_023965	2.20	6.92E-03	
77	Ficolin A (Fcna)	Fcna	NM_031348	2.20	7.19E-03	
78	Mitogen-activated protein kinase kinase kinase 8 (Map3k8)	Map3k8	NM_053847	2.19	2.25E-02	

#	Gene Name	Gene ID	Gene Identifier	Ratio	p-value	Reference, if HIF target
79	Basic helix-loop-helix domain containing, class B, 3 (Bhlhb3, DEC2)	Bhlhb3	NM_133303	2.10	8.33E-03	(286)
80	Flavin-containing monooxygenase 3 (Fmo3)	Fmo3	NM_053433	2.08	2.62E-02	
81	Glycoprotein (transmembrane) nmb (Gpnmb)	Gpnmb	NM_133298	2.07	1.05E-02	
82	CC chemokine ST38 precursor	Ccl20	AF053312	2.07	1.59E-03	
83	Clone N27 mRNA	Txnip	U30789	2.06	3.58E-02	
84	Basic helix-loop-helix domain containing, class B2 (Bhlhb2, DEC1)	Bhlhb2	NM_053328	2.06	2.84E-04	(286)
85	Lectin, galactose binding, soluble 3 (Lgals3)	Lgals3	NM_031832	2.05	1.64E-03	
86	UDP-glucuronosyltransferase (Ugt2b12)	-	NM_031980	2.04	1.35E-02	
87	Complement component 4 binding protein, beta (C4bpb)	C4bp-ps1	NM_016995	2.04	4.23E-02	
88	MHC class II antigen RT1.B-1 beta-chain	RT1-Bb	AI715202	2.02	8.55E-05	
89	ATP-sensitive K ⁺ channel subunit Kir6.1	Kcnj8	AB043636	2.01	1.95E-03	
90	Glutaredoxin	Glrx1	AF319950	2.01	5.84E-03	
91	Aldolase A, fructose-bisphosphate (Aldoa)	Aldoa	NM_012495	2.00	6.18E-03	(277, 287)
92	H3 histone, family 3B	-	AI177503	2.00	2.12E-04	
93	Tissue inhibitor of metalloproteinase 3	Timp3	AI009159	1.99	2.16E-02	
94	K-kininogen, differential splicing leads to HMW Kngk (Kngk)	MGC10874 7	NM_012741	1.98	2.05E-02	
95	UDP-glucuronosyltransferase	Udpgt	M31109	1.97	5.00E-02	
96	Lactate dehydrogenase A (Ldha),	Ldha		1.96	6.88E-04	(287-289)

#	Gene Name	Gene ID	Gene Identifier	Ratio	p-value	Reference, if HIF target
			NM_017025			
97	Serine proteinase inhibitor, clade H (heat shock protein 47), member 1 (Serpinh1)	Serpinh1	NM_017173	1.95	8.81E-03	
98	p21 (WAF1)	Cdkn1a	U24174	1.93	8.13E-03	
99	Selenoprotein P, plasma, 1	-	AA799627	1.92	4.83E-02	
100	Cathepsin Y	LOC252929	AA849399	1.91	1.11E-02	
101	Soluble adenylyl cyclase (LOC59320)	Sac	NM_021684	1.89	3.56E-02	
102	Pyruvate dehydrogenase kinase, isoenzyme 1 (Pdk1)	Pdk1	NM_053826	1.88	1.29E-02	(169)
103	Acyl-coenzyme A:cholesterol acyltransferase	Soat1	A1548897	1.86	1.58E-02	
104	Rat liver UDP-glucuronosyltransferase, phenobarbital-inducible form	Udpgr2	M13506	1.86	4.08E-02	
105	CD14 antigen (Cd14)	-	NM_021744	1.86	3.95E-02	
106	Superoxide dismutase 2, mitochondrial	-	BG671549	1.85	3.31E-02	
107	Neuron-specific enolase (NSE)	Eno2	AF019973	1.85	2.60E-02	
108	Brain hexokinase	Hk1	J04526	1.84	9.34E-03	
109	Cytochrome P450, subfamily IIC (mephenytoin 4-hydroxylase) (Cyp2c)	Cyp2c	NM_019184	1.84	4.02E-02	
110	Rat sterol carrier protein-2 (SCP-2)	Scp2	M34728	1.83	3.91E-02	
111	GABA transporter (RNU28927).	Slc6a12	NM_017335	1.79	2.42E-02	
112	Acid phosphatase 5, tartrate resistant (Acp5)	Acp5	NM_019144	1.79	4.73E-02	
113	Low molecular weight (LMW) K-kininogen	Kng1	M11884	1.78	2.41E-02	

#	Gene Name	Gene ID	Gene Identifier	Ratio	p-value	Reference, if HIF target
114	Triosephosphate isomerase 1 (Tpi1)	Tpi1	NM_022922	1.78	1.42E-02	(290, 291)
115	Peroxisomal biogenesis factor 3 (Pex3)	Pex3	NM_031350	1.77	8.23E-03	
116	Urinary protein 2 precursor	-	AF198441	1.75	2.79E-02	
117	Apoptosis inhibitor 2 (Api2)	Api2	NM_021752	1.75	1.91E-02	
118	H3 histone, family 3B	H3f3b	BG663226	1.74	1.56E-04	
119	Glucose-6-phosphate dehydrogenase (G6pd)	G6pdx	NM_017006	1.74	4.68E-04	(292)
120	Cystatin beta	Cstb	AI409867	1.73	1.59E-04	
121	HIF-1 responsive RTP801 (Rtp801)	Ddit4	NM_080906	1.72	1.39E-02	(293)
122	Aldose reductase-like protein	Akr1b8	AI233740	1.72	4.22E-04	
123	Hypoxia induced gene 1 (Hig1)	Hig1	NM_080902	1.72	2.81E-03	(294)
124	Cyclophilin D mRNA, nuclear gene encoding mitochondrial protein	Ppif	U68544	1.71	1.65E-02	
125	Myristoylated alanine-rich protein kinase C substrate	Marcks	BE111604	1.70	4.56E-02	
126	Pyridoxine 5-phosphate oxidase (U91561)	-	NM_022601	1.69	1.10E-02	
127	Glutamate-cysteine ligase, modifier subunit (Gclm)	Gclm	NM_017305	1.68	3.02E-02	
128	Sprague Dawley testosterone 6-beta-hydroxylase, cytochrome P4506-beta-A, (CYP3A2)	Cyp3a11	U09742	1.67	3.76E-02	
129	ATPase, vacuolar, 14 kD (Atp6s14)	Atp6v1f	NM_053884	1.67	1.56E-04	
130	92-kDa type IV collagenase	Mmp9	U36476	1.67	2.76E-02	
131	Inhibitor of DNA binding 2, dominant negative helix-loop-helix protein	Id2	AI008792	1.67	8.82E-03	(295)

#	Gene Name	Gene ID	Gene Identifier	Ratio	p-value	Reference, if HIF target
132	Contrapsin-like protease inhibitor related protein (CPi-23)	Spin2a	D00752	1.66	4.26E-02	
133	T-kininogen, see also D11Elh1 and D11Mit8 (Kng)	Kng1	NM_012696	1.65	7.55E-03	
134	Acid phosphatase 1, soluble (Acp1)	Acp1	NM_021262	1.64	1.72E-02	
135	Peripheral myelin protein	Pmp22	AA943163	1.64	4.12E-02	
136	F1-ATPase epsilon subunit, nuclear gene encoding mitochondrial protein	Atp5e	AF010323	1.63	7.68E-03	
137	Colony stimulating factor 3 (granulocyte) (Csf3)	Csf3	NM_017104	1.62	1.01E-03	
138	Early growth response 2 (Egr2)	Egr2	NM_053633	1.62	3.40E-02	
139	3 non-translated beta-F1-ATPase mRNA-binding protein	-	AF368860	1.62	2.06E-02	
140	Serum glucocorticoid regulated kinase (Sgk)	Sgk	NM_019232	1.61	3.01E-04	
141	CD74 antigen (invariant polypeptide of major histocompatibility class II antigen-associated) (Cd74)	Cd74	NM_013069	1.61	3.51E-03	
142	endothelial differentiation sphingolipid G-protein-coupled receptor 1	Edg1	BI295971	1.61	4.39E-02	
143	Cathepsin L	Ctsl	A1232474	1.60	3.13E-02	
144	Serine protease inhibitor (Spin2b)	Spin2b	NM_012657	1.60	4.77E-02	
145	Kidney-derived aspartic protease-like protein (Kdap)	Napsa	NM_031670	1.59	1.79E-02	
146	Espin (Espn)	Espn	NM_019622	1.59	1.21E-02	

#	Gene Name	Gene ID	Gene Identifier	Ratio	p-value	Reference, if HIF target
147	Prostaglandin-endoperoxide synthase 1 (prostaglandin GH synthase and cyclooxygenase) (Ptgs1)	Ptgs1	NM_017043	1.57	3.83E-02	
148	Metallothionein-2 and metallothionein-1	-	BM383531	1.55	1.21E-02	
149	Rat insulin-like growth factor I (IGF-I)	Igf1	M15481	1.53	1.23E-02	
150	Rat homologue of Kex2 and furin proteins	Pcsk1	M83745	1.53	3.06E-02	
151	Legumain	Lgmn	AF154349	1.53	4.51E-03	
152	Hexokinase 1 (Hk1)	Hk1	NM_012734	1.52	5.12E-03	
153	Polyubiquitin (four repetitive ubiquitins in tandem)	Ubb	D16554	1.51	1.35E-03	
154	Inhibitor of DNA binding 2, dominant negative helix-loop-helix protein (Id2)	Id2	NM_013060	1.51	3.50E-02	(295)
155	Transaldolase 1 (Taldo1)	Taldo1	NM_031811	1.51	6.72E-03	
156	Thymus cell surface antigen	-	BI285183	1.51	4.85E-02	
157	ATPase, H ⁺ transporting, lysosomal (vacuolar proton pump), beta 5658 kDa, isoform 2 (Atp6b2)	Atp6b2	NM_057213	1.51	1.07E-02	
158	p47 protein (p47)	p47	NM_031981	1.50	4.43E-03	
159	Alpha-2micro-globulin	LOC298109	AB039823	1.50	2.87E-02	

APPENDIX C

**GENES DOWN-REGULATED BY 4 HR. HYPOXIA IN PRIMARY RAT
HEPATOCYTES (COMPLETE LISTING).**

Table 13: Genes down-regulated by 4 hr. hypoxia in primary rat hepatocytes (complete list). This list represents all 468 rat genes with decreased expression, as identified by Affymetrix analysis and GeneSifter software. Ratio = hypoxic/normoxic signals. ESTs were filtered out.

#	Gene Name	Gene ID	Gene Identifier	Ratio	p-value
1	Cyclin D1 (CCND1)	Ccnd1	X75207	-8.28	1.09E-02
2	Novel kinesin-related protein (KIF1D)	Kif1c	BF417285	-5.99	8.72E-03
3	Cytochrome c oxidase subunit VIa polypeptide 2 (heart) (Cox6a2)	Cox6a2	NM_012812	-5.39	4.95E-02
4	Insulin-like 6 (Insl6)	Insl6	NM_022583	-4.92	7.25E-03
5	Recoverin (Rcvrn)	Rcvrn	NM_080901	-4.80	3.03E-05
6	Pepsinogen F protein (Pepf)	Pga5	NM_021753	-4.61	2.52E-03
7	Bcl-2 modifying factor (Bmf)	Bmf	NM_139258	4.55	1.44E-02
8	Tektin 1 (Tekt1)	Tekt1	NM_053508	-4.46	3.64E-02
9	Calcium-calmodulin-dependent protein kinase phosphatase	Ppm1f	AB023634	-4.28	3.08E-05
10	G protein-coupled receptor kinase 6, splice variant C (GRK6)	Gprk6	AF040750	-4.13	1.29E-02
11	Phosphatidylinositol 3-kinase p45 subunit	Pik3r1	D64048	-4.08	3.89E-02
12	G protein-coupled receptor kinase 6 (Gprk6)	Gprk6	NM_031657	-3.95	3.46E-02
13	Sarcosine dehydrogenase (SarDH)	Sardh	AF067650	-3.81	1.16E-02
14	Hepatocyte F2alpha receptor.	Ptgfr	X83856	-3.70	1.16E-03
15	Neurofibromatosis 2	Nf2	BF566236	-3.70	2.77E-02
16	Leucine zipper protein 1 (Luzp1)	-	NM_030830	-3.62	8.23E-03
17	Hairy and enhancer of split 2 (Drosophila) (Hes2)	Hes2	NM_019236	-3.61	2.16E-02
18	Rat olfactory protein	Olr1082	M64381	-3.58	1.95E-02
19	Glutamine glutamic acid-rich protein isoform Cb (GRP-Cb)	Grpca	M58654	-3.58	2.62E-02

#	Gene Name	Gene ID	Gene Identifier	Ratio	p-value
20	Fibroblast growth factor FGF-5 (Fgf5)	Fgf5	NM_022211	-3.42	1.34E-02
21	Glucosidase 1	-	C06771	-3.31	6.48E-03
22	Branched chain aminotransferase 2, mitochondrial (Bcat2)	Bcat2	NM_022400	-3.30	1.22E-02
23	Synaptonemal complex protein 3 (Sycp3)	Sycp3	NM_013041	-3.24	3.11E-02
24	Leukocyte common antigen related protein	Ptprf	M60103	-3.19	2.09E-04
25	Guanine nucleotide-binding regulatory protein alpha subunit	Gnaz	J03773	-3.16	3.34E-02
26	Serine protease gene	-	L38482	-3.14	3.32E-02
27	Mitogen activated protein kinase kinase 5 (Map2k5)	Map2k5	NM_017246	-3.10	1.78E-03
28	CTD-binding SR-like (rA1)	Sr-a1	NM_019384	-2.96	3.59E-02
29	Ischemia related factor NYW-1 (Nyw1), mRNA.	-	NM_021683	-2.89	3.54E-02
30	CCAAT enhancer binding, protein (CEBP) delta	Cebpd	BF419200	-2.87	6.56E-03
31	SPA-1 like protein p1294	Sipa111	AF026504	-2.87	3.90E-03
32	Transmembrane 4 superfamily member 4 (Tm4sf4)	Tm4sf4	NM_053785	-2.86	3.23E-02
33	LL5 protein (L15)	-	NM_134397	-2.85	8.92E-04
34	Hydroxyindole-O-methyltransferase	Asmt	L78306	-2.78	1.83E-02
35	Secretory (zymogen) granule membrane glycoprotein GP2 (Gp2)	Gp2	NM_134418	-2.74	8.75E-03
36	Avian erythroblastosis oncogene B 3 (ErbB3)	ErbB3	NM_017218	-2.73	5.38E-03
37	Three-PDZ containing protein similar to C. elegans PAR3 (partitioning defect) (Par3)	Par3	NM_031235	-2.73	6.57E-04

#	Gene Name	Gene ID	Gene Identifier	Ratio	p-value
38	NAC-1 protein (Nac-1)	Btbd14b	NM_134413	-2.73	1.71E-03
39	Calcium calmodulin-dependent protein kinase kinase 1, alpha (Camkk1)	Camkk1	NM_031662	-2.72	6.25E-03
40	Somatostatin receptor subtype 2 (Sstr2)	Sstr2	NM_019348	-2.72	3.73E-03
41	Tuberin-like protein 1 (Tulip1)	-	NM_020083	-2.72	3.83E-03
42	Activin beta E (Inhbe)	Inhbe	NM_031815	-2.72	1.48E-03
43	Dishevelled 1 (Dvl1)	Dvl1	NM_031820	-2.71	2.74E-03
44	ArgAbl-interacting protein ArgBP2 (Argbp2)	Argbp2	NM_053770	-2.70	6.38E-03
45	Sprague-Dawley (clone LRB2) RAB16	Rab3d	M83681	-2.70	3.85E-02
46	Calcium channel, voltage-dependent, L type, alpha 1S subunit	Cacna1s	AI454679	-2.68	3.29E-02
47	Potassium channel modulatory protein 2 (Kcnip2)	Kcnip2	NM_020095	-2.68	1.22E-02
48	Gastrin-releasing peptide (Grp)	Grp	NM_133570	-2.63	2.96E-02
49	Peroxisome proliferative activated receptor, gamma, coactivator 1 (Ppargc1)	Ppargc1a	NM_031347	-2.63	1.08E-02
50	G alpha interacting protein (Gaip)	Rgs19	NM_021661	-2.62	3.35E-04
51	Vacuolar protein sorting protein 33a (Vps33a)	Vps33a	NM_022961	-2.61	3.72E-05
52	Inositol polyphosphate 5-phosphatase	Cebpd	BF282728	-2.59	2.42E-02
53	Actinin, alpha 1 (Actn1)	Actn1	NM_031005	-2.58	1.11E-03
54	Synaptosomal-associated protein, 29kD (Snap29)	Snap29	NM_053810	-2.58	4.75E-03
55	Short stature homeobox 2 (Shox2)	Shox2	NM_013028	-2.57	2.34E-02

#	Gene Name	Gene ID	Gene Identifier	Ratio	p-value
56	Potassium voltage gated channel, shaker related subfamily, beta member 3 (Kcnab3)	Kcnab3	NM_031652	-2.55	8.24E-03
57	Damage-specific DNA binding protein 1 (DDB1 gene)	Ddb1	AJ277077	-2.54	2.67E-03
58	AGR16	Edg5	AB016931	-2.54	9.14E-06
59	General transcription factor III C 1	Gtf3c1	AI234022	-2.50	4.16E-03
60	Ly-49.12 antigen	Klra22	U56822	-2.50	2.24E-03
61	CUG triplet repeat, RNA-binding protein 2	Cugbp2	AW140475	-2.46	3.22E-02
62	Osteoregulin (LOC79110)	Mepe	NM_024142	-2.43	4.97E-02
63	Rab geranylgeranyl transferase component, subunit beta (Rabggtb)	-	NM_013020	-2.41	2.96E-03
64	Sprague-Dawley glycerolphosphate dehydrogenase (mGPD)	Gpd2	U08027	-2.41	3.65E-02
65	Potassium voltage-gated channel, subfamily H (eag-related), member 2 (Kcnh2)	Kcnh2	NM_053949	-2.41	9.27E-03
66	Scaffolding protein SLIPR (Slipr)	Slipr	NM_139084	-2.40	1.36E-03
67	Myosin, heavy polypeptide 9, non-muscle (Myh9)	Myh9	NM_013194	-2.40	1.93E-03
68	Synaptotagmin 7	Syt7	AI713274	-2.39	1.66E-02
69	Glutamate receptor, ionotropic, N-methyl D-aspartate 2A (Grin2a)	-	NM_012573	-2.38	7.76E-03
70	Inhibitor of kappa light polypeptide enhancer in B-cells, kinase complex-associated protein (Ikbkap)	Ikbkap	NM_080899	-2.38	1.96E-04
71	3-phosphoglycerate	Phgdh	NM_031620	-2.36	6.01E-03

#	Gene Name	Gene ID	Gene Identifier	Ratio	p-value
	dehydrogenase (Phgdh)				
72	Follistatin-related protein precursor (Frp).	Fstl1	NM_024369	-2.36	1.47E-02
73	Sperm tail protein Spag5	Spag5	AF111111	-2.36	3.56E-02
74	Smoothened (Smoh)	Smo	NM_012807	-2.32	1.24E-02
75	Inwardly rectifying potassium channel (Kir2.4)	-	AI717104	-2.30	3.02E-02
76	Erythrocyte protein band 4.1-like 3 (Epb4.113)	Epb4.113	NM_053927	-2.30	3.79E-02
77	MLS2s mRNA for melastatin like 2	Trpm4	AB040807	-2.30	1.41E-04
78	Male germ cell-associated kinase (Mak)	Mak	NM_013136	-2.28	1.24E-02
79	RNA binding protein p45AUF1	-	BE097663	-2.28	3.56E-03
80	(clone erb62) thyroid (T3) hormone receptor	Thrb	J03819	-2.27	3.51E-02
81	DNA polymerase delta, catalytic subunit (Pold1)	Pold1	NM_021662	-2.27	1.38E-02
82	Sprague-Dawley glucose-6-phosphatase	G6pc	U07993	-2.26	3.59E-02
83	Synuclein, alpha (Snca)	Snca	NM_019169	-2.25	4.94E-02
84	Neurochondrin (Ncdn)	Ncdn	NM_053543	-2.25	2.12E-04
85	Guanine nucleotide binding protein, alpha (Gnaz)	Gnaz	NM_013189	-2.24	4.45E-02
86	Vasopressin receptor V1a (Avpr1a)	Avpr1a	NM_053019	-2.24	4.77E-02
87	Chymotrypsin B (Ctrb1).	Ctrb	NM_012536	-2.24	1.85E-02
88	Testis-specific kinase 2 (Tesk2)	Tesk2	NM_133396	-2.23	3.26E-02
89	Contactin 1 (Cntn1)	Cntn1	NM_057118	-2.22	1.89E-02
90	Activity and neurotransmitter-induced early gene protein 4 (ania-4)	Ania4	NM_021584	-2.20	3.36E-02

#	Gene Name	Gene ID	Gene Identifier	Ratio	p-value
91	Xylosyltransferase 2 (Xylt2)	Xylt2	NM_022296	-2.19	3.11E-03
92	Agrin	Agri	M64780	-2.19	5.36E-03
93	Mammary cancer associated protein RMT-1	Rmt1	AF308611	-2.19	1.76E-02
94	Inositol polyphosphate-4-phosphatase, type II, 105kD (Inpp4b)	Inpp4b	NM_053917	-2.19	3.41E-02
95	V-akt murine thymoma viral oncogene homolog 3 (protein kinase B gamma) (Akt3)	Akt3	NM_031575	-2.18	4.29E-02
96	Multidrug resistance protein 1a (Pgy1)	Abcb1a	AF257746	-2.16	4.39E-02
97	MEGF6 (Egfl3)	Egfl3	NM_022955	-2.16	3.78E-02
98	Na/K-ATPase beta 2 subunit (ATP1B2)	Atp1b2	U45946	-2.16	3.16E-02
99	Sodium channel, voltage-gated, type V, alpha polypeptide (Scn5a)	Scn5a	NM_013125	-2.15	2.26E-02
100	Centaurin alpha	Centa1	U51013	-2.13	3.66E-02
101	Apoptotic protease activating factor-1	Apaf1	AF218388	-2.13	2.09E-02
102	Iron-regulatory protein 2 (Ireb2)	Ireb2	NM_022863	-2.12	7.71E-03
103	Attractin (Atrn)	Atrn	AB038388	-2.12	3.92E-03
104	UDP-Gal:betaGlcNAc beta 1,3-galactosyltransferase, polypeptide 4 (B3galt4)	B3galt4	NM_133553	-2.12	5.23E-03
105	Spermatogenesis associated 2	Spata2	BM389931	-2.11	4.62E-04
106	Type 2X myosin heavy chain (MYHC)	Myh1	BI277545	-2.10	1.91E-02
107	Kv1.6 voltage-gated potassium channel (kcna6).	Kcna6	AJ276137	-2.10	4.88E-02
108	Apoptotic protease activating factor 1 (Apaf1)	Apaf1	NM_023979	-2.10	2.88E-03

#	Gene Name	Gene ID	Gene Identifier	Ratio	p-value
109	Murine thymoma viral (v-akt) oncogene homolog 1 (Akt1)	Akt1	NM_033230	-2.09	2.88E-03
110	X transporter protein 3 (Xtrp3)	Xtrp3	AI169634	-2.08	1.63E-02
111	SC65 synaptonemal complex protein (Sc65)	Sc65	NM_021581	-2.08	3.50E-02
112	Gene for BAF60b	-	AB003505	-2.08	1.78E-02
113	O-GlcNAc transferase-interacting protein of 98 kDa	Als2cr3	BG378620	-2.08	2.79E-04
114	PKC lambda	Pkel	AB020615	-2.07	8.11E-04
115	Met proto-oncogene (Met)	Met	NM_031517	-2.06	2.30E-03
116	Metabotropic glutamate receptor subtype	Grm6	D13963	-2.06	3.08E-02
117	Branched chain keto acid dehydrogenase kinase	Bckdk	BI277527	-2.04	1.05E-03
118	Guanosine monophosphate reductase (Gmpr)	Gmpr	NM_057188	-2.04	1.88E-02
119	Erythroid differentiation gene 1 (Edag1).	Hemgn	NM_133294	-2.04	4.42E-02
120	Protein kinase inhibitor, alpha	Pkia	AA996685	-2.03	4.18E-02
121	Vps54-like protein	Vps54	AJ010392	-2.03	9.42E-03
122	H-K-ATPase alpha 2b subunit (HKalpha2b)	Atp12a	U94913	-2.03	4.10E-02
123	Ajuba protein (ORF1)	Jub	AJ306292	-2.02	4.90E-03
124	SH3ankyrin domain gene 3 (Shank3)	Shank3	NM_021676	-2.02	3.54E-02
125	Inhibitor of kappa light polypeptide gene enhancer in B-cells, kinase beta (Ikbkb)	Ikbkb	NM_053355	-2.02	5.63E-05
126	Rat casein-alpha	CSN1S1	J00710	-2.02	4.74E-02
127	CCAAT enhancer binding, protein (CEBP) delta (Cebpd)	Cebpd	NM_013154	-2.02	2.17E-02
128	Murine thymoma viral (v-akt)	Akt2	AI105076	-2.02	2.05E-04

#	Gene Name	Gene ID	Gene Identifier	Ratio	p-value
	oncogene homolog 2				
129	SH3-domain binding protein 4 (Sh3bp4), mRNA.	Sh3bp4	NM_022693	-2.02	4.11E-02
130	Bardet-Biedl syndrome 2 (human) (Bbs2)	Bbs2	NM_053618	-2.01	7.06E-03
131	Lsc protein (Lsc)	Arhgef1	NM_021694	-2.01	1.80E-03
132	P2Y purinoceptor	P2ry1	U22830	-2.01	1.09E-02
133	Phospholamban	Pln	BI290034	-2.01	2.85E-02
134	LDL-receptor.	Ldlr	X13722	-2.00	2.41E-03
135	NTR2 receptor (Ntsr2)	Ntsr2	NM_022695	-1.99	1.43E-03
136	Tyrosine protein kinase pp60-c-src (Src)	Src	NM_031977	-1.99	2.91E-02
137	Protein tyrosine phosphatase 2E (Ptp2E)	Ptpn21	NM_133545	-1.98	1.35E-03
138	6-Phosphofructo-2-kinase fructose-2,6-bisphosphatase 1 (liver and muscle) (Pfkfb1)	Pfkfb1	NM_012621	-1.98	2.13E-02
139	Ventral anterior homeobox 2 (Vax2)	Vax2	NM_022637	-1.98	8.35E-03
140	Adenosine receptor A3 (Adora3)	Adora3	NM_012896	-1.97	2.45E-02
141	Glucosidase 1 (Gcs1-pending)	Gcs1	NM_031749	-1.97	1.37E-03
142	Organic anion transporter (LOC83500)	Slc22a8	NM_031332	-1.96	1.07E-02
143	Diacylglycerol kinase, alpha (80kD) (Dgka)	Dgka	NM_080787	-1.96	4.75E-03
144	A disintegrin and metalloprotease domain (ADAM) 22	Adam22	AI029994	-1.96	1.69E-02
145	Multiple PDZ domain protein (Mpdz)	Mpdz	NM_019196	-1.96	3.12E-02
146	Putative pheromone receptor VN1	Vnr1	U36785	-1.95	2.65E-02
147	LIM motif-containing protein	Limk2	NM_024135	-1.95	1.85E-04

#	Gene Name	Gene ID	Gene Identifier	Ratio	p-value
	kinase 2 (Link2)				
148	Opioid-binding protein cell adhesion molecule-like (Opcml)	Opcml	NM_053848	-1.95	1.69E-02
149	Pulmonary surfactant protein D (Sftpd)	Sftpd	NM_012878	-1.94	4.46E-06
150	Adenylyl cyclase type VI	Adcy6	L01115	-1.94	6.00E-04
151	Leucocyte common antigen-related protein	Ptprf	X83505	-1.94	2.99E-03
152	Iron-responsive element-binding protein (Ratireb)	Ratireb	NM_017321	-1.93	2.44E-02
153	Matrix metalloproteinase 24 (membrane-inserted) (Mmp24)	Mmp24	NM_031757	-1.93	2.24E-02
154	Spermatogenesis associated 2 (Spata2)	Spata2	NM_053675	-1.93	4.40E-04
155	Telomerase catalytic subunit	Tert	AF247818	-1.93	3.60E-02
156	Adducin 1, alpha (Add1)	Add1	NM_016990	-1.93	4.09E-03
157	NG,NG dimethylarginine dimethylaminohydrolase	-	BI281103	-1.93	7.26E-04
158	Mucin1	Muc1	BI274326	-1.92	2.51E-02
159	Insulin receptor-related receptor (Insrr)	-	NM_022212	-1.92	2.72E-02
160	Transgelin 3 (Tagln3)	Tagln3	NM_031676	-1.92	4.48E-02
161	Myomegalin (LOC64183)	LOC64183	NM_022382	-1.92	4.74E-03
162	MAP microtubule affinity-regulating kinase 3 (Mark3)	Mark3	NM_130749	-1.92	1.48E-04
163	Exchange factor for ARF6 (EFA6)	Psd	NM_134370	-1.91	4.10E-02
164	Beta isoform of catalytic subunit of cAMP-dependent protein kinase	-	D10770	-1.91	3.56E-03
165	Bruton agammaglobulinemia tyrosine kinase (Tyro3)	Tyro3	NM_017092	-1.91	2.41E-02

#	Gene Name	Gene ID	Gene Identifier	Ratio	p-value
166	Phospholipase C, gamma 1 (Plcg1)	Plcg1	NM_013187	-1.90	4.95E-02
167	MHC class Ib M4 (RT1.M4) pseudogene	-	AF024712	-1.90	4.14E-02
168	Sulfhydryl oxidase (SOx)	Qscn6	AB044285	-1.90	3.40E-02
169	Brain cytosolic acyl coenzyme A thioester hydrolase	Bach	U49694	-1.90	1.28E-02
170	Ovalbumin upstream promoter gamma nuclear receptor rCOUPg	Nr2f6	AA997437	-1.89	1.04E-02
171	Growth factor receptor bound protein 14 (Grb14)	Grb14	NM_031623	-1.89	2.91E-02
172	Procollagen C-proteinase 3	Bmp1	AB012139	-1.89	2.40E-04
173	Farnesyltransferase beta subunit	Fntb	M69056	-1.89	2.44E-03
174	Retinoid X receptor gamma	Rxrg	BE118450	-1.89	8.69E-03
175	Cortactin-binding protein 1	Shank2	AF060116	-1.88	2.89E-02
176	Strain F344N angiotensin-converting enzyme (Ace)	Ace	AF201331	-1.87	2.77E-02
177	Pro-protein convertase 5 isoform B (Pcsk5)	Pcsk5	BI289394	-1.87	3.76E-02
178	Thyroid hormone receptor alpha (Thra1)	Thra	NM_031134	-1.87	2.20E-02
179	Homer, neuronal immediate early gene, 3	Homer3	AW253366	-1.87	6.42E-04
180	ATP-binding cassette, sub-family B (MDRTAP), member 6 (Abcb6)	Abcb6	NM_080582	-1.86	1.48E-02
181	Adaptor-related protein complex 3, mu 2 subunit (Ap3m2)	Ap3m2	NM_133305	-1.86	2.48E-02
182	Protein kinase, lysine deficient 1 (Prkwnk1)	Prkwnk1	NM_053794	-1.86	5.46E-03
183	Zinc finger protein 22 (KOX 15)	Znf22	AI232806	-1.86	1.80E-02
184	Nuclear pore membrane glycoprotein 210 (Pom210)	Pom210	NM_053322	-1.85	1.95E-02

#	Gene Name	Gene ID	Gene Identifier	Ratio	p-value
185	Small nuclear ribonucleoparticle-associated protein (snRNP)	Snrpn	M29294	-1.85	3.35E-02
186	Drosophila polarity gene (frizzled) homologue	Fzd1	AA944349	-1.85	2.05E-02
187	Platelet-derived growth factor, C polypeptide (Pdgfc)	Pdgfc	NM_031317	-1.85	4.67E-03
188	Peptidyl-glycine alpha-amidating monooxygenase (rPAM-2)	Pam	M25719	-1.85	4.93E-02
189	Insulin receptor-related receptor-alpha subunit	Insrr	M90661	-1.85	4.43E-02
190	Zona pellucida glycoprotein 1 (Zp1)	Zp1	NM_053509	-1.84	3.61E-02
191	Tumor-associated protein 1 (TA1)	Slc7a5	NM_017353	-1.84	4.07E-04
192	Translin (Tsn)	Tsn	NM_021762	-1.84	9.20E-04
193	MAD (mothers against decapentaplegic, Drosophila) homolog 7	Madh7	AW521447	-1.83	3.22E-02
194	FSH-regulated protein	-	L26293	-1.83	4.20E-02
195	Asparagine synthetase	Asns	U07202	-1.83	2.92E-03
196	Casein kinase 1 gamma 2 isoform (Csnk1g2)	Csnk1g2	NM_023102	-1.82	4.23E-04
197	Ectonucleoside triphosphate diphosphohydrolase 6 (Entpd6)	Entpd6	NM_053498	-1.82	1.85E-02
198	Zinc finger protein HIT-4	Hit4	AF277900	-1.82	2.42E-02
199	Alpha-tubulin	-	AA956714	-1.82	3.76E-02
200	Skn-1a	Pou2f3	L23862	-1.81	1.62E-02
201	Histone 2a (H2a)	H2a	NM_021840	-1.81	3.94E-02
202	Transcription factor 1, hepatic; LF-B1, hepatic nuclear factor (HNF1): albumin proximal factor, also TCF1 (Tcf1)	Tcf1	NM_012669	-1.81	4.29E-02

#	Gene Name	Gene ID	Gene Identifier	Ratio	p-value
203	Pancreas zinc finger protein, see also D1Bda10 (Znf146)	Zfp260	NM_017364	-1.81	4.85E-03
204	Striatin (Strn)	Strn	NM_019148	-1.81	3.25E-02
205	Androgen receptor-related apoptosis-associated protein CBL27	Cbl27	AF275151	-1.81	2.53E-02
206	Cortactin isoform C	Ctnn	AF054618	-1.81	6.99E-03
207	Type II collagen	Col2a1	AF305418	-1.81	4.99E-02
208	CLIP-associating protein 2 (Clasp2)	Clasp2	NM_053722	-1.81	2.58E-02
209	Voltage-gated Ca channel	Tpcn1	AB018253	-1.81	1.92E-05
210	Prolactin-like protein H (PLP-H)	PLP-I	AB019791	-1.80	5.39E-03
211	Strain SHROla ADD1SREBP-1c (Srebf1)	Srebf1	AF286470	-1.80	4.86E-02
212	Interleukin 23, alpha subunit p19 (Il23a)	Il23a	NM_130410	-1.80	9.32E-03
213	Solute carrier family 8 (Na/Ca exchanger), member 3 (Slc8a3)	Slc8a3	NM_078620	-1.80	1.47E-02
214	Ribosomal protein L30	-	AI170773	-1.80	5.51E-04
215	Androgen binding protein (ABP)	Hdc	M38759	-1.80	4.87E-02
216	Leucocyte specific transcript 1 (Lst1)	Lst1	NM_022634	-1.80	2.38E-02
217	Aryl hydrocarbon receptor (AHR) mRNA, alternatively spliced shorter insertion variant	Ahr	AF082125	-1.80	2.15E-03
218	Rattus sp. mRNA for kinase	-	AB020967	-1.79	5.21E-03
219	Ion transporter protein (NRITP)	Nritp	AF184921	-1.79	4.42E-02
220	Activity-dependent neuroprotective protein (Adnp)	Adnp	NM_022681	-1.79	1.81E-03
221	SH2-B PH domain containing signaling mediator 1 (Sh2bpsm1)	Sh2bpsm1	NM_134456	-1.79	9.47E-04

#	Gene Name	Gene ID	Gene Identifier	Ratio	p-value
222	Moloney murine sarcoma viral (v-mos) oncogene homolog (Mos)	Mos	NM_020102	-1.79	2.23E-02
223	Selectin, endothelial cell, ligand (Selel)	Glg1	NM_017211	-1.79	1.81E-02
224	Histone deacetylase 2	Hdac2	AA892297	-1.78	1.76E-02
225	MIC2 like 1 (Mic2l1)	Mic2l1	NM_134459	-1.78	1.67E-02
226	RP58 protein (Rp58)	Rp58	NM_022678	-1.78	2.24E-04
227	Acetyl-coenzyme A carboxylase (EC 6.4.1.2.)	Acaca	BI296153	-1.78	1.27E-03
228	Kinesin light chain 1	Klc1	AI576961	-1.78	7.81E-04
229	Solute carrier family 13 (sodium sulphate symporters), member 1	Slc13a1	AI454619	-1.77	4.53E-02
230	Bladder cancer associated protein (Blcap)	Blcap	NM_133582	-1.77	1.71E-03
231	Guanine nucleotide binding protein (G protein) alpha 12 (Gna12)	Gna12	NM_031034	-1.77	1.11E-02
232	Casein kinase I delta	Csnk1d	AA946432	-1.77	9.39E-04
233	Gamma-aminobutyric acid (GABA-A) receptor, subunit alpha 4 (Gabra4)	Gabra4	NM_080587	-1.77	2.10E-02
234	Nuclear receptor coactivator 2 (Ncoa2)	Ncoa2	NM_031822	-1.76	3.46E-02
235	Enigma homolog (Enh)	Enh	NM_053326	-1.76	7.64E-03
236	Transcription factor E2a (Tcfe2a)	Tcfe2a	NM_133524	-1.76	2.53E-02
237	A kinase (PRKA) anchor protein 1 (Akap1)	Akap1	NM_053665	-1.76	1.37E-03
238	Neurofibromatosis type 1 (Nf1)	Nf1	NM_012609	-1.76	4.60E-02
239	Lamin B1 (Lmnb1)	Lmnb1	NM_053905	-1.75	2.54E-02
240	LIM-domain containing, protein kinase (Limk1)	Limk1	NM_031727	-1.75	4.82E-02

#	Gene Name	Gene ID	Gene Identifier	Ratio	p-value
241	Rho interacting protein 3 (Rhoip3)	Rhoip3	NM_053814	-1.75	1.02E-02
242	C-terminal binding protein 1 (Ctbp1)	Ctbp1	NM_019201	-1.75	6.69E-04
243	TANK protein	Tank	AW140505	-1.75	9.35E-04
244	Arachidonate 12-lipoxygenase (Alox12)	Alox15	NM_031010	-1.75	1.01E-02
245	p75-like apoptosis-inducing death domain protein PLAIDD (LOC246143)	LOC246143	NM_139259	-1.75	4.60E-02
246	bcl-2 associated death agonist beta (Bad-beta)	Bad	AF279911	-1.74	1.72E-02
247	Solute carrier family 25 (mitochondrial carrier; citrate transporter) member 1 (Slc25a1), nuclear gene encoding mitochondrial protein	Slc25a1	NM_017307	-1.74	1.29E-03
248	CTL target antigen (Cth)	Cth	NM_017074	-1.74	1.88E-02
249	Phytanoyl-CoA hydroxylase (Refsum disease) (Phyh).	Phyh	NM_053674	-1.74	7.25E-03
250	p38 mitogen activated protein kinase (Mapk14)	Mapk14	NM_031020	-1.74	5.07E-03
251	Putative pheromone receptor VN7	V1rb7	U36786	-1.74	2.12E-02
252	Activine receptor 2b (transmembrane serine kinase)	Acvr2b	AI548799	-1.73	8.43E-03
253	Selenium binding protein 2 (Selenbp2)	Selenbp1	NM_080892	-1.73	4.31E-03
254	RalBP1	Ralbp1	U28830	-1.73	1.93E-02
255	Guanine nucleotide binding protein, alpha inhibiting 1 (Gnai1)	Gnai1	NM_013145	-1.73	3.99E-03
256	Putative protein phosphatase 1	Ppp1r10	NM_022951	-1.73	7.12E-04

#	Gene Name	Gene ID	Gene Identifier	Ratio	p-value
	nuclear targeting subunit (Ppp1r10)				
257	Cyclin D3 (Ccnd3)	Ccnd3	NM_012766	-1.73	7.03E-04
258	Rattus sp. DNA binding protein (URE-B1)	-	U08214	-1.73	3.31E-03
259	Testis specific protein	AF146738	AF146738	-1.72	2.84E-03
260	Phosphoribosyl pyrophosphate amidotransferase (Ppat).	-	NM_057198	-1.72	2.47E-05
261	Low density lipoprotein receptor-related protein associated protein 1	-	AI008974	-1.72	2.67E-03
262	WW domain binding protein 2 (Wbp2)	Wbp2	NM_138975	-1.72	3.52E-02
263	Gamma-aminobutyric acid (GABA) A receptor, alpha 3 (Gabra3)	Gabra3	NM_017069	-1.72	6.60E-03
264	ATP-binding cassette protein B1b	Abcb1	AY082609	-1.72	4.93E-02
265	Ras-related small GTP binding protein 4	Rab4a	BF281403	-1.72	2.83E-02
266	Glucocorticoid-induced leucine zipper (Gilz)	Dsipi	NM_031345	-1.71	9.27E-04
267	D1 dopamine receptor	Drd1a	M35077	-1.71	7.05E-03
268	Caspase-9 CTD isoform	Casp9	AY008275	-1.71	1.41E-02
269	F-spondin	LOC17156 9	AA801238	-1.71	3.20E-02
270	Damage-specific DNA binding protein 1	Ddb1	BF284000	-1.71	3.10E-02
271	Activin type I receptor (Acvr1)	Acvr1	NM_024486	-1.71	1.26E-03
272	Cyclin-dependent kinase 4 (Cdk4)	Cdk4	NM_053593	-1.71	5.57E-04
273	HLA-B associated transcript 3 (Bat3)	Bat3	NM_053609	-1.71	7.56E-03
274	RSS	-	D89965	-1.70	2.97E-02

#	Gene Name	Gene ID	Gene Identifier	Ratio	p-value
275	DNA polymerase beta (Polb)	Polb	NM_017141	-1.70	2.50E-02
276	RIN1	Rin1	U80076	-1.70	4.81E-02
277	Proline rich synapse associated protein 1 (ProSAP1)	Shank2	NM_133440	-1.70	1.92E-03
278	Insulin receptor (Insr)	Insr	NM_017071	-1.70	1.69E-02
279	Amino-terminal enhancer of split	Aes	BI274118	-1.70	1.26E-02
280	LIC-2 dynein light intermediate chain 5355 (Dncli2)	Dncli2	NM_031026	-1.70	9.22E-03
281	DNA fragmentation factor, 40 kD, beta polypeptide (caspase-activated DNase) (Dffb)	Dffb	NM_053362	-1.70	2.57E-02
282	Calpain 10 (Capn10).	Capn10	NM_031673	-1.70	8.93E-03
283	crp-ductin (Crdp)	-	NM_022849	-1.69	2.26E-02
284	Gustatory receptor 43 (Gust43)	Gust43	NM_020106	-1.69	3.44E-02
285	Hairless (hr)	Hr	NM_024364	-1.69	5.67E-03
286	Afadin (AF-6)	Af6	NM_013217	-1.69	3.15E-03
287	Adenylate kinase 3 (Ak3)	Ak3	NM_013218	-1.69	2.09E-03
288	Guanylate-cyclase regulatory protein (GCRP)	Rap2ip	AF288611	-1.69	1.32E-02
289	NF1-B3	Nfib	AB012232	-1.69	3.39E-02
290	Ischemia responsive 94 kDa protein (irp94)	Hspa4	AF077354	-1.69	1.32E-02
291	N-type calcium channel pore-forming subunit alpha 1B	Cacna1b	AF389419	-1.69	2.38E-03
292	Tumor necrosis factor (ligand) superfamily, member 6 (apoptosis (APO-1) antigen ligand 1) (Fas antigen ligand) (Tnfsf6)	Tnfsf6	NM_012908	-1.69	8.17E-03
293	Thymopoietin (lamina associated polypeptide 2) (Tmpos)	Tmpos	NM_012887	-1.68	6.66E-03
294	Rabin 3 (RABIN3)	RABIN3	NM_017313	-1.68	5.21E-03

#	Gene Name	Gene ID	Gene Identifier	Ratio	p-value
295	Maternal G10 transcript	G10	AI599413	-1.68	2.23E-02
296	Potassium inwardly-rectifying, channel, subfamily J, member 6 (Kcnj6)	-	NM_013192	-1.68	4.51E-02
297	Putative protein serinethreonine phosphatase 4-associated protein	Ppp4r1	BI285346	-1.68	4.73E-02
298	Proteinase-activated receptor-2, G protein-coupled receptor 11 (F2r11)	F2r11	NM_053897	-1.68	3.80E-02
299	G-protein-coupled receptor induced protein GIG2	Trib1	BM387324	-1.68	1.39E-03
300	GABA-BR1a receptor	Gabbr1	Y10369	-1.67	9.25E-04
301	Unknown Glu-Pro dipeptide repeat protein	Rab10	AA945841	-1.67	2.94E-03
302	Gastric inhibitory peptide receptor (Gipr)	Gipr	NM_012714	-1.67	4.17E-02
303	Phosphodiesterase 3B, cGMP-inhibited (Pde3b)	Pde3b	NM_017229	-1.67	1.45E-02
304	Granuphilin B	Sytl4	AF419342	-1.67	5.88E-03
305	Transforming growth factor beta stimulated clone 22 (Tgfb1i4)	-	NM_013043	-1.67	1.04E-02
306	Putative zinc finger protein SERZ-1 (Serz-1)	Zdhhc7	NM_133394	-1.67	7.73E-03
307	Myotonic dystrophy kinase-related Cdc42-binding kinase MRCK-beta (MRCK-beta)	Cdc42bpb	AF021936	-1.67	4.28E-02
308	Growth supressor 1 (Gros1)	Lepre1	NM_053667	-1.67	8.22E-03
309	Potassium inwardly-rectifying channel,subfamily J, member 13 (Kcnj13)	Kcnj13	NM_053608	-1.67	3.11E-02
310	Prolyl endopeptidase (Prep)	Prep	NM_031324	-1.67	2.48E-03
311	Butyrylcholinesterase (Bche)	Bche	NM_022942	-1.67	4.56E-02
312	Crystallin, beta B3 (Crybb3)	Crybb3	NM_031690	-1.67	2.17E-02

#	Gene Name	Gene ID	Gene Identifier	Ratio	p-value
313	Potassium voltage gated channel, shaker related subfamily, beta member 2 (Kcnab2)	Kcnab2	NM_017304	-1.66	1.20E-02
314	Protein tyrosine phosphatase, non-receptor type 1 (Ptpn1)	Ptpn1	NM_012637	-1.66	3.36E-02
315	Junction plakoglobin (Jup)	Jup	NM_031047	-1.66	2.55E-03
316	Peroxisomal multifunctional enzyme type II (Hsd17b4)	Hsd17b4	NM_024392	-1.66	9.03E-03
317	DNA polymerase gamma (Polg)	Polg	NM_053528	-1.66	7.97E-05
318	Slit (Drosophila) homolog 3 (Slit3)	Slit3	NM_031321	-1.66	3.23E-02
319	Chymotrypsin-like (Ctrl)	Ctrl	NM_054009	-1.66	3.84E-02
320	Ring finger protein 22 (Rnf22)	Trim3	NM_031786	-1.65	5.38E-03
321	Gap junction membrane channel protein alpha 5 (connexin 40) (Gja5)	Gja5	NM_019280	-1.65	2.91E-02
322	Moesin (Msn)	Msn	NM_030863	-1.65	4.08E-03
323	GATA-binding protein 6 (Gata6)	Gata6	NM_019185	-1.65	4.50E-02
324	Zinc finger protein (pMLZ-4)	-	AF151710	-1.65	9.16E-04
325	Clone GB1B21a phosphodiesterase 1B (Pde1B)	Pde1b	AF327906	-1.65	4.10E-02
326	Ankyrin repeat-rich membrane-spanning protein (ARMS)	Kidins220	AF313464	-1.65	4.19E-02
327	Meningioma expressed antigen 5 (hyaluronidase) (Mgea5)	Mgea5	NM_131904	-1.65	3.69E-02
328	Sprague-Dawley (clone LRB6) RAB12	Rab12	M83676	-1.65	2.89E-02
329	Rat alternative brain Ca ⁺ 2-ATPase	-	J04024	-1.65	6.96E-03
330	Scaffolding protein SLIPR (Slipr)	Slipr	AF255614	-1.64	2.77E-02
331	p53-activated gene 608 (PAG608)	Wig1	NM_022548	-1.64	6.63E-03

#	Gene Name	Gene ID	Gene Identifier	Ratio	p-value
332	Amino acid transporter system A (ATA2)	Slc38a2	AF249673	-1.64	9.83E-03
333	Nucleoporin 155kD (Nup155)	Nup155	NM_053952	-1.64	5.60E-03
334	Protein serine/threonine kinase CPG16 (cpg16)	Ania4	U78857	-1.64	1.52E-02
335	Myosin IXb	Myo9b	AI178160	-1.64	1.77E-04
336	TEMO	-	AI180458	-1.64	3.41E-02
337	Rat brain-specific identifier sequence (ID) clone p1B337.	Eif5	K01677	-1.64	1.71E-02
338	Myosin Ic (Myo1c)	Myo1c	NM_012983	-1.64	7.77E-03
339	Diphosphoinositol polyphosphate phosphohydrolase type II	Nudt4	AI602300	-1.64	2.70E-02
340	Protein phosphatase 2 (formerly 2A), catalytic subunit, beta isoform (Ppp2cb)	Ppp2cb	NM_017040	-1.63	6.83E-04
341	Purinergic receptor P2X, ligand-gated ion channel, 7 (P2rx7)	P2rx7	NM_019256	-1.63	4.07E-03
342	Myosin Vb (Myo5b)	Myo5b	NM_017083	-1.63	9.10E-03
343	Nuclear receptor subfamily 2, group F, member 6 (Nr2f6)	Nr2f6	NM_139113	-1.63	6.58E-04
344	Phosphatidylinositol 3-kinase, C2 domain containing, gamma polypeptide (Pik3c2g)	Pik3c2g	NM_053923	-1.63	4.67E-02
345	TEMO (Temo)	-	NM_023986	-1.63	8.58E-03
346	Tyrosine protein kinase pp60-c-src	Src	AI175966	-1.63	2.40E-02
347	CTD-binding SR-like protein rA9	LOC24592 5	U49057	-1.63	1.19E-02
348	RNA helicase with arginine-serine-rich domain	Ddx46	U25746	-1.62	1.57E-02
349	Unconventional myosin Myr2 I heavy chain (Myr2)	Myr2	NM_023092	-1.62	2.94E-02

#	Gene Name	Gene ID	Gene Identifier	Ratio	p-value
350	SH2-containing inositol phosphatase 2 (Inpp1)	Inpp1	NM_022944	-1.62	8.55E-03
351	Poly(ADP-ribose) glycohydrolase (Parg)	Parg	AB019366	-1.62	3.69E-03
352	Activity and neurotransmitter-induced early gene 3 (ania-3)	Homer1	AF030088	-1.62	3.68E-02
353	AKAP95	Akap8	U01914	-1.62	1.54E-03
354	exo84	Exoc8	AF032669	-1.62	1.92E-02
355	Erythropoietin receptor (Epor)	Epor	NM_017002	-1.62	2.37E-02
356	NonOp54nrb homolog	Sfpq	AI599699	-1.61	4.00E-02
357	Endothelial differentiation, sphingolipid G-protein-coupled receptor, 5 (Edg5)	Edg5	NM_017192	-1.61	7.13E-03
358	Multiple endocrine neoplasia 1 (Men1)	Men1	NM_019208	-1.61	4.95E-03
359	Upstream transcription factor 1 (Usf1)	Usf1	NM_031777	-1.61	1.50E-02
360	Murine thymoma viral (v-akt) oncogene homolog 2 (Akt2)	Akt2	NM_017093	-1.61	2.15E-02
361	Fertility related protein WMP1	Wmp1	AF094609	-1.61	7.16E-03
362	Laminin, gamma 1	Lamc1	BI275624	-1.60	3.11E-03
363	Preoptic regulatory factor-2 (PORF-2).	PORF-2	X53232	-1.60	1.18E-02
364	Natriuretic peptide clearance receptor	Npr3	X78595	-1.60	4.83E-02
365	Mevalonate kinase (Mvk)	Mvk	NM_031063	-1.60	2.40E-02
366	Nucleosome assembly protein 1-like 1	Nap111	BM386384	-1.60	8.57E-03
367	v-crk avian sarcoma virus CT10 oncogene homolog (Crk)	Crk	NM_019302	-1.60	2.11E-02
368	Beta II spectrin-short isoform	Spnb2	AW920849	-1.60	4.04E-02
369	RAP2B, member of RAS	Rap2b	NM_133410	-1.60	1.67E-02

#	Gene Name	Gene ID	Gene Identifier	Ratio	p-value
	oncogene family (Rap2b)				
370	UDP-glucose glycoprotein: glucosyltransferase UGGT (Uggt)	Ugcgl1	NM_133596	-1.60	1.94E-02
371	Beta adaptin	Ap2b1	M34176	-1.59	2.22E-02
372	CDC37 (cell division cycle 37, S. cerevisiae, homolog) (Cdc37)	Cdc37	NM_053743	-1.59	1.14E-03
373	Avian sarcoma virus 17 (v-jun) oncogene homolog (Jun)	Jun	NM_021835	-1.59	7.39E-04
374	Neuroblastoma RAS viral (v-ras) oncogene homolog (Nras)	Nras	NM_080766	-1.59	3.33E-02
375	SPASIC protein	Accn4	BM386997	-1.59	4.17E-02
376	Tspan-2 protein (Tspan-2)	Tspan2	NM_022589	-1.59	4.61E-02
377	Syntaxin 1 a	Stx1a	BI290256	-1.59	1.59E-02
378	Neural visinin-like protein 1 (Vsn1)	Vsn1	NM_012686	-1.59	4.18E-02
379	Dopamine receptor interacting protein (Drip78)	Drip78	NM_053690	-1.59	2.67E-03
380	Ryk mRNA for tyrosine kinase-related protein	Ryk	AB073721	-1.58	7.92E-03
381	Acetylcholine receptor beta (Chrb1)	Chrb1	NM_012528	-1.58	4.68E-02
382	Guanine nucleotide-binding protein beta 1	Gnb1	AI103622	-1.58	1.07E-02
383	MafG-2	Mafg	AB050011	-1.58	4.68E-04
384	s-Afadin	Af6	U83231	-1.58	2.60E-02
385	ATP-binding cassette, sub-family C (CFTRMRP), member 2 (Abcc2)	Abcc2	NM_012833	-1.58	2.95E-03
386	Myelin oligodendrocyte glycoprotein	Zfp57	BE103960	-1.58	2.92E-02
387	Sprague-Dawley N-methyl-D-aspartate receptor NMDAR2C	Grin2c	U08259	-1.58	4.57E-02

#	Gene Name	Gene ID	Gene Identifier	Ratio	p-value
	subunit				
388	Fos-related antigen (Fra)	Rabep2	NM_030585	-1.58	1.92E-02
389	Adenylyl cyclase 2 (Adcy2)	Adcy2	NM_031007	-1.58	2.91E-02
390	Rabaptin	Rabep1	U70777	-1.57	1.43E-02
391	Discs, large homolog 3 (Drosophila)	Dlgh3	BI290059	-1.57	4.46E-02
392	Calpain 8 (Capn8)	Capn8	NM_133309	-1.57	4.20E-02
393	SNRPN upstream reading frame (Snurf)	Snrpn	NM_130738	-1.57	3.12E-03
394	2,3-oxidosqualene:lanosterol cyclase	Lss	D45252	-1.57	4.80E-02
395	5-AMP-activated protein kinase, beta subunit (Prkab1)	Prkab1	NM_031976	-1.57	1.87E-02
396	Noerythroid alpha-spectrin 2	Spna2	BM387423	-1.56	3.57E-03
397	Substance P receptor	Tacr1	M31477	-1.56	4.40E-02
398	Pancreatitis associated protein III (PAPIII0)	Reg3g	L20869	-1.56	4.97E-02
399	Nuclear pore membrane glycoprotein 121 kD (Pom121),	Pom121	NM_053622	-1.56	3.46E-03
400	Cysteine desulfurase	Nifs	AI410876	-1.56	5.15E-03
401	Transporter protein; system N1 Na ⁺ and H ⁺ -coupled glutamine transporter	Hnrpu	AI177494	-1.56	3.35E-03
402	Peptide histidine transporter	Slc15a4	AB000280	-1.56	1.68E-03
403	Drosophila polarity gene (frizzled) homologue	Fzd2	L02530	-1.56	1.11E-02
404	Actinin, alpha 4 (Actn4)	Actn4	NM_031675	-1.56	1.91E-02
405	Unconventional myosin Myr2 I heavy chain	Myr2	AI012566	-1.56	4.13E-02
406	Matrix metalloproteinase 24 (membrane-inserted)	Mmp24	AI175506	-1.56	4.39E-02

#	Gene Name	Gene ID	Gene Identifier	Ratio	p-value
407	Calmodulin III (Calm3)	Calm3	AI411316	-1.56	5.72E-03
408	Metabotropic glutamate receptor 8 (Grm8)	Grm8	NM_022202	-1.55	4.87E-02
409	Synaptotagmin 6 (Syt6)	Syt6	NM_022191	-1.55	2.62E-02
410	Sialyltransferase (N-acetylglucosaminidase alpha 2,3-sialyltransferase) (Siat6)	Siat6	NM_031697	-1.55	3.53E-02
411	Cytoplasmic linker 2 (Cyln2)	Cyln2	NM_021997	-1.55	3.11E-02
412	Homolog of yeast nuclear protein localization 4 (Npl4)	Npl4	NM_080577	-1.55	6.62E-03
413	Vesicle associated protein (VAP1)	Sec3111	NM_033021	-1.55	9.19E-04
414	Spermidine synthase (Srm)	Srm	NM_053464	-1.55	3.89E-03
415	Cell division cycle 25A (Cdc25a)	Cdc25a	NM_133571	-1.55	1.04E-02
416	V1-type AVP membrane receptor	Itgb5	AW520594	-1.55	2.85E-02
417	Septin 2 (Sept2)	2-Sep	NM_057148	-1.55	1.53E-02
418	presenilin-2	Psen2	AB004454	-1.55	2.38E-02
419	Rattus sp. pre-mtHSP70; nuclear gene for mitochondrial product.	-	S75280	-1.55	2.63E-02
420	Zinc finger protein 22 (KOX 15) (Znf22)	Znf22	NM_133579	-1.55	4.29E-04
421	Epithelial sodium channel alpha subunit (rEnaca)	Senn1a	U54699	-1.55	4.17E-02
422	Unknown Glu-Pro dipeptide repeat protein	-	BI294751	-1.55	6.11E-03
423	Rat metalloendopeptidase	Thop1	M61142	-1.55	8.62E-03
424	myosin IB (Myo1b)	Myo1b	NM_053986	-1.55	2.80E-03
425	Gamma-glutamyl carboxylase (Ggcx)	Ggcx	NM_031756	-1.55	3.04E-02
426	S-Adenosylmethionine decarboxylase 1 (Amd1)	Amd1	NM_031011	-1.55	1.73E-03
427	Glutamate dehydrogenase	Glud1	BI284411	-1.54	6.23E-03

#	Gene Name	Gene ID	Gene Identifier	Ratio	p-value
428	Transforming growth factor, beta receptor III (Tgfbr3)	Tgfbr3	NM_017256	-1.54	1.74E-02
429	Malic enzyme 1, soluble (Me1)	Me1	NM_012600	-1.54	5.94E-03
430	Hsp70 binding protein HspBP	Hspbp1	AF187860	-1.54	7.39E-03
431	Selective LIM binding factor, rat homolog (Slb)	Slb	NM_053792	-1.54	4.49E-02
432	Castration Induced Prostatic Apoptosis Related protein-1 (CIPAR-1)	Cipar1	AI136555	-1.53	2.14E-02
433	Colony stimulating factor 2 receptor, beta 1, low-affinity (granulocyte-macrophage) (Csf2rb1)-	Csf2rb1	NM_133555	-1.53	3.95E-02
434	Clone 15 phosphodiesterase 1C (PDE1C)	Pde1c	AF328800	-1.53	4.78E-02
435	Protease, serine, 15 (Prss15)	Prss15	NM_133404	-1.53	2.17E-02
436	NM23-R7 (Nm23-R7)	Nme7	AF202049	-1.53	8.71E-03
437	GPI-anchored metastasis-associated protein homolog (C4.4a)	C4.4a	NM_021759	-1.53	2.38E-02
438	Rat adult liver mRNA for S1-1 protein	Rbm10	D83948	-1.53	1.37E-02
439	Fatty acid synthase (Fasn)	Fasn	NM_017332	-1.53	3.36E-02
440	Galactosyltransferase associated kinase (GTA)	Cdc211	L24388	-1.53	1.66E-02
441	Protein phosphatase type 1A (formely 2C), Mg-dependent, alpha isoform (Ppm1a)	Ppm1a	NM_017038	-1.53	3.58E-03
442	Phosphatidylinositol 4-kinase (Pik4cb)	Pik4cb	NM_031083	-1.52	9.20E-03
443	Dipeptidylpeptidase III (Dpp3)	Dpp3	NM_053748	-1.52	2.06E-02
444	Rapamycin and FKBP12 target-1 protein (Frap1)	Frap1	NM_019906	-1.52	1.41E-02

#	Gene Name	Gene ID	Gene Identifier	Ratio	p-value
445	Limkain b1 (Lkap)	Lkap	NM_133421	-1.52	4.87E-02
446	Alcohol dehydrogenase family 3, subfamily A2 (Aldh3a2)	Aldh3a2	NM_031731	-1.52	6.86E-03
447	Phospholipase D	Pld1	AB000779	-1.52	1.45E-02
448	ADP-ribosylation-like 2 (Arl2)	Arl2	NM_031711	-1.52	1.53E-02
449	Gamma-synergin	Ap1gbp1	AF169549	-1.52	6.36E-03
450	Collagen type XVIII, alpha 1 chain	Col18a1	BI288582	-1.52	7.81E-03
451	Acetyl-CoA transporter (Acatn)	Slc33a1	NM_022252	-1.52	7.76E-04
452	Neurolysin (metallopeptidase M3 family) (Nln)	Nln	NM_053970	-1.51	1.29E-02
453	Heat shock transcription factor 1	Hsf1	AI172496	-1.51	2.87E-05
454	ATPase, Class II, type 9A	Atp9a	BG380816	-1.51	2.44E-03
455	Prostaglandin transporter subtype 2 (Pgt2)	Slco3a1	AF239219	-1.51	3.37E-02
456	CPG2 protein (CPG2)	-	NM_019355	-1.51	1.46E-02
457	Thymine-DNA glycosylase (Tdg)	Tdg	NM_053729	-1.51	3.10E-02
458	Ryk mRNA for tyrosine kinase-related protein	Ryk	BE113287	-1.51	3.17E-02
459	UNC-119 homolog (C. elegans) (Unc119)	Unc119	NM_017188	-1.51	3.64E-02
460	Endo-alpha-mannosidase (Enman)	Enman	NM_080785	-1.50	4.59E-02
461	Hepatoma-derived growth factor (Hdgf)	Hdgf	NM_053707	-1.50	7.84E-03
462	Shank-interacting protein (Conneck1)	Sharpin	NM_031153	-1.50	9.14E-03
463	A disintegrin and metalloproteinase domain (ADAM) 15 (metargidin) (Adam15)	Adam15	NM_020308	-1.50	2.19E-02
464	G protein-coupled receptor LGR4	Gpr48	BI300274	-1.50	2.57E-02

#	Gene Name	Gene ID	Gene Identifier	Ratio	<i>p</i> -value
	(LGR4)				
465	Ectonucleotide pyrophosphatase phosphodiesterase 2 (Enpp2)	Enpp2	NM_057104	-1.50	1.06E-02
466	Xrcc5	Xrcc5	AA893188	-1.50	4.26E-03
467	Chloride channel 7 (Clcn7)	Clcn7	NM_031568	-1.50	7.07E-03
468	Cytochrome P450 Lanosterol 14 alpha-demethylase (Cyp51)	Cyp51	NM_012941	-1.50	2.09E-02

BIBLIOGRAPHY

1. Miyake T, Kung CK, Goldwasser E. Purification of human erythropoietin. *J Biol Chem* 1977;252:5558-5564.
2. Eckardt KU, Kurtz A. Regulation of erythropoietin production. *Eur J Clin Invest* 2005;35 Suppl 3:13-19.
3. Goldberg MA, Glass GA, Cunningham JM, Bunn HF. The regulated expression of erythropoietin by two human hepatoma cell lines. *Proc Natl Acad Sci U S A* 1987;84:7972-7976.
4. Goldberg MA, Dunning SP, Bunn HF. Regulation of the erythropoietin gene: evidence that the oxygen sensor is a heme protein. *Science* 1988;242:1412-1415.
5. Semenza GL, Koury ST, Nejfelt MK, Gearhart JD, Antonarakis SE. Cell-type-specific and hypoxia-inducible expression of the human erythropoietin gene in transgenic mice. *Proc Natl Acad Sci U S A* 1991;88:8725-8729.
6. Semenza GL, Nejfelt MK, Chi SM, Antonarakis SE. Hypoxia-inducible nuclear factors bind to an enhancer element located 3' to the human erythropoietin gene. *Proc Natl Acad Sci U S A* 1991;88:5680-5684.
7. Semenza GL, Wang GL. A nuclear factor induced by hypoxia via de novo protein synthesis binds to the human erythropoietin gene enhancer at a site required for transcriptional activation. *Mol Cell Biol* 1992;12:5447-5454.
8. Wang GL, Semenza GL. Characterization of hypoxia-inducible factor 1 and regulation of DNA binding activity by hypoxia. *J Biol Chem* 1993;268:21513-21518.
9. Wang GL, Semenza GL. General involvement of hypoxia-inducible factor 1 in transcriptional response to hypoxia. *Proc Natl Acad Sci U S A* 1993;90:4304-4308.
10. Wang GL, Semenza GL. Purification and characterization of hypoxia-inducible factor 1. *J Biol Chem* 1995;270:1230-1237.
11. Wang GL, Jiang BH, Rue EA, Semenza GL. Hypoxia-inducible factor 1 is a basic-helix-loop-helix-PAS heterodimer regulated by cellular O₂ tension. *Proc Natl Acad Sci U S A* 1995;92:5510-5514.

12. Huang ZJ, Edery I, Rosbash M. PAS is a dimerization domain common to *Drosophila* period and several transcription factors. *Nature* 1993;364:259-262.
13. Dolwick KM, Swanson HI, Bradfield CA. In vitro analysis of Ah receptor domains involved in ligand-activated DNA recognition. *Proc Natl Acad Sci U S A* 1993;90:8566-8570.
14. Reisz-Porszasz S, Probst MR, Fukunaga BN, Hankinson O. Identification of functional domains of the aryl hydrocarbon receptor nuclear translocator protein (ARNT). *Mol Cell Biol* 1994;14:6075-6086.
15. Hirose K, Morita M, Ema M, Mimura J, Hamada H, Fujii H, Saijo Y, et al. cDNA cloning and tissue-specific expression of a novel basic helix-loop-helix/PAS factor (Arnt2) with close sequence similarity to the aryl hydrocarbon receptor nuclear translocator (Arnt). *Mol Cell Biol* 1996;16:1706-1713.
16. Takahata S, Sogawa K, Kobayashi A, Ema M, Mimura J, Ozaki N, Fujii-Kuriyama Y. Transcriptionally active heterodimer formation of an Arnt-like PAS protein, Arnt3, with HIF-1a, HLF, and clock. *Biochem Biophys Res Commun* 1998;248:789-794.
17. Semenza GL. Regulation of mammalian O₂ homeostasis by hypoxia-inducible factor 1. *Annu Rev Cell Dev Biol* 1999;15:551-578.
18. Chan WK, Yao G, Gu YZ, Bradfield CA. Cross-talk between the aryl hydrocarbon receptor and hypoxia inducible factor signaling pathways. Demonstration of competition and compensation. *J Biol Chem* 1999;274:12115-12123.
19. Franks RG, Crews ST. Transcriptional activation domains of the single-minded bHLH protein are required for CNS midline cell development. *Mech Dev* 1994;45:269-277.
20. UniProt Universal Protein Knowledgebase. (<http://www.ebi.uniprot.org>): UniProt Consortium: European Bioinformatics Institute (EBI), Swiss Institute of Bioinformatics (SIB), and Protein Information Resource (PIR): Accessed 1/13/2006.
21. Luo G, Gu YZ, Jain S, Chan WK, Carr KM, Hogenesch JB, Bradfield CA. Molecular characterization of the murine Hif-1 alpha locus. *Gene Expr* 1997;6:287-299.
22. Ladoux A, Frelin C. Cardiac expressions of HIF-1 alpha and HLF/EPAS, two basic loop helix/PAS domain transcription factors involved in adaptative responses to hypoxic stresses. *Biochem Biophys Res Commun* 1997;240:552-556.
23. Li H, Ko HP, Whitlock JP. Induction of phosphoglycerate kinase 1 gene expression by hypoxia. Roles of Arnt and HIF1alpha. *J Biol Chem* 1996;271:21262-21267.
24. Wenger RH, Rolfs A, Marti HH, Guenet JL, Gassmann M. Nucleotide sequence, chromosomal assignment and mRNA expression of mouse hypoxia-inducible factor-1 alpha. *Biochem Biophys Res Commun* 1996;223:54-59.

25. Luo JC, Shibuya M. A variant of nuclear localization signal of bipartite-type is required for the nuclear translocation of hypoxia inducible factors (1alpha, 2alpha and 3alpha). *Oncogene* 2001;20:1435-1444.
26. Jiang BH, Zheng JZ, Leung SW, Roe R, Semenza GL. Transactivation and inhibitory domains of hypoxia-inducible factor 1alpha. Modulation of transcriptional activity by oxygen tension. *J Biol Chem* 1997;272:19253-19260.
27. Arany Z, Huang LE, Eckner R, Bhattacharya S, Jiang C, Goldberg MA, Bunn HF, et al. An essential role for p300/CBP in the cellular response to hypoxia. *Proc Natl Acad Sci U S A* 1996;93:12969-12973.
28. Ebert BL, Bunn HF. Regulation of transcription by hypoxia requires a multiprotein complex that includes hypoxia-inducible factor 1, an adjacent transcription factor, and p300/CREB binding protein. *Mol Cell Biol* 1998;18:4089-4096.
29. Kallio PJ, Okamoto K, O'Brien S, Carrero P, Makino Y, Tanaka H, Poellinger L. Signal transduction in hypoxic cells: inducible nuclear translocation and recruitment of the CBP/p300 coactivator by the hypoxia-inducible factor-1alpha. *Embo J* 1998;17:6573-6586.
30. Lando D, Peet DJ, Whelan DA, Gorman JJ, Whitelaw ML. Asparagine hydroxylation of the HIF transactivation domain a hypoxic switch. *Science* 2002;295:858-861.
31. Lando D, Peet DJ, Gorman JJ, Whelan DA, Whitelaw ML, Bruick RK. FIH-1 is an asparaginyl hydroxylase enzyme that regulates the transcriptional activity of hypoxia-inducible factor. *Genes Dev* 2002;16:1466-1471.
32. McNeill LA, Hewitson KS, Claridge TD, Seibel JF, Horsfall LE, Schofield CJ. Hypoxia-inducible factor asparaginyl hydroxylase (FIH-1) catalyses hydroxylation at the beta-carbon of asparagine-803. *Biochem J* 2002;367:571-575.
33. Rogers S, Wells R, Rechsteiner M. Amino acid sequences common to rapidly degraded proteins: the PEST hypothesis. *Science* 1986;234:364-368.
34. Huang LE, Gu J, Schau M, Bunn HF. Regulation of hypoxia-inducible factor 1alpha is mediated by an O₂-dependent degradation domain via the ubiquitin-proteasome pathway. *Proc Natl Acad Sci U S A* 1998;95:7987-7992.
35. Masson N, Willam C, Maxwell PH, Pugh CW, Ratcliffe PJ. Independent function of two destruction domains in hypoxia-inducible factor-alpha chains activated by prolyl hydroxylation. *Embo J* 2001;20:5197-5206.
36. Bruick RK, McKnight SL. A conserved family of prolyl-4-hydroxylases that modify HIF. *Science* 2001;294:1337-1340.

37. Jeong JW, Bae MK, Ahn MY, Kim SH, Sohn TK, Bae MH, Yoo MA, et al. Regulation and destabilization of HIF-1 α by ARD1-mediated acetylation. *Cell* 2002;111:709-720.
38. Vitale N, Moss J, Vaughan M. ARD1, a 64-kDa bifunctional protein containing an 18-kDa GTP-binding ADP-ribosylation factor domain and a 46-kDa GTPase-activating domain. *Proc Natl Acad Sci U S A* 1996;93:1941-1944.
39. Arnesen T, Anderson D, Baldersheim C, Lanotte M, Varhaug JE, Lillehaug JR. Identification and characterization of the human ARD1-NATH protein acetyltransferase complex. *Biochem J* 2005;386:433-443.
40. Hara S, Hamada J, Kobayashi C, Kondo Y, Imura N. Expression and characterization of hypoxia-inducible factor (HIF)-3 α in human kidney: suppression of HIF-mediated gene expression by HIF-3 α . *Biochem Biophys Res Commun* 2001;287:808-813.
41. Maynard MA, Qi H, Chung J, Lee EH, Kondo Y, Hara S, Conaway RC, et al. Multiple splice variants of the human HIF-3 α locus are targets of the von Hippel-Lindau E3 ubiquitin ligase complex. *J Biol Chem* 2003;278:11032-11040.
42. Makino Y, Cao R, Svensson K, Bertilsson G, Asman M, Tanaka H, Cao Y, et al. Inhibitory PAS domain protein is a negative regulator of hypoxia-inducible gene expression. *Nature* 2001;414:550-554.
43. Makino Y, Kanopka A, Wilson WJ, Tanaka H, Poellinger L. Inhibitory PAS domain protein (IPAS) is a hypoxia-inducible splicing variant of the hypoxia-inducible factor-3 α locus. *J Biol Chem* 2002;277:32405-32408.
44. Min JH, Yang H, Ivan M, Gertler F, Kaelin WG, Jr., Pavletich NP. Structure of an HIF-1 α -pVHL complex: hydroxyproline recognition in signaling. *Science* 2002;296:1886-1889.
45. Hon WC, Wilson MI, Harlos K, Claridge TD, Schofield CJ, Pugh CW, Maxwell PH, et al. Structural basis for the recognition of hydroxyproline in HIF-1 α by pVHL. *Nature* 2002;417:975-978.
46. Jaakkola P, Mole DR, Tian YM, Wilson MI, Gielbert J, Gaskell SJ, Kriegsheim A, et al. Targeting of HIF- α to the von Hippel-Lindau ubiquitylation complex by O₂-regulated prolyl hydroxylation. *Science* 2001;292:468-472.
47. Traenckner EB, Baeuerle PA. Appearance of apparently ubiquitin-conjugated I κ B- α during its phosphorylation-induced degradation in intact cells. *J Cell Sci Suppl* 1995;19:79-84.
48. Ivan M, Kondo K, Yang H, Kim W, Valiando J, Ohh M, Salic A, et al. HIF α targeted for VHL-mediated destruction by proline hydroxylation: implications for O₂ sensing. *Science* 2001;292:464-468.

49. Berra E, Benizri E, Ginouves A, Volmat V, Roux D, Pouyssegur J. HIF prolyl-hydroxylase 2 is the key oxygen sensor setting low steady-state levels of HIF-1alpha in normoxia. *Embo J* 2003;22:4082-4090.
50. Jiang BH, Rue E, Wang GL, Roe R, Semenza GL. Dimerization, DNA binding, and transactivation properties of hypoxia-inducible factor 1. *J Biol Chem* 1996;271:17771-17778.
51. Freedman SJ, Sun ZY, Poy F, Kung AL, Livingston DM, Wagner G, Eck MJ. Structural basis for recruitment of CBP/p300 by hypoxia-inducible factor-1 alpha. *Proc Natl Acad Sci U S A* 2002;99:5367-5372.
52. Zelzer E, Levy Y, Kahana C, Shilo BZ, Rubinstein M, Cohen B. Insulin induces transcription of target genes through the hypoxia-inducible factor HIF-1alpha/ARNT. *Embo J* 1998;17:5085-5094.
53. Feldser D, Agani F, Iyer NV, Pak B, Ferreira G, Semenza GL. Reciprocal positive regulation of hypoxia-inducible factor 1alpha and insulin-like growth factor 2. *Cancer Res* 1999;59:3915-3918.
54. Zhong H, Chiles K, Feldser D, Laughner E, Hanrahan C, Georgescu MM, Simons JW, et al. Modulation of hypoxia-inducible factor 1alpha expression by the epidermal growth factor/phosphatidylinositol 3-kinase/PTEN/AKT/FRAP pathway in human prostate cancer cells: implications for tumor angiogenesis and therapeutics. *Cancer Res* 2000;60:1541-1545.
55. Ehleben W, Porwol T, Fandrey J, Kummer W, Acker H. Cobalt and desferrioxamine reveal crucial members of the oxygen sensing pathway in HepG2 cells. *Kidney Int* 1997;51:483-491.
56. Semenza GL. Perspectives on oxygen sensing. *Cell* 1999;98:281-284.
57. Gong W, Hao B, Mansy SS, Gonzalez G, Gilles-Gonzalez MA, Chan MK. Structure of a biological oxygen sensor: a new mechanism for heme-driven signal transduction. *Proc Natl Acad Sci U S A* 1998;95:15177-15182.
58. Epstein AC, Gleadle JM, McNeill LA, Hewitson KS, O'Rourke J, Mole DR, Mukherji M, et al. *C. elegans* EGL-9 and mammalian homologs define a family of dioxygenases that regulate HIF by prolyl hydroxylation. *Cell* 2001;107:43-54.
59. Trent C, Tsuing N, Horvitz HR. Egg-laying defective mutants of the nematode *Caenorhabditis elegans*. *Genetics* 1983;104:619-647.
60. Hirsila M, Koivunen P, Gunzler V, Kivirikko KI, Myllyharju J. Characterization of the human prolyl 4-hydroxylases that modify the hypoxia-inducible factor. *J Biol Chem* 2003;278:30772-30780.

61. Oehme F, Jonghaus W, Narouz-Ott L, Huetter J, Flamme I. A nonradioactive 96-well plate assay for the detection of hypoxia-inducible factor prolyl hydroxylase activity. *Anal Biochem* 2004;330:74-80.
62. Hewitson KS, McNeill LA, Riordan MV, Tian YM, Bullock AN, Welford RW, Elkins JM, et al. Hypoxia-inducible factor (HIF) asparagine hydroxylase is identical to factor inhibiting HIF (FIH) and is related to the cupin structural family. *J Biol Chem* 2002;277:26351-26355.
63. Dann CE, 3rd, Bruick RK, Deisenhofer J. Structure of factor-inhibiting hypoxia-inducible factor 1: An asparaginyl hydroxylase involved in the hypoxic response pathway. *Proc Natl Acad Sci U S A* 2002;99:15351-15356.
64. Lee E, Yim S, Lee SK, Park H. Two transactivation domains of hypoxia-inducible factor-1alpha regulated by the MEK-1/p42/p44 MAPK pathway. *Mol Cells* 2002;14:9-15.
65. Elkins JM, Hewitson KS, McNeill LA, Seibel JF, Schlemminger I, Pugh CW, Ratcliffe PJ, et al. Structure of factor-inhibiting hypoxia-inducible factor (HIF) reveals mechanism of oxidative modification of HIF-1 alpha. *J Biol Chem* 2003;278:1802-1806.
66. Lancaster DE, McNeill LA, McDonough MA, Aplin RT, Hewitson KS, Pugh CW, Ratcliffe PJ, et al. Disruption of dimerization and substrate phosphorylation inhibit factor inhibiting hypoxia-inducible factor (FIH) activity. *Biochem J* 2004;383:429-437.
67. Stenflo J, Lundwall A, Dahlback B. beta-Hydroxyasparagine in domains homologous to the epidermal growth factor precursor in vitamin K-dependent protein S. *Proc Natl Acad Sci U S A* 1987;84:368-372.
68. Dinchuk JE, Focht RJ, Kelley JA, Henderson NL, Zolotarjova NI, Wynn R, Neff NT, et al. Absence of post-translational aspartyl beta-hydroxylation of epidermal growth factor domains in mice leads to developmental defects and an increased incidence of intestinal neoplasia. *J Biol Chem* 2002;277:12970-12977.
69. Bruick RK. Oxygen sensing in the hypoxic response pathway: regulation of the hypoxia-inducible transcription factor. *Genes Dev* 2003;17:2614-2623.
70. Li D, Hirsila M, Koivunen P, Brenner MC, Xu L, Yang C, Kivirikko KI, et al. Many amino acid substitutions in a hypoxia-inducible transcription factor (HIF)-1alpha-like peptide cause only minor changes in its hydroxylation by the HIF prolyl 4-hydroxylases: substitution of 3,4-dehydroproline or azetidine-2-carboxylic acid for the proline leads to a high rate of uncoupled 2-oxoglutarate decarboxylation. *J Biol Chem* 2004;279:55051-55059.
71. Laughner E, Taghavi P, Chiles K, Mahon PC, Semenza GL. HER2 (neu) signaling increases the rate of hypoxia-inducible factor 1alpha (HIF-1alpha) synthesis: novel mechanism for HIF-1-mediated vascular endothelial growth factor expression. *Mol Cell Biol* 2001;21:3995-4004.

72. del Peso L, Castellanos MC, Temes E, Martin-Puig S, Cuevas Y, Olmos G, Landazuri MO. The von Hippel Lindau/hypoxia-inducible factor (HIF) pathway regulates the transcription of the HIF-proline hydroxylase genes in response to low oxygen. *J Biol Chem* 2003;278:48690-48695.
73. Marxsen JH, Stengel P, Doege K, Heikkinen P, Jokilehto T, Wagner T, Jelkmann W, et al. Hypoxia-inducible factor-1 (HIF-1) promotes its degradation by induction of HIF- α -prolyl-4-hydroxylases. *Biochem J* 2004;381:761-767.
74. Pescador N, Cuevas Y, Naranjo S, Alcaide M, Villar D, Landazuri MO, Del Peso L. Identification of a functional hypoxia-responsive element that regulates the expression of the egl nine homologue 3 (egln3/phd3) gene. *Biochem J* 2005;390:189-197.
75. D'Angelo G, Duplan E, Boyer N, Vigne P, Frelin C. Hypoxia up-regulates prolyl hydroxylase activity: a feedback mechanism that limits HIF-1 responses during reoxygenation. *J Biol Chem* 2003;278:38183-38187.
76. Nakayama K, Frew IJ, Hagensen M, Skals M, Habelhah H, Bhoumik A, Kadoya T, et al. Siah2 regulates stability of prolyl-hydroxylases, controls HIF1 α abundance, and modulates physiological responses to hypoxia. *Cell* 2004;117:941-952.
77. Erez N, Stambolsky P, Shats I, Milyavsky M, Kachko T, Rotter V. Hypoxia-dependent regulation of PHD1: cloning and characterization of the human PHD1/EGLN2 gene promoter. *FEBS Lett* 2004;567:311-315.
78. Choi KO, Lee T, Lee N, Kim JH, Yang EG, Yoon JM, Kim JH, et al. Inhibition of the catalytic activity of hypoxia-inducible factor-1 α -prolyl-hydroxylase 2 by a MYND-type zinc finger. *Mol Pharmacol* 2005;68:1803-1809.
79. Hopfer U, Hopfer H, Jablonski K, Stahl RA, Wolf G. The Novel WD-repeat Protein Morg1 Acts as a Molecular Scaffold for Hypoxia-inducible Factor Prolyl Hydroxylase 3 (PHD3). *J Biol Chem* 2006;281:8645-8655.
80. Baek JH, Mahon PC, Oh J, Kelly B, Krishnamachary B, Pearson M, Chan DA, et al. OS-9 interacts with hypoxia-inducible factor 1 α and prolyl hydroxylases to promote oxygen-dependent degradation of HIF-1 α . *Mol Cell* 2005;17:503-512.
81. Abbott BD, Probst MR. Developmental expression of two members of a new class of transcription factors: II. Expression of aryl hydrocarbon receptor nuclear translocator in the C57BL/6N mouse embryo. *Dev Dyn* 1995;204:144-155.
82. Blancher C, Moore JW, Talks KL, Houlbrook S, Harris AL. Relationship of hypoxia-inducible factor (HIF)-1 α and HIF-2 α expression to vascular endothelial growth factor induction and hypoxia survival in human breast cancer cell lines. *Cancer Res* 2000;60:7106-7113.

83. Stroka DM, Burkhardt T, Desbaillets I, Wenger RH, Neil DA, Bauer C, Gassmann M, et al. HIF-1 is expressed in normoxic tissue and displays an organ-specific regulation under systemic hypoxia. *Faseb J* 2001;15:2445-2453.
84. Ema M, Taya S, Yokotani N, Sogawa K, Matsuda Y, Fujii-Kuriyama Y. A novel bHLH-PAS factor with close sequence similarity to hypoxia-inducible factor 1alpha regulates the VEGF expression and is potentially involved in lung and vascular development. *Proc Natl Acad Sci U S A* 1997;94:4273-4278.
85. Rajakumar A, Conrad KP. Expression, ontogeny, and regulation of hypoxia-inducible transcription factors in the human placenta. *Biol Reprod* 2000;63:559-569.
86. Wiesener MS, Jurgensen JS, Rosenberger C, Scholze CK, Horstrup JH, Warnecke C, Mandriota S, et al. Widespread hypoxia-inducible expression of HIF-2alpha in distinct cell populations of different organs. *Faseb J* 2003;17:271-273.
87. Sowter HM, Raval RR, Moore JW, Ratcliffe PJ, Harris AL. Predominant role of hypoxia-inducible transcription factor (Hif)-1alpha versus Hif-2alpha in regulation of the transcriptional response to hypoxia. *Cancer Res* 2003;63:6130-6134.
88. Hu CJ, Iyer S, Sataur A, Covello KL, Chodosh LA, Simon MC. Differential Regulation of the Transcriptional Activities of Hypoxia-Inducible Factor 1 Alpha (HIF-1{alpha}) and HIF-2{alpha} in Stem Cells. *Mol Cell Biol* 2006;26:3514-3526.
89. Park SK, Dadak AM, Haase VH, Fontana L, Giaccia AJ, Johnson RS. Hypoxia-induced gene expression occurs solely through the action of hypoxia-inducible factor 1alpha (HIF-1alpha): role of cytoplasmic trapping of HIF-2alpha. *Mol Cell Biol* 2003;23:4959-4971.
90. Covello KL, Simon MC, Keith B. Targeted replacement of hypoxia-inducible factor-1alpha by a hypoxia-inducible factor-2alpha knock-in allele promotes tumor growth. *Cancer Res* 2005;65:2277-2286.
91. Covello KL, Kehler J, Yu H, Gordan JD, Arsham AM, Hu CJ, Labosky PA, et al. HIF-2alpha regulates Oct-4: effects of hypoxia on stem cell function, embryonic development, and tumor growth. *Genes Dev* 2006;20:557-570.
92. Gu YZ, Moran SM, Hogenesch JB, Wartman L, Bradfield CA. Molecular characterization and chromosomal localization of a third alpha-class hypoxia inducible factor subunit, HIF3alpha. *Gene Expr* 1998;7:205-213.
93. Lieb ME, Menzies K, Moschella MC, Ni R, Taubman MB. Mammalian EGLN genes have distinct patterns of mRNA expression and regulation. *Biochem Cell Biol* 2002;80:421-426.
94. Oehme F, Ellinghaus P, Kolkhof P, Smith TJ, Ramakrishnan S, Hutter J, Schramm M, et al. Overexpression of PH-4, a novel putative proline 4-hydroxylase, modulates activity of

- hypoxia-inducible transcription factors. *Biochem Biophys Res Commun* 2002;296:343-349.
95. Ram PA, Waxman DJ. Dehydroepiandrosterone 3 beta-sulphate is an endogenous activator of the peroxisome-proliferation pathway: induction of cytochrome P-450 4A and acyl-CoA oxidase mRNAs in primary rat hepatocyte culture and inhibitory effects of Ca(2+)-channel blockers. *Biochem J* 1994;301 (Pt 3):753-758.
 96. Wax SD, Tsao L, Lieb ME, Fallon JT, Taubman MB. SM-20 is a novel 40-kd protein whose expression in the arterial wall is restricted to smooth muscle. *Lab Invest* 1996;74:797-808.
 97. Lipscomb EA, Sarmiere PD, Freeman RS. SM-20 is a novel mitochondrial protein that causes caspase-dependent cell death in nerve growth factor-dependent neurons. *J Biol Chem* 2001;276:5085-5092.
 98. Soilleux EJ, Turley H, Tian YM, Pugh CW, Gatter KC, Harris AL. Use of novel monoclonal antibodies to determine the expression and distribution of the hypoxia regulatory factors PHD-1, PHD-2, PHD-3 and FIH in normal and neoplastic human tissues. *Histopathology* 2005;47:602-610.
 99. Iyer NV, Kotch LE, Agani F, Leung SW, Laughner E, Wenger RH, Gassmann M, et al. Cellular and developmental control of O₂ homeostasis by hypoxia-inducible factor 1 alpha. *Genes Dev* 1998;12:149-162.
 100. Ryan HE, Lo J, Johnson RS. HIF-1 alpha is required for solid tumor formation and embryonic vascularization. *Embo J* 1998;17:3005-3015.
 101. Semenza GL, Agani F, Iyer N, Kotch L, Laughner E, Leung S, Yu A. Regulation of cardiovascular development and physiology by hypoxia-inducible factor 1. *Ann N Y Acad Sci* 1999;874:262-268.
 102. Compernelle V, Brusselmans K, Franco D, Moorman A, Dewerchin M, Collen D, Carmeliet P. Cardia bifida, defective heart development and abnormal neural crest migration in embryos lacking hypoxia-inducible factor-1alpha. *Cardiovasc Res* 2003;60:569-579.
 103. Compernelle V, Brusselmans K, Acker T, Hoet P, Tjwa M, Beck H, Plaisance S, et al. Loss of HIF-2alpha and inhibition of VEGF impair fetal lung maturation, whereas treatment with VEGF prevents fatal respiratory distress in premature mice. *Nat Med* 2002;8:702-710.
 104. Tian H, Hammer RE, Matsumoto AM, Russell DW, McKnight SL. The hypoxia-responsive transcription factor EPAS1 is essential for catecholamine homeostasis and protection against heart failure during embryonic development. *Genes Dev* 1998;12:3320-3324.

105. Scortegagna M, Ding K, Oktay Y, Gaur A, Thurmond F, Yan LJ, Marck BT, et al. Multiple organ pathology, metabolic abnormalities and impaired homeostasis of reactive oxygen species in *Epas1*^{-/-} mice. *Nat Genet* 2003;35:331-340.
106. Scortegagna M, Morris MA, Oktay Y, Bennett M, Garcia JA. The HIF family member EPAS1/HIF-2alpha is required for normal hematopoiesis in mice. *Blood* 2003;102:1634-1640.
107. Cramer T, Johnson RS. A novel role for the hypoxia inducible transcription factor HIF-1alpha: critical regulation of inflammatory cell function. *Cell Cycle* 2003;2:192-193.
108. Schipani E, Ryan HE, Didrickson S, Kobayashi T, Knight M, Johnson RS. Hypoxia in cartilage: HIF-1alpha is essential for chondrocyte growth arrest and survival. *Genes Dev* 2001;15:2865-2876.
109. Helton R, Cui J, Scheel JR, Ellison JA, Ames C, Gibson C, Blouw B, et al. Brain-specific knock-out of hypoxia-inducible factor-1alpha reduces rather than increases hypoxic-ischemic damage. *J Neurosci* 2005;25:4099-4107.
110. Appelhoff RJ, Tian YM, Raval RR, Turley H, Harris AL, Pugh CW, Ratcliffe PJ, et al. Differential function of the prolyl hydroxylases PHD1, PHD2, and PHD3 in the regulation of hypoxia-inducible factor. *J Biol Chem* 2004;279:38458-38465.
111. Mazure NM, Brahimi-Horn MC, Berta MA, Benizri E, Bilton RL, Dayan F, Ginouves A, et al. HIF-1: master and commander of the hypoxic world. A pharmacological approach to its regulation by siRNAs. *Biochem Pharmacol* 2004;68:971-980.
112. Ji YS, Xu Q, Schmedtje JF, Jr. Hypoxia induces high-mobility-group protein I(Y) and transcription of the cyclooxygenase-2 gene in human vascular endothelium. *Circ Res* 1998;83:295-304.
113. Semenza GL. Hydroxylation of HIF-1: oxygen sensing at the molecular level. *Physiology (Bethesda)* 2004;19:176-182.
114. Schofield CJ, Ratcliffe PJ. Oxygen sensing by HIF hydroxylases. *Nat Rev Mol Cell Biol* 2004;5:343-354.
115. Wenger RH, Stiehl DP, Camenisch G. Integration of oxygen signaling at the consensus HRE. *Sci STKE* 2005;2005:re12.
116. Hu CJ, Wang LY, Chodosh LA, Keith B, Simon MC. Differential roles of hypoxia-inducible factor 1alpha (HIF-1alpha) and HIF-2alpha in hypoxic gene regulation. *Mol Cell Biol* 2003;23:9361-9374.
117. Seagroves TN, Ryan HE, Lu H, Wouters BG, Knapp M, Thibault P, Laderoute K, et al. Transcription factor HIF-1 is a necessary mediator of the pasteur effect in mammalian cells. *Mol Cell Biol* 2001;21:3436-3444.

118. Tsuzuki Y, Fukumura D, Oosthuysen B, Koike C, Carmeliet P, Jain RK. Vascular endothelial growth factor (VEGF) modulation by targeting hypoxia-inducible factor-1alpha--> hypoxia response element--> VEGF cascade differentially regulates vascular response and growth rate in tumors. *Cancer Res* 2000;60:6248-6252.
119. Jokilehto T, Rantanen K, Luukkaa M, Heikkinen P, Grenman R, Minn H, Kronqvist P, et al. Overexpression and nuclear translocation of hypoxia-inducible factor prolyl hydroxylase PHD2 in head and neck squamous cell carcinoma is associated with tumor aggressiveness. *Clin Cancer Res* 2006;12:1080-1087.
120. Maltepe E, Schmidt JV, Baunoch D, Bradfield CA, Simon MC. Abnormal angiogenesis and responses to glucose and oxygen deprivation in mice lacking the protein ARNT. *Nature* 1997;386:403-407.
121. Carmeliet P, Jain RK. Angiogenesis in cancer and other diseases. *Nature* 2000;407:249-257.
122. Larcher F, Murillas R, Bolontrade M, Conti CJ, Jorcano JL. VEGF/VPF overexpression in skin of transgenic mice induces angiogenesis, vascular hyperpermeability and accelerated tumor development. *Oncogene* 1998;17:303-311.
123. Vincent KA, Feron O, Kelly RA. Harnessing the response to tissue hypoxia: HIF-1 alpha and therapeutic angiogenesis. *Trends Cardiovasc Med* 2002;12:362-367.
124. Percy MJ, Zhao Q, Flores A, Harrison C, Lappin TR, Maxwell PH, McMullin MF, et al. A family with erythrocytosis establishes a role for prolyl hydroxylase domain protein 2 in oxygen homeostasis. *Proc Natl Acad Sci U S A* 2006;103:654-659.
125. Jungermann K, Kietzmann T. Oxygen: modulator of metabolic zonation and disease of the liver. *Hepatology* 2000;31:255-260.
126. Singh A, Chu I, Villeneuve DC. Subchronic toxicity of 2,4,4'-trichlorobiphenyl in the rat liver: an ultrastructural and biochemical study. *Ultrastruct Pathol* 1996;20:275-284.
127. Bangoura G, Yang LY, Huang GW, Wang W. Expression of HIF-2alpha/EPAS1 in hepatocellular carcinoma. *World J Gastroenterol* 2004;10:525-530.
128. James LP, Donahower B, Burke AS, McCullough S, Hinson JA. Induction of the nuclear factor HIF-1alpha in acetaminophen toxicity: Evidence for oxidative stress. *Biochem Biophys Res Commun* 2006.
129. Corpechot C, Barbu V, Wendum D, Chignard N, Housset C, Poupon R, Rosmorduc O. Hepatocyte growth factor and c-Met inhibition by hepatic cell hypoxia: a potential mechanism for liver regeneration failure in experimental cirrhosis. *Am J Pathol* 2002;160:613-620.

130. Corpechot C, Barbu V, Wendum D, Kinnman N, Rey C, Poupon R, Housset C, et al. Hypoxia-induced VEGF and collagen I expressions are associated with angiogenesis and fibrogenesis in experimental cirrhosis. *Hepatology* 2002;35:1010-1021.
131. Seglen PO. Preparation of isolated rat liver cells. *Methods Cell Biol* 1976;13:29-83.
132. Runge D, Runge DM, Jager D, Lubecki KA, Beer Stolz D, Karathanasis S, Kietzmann T, et al. Serum-free, long-term cultures of human hepatocytes: maintenance of cell morphology, transcription factors, and liver-specific functions. *Biochem Biophys Res Commun* 2000;269:46-53.
133. Block GD, Locker J, Bowen WC, Petersen BE, Katyal S, Strom SC, Riley T, et al. Population expansion, clonal growth, and specific differentiation patterns in primary cultures of hepatocytes induced by HGF/SF, EGF and TGF alpha in a chemically defined (HGM) medium. *J Cell Biol* 1996;132:1133-1149.
134. Jiang BH, Semenza GL, Bauer C, Marti HH. Hypoxia-inducible factor 1 levels vary exponentially over a physiologically relevant range of O₂ tension. *Am J Physiol* 1996;271:C1172-1180.
135. Ljungkvist AS, Bussink J, Rijken PF, Raleigh JA, Denekamp J, Van Der Kogel AJ. Changes in tumor hypoxia measured with a double hypoxic marker technique. *Int J Radiat Oncol Biol Phys* 2000;48:1529-1538.
136. Mosmann T. Rapid colorimetric assay for cellular growth and survival: application to proliferation and cytotoxicity assays. *J Immunol Methods* 1983;65:55-63.
137. Korzeniewski C, Callewaert DM. An enzyme-release assay for natural cytotoxicity. *J Immunol Methods* 1983;64:313-320.
138. Novicki DL, Jirtle RL, Michalopoulos G. Establishment of two rat hepatoma cell strains produced by a carcinogen initiation, phenobarbital promotion protocol. *In Vitro* 1983;19:191-202.
139. Higgins GM, Anderson RM. Experimental pathology of the liver, I: restoration of the liver of the white rat following partial surgical removal. *Arch Pathol* 1931;12:186-202.
140. Muzio G, Maggiora M, Trombetta A, Martinasso G, Reffo P, Colombatto S, Canuto RA. Mechanisms involved in growth inhibition induced by clofibrate in hepatoma cells. *Toxicology* 2003;187:149-159.
141. Stolz DB, Zamora R, Vodovotz Y, Loughran PA, Billiar TR, Kim YM, Simmons RL, et al. Peroxisomal localization of inducible nitric oxide synthase in hepatocytes. *Hepatology* 2002;36:81-93.
142. Runge D, Runge DM, Bowen WC, Locker J, Michalopoulos GK. Matrix induced re-differentiation of cultured rat hepatocytes and changes of CCAAT/enhancer binding proteins. *Biol Chem* 1997;378:873-881.

143. Laemmli UK. Cleavage of structural proteins during the assembly of the head of bacteriophage T4. *Nature* 1970;227:680-685.
144. Zhang SX, Gozal D, Sachleben LR, Jr., Rane M, Klein JB, Gozal E. Hypoxia induces an autocrine-paracrine survival pathway via platelet-derived growth factor (PDGF)-B/PDGF-beta receptor/phosphatidylinositol 3-kinase/Akt signaling in RN46A neuronal cells. *Faseb J* 2003;17:1709-1711.
145. Michalopoulos GK, Bowen WC, Mule K, Luo J. HGF-, EGF-, and dexamethasone-induced gene expression patterns during formation of tissue in hepatic organoid cultures. *Gene Expr* 2003;11:55-75.
146. Kietzmann T, Cornesse Y, Brechtel K, Modaressi S, Jungermann K. Perivenous expression of the mRNA of the three hypoxia-inducible factor alpha-subunits, HIF1alpha, HIF2alpha and HIF3alpha, in rat liver. *Biochem J* 2001;354:531-537.
147. Scharf JG, Unterman TG, Kietzmann T. Oxygen-dependent modulation of insulin-like growth factor binding protein biosynthesis in primary cultures of rat hepatocytes. *Endocrinology* 2005;146:5433-5443.
148. Tian YM, Mole DR, Ratcliffe PJ, Gleadle JM. Characterization of different isoforms of the HIF prolyl hydroxylase PHD1 generated by alternative initiation. *Biochem J* 2006.
149. Groulx I, Lee S. Oxygen-dependent ubiquitination and degradation of hypoxia-inducible factor requires nuclear-cytoplasmic trafficking of the von Hippel-Lindau tumor suppressor protein. *Mol Cell Biol* 2002;22:5319-5336.
150. Heiland I, Erdmann R. Biogenesis of peroxisomes. Topogenesis of the peroxisomal membrane and matrix proteins. *Febs J* 2005;272:2362-2372.
151. Olivier LM, Kovacs W, Masuda K, Keller GA, Krisans SK. Identification of peroxisomal targeting signals in cholesterol biosynthetic enzymes. AA-CoA thiolase, hmg-coa synthase, MPPD, and FPP synthase. *J Lipid Res* 2000;41:1921-1935.
152. Huber PA, Birdsey GM, Lumb MJ, Prowse DT, Perkins TJ, Knight DR, Danpure CJ. Peroxisomal import of human alanine:glyoxylate aminotransferase requires ancillary targeting information remote from its C terminus. *J Biol Chem* 2005;280:27111-27120.
153. Paton VG, Shackelford JE, Krisans SK. Cloning and subcellular localization of hamster and rat isopentenyl diphosphate dimethylallyl diphosphate isomerase. A PTS1 motif targets the enzyme to peroxisomes. *J Biol Chem* 1997;272:18945-18950.
154. Loughran PA, Stolz DB, Vodovotz Y, Watkins SC, Simmons RL, Billiar TR. Monomeric inducible nitric oxide synthase localizes to peroxisomes in hepatocytes. *Proc Natl Acad Sci U S A* 2005;102:13837-13842.
155. McNew JA, Goodman JM. An oligomeric protein is imported into peroxisomes in vivo. *J Cell Biol* 1994;127:1245-1257.

156. Haase VH, Glickman JN, Socolovsky M, Jaenisch R. Vascular tumors in livers with targeted inactivation of the von Hippel-Lindau tumor suppressor. *Proc Natl Acad Sci U S A* 2001;98:1583-1588.
157. Jungermann K, Katz N. Functional specialization of different hepatocyte populations. *Physiol Rev* 1989;69:708-764.
158. Berra E, Roux D, Richard DE, Pouyssegur J. Hypoxia-inducible factor-1 alpha (HIF-1 alpha) escapes O(2)-driven proteasomal degradation irrespective of its subcellular localization: nucleus or cytoplasm. *EMBO Rep* 2001;2:615-620.
159. Tuckerman JR, Zhao Y, Hewitson KS, Tian YM, Pugh CW, Ratcliffe PJ, Mole DR. Determination and comparison of specific activity of the HIF-prolyl hydroxylases. *FEBS Lett* 2004;576:145-150.
160. Haase VH. Hypoxia-Inducible Factors in the Kidney. *Am J Physiol Renal Physiol* 2006.
161. Metzen E, Berchner-Pfannschmidt U, Stengel P, Marxsen JH, Stolze I, Klinger M, Huang WQ, et al. Intracellular localisation of human HIF-1 alpha hydroxylases: implications for oxygen sensing. *J Cell Sci* 2003;116:1319-1326.
162. Kuznetsova AV, Meller J, Schnell PO, Nash JA, Ignacak ML, Sanchez Y, Conaway JW, et al. von Hippel-Lindau protein binds hyperphosphorylated large subunit of RNA polymerase II through a proline hydroxylation motif and targets it for ubiquitination. *Proc Natl Acad Sci U S A* 2003;100:2706-2711.
163. Jansen GA, Ofman R, Denis S, Ferdinandusse S, Hogenhout EM, Jakobs C, Wanders RJ. Phytanoyl-CoA hydroxylase from rat liver. Protein purification and cDNA cloning with implications for the subcellular localization of phytanic acid alpha-oxidation. *J Lipid Res* 1999;40:2244-2254.
164. Mihalik SJ, Rainville AM, Watkins PA. Phytanic acid alpha-oxidation in rat liver peroxisomes. Production of alpha-hydroxyphytanoyl-CoA and formate is enhanced by dioxygenase cofactors. *Eur J Biochem* 1995;232:545-551.
165. Wenger RH. Mitochondria: Oxygen sinks rather than sensors? *Med Hypotheses* 2006;66:380-383.
166. De Duve C, Baudhuin P. Peroxisomes (microbodies and related particles). *Physiol Rev* 1966;46:323-357.
167. Hagen T, Taylor CT, Lam F, Moncada S. Redistribution of intracellular oxygen in hypoxia by nitric oxide: effect on HIF1alpha. *Science* 2003;302:1975-1978.
168. Metzen E, Zhou J, Jelkmann W, Fandrey J, Brune B. Nitric oxide impairs normoxic degradation of HIF-1alpha by inhibition of prolyl hydroxylases. *Mol Biol Cell* 2003;14:3470-3481.

169. Papandreou I, Cairns RA, Fontana L, Lim AL, Denko NC. HIF-1 mediates adaptation to hypoxia by actively downregulating mitochondrial oxygen consumption. *Cell Metab* 2006;3:187-197.
170. Selak MA, Armour SM, MacKenzie ED, Boulahbel H, Watson DG, Mansfield KD, Pan Y, et al. Succinate links TCA cycle dysfunction to oncogenesis by inhibiting HIF- α prolyl hydroxylase. *Cancer Cell* 2005;7:77-85.
171. Kim JW, Tchernyshyov I, Semenza GL, Dang CV. HIF-1-mediated expression of pyruvate dehydrogenase kinase: A metabolic switch required for cellular adaptation to hypoxia. *Cell Metab* 2006;3:177-185.
172. Michalopoulos GK, DeFrances MC. Liver regeneration. *Science* 1997;276:60-66.
173. Martinez-Hernandez A, Amenta PS. The extracellular matrix in hepatic regeneration. *Faseb J* 1995;9:1401-1410.
174. Ross MA, Sander CM, Kleeb TB, Watkins SC, Stolz DB. Spatiotemporal expression of angiogenesis growth factor receptors during the revascularization of regenerating rat liver. *Hepatology* 2001;34:1135-1148.
175. Sato T, El-Assal ON, Ono T, Yamanoi A, Dhar DK, Nagasue N. Sinusoidal endothelial cell proliferation and expression of angiopoietin/Tie family in regenerating rat liver. *J Hepatol* 2001;34:690-698.
176. Shimizu H, Miyazaki M, Wakabayashi Y, Mitsuhashi N, Kato A, Ito H, Nakagawa K, et al. Vascular endothelial growth factor secreted by replicating hepatocytes induces sinusoidal endothelial cell proliferation during regeneration after partial hepatectomy in rats. *J Hepatol* 2001;34:683-689.
177. Taniguchi E, Sakisaka S, Matsuo K, Tanikawa K, Sata M. Expression and role of vascular endothelial growth factor in liver regeneration after partial hepatectomy in rats. *J Histochem Cytochem* 2001;49:121-130.
178. Kraizer Y, Mawasi N, Seagal J, Paizi M, Assy N, Spira G. Vascular endothelial growth factor and angiopoietin in liver regeneration. *Biochem Biophys Res Commun* 2001;287:209-215.
179. LeCouter J, Moritz DR, Li B, Phillips GL, Liang XH, Gerber HP, Hillan KJ, et al. Angiogenesis-independent endothelial protection of liver: role of VEGFR-1. *Science* 2003;299:890-893.
180. Li W, Liang X, Leu JI, Kovalovich K, Ciliberto G, Taub R. Global changes in interleukin-6-dependent gene expression patterns in mouse livers after partial hepatectomy. *Hepatology* 2001;33:1377-1386.
181. Cressman DE, Diamond RH, Taub R. Rapid activation of the Stat3 transcription complex in liver regeneration. *Hepatology* 1995;21:1443-1449.

182. Stolz DB, Mars WM, Petersen BE, Kim TH, Michalopoulos GK. Growth factor signal transduction immediately after two-thirds partial hepatectomy in the rat. *Cancer Res* 1999;59:3954-3960.
183. Fausto N. Liver regeneration. *J Hepatol* 2000;32:19-31.
184. Lindroos PM, Zarnegar R, Michalopoulos GK. Hepatocyte growth factor (hepatopoietin A) rapidly increases in plasma before DNA synthesis and liver regeneration stimulated by partial hepatectomy and carbon tetrachloride administration. *Hepatology* 1991;13:743-750.
185. Padiaditakis P, Lopez-Talavera JC, Petersen B, Monga SP, Michalopoulos GK. The processing and utilization of hepatocyte growth factor/scatter factor following partial hepatectomy in the rat. *Hepatology* 2001;34:688-693.
186. Zarnegar R, DeFrances MC, Kost DP, Lindroos P, Michalopoulos GK. Expression of hepatocyte growth factor mRNA in regenerating rat liver after partial hepatectomy. *Biochem Biophys Res Commun* 1991;177:559-565.
187. Patijn GA, Lieber A, Schowalter DB, Schwall R, Kay MA. Hepatocyte growth factor induces hepatocyte proliferation in vivo and allows for efficient retroviral-mediated gene transfer in mice. *Hepatology* 1998;28:707-716.
188. Huh CG, Factor VM, Sanchez A, Uchida K, Conner EA, Thorgeirsson SS. Hepatocyte growth factor/c-met signaling pathway is required for efficient liver regeneration and repair. *Proc Natl Acad Sci U S A* 2004;101:4477-4482.
189. Borowiak M, Garratt AN, Wustefeld T, Strehle M, Trautwein C, Birchmeier C. Met provides essential signals for liver regeneration. *Proc Natl Acad Sci U S A* 2004;101:10608-10613.
190. Birchmeier C, Gherardi E. Developmental roles of HGF/SF and its receptor, the c-Met tyrosine kinase. *Trends Cell Biol* 1998;8:404-410.
191. Phaneuf D, Moscioni AD, LeClair C, Raper SE, Wilson JM. Generation of a mouse expressing a conditional knockout of the hepatocyte growth factor gene: demonstration of impaired liver regeneration. *Dev Cell Biol* 2004;23:592-603.
192. Pennacchietti S, Michieli P, Galluzzo M, Mazzone M, Giordano S, Comoglio PM. Hypoxia promotes invasive growth by transcriptional activation of the met protooncogene. *Cancer Cell* 2003;3:347-361.
193. Hara S, Nakashiro KI, Klosek SK, Ishikawa T, Shintani S, Hamakawa H. Hypoxia enhances c-Met/HGF receptor expression and signaling by activating HIF-1alpha in human salivary gland cancer cells. *Oral Oncol* 2006.
194. Scarpino S, Cancellario d'Alena F, Di Napoli A, Pasquini A, Marzullo A, Ruco LP. Increased expression of Met protein is associated with up-regulation of hypoxia inducible

- factor-1 (HIF-1) in tumour cells in papillary carcinoma of the thyroid. *J Pathol* 2004;202:352-358.
195. Tacchini L, De Ponti C, Matteucci E, Follis R, Desiderio MA. Hepatocyte growth factor-activated NF-kappaB regulates HIF-1 activity and ODC expression, implicated in survival, differently in different carcinoma cell lines. *Carcinogenesis* 2004;25:2089-2100.
 196. Tacchini L, Matteucci E, De Ponti C, Desiderio MA. Hepatocyte growth factor signaling regulates transactivation of genes belonging to the plasminogen activation system via hypoxia inducible factor-1. *Exp Cell Res* 2003;290:391-401.
 197. Tacchini L, Dansi P, Matteucci E, Desiderio MA. Hepatocyte growth factor signalling stimulates hypoxia inducible factor-1 (HIF-1) activity in HepG2 hepatoma cells. *Carcinogenesis* 2001;22:1363-1371.
 198. Hayashi S, Morishita R, Nakamura S, Yamamoto K, Moriguchi A, Nagano T, Taiji M, et al. Potential role of hepatocyte growth factor, a novel angiogenic growth factor, in peripheral arterial disease: downregulation of HGF in response to hypoxia in vascular cells. *Circulation* 1999;100:II301-308.
 199. Su Y, Li H, Zhang J, Xiu R. Down-regulation of hepatocyte growth factor mRNA in rat cardiac myocytes under hypoxia mimicked by cobalt chloride. *Clin Hemorheol Microcirc* 2006;34:201-206.
 200. Yamamoto K, Morishita R, Hayashi S, Matsushita H, Nakagami H, Moriguchi A, Matsumoto K, et al. Contribution of Bcl-2, but not Bcl-xL and Bax, to antiapoptotic actions of hepatocyte growth factor in hypoxia-conditioned human endothelial cells. *Hypertension* 2001;37:1341-1348.
 201. Ozaki M, Haga S, Zhang HQ, Irani K, Suzuki S. Inhibition of hypoxia/reoxygenation-induced oxidative stress in HGF-stimulated antiapoptotic signaling: role of PI3-K and Akt kinase upon rac1. *Cell Death Differ* 2003;10:508-515.
 202. Rubin RA, O'Keefe EJ, Earp HS. Alteration of epidermal growth factor-dependent phosphorylation during rat liver regeneration. *Proc Natl Acad Sci U S A* 1982;79:776-780.
 203. Earp HS, Dawson TL, Li X, Yu H. Heterodimerization and functional interaction between EGF receptor family members: a new signaling paradigm with implications for breast cancer research. *Breast Cancer Res Treat* 1995;35:115-132.
 204. Earp HS, 3rd, Calvo BF, Sartor CI. The EGF receptor family--multiple roles in proliferation, differentiation, and neoplasia with an emphasis on HER4. *Trans Am Clin Climatol Assoc* 2003;114:315-333; discussion 333-314.
 205. Carver RS, Stevenson MC, Scheving LA, Russell WE. Diverse expression of ErbB receptor proteins during rat liver development and regeneration. *Gastroenterology* 2002;123:2017-2027.

206. Stern DF. Tyrosine kinase signalling in breast cancer: ErbB family receptor tyrosine kinases. *Breast Cancer Res* 2000;2:176-183.
207. Carraway KL, 3rd, Sweeney C. Localization and modulation of ErbB receptor tyrosine kinases. *Curr Opin Cell Biol* 2001;13:125-130.
208. O'Reilly SM, Leonard MO, Kieran N, Comerford KM, Cummins E, Pouliot M, Lee SB, et al. Hypoxia induces epithelial amphiregulin gene expression in a CREB-dependent manner. *Am J Physiol Cell Physiol* 2006;290:C592-600.
209. Jin K, Mao XO, Sun Y, Xie L, Jin L, Nishi E, Klagsbrun M, et al. Heparin-binding epidermal growth factor-like growth factor: hypoxia-inducible expression in vitro and stimulation of neurogenesis in vitro and in vivo. *J Neurosci* 2002;22:5365-5373.
210. Schultz K, Fanburg BL, Beasley D. Hypoxia and hypoxia-inducible factor-1{alpha} promote growth factor-induced proliferation of human vascular smooth muscle cells. *Am J Physiol Heart Circ Physiol* 2006.
211. Huang GW, Yang LY, Lu WQ. Effects of PI3K and p42/p44 MAPK on overexpression of vascular endothelial growth factor in hepatocellular carcinoma. *World J Gastroenterol* 2004;10:809-812.
212. Jiang BH, Jiang G, Zheng JZ, Lu Z, Hunter T, Vogt PK. Phosphatidylinositol 3-kinase signaling controls levels of hypoxia-inducible factor 1. *Cell Growth Differ* 2001;12:363-369.
213. Maity A, Pore N, Lee J, Solomon D, O'Rourke DM. Epidermal growth factor receptor transcriptionally up-regulates vascular endothelial growth factor expression in human glioblastoma cells via a pathway involving phosphatidylinositol 3'-kinase and distinct from that induced by hypoxia. *Cancer Res* 2000;60:5879-5886.
214. Levy R, Smith SD, Chandler K, Sadovsky Y, Nelson DM. Apoptosis in human cultured trophoblasts is enhanced by hypoxia and diminished by epidermal growth factor. *Am J Physiol Cell Physiol* 2000;278:C982-988.
215. Perkins J, St John J, Ahmed A. Modulation of trophoblast cell death by oxygen and EGF. *Mol Med* 2002;8:847-856.
216. Kothari S, Cizeau J, McMillan-Ward E, Israels SJ, Bailes M, Ens K, Kirshenbaum LA, et al. BNIP3 plays a role in hypoxic cell death in human epithelial cells that is inhibited by growth factors EGF and IGF. *Oncogene* 2003;22:4734-4744.
217. Pillai SB, Turman MA, Besner GE. Heparin-binding EGF-like growth factor is cytoprotective for intestinal epithelial cells exposed to hypoxia. *J Pediatr Surg* 1998;33:973-978; discussion 978-979.

218. Pillai SB, Hinman CE, Luquette MH, Nowicki PT, Besner GE. Heparin-binding epidermal growth factor-like growth factor protects rat intestine from ischemia/reperfusion injury. *J Surg Res* 1999;87:225-231.
219. Krogh A. The number and distribution of capillaries in muscles with calculations of the oxygen pressure head necessary for supplying the tissue. *J. Physiol. (London)* 1919;52:409-415.
220. Jewell UR, Kvietikova I, Scheid A, Bauer C, Wenger RH, Gassmann M. Induction of HIF-1alpha in response to hypoxia is instantaneous. *Faseb J* 2001;15:1312-1314.
221. Isom HC, Secott T, Georgoff I, Woodworth C, Mummaw J. Maintenance of differentiated rat hepatocytes in primary culture. *Proc Natl Acad Sci U S A* 1985;82:3252-3256.
222. Yang X, Lu P, Fujii C, Nakamoto Y, Gao JL, Kaneko S, Murphy PM, et al. Essential contribution of a chemokine, CCL3, and its receptor, CCR1, to hepatocellular carcinoma progression. *Int J Cancer* 2006;118:1869-1876.
223. Cormier-Regard S, Nguyen SV, Claycomb WC. Adrenomedullin gene expression is developmentally regulated and induced by hypoxia in rat ventricular cardiac myocytes. *J Biol Chem* 1998;273:17787-17792.
224. Nguyen SV, Claycomb WC. Hypoxia regulates the expression of the adrenomedullin and HIF-1 genes in cultured HL-1 cardiomyocytes. *Biochem Biophys Res Commun* 1999;265:382-386.
225. Garayoa M, Martinez A, Lee S, Pio R, An WG, Neckers L, Trepel J, et al. Hypoxia-inducible factor-1 (HIF-1) up-regulates adrenomedullin expression in human tumor cell lines during oxygen deprivation: a possible promotion mechanism of carcinogenesis. *Mol Endocrinol* 2000;14:848-862.
226. Qing X, Svaren J, Keith IM. mRNA expression of novel CGRP1 receptors and their activity-modifying proteins in hypoxic rat lung. *Am J Physiol Lung Cell Mol Physiol* 2001;280:L547-554.
227. Tazuke SI, Mazure NM, Sugawara J, Carland G, Faessen GH, Suen LF, Irwin JC, et al. Hypoxia stimulates insulin-like growth factor binding protein 1 (IGFBP-1) gene expression in HepG2 cells: a possible model for IGFBP-1 expression in fetal hypoxia. *Proc Natl Acad Sci U S A* 1998;95:10188-10193.
228. Popovici RM, Lu M, Bhatia S, Faessen GH, Giaccia AJ, Giudice LC. Hypoxia regulates insulin-like growth factor-binding protein 1 in human fetal hepatocytes in primary culture: suggestive molecular mechanisms for in utero fetal growth restriction caused by uteroplacental insufficiency. *J Clin Endocrinol Metab* 2001;86:2653-2659.
229. Katz AI, Toback FG, Lindheimer MD. Independence of onset of compensatory kidney growth from changes in renal function. *Am J Physiol* 1976;230:1067-1071.

230. Alvarez FE, Greco RS. Regeneration of the spleen after ectopic implantation and partial splenectomy. *Arch Surg* 1980;115:772-775.
231. Kietzmann T, Dimova EY, Flugel D, Scharf JG. Oxygen: modulator of physiological and pathophysiological processes in the liver. *Z Gastroenterol* 2006;44:67-76.
232. Immenschuh S, Hinke V, Ohlmann A, Gifhorn-Katz S, Katz N, Jungermann K, Kietzmann T. Transcriptional activation of the haem oxygenase-1 gene by cGMP via a cAMP response element/activator protein-1 element in primary cultures of rat hepatocytes. *Biochem J* 1998;334 (Pt 1):141-146.
233. Kietzmann T, Roth U, Jungermann K. Induction of the plasminogen activator inhibitor-1 gene expression by mild hypoxia via a hypoxia response element binding the hypoxia-inducible factor-1 in rat hepatocytes. *Blood* 1999;94:4177-4185.
234. Kietzmann T, Samoylenko A, Roth U, Jungermann K. Hypoxia-inducible factor-1 and hypoxia response elements mediate the induction of plasminogen activator inhibitor-1 gene expression by insulin in primary rat hepatocytes. *Blood* 2003;101:907-914.
235. Maeno H, Ono T, Dhar DK, Sato T, Yamanoi A, Nagasue N. Expression of hypoxia inducible factor-1alpha during liver regeneration induced by partial hepatectomy in rats. *Liver Int* 2005;25:1002-1009.
236. Bianciardi P, Fantacci M, Caretti A, Ronchi R, Milano G, Morel S, von Segesser L, et al. Chronic in vivo hypoxia in various organs: hypoxia-inducible factor-1alpha and apoptosis. *Biochem Biophys Res Commun* 2006;342:875-880.
237. Samaja M. Prediction of the oxygenation of human organs at varying blood oxygen carrying properties. *Respir Physiol* 1988;72:211-217.
238. Knowles HJ, Tian YM, Mole DR, Harris AL. Novel mechanism of action for hydralazine: induction of hypoxia-inducible factor-1alpha, vascular endothelial growth factor, and angiogenesis by inhibition of prolyl hydroxylases. *Circ Res* 2004;95:162-169.
239. Chan DA, Sutphin PD, Denko NC, Giaccia AJ. Role of prolyl hydroxylation in oncogenically stabilized hypoxia-inducible factor-1alpha. *J Biol Chem* 2002;277:40112-40117.
240. Kageyama Y, Koshiji M, To KK, Tian YM, Ratcliffe PJ, Huang LE. Leu-574 of human HIF-1alpha is a molecular determinant of prolyl hydroxylation. *Faseb J* 2004;18:1028-1030.
241. Lu H, Dalgard CL, Mohyeldin A, McFate T, Tait AS, Verma A. Reversible Inactivation of HIF-1 Prolyl Hydroxylases Allows Cell Metabolism to Control Basal HIF-1. *J Biol Chem* 2005;280:41928-41939.

242. Briere JJ, Favier J, Benit P, El Ghouzzi V, Lorenzato A, Rabier D, Di Renzo MF, et al. Mitochondrial succinate is instrumental for HIF1alpha nuclear translocation in SDHA-mutant fibroblasts under normoxic conditions. *Hum Mol Genet* 2005;14:3263-3269.
243. Isaacs JS, Jung YJ, Mole DR, Lee S, Torres-Cabala C, Chung YL, Merino M, et al. HIF overexpression correlates with biallelic loss of fumarate hydratase in renal cancer: Novel role of fumarate in regulation of HIF stability. *Cancer Cell* 2005;8:143-153.
244. Jezek P, Hlavata L. Mitochondria in homeostasis of reactive oxygen species in cell, tissues, and organism. *Int J Biochem Cell Biol* 2005;37:2478-2503.
245. Gupta M, Dobashi K, Greene EL, Orak JK, Singh I. Studies on hepatic injury and antioxidant enzyme activities in rat subcellular organelles following in vivo ischemia and reperfusion. *Mol Cell Biochem* 1997;176:337-347.
246. Kremser K, Kremser-Jezik M, Singh I. Effect of hypoxia-reoxygenation on peroxisomal functions in cultured human skin fibroblasts from control and Zellweger syndrome patients. *Free Radic Res* 1995;22:39-46.
247. Baumgart E, Fahimi HD, Steininger H, Grabenbauer M. A review of morphological techniques for detection of peroxisomal (and mitochondrial) proteins and their corresponding mRNAs during ontogenesis in mice: application to the PEX5-knockout mouse with Zellweger syndrome. *Microsc Res Tech* 2003;61:121-138.
248. Yanago E, Hiromasa T, Matsumura T, Kinoshita N, Fujiki Y. Isolation of Chinese hamster ovary cell pex mutants: two PEX7-defective mutants. *Biochem Biophys Res Commun* 2002;293:225-230.
249. Baes M, Gressens P, Baumgart E, Carmeliet P, Casteels M, Franssen M, Evrard P, et al. A mouse model for Zellweger syndrome. *Nat Genet* 1997;17:49-57.
250. Baumgart E, Vanhorebeek I, Grabenbauer M, Borgers M, Declercq PE, Fahimi HD, Baes M. Mitochondrial alterations caused by defective peroxisomal biogenesis in a mouse model for Zellweger syndrome (PEX5 knockout mouse). *Am J Pathol* 2001;159:1477-1494.
251. Jungermann K, Kietzmann T. Zonation of parenchymal and nonparenchymal metabolism in liver. *Annu Rev Nutr* 1996;16:179-203.
252. Jungermann K, Kietzmann T. Role of oxygen in the zonation of carbohydrate metabolism and gene expression in liver. *Kidney Int* 1997;51:402-412.
253. Wolfle D, Schmidt H, Jungermann K. Short-term modulation of glycogen metabolism, glycolysis and gluconeogenesis by physiological oxygen concentrations in hepatocyte cultures. *Eur J Biochem* 1983;135:405-412.
254. Wolfle D, Jungermann K. Long-term effects of physiological oxygen concentrations on glycolysis and gluconeogenesis in hepatocyte cultures. *Eur J Biochem* 1985;151:299-303.

255. Nauck M, Wolfle D, Katz N, Jungermann K. Modulation of the glucagon-dependent induction of phosphoenolpyruvate carboxykinase and tyrosine aminotransferase by arterial and venous oxygen concentrations in hepatocyte cultures. *Eur J Biochem* 1981;119:657-661.
256. Kota BP, Huang TH, Roufogalis BD. An overview on biological mechanisms of PPARs. *Pharmacol Res* 2005;51:85-94.
257. Issemann I, Green S. Activation of a member of the steroid hormone receptor superfamily by peroxisome proliferators. *Nature* 1990;347:645-650.
258. Dreyer C, Krey G, Keller H, Givel F, Helftenbein G, Wahli W. Control of the peroxisomal beta-oxidation pathway by a novel family of nuclear hormone receptors. *Cell* 1992;68:879-887.
259. Kliewer SA, Forman BM, Blumberg B, Ong ES, Borgmeyer U, Mangelsdorf DJ, Umesono K, et al. Differential expression and activation of a family of murine peroxisome proliferator-activated receptors. *Proc Natl Acad Sci U S A* 1994;91:7355-7359.
260. Zhang HL, Zhang ZX, Xu YJ. [Influence of hypoxia on peroxisome proliferator activated receptor alpha and its mechanisms]. *Zhonghua Jie He He Hu Xi Za Zhi* 2003;26:535-538.
261. Narravula S, Colgan SP. Hypoxia-inducible factor 1-mediated inhibition of peroxisome proliferator-activated receptor alpha expression during hypoxia. *J Immunol* 2001;166:7543-7548.
262. Huss JM, Levy FH, Kelly DP. Hypoxia inhibits the peroxisome proliferator-activated receptor alpha/retinoid X receptor gene regulatory pathway in cardiac myocytes: a mechanism for O₂-dependent modulation of mitochondrial fatty acid oxidation. *J Biol Chem* 2001;276:27605-27612.
263. Chen B, Lam KS, Wang Y, Wu D, Lam MC, Shen J, Wong L, et al. Hypoxia dysregulates the production of adiponectin and plasminogen activator inhibitor-1 independent of reactive oxygen species in adipocytes. *Biochem Biophys Res Commun* 2006;341:549-556.
264. Tien ES, Davis JW, Vanden Heuvel JP. Identification of the CREB-binding protein/p300-interacting protein CITED2 as a peroxisome proliferator-activated receptor alpha coregulator. *J Biol Chem* 2004;279:24053-24063.
265. Freedman SJ, Sun ZY, Kung AL, France DS, Wagner G, Eck MJ. Structural basis for negative regulation of hypoxia-inducible factor-1alpha by CITED2. *Nat Struct Biol* 2003;10:504-512.
266. Reddy JK, Azarnoff DL, Hignite CE. Hypolipidaemic hepatic peroxisome proliferators form a novel class of chemical carcinogens. *Nature* 1980;283:397-398.

267. Peters JM, Cheung C, Gonzalez FJ. Peroxisome proliferator-activated receptor-alpha and liver cancer: where do we stand? *J Mol Med* 2005;83:774-785.
268. Fruchart JC, Brewer HB, Jr., Leitersdorf E. Consensus for the use of fibrates in the treatment of dyslipoproteinemia and coronary heart disease. Fibrate Consensus Group. *Am J Cardiol* 1998;81:912-917.
269. Palmer CN, Hsu MH, Griffin KJ, Raucy JL, Johnson EF. Peroxisome proliferator activated receptor-alpha expression in human liver. *Mol Pharmacol* 1998;53:14-22.
270. Tugwood JD, Aldridge TC, Lambe KG, Macdonald N, Woodyatt NJ. Peroxisome proliferator-activated receptors: structures and function. *Ann N Y Acad Sci* 1996;804:252-265.
271. Walgren JE, Kurtz DT, McMillan JM. Expression of PPAR(alpha) in human hepatocytes and activation by trichloroacetate and dichloroacetate. *Res Commun Mol Pathol Pharmacol* 2000;108:116-132.
272. Ganning AE, Brunk U, Dallner G. Phthalate esters and their effect on the liver. *Hepatology* 1984;4:541-547.
273. Hurst CH, Waxman DJ. Activation of PPARalpha and PPARgamma by environmental phthalate monoesters. *Toxicol Sci* 2003;74:297-308.
274. Bility MT, Thompson JT, McKee RH, David RM, Butala JH, Vanden Heuvel JP, Peters JM. Activation of mouse and human peroxisome proliferator-activated receptors (PPARs) by phthalate monoesters. *Toxicol Sci* 2004;82:170-182.
275. Shaw D, Lee R, Roberts RA. Species differences in response to the phthalate plasticizer monoisononylphthalate (MINP) in vitro: a comparison of rat and human hepatocytes. *Arch Toxicol* 2002;76:344-350.
276. Kamendulis LM, Isenberg JS, Smith JH, Pugh G, Jr., Lington AW, Klaunig JE. Comparative effects of phthalate monoesters on gap junctional intercellular communication and peroxisome proliferation in rodent and primate hepatocytes. *J Toxicol Environ Health A* 2002;65:569-588.
277. Semenza GL, Roth PH, Fang HM, Wang GL. Transcriptional regulation of genes encoding glycolytic enzymes by hypoxia-inducible factor 1. *J Biol Chem* 1994;269:23757-23763.
278. Cha HS, Ahn KS, Jeon CH, Kim J, Song YW, Koh EM. Influence of hypoxia on the expression of matrix metalloproteinase-1, -3 and tissue inhibitor of metalloproteinase-1 in rheumatoid synovial fibroblasts. *Clin Exp Rheumatol* 2003;21:593-598.
279. Staller P, Sulitkova J, Lisztwan J, Moch H, Oakeley EJ, Krek W. Chemokine receptor CXCR4 downregulated by von Hippel-Lindau tumour suppressor pVHL. *Nature* 2003;425:307-311.

280. Lee PJ, Jiang BH, Chin BY, Iyer NV, Alam J, Semenza GL, Choi AM. Hypoxia-inducible factor-1 mediates transcriptional activation of the heme oxygenase-1 gene in response to hypoxia. *J Biol Chem* 1997;272:5375-5381.
281. Nikitenko LL, Smith DM, Bicknell R, Rees MC. Transcriptional regulation of the CRLR gene in human microvascular endothelial cells by hypoxia. *Faseb J* 2003;17:1499-1501.
282. Teh BG. [Pim-1 induced by hypoxia is involved in drug resistance and tumorigenesis of solid tumor cells]. *Hokkaido Igaku Zasshi* 2004;79:19-26.
283. Bertges DJ, Berg S, Fink MP, Delude RL. Regulation of hypoxia-inducible factor 1 in enterocytic cells. *J Surg Res* 2002;106:157-165.
284. Ebert BL, Firth JD, Ratcliffe PJ. Hypoxia and mitochondrial inhibitors regulate expression of glucose transporter-1 via distinct Cis-acting sequences. *J Biol Chem* 1995;270:29083-29089.
285. Louis CA, Reichner JS, Henry WL, Jr., Mastrofrancesco B, Gotoh T, Mori M, Albina JE. Distinct arginase isoforms expressed in primary and transformed macrophages: regulation by oxygen tension. *Am J Physiol* 1998;274:R775-782.
286. Miyazaki K, Kawamoto T, Tanimoto K, Nishiyama M, Honda H, Kato Y. Identification of functional hypoxia response elements in the promoter region of the DEC1 and DEC2 genes. *J Biol Chem* 2002;277:47014-47021.
287. Semenza GL, Jiang BH, Leung SW, Passantino R, Concordet JP, Maire P, Giallongo A. Hypoxia response elements in the aldolase A, enolase 1, and lactate dehydrogenase A gene promoters contain essential binding sites for hypoxia-inducible factor 1. *J Biol Chem* 1996;271:32529-32537.
288. Firth JD, Ebert BL, Pugh CW, Ratcliffe PJ. Oxygen-regulated control elements in the phosphoglycerate kinase 1 and lactate dehydrogenase A genes: similarities with the erythropoietin 3' enhancer. *Proc Natl Acad Sci U S A* 1994;91:6496-6500.
289. Firth JD, Ebert BL, Ratcliffe PJ. Hypoxic regulation of lactate dehydrogenase A. Interaction between hypoxia-inducible factor 1 and cAMP response elements. *J Biol Chem* 1995;270:21021-21027.
290. Yamaji R, Fujita K, Nakanishi I, Nagao K, Naito M, Tsuruo T, Inui H, et al. Hypoxic up-regulation of triosephosphate isomerase expression in mouse brain capillary endothelial cells. *Arch Biochem Biophys* 2004;423:332-342.
291. Gess B, Hofbauer KH, Deutzmann R, Kurtz A. Hypoxia up-regulates triosephosphate isomerase expression via a HIF-dependent pathway. *Pflugers Arch* 2004;448:175-180.
292. Gao L, Mejias R, Echevarria M, Lopez-Barneo J. Induction of the glucose-6-phosphate dehydrogenase gene expression by chronic hypoxia in PC12 cells. *FEBS Lett* 2004;569:256-260.

293. Shoshani T, Faerman A, Mett I, Zelin E, Tenne T, Gorodin S, Moshel Y, et al. Identification of a novel hypoxia-inducible factor 1-responsive gene, RTP801, involved in apoptosis. *Mol Cell Biol* 2002;22:2283-2293.
294. Bedo G, Vargas M, Ferreiro MJ, Chalar C, Agrati D. Characterization of hypoxia induced gene 1: expression during rat central nervous system maturation and evidence of antisense RNA expression. *Int J Dev Biol* 2005;49:431-436.
295. Lofstedt T, Jogi A, Sigvardsson M, Gradin K, Poellinger L, Pahlman S, Axelson H. Induction of ID2 expression by hypoxia-inducible factor-1: a role in dedifferentiation of hypoxic neuroblastoma cells. *J Biol Chem* 2004;279:39223-39231.